



# **From Phosphinoboranes to Mercaptopyridines: A Journey into the Reactivity of not so Frustrated Lewis Pairs**

**Thèse**

**Étienne Rochette**

**Doctorat en chimie**  
Philosophiæ doctor (Ph. D.)

Québec, Canada

© Étienne Rochette, 2019



## Résumé

La catalyse est une des pierres d'assise de la chimie moderne. Elle permet de faire des transformations difficiles d'une manière efficace et sélective, rendant possible des voies de synthèse plus courtes qui permettent ainsi à l'industrie chimique des économies de temps et d'argent. Par conséquent, le développement de la catalyse est d'une grande importance. Dans les dernières décennies, la plupart des efforts ont été orientés vers l'utilisation de métaux de transition de la seconde et troisième rangée, une approche couronnée de succès. Cependant, la maturité de ce sous-domaine et les améliorations des méthodes de caractérisation et de modélisation ont encouragé les chercheurs académiques à explorer le potentiel d'autres éléments du tableau périodique pour la catalyse.

Cette thèse explore la catalyse sans métal, ou comme nous aimons l'appeler, la chimie organométallique sans métal. Elle présente des avancées dans le domaine des paires de Lewis frustrées (PLFs), qui utilisent des molécules comportant des fonctions acide de Lewis et base de Lewis pour rendre possible des transformations qui ne le seraient pas en utilisant seulement l'une ou l'autre des fonctions. Le focus particulier du travail est de comprendre et d'exploiter la chimie des PLFs. Par conséquent, nous ne nous sommes pas limités à seulement une sous-classe de PLFs ni à une seule transformation chimique. Les sujets contenus dans la thèse sont diversifiés et incluent la réduction du  $\text{CO}_2$ , la fonctionnalisation de liens C-H, la chimie des liens B-B, la chimie des liens B-S ainsi que des discussions plus fondamentales sur le futur de la catalyse utilisant les PLFs.

## Abstract

Catalysis is one of the cornerstones of modern chemistry. It allows difficult transformations to take place in an efficient and selective manner, making possible the design of shorter synthetic pathways and saving the chemical industry time and money. Thus, the improvement of catalysis is of great importance. In the past decades, most efforts have been oriented toward the use of second and third row transition metals, an approach that has been very successful. However, the maturity of that sub-field and the improvement of characterization and modelization techniques have been leading academic researchers in exploring catalysis with other elements of the periodic table.

This thesis explores metal-free catalysis, or as we like to call it metal-free organometallic chemistry. It presents advances in frustrated Lewis pair (FLP) chemistry, which uses molecules containing Lewis basic and Lewis acidic functions to access transformations that would not be possible using only one or the other. The focus of the work is mostly on understanding and exploiting FLP chemistry. Thus, we did not limit ourselves to some sub-class of FLP nor to only one transformation. The subjects contained in the thesis are quite diverse and include CO<sub>2</sub> reduction, C-H bond functionalization, B-B bond chemistry, B-S bond chemistry as well as more fundamental discussions on future FLP catalysis development.

## Table of contents

Résumé .....	iii
Abstract.....	iv
List of Figures.....	vii
List of Schemes .....	x
List of Tables .....	xii
List of Abbreviations .....	xiii
Remerciements .....	xiv
Introduction .....	1
Green Chemistry .....	1
Catalysis .....	3
Frustrated Lewis Pairs.....	6
A Brief History of FLP.....	10
Details on the thesis content.....	12
Literature overview of subjects discussed in the thesis.....	14
CO <sub>2</sub> reduction.....	14
Csp <sup>2</sup> -H borylation.....	17
Diboranes .....	20
Chapter 1   Methodology.....	22
1.1   Inert synthetic methods .....	23
1.2 <sup>11</sup> B NMR spectroscopy.....	26
1.3   Density functional theory .....	29
1.3.1   Theoretical background.....	29
1.3.2   Utilization of DFT in the work presented .....	30
Chapter 2   Metal-free reduction of CO <sub>2</sub> : from phosphinoboranes to aminoboranes ....	34
2.1   Previous work on phosphinoborane FLP catalyzed reduction of CO <sub>2</sub> .....	34
2.2   Aminoborane FLPs for the hydrogenation of CO <sub>2</sub> .....	39
2.3   Aminoborane FLPs Exhibiting High Robustness and Reversible Formic Acid, Water and Methanol Cleavage.....	44
Chapter 3   Metal-free Csp <sup>2</sup> -H borylation of heteroarenes.....	48
3.1   Improvements on the C-H borylation system.....	61
3.1.1   Initial objectives and ideas .....	61
3.1.2   Discovery of bench stable pre-catalysts .....	64
3.1.3   Derivatives comporting less hindered amino group.....	69
3.1.4   Final attempts at improving the system.....	74

Chapter 4	From alkyne hydrogenation to B-B bond formation .....	78
4.1	FLP catalyzed alkyne hydrogenation .....	78
4.2	The discovery of the diborane (NMe <sub>2</sub> -C <sub>6</sub> H <sub>4</sub> -BH) <sub>2</sub> .....	84
4.3	The reactivity of the diborane (NMe <sub>2</sub> -C <sub>6</sub> H <sub>4</sub> -BH) <sub>2</sub> .....	95
Chapter 5	FLP promoted intra-molecular Csp <sup>3</sup> -H bond cleavage and subsequent rearrangements.....	104
Chapter 6	S-H bond borylation and the σ-bond metathesis .....	119
Chapter 7	Transfer borylation: from N/B to N/S .....	132
Conclusion	.....	144
	Perspectives.....	144
	Final conclusion .....	149
Annexes – Experimental Section.....		151
	Organization of the section .....	151
	General experimental .....	151
Chapter 2	.....	152
Chapter 3	.....	155
Chapter 4	.....	168
	Reactivity of <b>4.1</b> as nucleophile in S <sub>N</sub> <sup>2</sup> reactions .....	169
	Substitution of the B-N bond of <b>4.1</b> by another L or X type “ligand” .....	188
	Reactivity of <b>4.1</b> with S <sub>8</sub> and Se <sub>(s)</sub> .....	194
Chapter 5	.....	200
Chapter 6	.....	209
Chapter 7	.....	213
Bibliography	.....	217

## List of Figures

<b>Figure 1</b> The twelve principles of green chemistry. <sup>4</sup> .....	1
<b>Figure 2</b> Energy profile of a catalytic reaction versus a stoichiometric one. ....	3
<b>Figure 3</b> GWP/kg, in e-CO <sub>2</sub> of various elements. <sup>10</sup> .....	4
<b>Figure 4</b> Classical FLP reactivity. ....	8
<b>Figure 5</b> Advantages and disadvantages of inter-molecular, intra-molecular and auto-assembling FLP.....	9
<b>Figure 6</b> Major “deactivation” pathways in intra-molecular FLP depending on the spacer.....	10
<b>Figure 7</b> Early examples of FLP chemistry.....	11
<b>Figure 8</b> Transition metal catalyzed reduction of CO <sub>2</sub> . ....	15
<b>Figure 9</b> Metal-free reduction of CO <sub>2</sub> . ....	16
<b>Figure 10</b> Selected 2 <sup>nd</sup> or 3 <sup>rd</sup> row transition metal catalysts for the Csp <sup>2</sup> -H bond borylation reaction. ....	18
<b>Figure 11</b> Selected 1 <sup>st</sup> row transition metal catalysts for the Csp <sup>2</sup> -H bond borylation reaction. ....	18
<b>Figure 12</b> Selected stoichiometric metal-free borylation reagents. ....	19
<b>Figure 13</b> Selected metal-free catalysts for the Csp <sup>2</sup> -H bond borylation reaction. ....	19
<b>Figure 14</b> Selected examples of commercially available diboranes.....	20
<b>Figure 15</b> Selected examples of diboranes reported in the literature. ....	21
<b>Figure 16</b> A) a glovebox B) a J-Young tube C) a Schlenk line.....	23
<b>Figure 17</b> <sup>11</sup> B NMR shifts of various boron containing compounds. <sup>115</sup> .....	27
<b>Figure 18</b> Previous work on CO <sub>2</sub> reactivity and FLP.....	35
<b>Figure 19</b> DFT calculated hydrogenation and the hydroboration of CO <sub>2</sub> using HBCat. ....	36
<b>Figure 20</b> Examples of a Lewis base CO <sub>2</sub> adduct (A) and a FLP CO <sub>2</sub> adduct (B).....	37
<b>Figure 21</b> Proposed catalytic cycle for the hydrogenation of CO <sub>2</sub> (A) and ideal relative energy of different states in the mechanism (B).....	38
<b>Figure 22</b> DFT calculated CO <sub>2</sub> and H <sub>2</sub> adducts energy and enthalpy with different atom combinations (N, P, B, Al).....	39
<b>Figure 23</b> Summary of the DFT investigation of the aminoborane mediated CO <sub>2</sub> hydrogenation mechanism.....	43
<b>Figure 24</b> Problem caused by formic acid, CO <sub>2</sub> first reduction product (A) and proposed solution, partial FLP catalyzed CO <sub>2</sub> hydrogenation.....	44
<b>Figure 25</b> DFT calculated intermediate and transition state free energies for the hydrogenation of CO <sub>2</sub> , benzaldehyde and acetone using a pyridine based FLP. ....	47
<b>Figure 26</b> Micro-reversibility of the protodeborylation and C-H cleavage functionalization.....	48
<b>Figure 27</b> Selected results concerning <b>3.1</b> reported by the Repo group A) Synthesis B) Crystallographic structure. ....	50
<b>Figure 28</b> Initial mechanistic hypothesis for the catalytic borylation of C-H bonds.....	50
<b>Figure 29</b> <sup>11</sup> B{ <sup>1</sup> H} NMR spectra of <b>3.2</b> (top), the reaction of <b>3.2</b> and HBPin (middle) and of <b>3.1</b> (bottom).....	52
<b>Figure 30</b> A) DFT studies of <b>3.1</b> mediated catalytic C-H bond borylation of <i>N</i> -methylpyrrole. B) Optimized transition states geometries. ....	54
<b>Figure 31</b> Substrate scope of the borylation using <b>3.1</b> as catalyst.....	57
<b>Figure 32</b> Functional group tolerance study results for the borylation of <i>N</i> -methylpyrrole using <b>3.1</b> as catalyst. ....	59
<b>Figure 33</b> ΔG (kcal/mol) for the C-H cleavage transition state between <b>3.3</b> and a variety of arenes and heteroarenes.....	62

<b>Figure 34</b> Potential of <i>ortho</i> -to-boron-substituted catalysts to favor the monomer. ....	63
<b>Figure 35</b> A) Crystal structure of <b>3.6</b> . B) Crystal structure of <b>3.7</b> .....	65
<b>Figure 36</b> <sup>1</sup> H NMR monitoring of the borylation reaction of 1-methylpyrrole catalyzed by ambiphilic fluoroborate salts using HBPIn. ....	68
<b>Figure 37</b> Different possible dimeric forms of amino-hydroboranes.....	70
<b>Figure 38</b> Summary of the mechanistic investigation of the amino-hydroborane catalysed C-H borylation of heteroarenes.....	72
<b>Figure 39</b> DFT comparison of amino-hydroboranes catalysts with unsaturated and saturated backbones.....	75
<b>Figure 40</b> A) Initial and potential FLP alkyne hydrogenation catalysts. B) Proposed mechanism for the FLP catalyzed alkyne hydrogenation as reported by Repo and Papai. <sup>133</sup> .....	79
<b>Figure 41</b> Filtration apparatus used to synthesize <b>3.3</b> . ....	80
<b>Figure 42</b> Crystal structure of <b>3.3</b> .....	81
<b>Figure 43</b> Multi insertion product characterized by Aldridge <i>et al.</i> ....	83
<b>Figure 44</b> Crystal structure of <b>4.1</b> .....	84
<b>Figure 45</b> <sup>1</sup> H NMR (500 MHz, CDCl <sub>3</sub> ) of <b>3.3</b> .....	86
<b>Figure 46</b> <sup>13</sup> C{ <sup>1</sup> H} NMR (126 MHz, CDCl <sub>3</sub> ) of <b>3.3</b> .....	87
<b>Figure 47</b> <sup>11</sup> B{ <sup>1</sup> H} NMR (160 MHz, CDCl <sub>3</sub> ) of <b>3.3</b> .....	88
<b>Figure 48</b> ΔG in function of temperature for the equilibrium between <b>3.3</b> and <b>3.3*</b> . ....	89
<b>Figure 49</b> DFT calculated mechanism for the formation of <b>4.1</b> from <b>3.3</b> , .....	91
<b>Figure 50</b> ln of the relative integration of <b>3.3</b> CH <sub>3</sub> signal at 2.35 ppm (conversion) over time at different temperature.....	92
<b>Figure 51</b> Eyring plot for the transformation of compound <b>3.3</b> in compound <b>4.1</b> . ....	93
<b>Figure 52</b> DFT calculated transition states for the S <sub>N</sub> <sup>2</sup> reaction of <b>4.1</b> with different substrates.....	96
<b>Figure 53</b> Crystal structure of [NMe <sub>2</sub> -C <sub>6</sub> H <sub>4</sub> -B(Bu)] <sub>2</sub> -O. ....	97
<b>Figure 54</b> Crystallographic structures of the various diborane species synthesized ( <b>4.2</b> , <b>4.3</b> , <b>4.5</b> and <b>4.9</b> ). ....	99
<b>Figure 55</b> DFT calculated potential lability of the B-N bond.....	100
<b>Figure 56</b> Proposed pathway form the formation of the products observed in the reaction of <b>4.1</b> with S <sub>8</sub> and Se <sub>(s)</sub> .....	102
<b>Figure 57</b> Crystal structure of <b>5.4</b> .....	105
<b>Figure 58</b> DFT investigation of the rearrangement mechanism forming <b>5.4</b> . ....	106
<b>Figure 59</b> DFT investigation of the FLP promoted Csp <sup>3</sup> -H bond cleavage. ....	107
<b>Figure 60</b> Stability of the adducts between <b>5.3</b> with different Lewis bases calculated by DFT. ...	109
<b>Figure 61</b> Crystal structure of <b>5.2</b> .....	110
<b>Figure 62</b> DFT investigation to explain the formation of <b>5.8</b> .....	113
<b>Figure 63</b> Comparison between the observed rearrangement, the Wagner-Meerwein rearrangement and the Petasis reaction. ....	114
<b>Figure 64</b> Crystal structure of <b>5.8</b> .....	114
<b>Figure 65</b> Comparison of the DFT investigation of the rearengement of <b>3.3</b> and <b>3.9</b> .....	117
<b>Figure 66</b> DFT investigation of the borylation of <i>tert</i> -butylamine and <i>tert</i> -butylthiol.....	121
<b>Figure 67</b> Scope of the catalytic borylation of thiols and time required for full <sup>1</sup> H NMR conversion. .....	124
<b>Figure 68</b> Proposed mechanism for the FLP catalyzed borylation of thiol. ....	125
<b>Figure 69</b> Top: <sup>11</sup> B{ <sup>1</sup> H} NMR (160 MHz, CDCl <sub>3</sub> ) during the catalytic borylation of decanethiol. Bottom: <sup>11</sup> B NMR (160 MHz, CDCl <sub>3</sub> ) during the <b>3.3</b> catalyzed borylation of decanethiol. ....	126



<b>Figure 70</b> Top: $^{11}\text{B}\{^1\text{H}\}$ NMR (160 MHz, $\text{CDCl}_3$ ) during the catalytic borylation of <i>t</i> Bu-SH. Bottom: $^{11}\text{B}$ NMR (160 MHz, $\text{CDCl}_3$ ) during the <b>3.3</b> catalyzed borylation of <i>t</i> Bu-SH. ....	127
<b>Figure 71</b> Proposed potential catalytic cycle for a metal-free hydro-heteroelement addition reaction. .....	129
<b>Figure 72</b> Potential metal-free transfer borylation catalytic cycle. ....	136
<b>Figure 73</b> Thermodynamics of the transfer borylation reaction. ....	137
<b>Figure 74</b> Initial catalyst and boron source screening. ....	138
<b>Figure 75</b> Substrate scope of the <b>7.1</b> catalyzed transfer borylation. ....	141
<b>Figure 76</b> Proposed catalytic cycle of the 2-mercaptopyridine catalyzed transfer borylation. ....	143
<b>Figure 77</b> Potential hydrogenation catalytic cycle using auto-assembling FLP. ....	145
<b>Figure 78</b> Different type of potential C-H transfer borylation catalyst. ....	146
<b>Figure 79</b> Potential hydroaddition catalytic cycle using auto-assembling FLP. ....	147

## List of Schemes

<b>Scheme 1</b> Planned and tried synthesis of compound <b>2.1</b> .....	38
<b>Scheme 2</b> Synthesis of the lithiated precursors <b>2.8</b> and <b>2.9</b> for the synthesis of aminoboranes <b>2.2-2.7</b> .....	40
<b>Scheme 3</b> Synthesis of the various N/B FLPs. ....	41
<b>Scheme 4</b> Stoichiometric CO <sub>2</sub> hydrogenation by <b>2.2</b> and <b>2.4</b> .....	41
<b>Scheme 5</b> Summary of the experimental mechanistic investigation.....	42
<b>Scheme 6</b> DFT calculations on the reversibility of the <b>2.7</b> adducts with various CO <sub>2</sub> reduction products, HCOOH, H <sub>2</sub> O and MeOH. ....	46
<b>Scheme 7</b> Proposed sequence for the <b>2.11</b> catalyzed H/D scrambling between C <sub>6</sub> D <sub>6</sub> and H <sub>2</sub> . ....	49
<b>Scheme 8</b> General aminoborane synthesis reporter by the Ritter group. ....	63
<b>Scheme 9</b> <b>3.1</b> Synthesis (A) vs <b>3.3</b> synthesis (B). ....	64
<b>Scheme 10</b> Synthesis of <b>3.6-3.8</b> , fluoroborate analogue of <b>3.1</b> . ....	65
<b>Scheme 11</b> Structure of the targeted morpholino derivative.....	69
<b>Scheme 12</b> A) Synthesis of <b>3.9</b> B) synthesis of <b>3.10</b> . ....	71
<b>Scheme 13</b> Catalyst deactivation pathway while using more active hydroboranes as borylating reagent. ....	74
<b>Scheme 14</b> Deactivation pathway while using BH <sub>3</sub> as as borylating reagent.....	74
<b>Scheme 15</b> Synthesis of [NisoBu <sub>2</sub> -C <sub>6</sub> H <sub>10</sub> -BH <sub>2</sub> ] <sub>2</sub> ( <b>3.11</b> ). ....	76
<b>Scheme 16</b> Synthesis of N(pyrollidino)H-C <sub>6</sub> H <sub>10</sub> -BF <sub>3</sub> ( <b>3.12</b> ). ....	76
<b>Scheme 17</b> Retrosynthesis of [N(piperidine)-C <sub>6</sub> F <sub>4</sub> -BH <sub>2</sub> ] <sub>2</sub> and N(piperidine)(H)-C <sub>6</sub> F <sub>4</sub> -BF <sub>3</sub> . ....	77
<b>Scheme 18</b> Experimental results for the S <sub>N</sub> <sup>2</sup> reaction of <b>4.1</b> with different substrates. ....	96
<b>Scheme 19</b> Re-optimized synthesis of <b>4.1</b> . ....	98
<b>Scheme 20</b> Reaction of <b>4.1</b> with IMes and crystal structure of the compound formed. ....	101
<b>Scheme 21</b> Proposed reaction of <b>4.1</b> with NEt <sub>3</sub> •HCl. ....	101
<b>Scheme 22</b> Proposed products from the reaction of <b>4.1</b> with S <sub>8</sub> ( <b>4.10</b> ) and Se <sub>(s)</sub> ( <b>4.11</b> ). ....	102
<b>Scheme 23</b> Reactivity of a diborane with disulfide reported by the Himmel group. <sup>205</sup> ....	103
<b>Scheme 24</b> Synthesis of <b>5.1</b> . ....	104
<b>Scheme 25</b> Attempted synthesis of <b>5.3</b> . ....	105
<b>Scheme 26</b> Synthesis of <b>5.7</b> . ....	108
<b>Scheme 27</b> Alternative synthesis of <b>5.1</b> . ....	108
<b>Scheme 28</b> Reaction of <b>5.2</b> with PPh <sub>3</sub> •HBr forming <b>5.3</b> •PPh <sub>3</sub> and <b>5.4</b> after mild heating. ....	110
<b>Scheme 29</b> Synthesis of <b>5.3</b> •Pyridine. ....	111
<b>Scheme 30</b> Reactivity of <b>5.3</b> •Pyridine upon heating. ....	112
<b>Scheme 31</b> Formation of species <b>5.9</b> from <b>3.9</b> . ....	115
<b>Scheme 32</b> Small changes, divergent outcome. ....	118
<b>Scheme 33</b> Stoichiometric reactions between <b>3.3</b> and <i>tert</i> -butanol, <i>tert</i> -butylamine and <i>tert</i> -butylthiol. ....	122
<b>Scheme 34</b> One-pot Michael addition of 4-methylthiophenol on 4-phenyl-3-buten-2-one through catalytic borylation. ....	128
<b>Scheme 35</b> Attempted catalytic thioaddition on α,β-unsaturated ketones (A) and carboboration (B). ....	130
<b>Scheme 36</b> Examples of isodesmic reactions. ....	133
<b>Scheme 37</b> Different synthesis of phenylboronic acid. ....	134
<b>Scheme 38</b> Synthesis of various borylating reagent. ....	135

**Scheme 39** A) Example of the reactivity of Se-B bond with ynone. B) Example of the reactivity of B-N bond with isocyanate. .... 148

## List of Tables

<b>Table 1</b> Half-life reaction times function of the TS energy and of the temperature.....	32
<b>Table 2</b> Computed binding energies of small molecules by a TMP-C <sub>6</sub> H <sub>4</sub> -BF <sub>2</sub> FLP.....	66
<b>Table 3</b> Yield comparison for representative substrates using <b>3.1</b> and <b>3.7</b> .....	67
<b>Table 4</b> DFT calculated $\Delta G$ (kcal/mol) of amino-hydroboranes bearing different amine substituents in different dimeric form and $\Delta G^\ddagger$ (kcal/mol) of the C-H bond cleavage transition state for <i>N</i> -methylpyrrole and thiophene.....	70
<b>Table 5</b> Alkyne hydrogenation results.....	82
<b>Table 6</b> VT <sup>1</sup> H NMR data of the equilibrium between <b>3.3</b> and <b>3.3*</b> .....	89
<b>Table 7</b> DFT calculated relative B-H bond strength.....	97
<b>Table 8</b> The <sup>11</sup> B NMR shifts of the various diborane species synthesized.....	99
<b>Table 9</b> Optimization of the borylation of thiophenol catalyzed by <b>3.3</b> .....	122
<b>Table 10</b> Condition screening of the C-H transfer borylation reaction.....	139

## List of Abbreviations

BBN = 9-Borabicyclo[3.3.1]nonane or 9-Borabicyclo[3.3.1]nonyl  
DFT = Density functional theory  
DME = 1,2-Dimethoxyethane  
Dur' = 2,4,5,-Trimethylphenyl  
e-CO<sub>2</sub> = equivalents of CO<sub>2</sub>  
*e.g.* = *exempli gratia*, which means for example  
equiv. = equivalents  
FLP = Frustrated Lewis pair  
GWP = Global warming potential  
Pin = Pinacol  
ICH = International Council for Harmonisation of Technical Requirements for Pharmaceuticals for Human Use  
IMes = 1,3-Dimesitylimidazol-2-ylidene  
Me = Methyl  
Mes = Mesityl, or 2,4,6,-Trimethylphenyl  
NMR = Nuclear magnetic resonance  
Ph = Phenyl  
SMD = Solvation model based on density  
*t*Bu = *tert*-butyl  
THF = Tetrahydrofuran  
TMP = 2,2,6,6-Tetramethylpiperidine  
TMSBr = Bromotrimethylsilane  
TMSCl = Chlorotrimethylsilane  
TS = Transition state  
US EPA = United States Environmental Protection Agency  
USP = United States Pharmacopeial Convention  
UV-Vis = Ultraviolet and visible  
VT NMR = Nuclear magnetic resonance spectroscopy at variable temperature  
 $\Delta G$  = Difference in free energy  
 $\Delta G^\ddagger$  = Difference in free energy for a transition state  
 $\Delta H$  = Difference in enthalpy  
 $\Delta H^\ddagger$  = Difference in enthalpy for a transition state  
 $\Delta S$  = Difference in entropy  
 $\Delta S^\ddagger$  = Difference in entropy for a transition state

## Remerciements

Cette thèse n'aurait jamais vu le jour sans l'aide d'un nombre incalculable de personnes et j'aimerais profiter de l'occasion pour souligner l'impact que quelques-unes d'entre elles ont eu dans mon cheminement à la maîtrise, puis au doctorat. Évidemment, il est impossible de souligner la contribution de tous, mais sachez que grande ou petite, toute l'aide que vous avez pu m'apporter a été grandement appréciée.

Tout d'abord j'aimerais remercier infiniment Claudia, ma partenaire de vie depuis le début de nos études. Avoir quelqu'un à ses côtés qui nous comprend est absolument inestimable et je ne sais honnêtement pas comment j'aurais pu passer à travers mon doctorat sans ton aide. J'espère sincèrement pouvoir t'aider autant que tu as pu le faire pour moi à terminer le tien et que nous écrivons ensuite plusieurs autres chapitres de nos vies ensemble.

J'aimerais également remercier mes mentors, lors de mes débuts dans le groupe Fontaine, Marc-André Courtemanche et Marc-André Légaré. Comme le dit le dicton : «Un Marc-André c'est bien, mais deux c'est mieux.» Vous m'avez appris bien plus que vous pouvez le croire et mes moments avec vous ont certainement été parmi les plus heureux de mon doctorat. J'aimerais aussi remercier plus particulièrement Julien Légaré Lavergne, Nicolas Bouchard et Hugo Boutin avec qui j'ai collaboré étroitement pour bon nombre des travaux présentés dans la thèse. Un énorme merci à vous pour l'aide que vous avez apporté aux travaux, mais également pour tous les bons moments à l'extérieur du laboratoire. À ce sujet je voudrais également remercier les autres personnes ayant séjourné avec moi dans le groupe Fontaine au fil des ans, Ambreen Mushtaq, Maria Zakharova, Yimu Hu, Luis Misal, Théo Rongère, Thomas Bossé-Demers, ainsi que toutes les autres que j'ai côtoyées pendant c'est cinq années. Un énorme merci, pour votre présence et votre bonne humeur et je vous souhaite de réussir tout ce que vous entreprendrez dans le futur. Un merci tout spécial également au Pr. Paul Chirik et aux membres de son groupe pour m'avoir accueilli parmi eux lors de la session d'automne 2017.

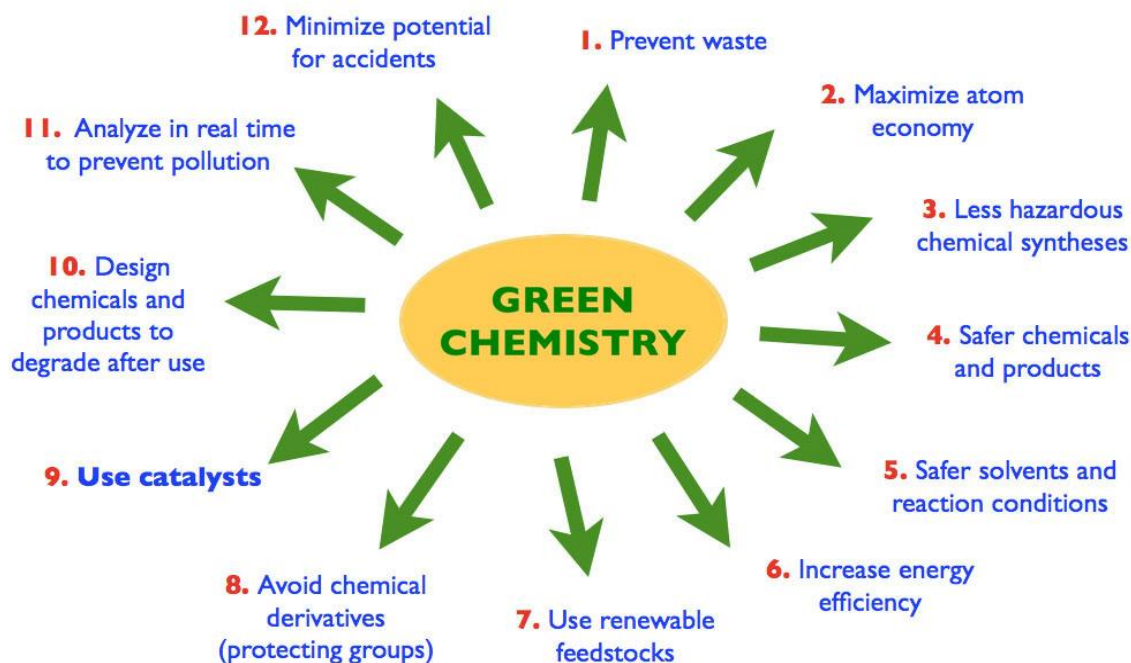
J'aimerais également remercier le personnel de soutien du département de chimie de l'Université Laval, particulièrement Pierre Audet, Christian Côté et Mélanie Tremblay, qui travaille souvent dans l'ombre et à qui on devrait sans aucun doute dire merci plus souvent. Merci également au corps professoral pour leurs commentaires et conseils, et un merci particulier à M. Dang pour m'avoir permis de suivre les cours nécessaires à l'obtention de mon diplôme.

Finalement, j'aimerais bien évidemment remercier mon directeur de recherche Pr. Frédéric-Georges Fontaine, tout d'abord pour avoir accepté de demander avec moi une bourse CRSNG maîtrise à une semaine de la date limite il y a de cela cinq ans, puis pour m'avoir continuellement encouragé et supporté pendant les cinq dernières années.

## Introduction

### *Green Chemistry*

The term “green chemistry” was first introduced in the early 1990’s by Dr. Paul T. Anastas while working at the United States Environmental Protection Agency (US EPA) and certainly gained much of its momentum with the publication of its twelve principles in 1998 (**Figure 1**).<sup>1</sup> Twenty years later, with growing environmental concern of the general population, green chemistry is stronger than ever. The conceptual simplicity of some of its principles (*e.g.* the atom economy) and the many real world successful examples of its application makes it easy to grasp for students and certainly helped it to be taught in the undergraduate chemistry curriculum. Moreover, thanks to its usual alignment with economic priorities, it avoided detractors from industry. However, this positive attention turned green chemistry into a “buzzword” and it is now often used for marketing purposes instead of a tool to improve chemical processes.<sup>2</sup> To make things worse, calculating the “greenness” of reactions or processes is far from being an easy task. Whereas industry is forced by regulation<sup>3</sup> to invest the time and resources to carefully measure the ecological impact of large scale processes, the reality in academia is very different. The plurality and complexity of metrics created a landscape where a new reaction is often claimed “green” if any of the twelve principles is improved.



**Figure 1** The twelve principles of green chemistry.<sup>4</sup>

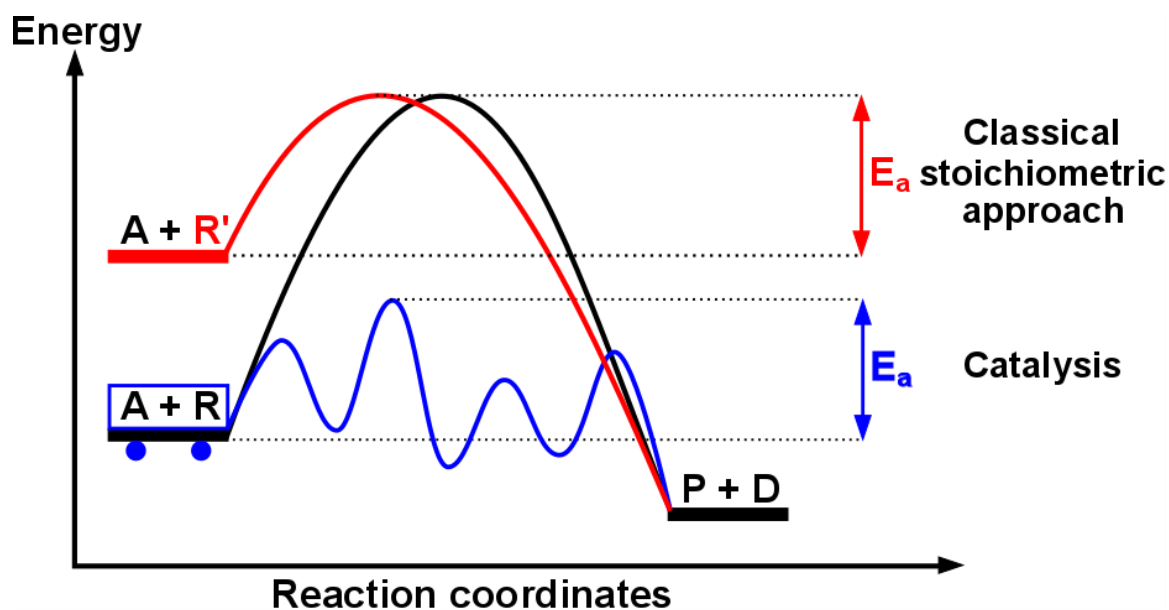
Metrics can be very simple, such as reaction yield or atom economy.<sup>5</sup> Such parameters are very easy to calculate, but do not include many crucial aspects of green chemistry, such as solvent and hazardous materials used or energy input. More accurate metrics such as the E-factor<sup>6</sup> and Eco-scale<sup>7,8</sup> fixed those problems to some extent, but in the same time made the calculation of the “greenness” of a process more complex (and sometimes arguably biased). In short, the E factor is the ratio of waste generated per kg of product (in which a subjective “environmental quotient” can be used to adjust for the “dirtiness” of the waste) and the Eco-scale is a scoring method (from 100-0) that gives penalty (once again quite subjective) according to yield, safety, technical setup, temperature/time, workup and purification. Moreover, the E factor, being a ratio per mass unit of product, will be lower for massive molecules compared to light ones, especially if a massive “useless” group, such as solubilizing chains, are attached in a benign and wasteless manner. Thus, using it to compare the greenness of processes forming different products is unadvisable. However, it is fair to say that because green chemistry usually takes for granted the target legitimacy, green chemistry metrics are mostly used to compare methods that lead to the same target.

In sum, the current green chemistry metrics are still far from perfect, but are nevertheless useful. Maybe the future developments of computer assisted chemistry, by assessing important challenges such as giving a score to molecule complexity and by allowing faster synthetic pathway comparisons,<sup>9</sup> will help in the development of better green chemistry metrics that are able to take into account more accurately and objectively the entire chemical process, including the target choice and its end of life. This could make possible a green by design approach instead of the current greening one. However, one thing that is certain, the history of green chemistry is far from over.



## Catalysis

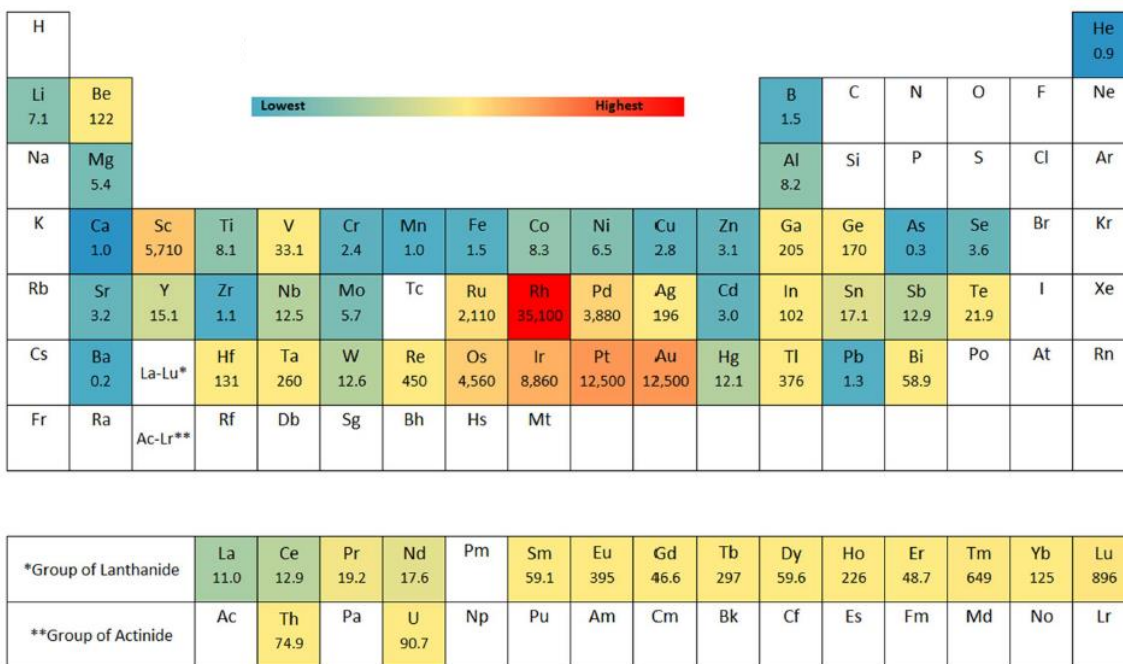
Catalysis is undoubtedly key in the development of greener reactions and processes. However, I think the reasons why catalysis is a part of the green chemistry principles is not so obvious and often misunderstood. In an ideal general chemical reaction,  $A + B \rightarrow C$ , all of the atoms contained in A and B end up in C and no waste is produced. Adding another molecule, including a catalyst, reduces the efficiency of the reaction. The power of catalysis arises from the fact that this type of ideal reaction is extremely rare. A green process requires using renewable or safer starting materials and produce fewer waste while using less energy. However, safe reagents are usually not very reactive, which leads to higher temperature requirements or the necessity to somehow activate the reagent. It is in that regard that catalysis is useful. It is much better to use a very small amount of a catalyst that is regenerated every cycle than a stoichiometric activator. In other words, it is not adding a catalyst to a reaction that makes it green, but catalysis allows greener transformations to take place.



**Figure 2** Energy profile of a catalytic reaction versus a stoichiometric one.

Another often neglected aspect of catalysis when it comes to green chemistry is the catalyst itself. It is usually better to use a catalytic amount of an additive compared to a stoichiometric amount of it because it produces less waste. However, if a catalytic additive, or the waste generated from it, is highly toxic, if the catalyst is hazardous or simply if the catalyst synthesis or its utilization requires a lot of energy and/or generate a lot of waste, it may counter balance the gain it procures by allowing greener synthetic pathways. Thus, the design of greener catalysts, and not only of greener reactions, is also of interest.

Looking objectively at the possibilities catalysis is now offering, one can only be in awe at the tremendous diversity of reactions that can be performed, often in an extremely selective and convenient fashion. While the most popular catalysts contribute at making chemical processes greener, one is forced to admit that the field is overwhelmingly dominated by second and third row transition metals, which are some of the most energetically demanding elements to extract. It has been estimated that the global warming potential (GWP) for the production of 1 kg of palladium is 3,880 kg equivalents of CO<sub>2</sub> (e-CO<sub>2</sub>).<sup>10</sup> For example, palladium catalysts are ubiquitous in C-C bond forming reactions such as the Heck,<sup>11–13</sup> Suzuki-Miyaura<sup>14,15</sup> and Sonogashira<sup>16–18</sup> cross-couplings as well as in C–N cross-couplings such as the Buchwald-Hartwig amination.<sup>19,20</sup> Similarly, other important pharmaceutical reactions such as the asymmetric hydrogenations are typically conducted with rhodium,<sup>21,22</sup> ruthenium (Noyori hydrogenation)<sup>23</sup>, and sometimes iridium<sup>24,25</sup> catalysts with respective GWP/kg of 35,100, 2,110 and 8,860 kg e-CO<sub>2</sub>.<sup>10</sup> In addition to their high cost, other arguments promoting a transition away from precious metal catalysts also include the potential depletion of their reserves, their sometimes important and sudden price variation which can lead to supply problems, and the requirement to remove traces of these metals in the final products (sometimes via tedious and costly procedures) in order to meet regulations such as those set by the United States Pharmacopeial Convention (USP) and the International Council for Harmonisation of Technical Requirements for Pharmaceuticals for Human Use (ICH).<sup>26,27</sup>



**Figure 3** GWP/kg, in e-CO<sub>2</sub> of various elements.<sup>10</sup>

In that context, it is not so surprising that in the last decades, a lot of efforts has been invested (particularly in academia, but now more and more from industry) in the development of alternatives.<sup>28</sup> First row transition metal catalysts using elements such as Fe, Co, Ni, Cu have received much of recent attention, have much more abundant reserves and are much less economically and environmentally costly to extract (their GWP/kg are all under 10 kg e-CO<sub>2</sub>). Many success stories came out from those efforts and describing them all is certainly out of the scope of the thesis. A very general and important conclusion generally still comes out of those studies: first row transition metals do not behave as second and third row transition metals do.<sup>29</sup> The mechanisms of first row transition metal catalyzed transformations are often new and unexpected and mimicking classical mechanisms (of second and third row transition metal catalysts) with a first row transition metal catalyst is often much harder than it may seem. That is of course great for academic researchers since it brings up a lot of questions leading to many publications. But more importantly, sometimes it also leads to the discovery of orthogonal reactivity, opening new synthetic pathways and giving more value to those new catalysts than if they were simply cheaper alternatives.

## ***Frustrated Lewis Pairs***

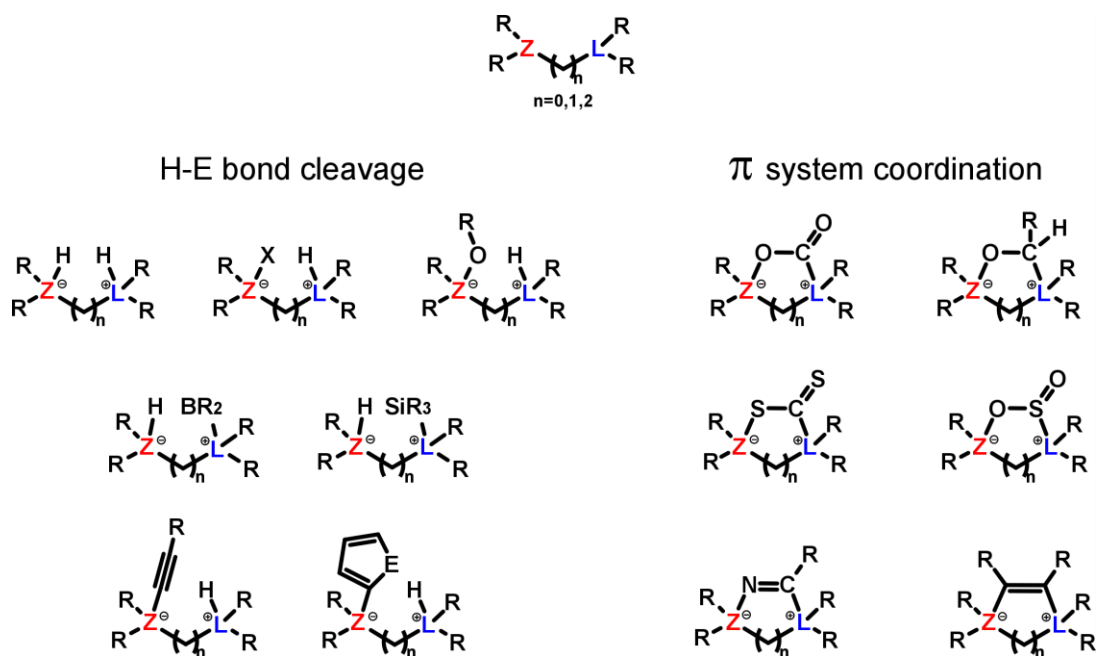
Another possible alternative to precious metal catalysts that is certainly more relevant to the thesis are metal-free catalysts. For most chemists, metal-free catalysis resonates more with classical organic chemistry than with organometallic chemistry. Indeed, important classes of metal-free catalysts include acids,<sup>30</sup> bases,<sup>31</sup> phase-transfer catalysts,<sup>32</sup> and hydrogen bonding catalysts.<sup>33</sup> They are usually used in “classic” organic reactions such as Diels-Alder,<sup>34</sup> Michael additions<sup>35</sup> and Mannich reactions,<sup>36</sup> often to render them asymmetric.<sup>37,38</sup> However, the discovery, in 2006, of the heterolytic cleavage of molecular hydrogen by the combination of a sterically hindered Lewis acid and Lewis base, later named frustrated Lewis pair (FLP), opened up the way to a new class of metal-free catalysts, able to perform reactions that were thought exclusive to transition metals, such as the catalytic hydrogenation.<sup>39</sup>

After more than a decade of developments, FLP chemistry exhibits an impressive array of reactivity. However, quite surprisingly, the definition of FLP escapes consensus and a recent review on the concept of FLP even concludes: «*an all-encompassing definition of the term ‘frustrated Lewis pair’ remains elusive*». <sup>40</sup> Thus, I guess that since even the field leaders fell short, defining FLP is out of the thesis scope. Nevertheless, I think that a short discussion on why this definition is so elusive is necessary. First of all, the Lewis definition of an acid and a base<sup>41</sup> (a Lewis acid is an electron pair acceptor and a Lewis base an electron pair donor) is formally extremely inclusive. For example the proton, key to other acid/base definitions such as the Brønsted one (an acid is a proton donor and a base a proton acceptor) can also be described as a Lewis acid and other compounds, such as boranes, that can accept an electron pair but cannot give a proton are also included in the Lewis definition of an acid, while they are excluded of the Brønsted one. Over the years, probably because initial acid/base chemistry teaching mostly focuses on aqueous chemistry which can be more easily visually represented and understood using the Brønsted definition, the Lewis acid, at least I think in most chemist minds, started to refer only to the subgroup of acids which cannot be described by the Brønsted definition. That very important distortion between the general perception and the formal definition of a Lewis acid certainly complicates the formulation of a general and accurate definition of FLPs, but it is only the tip of the iceberg.

The most challenging part in defining a FLP certainly resides in choosing the goal of the definition. In most people’s mind a definition only serves at clarifying a concept, but for a new one, it might have the opposite effect. A good definition helps understanding and promoting an idea and it helps to promote new research to prove that concept. In that sense, to be useful a definition must be inclusive enough to foster new ideas while avoiding being too general, which blurs the boundaries and

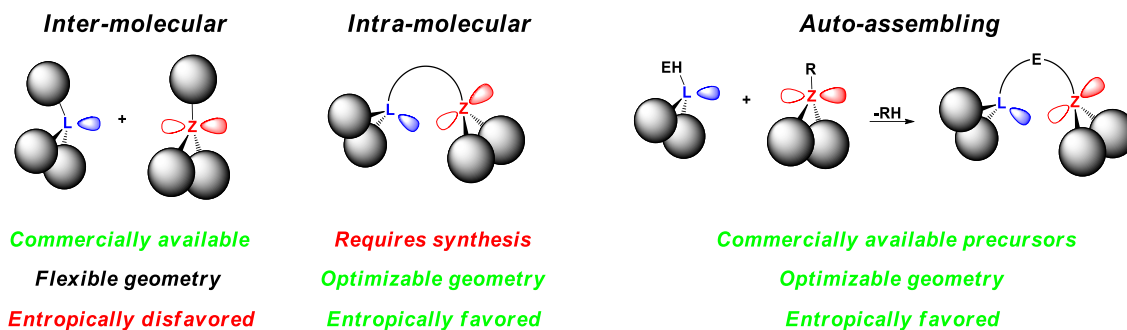
eventually make it less useful. This is why I think the initial tentative definitions of a FLP miserably failed and are no longer used by the leaders in the field. The most poignant example is certainly the definition still promoted by a popular online encyclopedia: “A frustrated Lewis pair is a compound or mixture containing a Lewis acid and a Lewis base that, because of steric hindrance, cannot combine to form a classical adduct.”<sup>42</sup> That definition is simple and easy to understand. However, it is far from useful and may even be misleading. The formation or absence of formation of a Lewis adduct does not help predicting the reactivity of a FLP. Using weak Lewis acids and bases, adduct formation can be prevented by minimal steric hindrance, but that rarely translates to interesting chemistry. Moreover, many important breakthroughs in FLP chemistry, some of which will be described in the thesis, have been made using compounds forming a Lewis adduct in their resting state. I would personally define a FLP as: *a compound or mixture of compounds that uses both Lewis acid and Lewis base functionalities to access a chemical transformation inaccessible using only one or the other*. I believe this definition could foster new ideas and it includes most FLP chemistry reported today. However, it defines FLPs not directly as a compound but as a tool to new reactivity, defined by its function rather than its composition, making it harder to grasp and manipulate. That definition also requires the presence of chemical reactivity and mechanistic understanding of the transformation. I think that would be good for the field in general, but may limit its reach and reduce the number of studies referring to FLPs, which is currently a buzzword. In today’s research context, the citation count more for some people than the quest to improve understanding. Anyway, despite (or maybe thanks to) the lack of a unanimous definition for FLPs, the field certainly thrived in the last decade. Many recent reviews provide a quite comprehensive view of the current possibilities offered by FLP.<sup>43-54</sup> I do not think including yet another one in the introduction of my thesis would be of much use, but a brief summary is certainly important for readers not familiar to the field. A brief history of FLP will also be presented at the end of that section.

In summary, the FLP reactivity can be separated in two major classes, the cleavage of H-E bonds (polar as well as non-polar) and the coordination to  $\pi$  systems (**Figure 4**). The two most prominent examples that helped popularize FLP are the reversible gas uptake, including hydrogen storage as well as CO<sub>2</sub> and other greenhouse gases capture, and the heterolytic H-H bond cleavage which paved the way for metal-free FLP promoted catalytic hydrogenation. The more recent examples taking advantage of C-H bond cleavage for the functionalization of heteroarenes will be discussed in more details later in the thesis.



**Figure 4** Classical FLP reactivity.

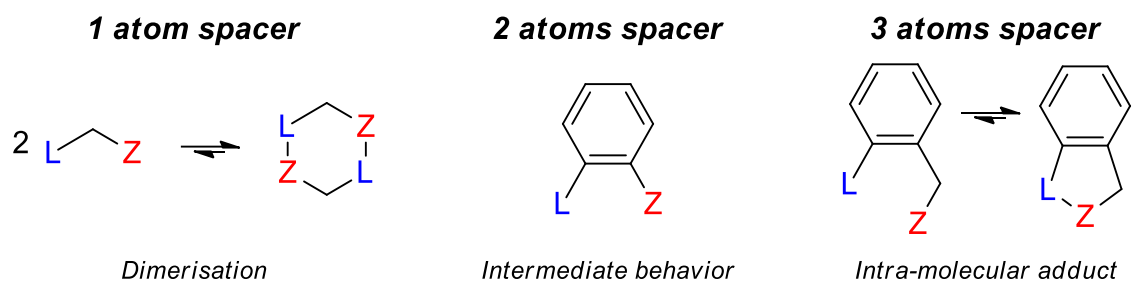
One of the advantages of FLPs, for academic studies in particular, include their high modularity. The reactivity is mostly dictated by the nature of the Lewis acid (Z), the nature of the Lewis base (L) and by their relative position in space. The substituents on the FLP will influence their acidity, basicity and ability to interact with each other and with a substrate. This brings up the important distinction between inter-molecular and intra-molecular FLP. As their name strongly suggest, an inter-molecular FLP will be composed of two independent molecules, the Lewis acid and the Lewis base, while an intra-molecular FLP has the Lewis acid and the Lewis base attached together by a spacer or backbone (**Figure 5**). The major advantage of inter-molecular FLPs is the broad diversity of commercially available Lewis acids and Lewis bases, which allows fast and easy screening of many possible combinations, making optimization easier. On the other hand, intra-molecular FLPs usually require some synthetic efforts, but open up the possibility of adjusting geometrical factors in order to prevent Lewis adduct formation, favor substrate interaction and reduce the entropic penalty in key transition states or intermediates, which often translates in increased activity. Finally, auto-assembling FLP, combining the advantages of inter- and intra-molecular FLP are possible, an example will be discussed in Chapter 7.



**Figure 5** Advantages and disadvantages of inter-molecular, intra-molecular and auto-assembling FLP.

More than a decade into FLP development, it is not surprising that the most interesting chemistry using inter-molecular FLP has been investigated, in particular using commercially available Lewis acids, bases and substrates. Today, most “novelty” in this field is now mostly limited in showcasing examples of new Lewis acids finely controlling steric bulk and acidity,<sup>55,56</sup> and the use of the common Lewis acid, mostly  $B(C_6F_5)_3$ , to promote reactions on complex pre-organized substrate.<sup>57</sup> On the other hand, the development of intra-molecular FLPs, probably because it requires more complex synthesis, has certainly lagged behind, but it is now getting up to speed and most interesting new developments in FLP chemistry are coming from these systems. Of crucial importance to intra-molecular FLP reactivity is the spacer or backbone. Its effect on reactivity is quite hard to predict, compared to increasing the bulk or the “strength” of the acid and basic moieties, and changing its structure often requires complete redesign of the synthetic pathway. On the other hand, using a new backbone may result in accessing completely new reactivity. The geometry affects the resting state by disfavoring adduct formation by geometrical constraints, making these FLPs potentially more reactive and - transition states more accessible since a well pre-organized FLP will reduce the entropic penalty. Many different types of backbones exist and are mostly carbon based, but can contain heteroatoms for controlling the geometrical parameters or facilitate synthesis.

The spacers are sometimes more rigid (aromatic ring) and sometimes more flexible (aliphatic chain) or a combination of both, spacing the acidic and basic moieties by one, two, three atoms or more. The number of atoms spacing the acidic and basic moieties and the flexibility of the spacer will greatly influence the resting state of the FLP. When using one atom spacer, great care should be taken in the design to avoid dimerization since 6-membered rings containing two Lewis adducts can form easily.<sup>58-60</sup> In the case of a three atoms spacer, the formation of an intra-molecular 5-membered ring is usually the major concern.<sup>61-64</sup> Backbones containing two atoms are a compromise and can adopt very different geometries depending on the substituents. The possibilities will be discussed in more detail in the thesis.



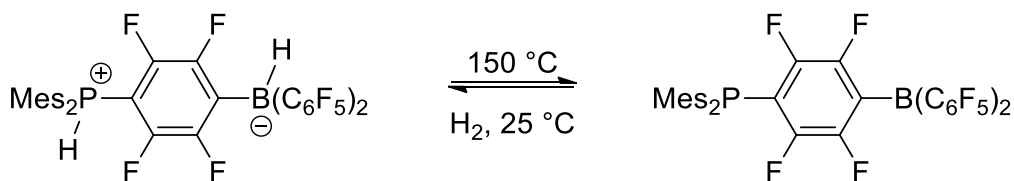
**Figure 6** Major “deactivation” pathways in intra-molecular FLP depending on the spacer.

### *A Brief History of FLP*

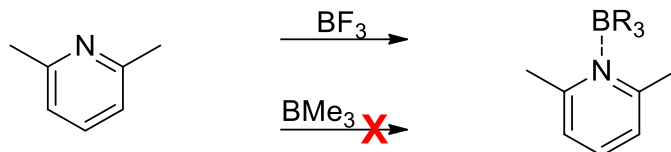
For most researchers in the field, FLPs started with the discovery of the molecular hydrogen splitting by a sterically hindered phosphinoborane in 2006 (**Figure 7 A**).<sup>39</sup> It is certainly true in the sense that it is this publication that brought attention to this chemistry, but as it is often the case when something gets popular and people go back in literature, earlier examples of what might be described as a FLP behavior can be found. Notably, Brown and co-workers made the interesting observation in 1942 that lutidine forms a Lewis adduct when combined with trifluoroborane (BF<sub>3</sub>), but does not with trimethylborane (BMe<sub>3</sub>). They even attributed this lack of reactivity between lutidine and BMe<sub>3</sub> to steric congestion.<sup>65</sup> In 1959, Benz and Wittig reported the reactivity of benzyne in presence of both PPh<sub>3</sub> and BPh<sub>3</sub>.<sup>66</sup> Finally, the closest example is certainly the report of Piers and co-workers in 2003 on the reactivity of aminoboranes with water and HCl in which they conclude: «*The basicity of the nitrogen center in an aminoborane would have to be significantly higher in order to thermodynamically favor the formation of a dihydrogen adduct over the elimination of hydrogen in the reaction.*»<sup>67</sup>



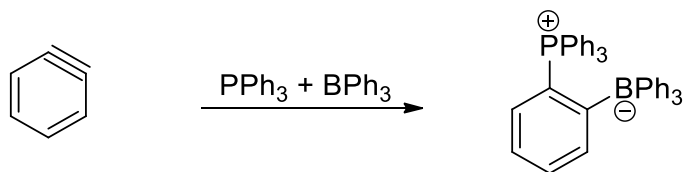
**A) Stephan 2006**



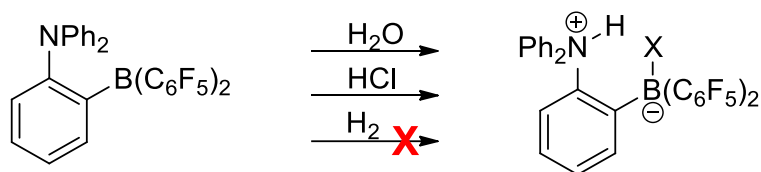
**B) Brown 1942**



**C) Benz and Wittig 1959**



**D) Piers 2003**



**Figure 7** Early examples of FLP chemistry.

After 2006, the number of reports concerning FLP chemistry raised quickly, with the Stephan and Erker groups leading the way. The first report of a FLP  $\text{CO}_2$  adduct,<sup>68</sup> of the cleavage of a  $\text{Csp-H}$ <sup>69</sup> bond and of catalytic imine<sup>70</sup> and enamine<sup>71</sup> hydrogenation, to only name a few transformations, were all published before 2010.

### ***Details on the thesis content***

After the introduction and methodology section, Chapter 2 of the thesis discusses of metal-free CO<sub>2</sub> reduction, with a focus on its hydrogenation. This project can be considered as the follow-up of the CO<sub>2</sub> hydroboration project that was at the core of my mentors' (Marc-André Courtemanche and Marc-André Légaré) thesis. The work presented in it was mostly performed under Marc-André Courtemanche supervision and was published in two papers:

Courtemanche, M.-A.; Pulis, A. P.; Rochette, É.; Légaré, M.-A.; Stephan, D. W.; Fontaine, F.-G. Intramolecular B/N Frustrated Lewis Pairs and the Hydrogenation of Carbon Dioxide. *Chem. Commun.* **2015**, *51*, 9797–9800.

Rochette, É.; Courtemanche, M.-A.; Pulis, A.; Bi, W.; Fontaine, F.-G. Ambiphilic Frustrated Lewis Pair Exhibiting High Robustness and Reversible Water Activation: Towards the Metal-Free Hydrogenation of Carbon Dioxide. *Molecules* **2015**, *20*, 11902–11914.

Chapter 3 discusses of metal-free C-H activation and catalytic borylation of heteroarenes, the initial discovery and the improvements made on the system afterward. This work was performed on an approximately 3-4 years span. Initially, the project was led by Marc-André Légaré, toward the end of his Ph.D., but along the years many people contributed to it: Marc-André Courtemanche, Julien Légaré Lavergne, Nicolas Bouchard, Luis Misal Castro and Arumugam Jayaraman. The content of three papers is discussed:

Légaré, M.-A.; Courtemanche, M.-A.; Rochette, É.; Fontaine, F.-G. Metal-Free Catalytic C-H Bond Activation and Borylation of Heteroarenes. *Science* **2015**, *349*, 513–516.

Légaré, M.-A.; Rochette, É.; Légaré-Lavergne, J.; Bouchard, N.; Fontaine, F.-G. Bench-Stable Frustrated Lewis Pair Chemistry: Fluoroborate Salts as Precatalysts for the C-H Borylation of Heteroarenes. *Chem. Commun.* **2016**, *52*, 5387–5390.

Légaré Lavergne, J.; Jayaraman, A.; Misal Castro, L. C.; Rochette, É.; Fontaine, F. G. Metal-Free Borylation of Heteroarenes Using Ambiphilic Aminoboranes: On the Importance of Sterics in Frustrated Lewis Pair C-H Bond Activation. *J. Am. Chem. Soc.* **2017**, *139*, 14714–14723.

Chapter 4 discusses of the discovery of an unusual rearrangement I discovered while studying aminohydroborane, the spontaneous formation of a B-B bond and of the reactivity of the diborane formed. The work contained in the first part of the chapter, the discovery and description of the rearrangement, was performed with the help of Nicolas Bouchard and Julien Légaré Lavergne and was published:

Rochette, É.; Bouchard, N.; Légaré Lavergne, J.; Matta, C. F.; Fontaine, F. G. Spontaneous Reduction of a Hydroborane To Generate a B-B Single Bond by the Use of a Lewis Pair. *Angew. Chem. Int. Ed.* **2016**, *55*, 12722–12726.

The second section of the chapter, the reactivity of the diborane is still an ongoing project to which nobody is currently assigned.

Chapter 5 discusses of another rearrangement I discovered while studying aminohydroborane, the intramolecular cleavage of a Csp<sup>3</sup>-H bond. The work presented in the first section was published:

Rochette, É.; Courtemanche, M. A.; Fontaine, F. G. Frustrated Lewis Pair Mediated Csp<sup>3</sup>-H Activation. *Chem. Eur. J.* **2017**, *23*, 3567–3571.

Later, the work was found to be very helpful in understanding the thermal behavior of a closely related species. This study is also discussed in the chapter, but was not published.

Chapter 6 discusses of catalytic S-H bond borylation and of the use of the similarity between this reaction and the C-H borylation to better understand their mechanism. This work was performed in close collaboration with Hugo Boutin and was published:

Rochette, É.; Boutin, H.; Fontaine, F. G. Frustrated Lewis Pair Catalyzed S-H Bond Borylation. *Organometallics* **2017**, *36*, 2870–2876.

Finally, Chapter 7 discusses of the potential of a new approach to C-H borylation, transfer borylation and of its proof of concept using 2-mercaptopyridine as catalyst. The project is still ongoing, but the initial results were published on the pre-print server ChemRxiv:

Rochette, É.; Fontaine, F.-G. Isodesmic C-H Borylation: Perspectives and Proof of Concept of Transfer Borylation Catalysis, **2018**. ChemRxiv. Preprint.

## ***Literature overview of subjects discussed in the thesis***

### *CO<sub>2</sub> reduction*

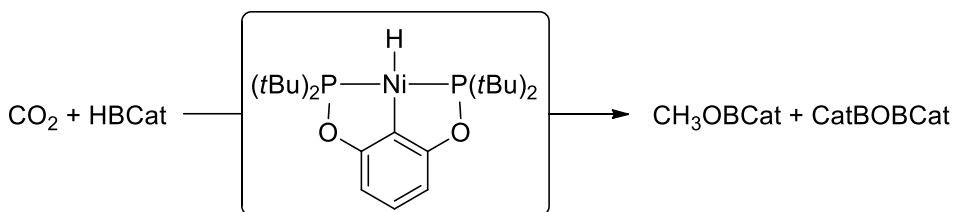
CO<sub>2</sub> is well known because of its raising concentration in the atmosphere and its contribution to global warming and climate change.<sup>72</sup> The glamorous hype associated with trying to solve such an important problem, and more importantly the easiness to get funding to do so, motivated many researchers to look for potential solutions. Using CO<sub>2</sub> as a chemical feedstock is one of them and among that sub-field of options, converting CO<sub>2</sub> to methanol in order to use it as an energy vector is certainly the most popular. It was even promoted by George A. Olah, Nobel laureate in 1994 for his unrelated work on carbocation chemistry.<sup>73</sup>

At the moment, methanol is mostly produced from methane through syngas, which is currently the most cost efficient process, but it is obviously not sustainable. It is possible to produce methanol by reducing CO<sub>2</sub> using different reductants such as hydroboranes, hydrosilanes, or ideally molecular hydrogen produced in a sustainable manner from a renewable source. Considering the simplicity of the reagents and products, and the potential scale of such an operation, heterogeneous catalysis (ideally composed from earth abundant elements) is certainly the most logical candidate and Cu/ZnO/Al<sub>2</sub>O<sub>3</sub> catalysts are indeed what is used at the George Olah CO<sub>2</sub> renewable methanol plant, which opened in 2012.<sup>74</sup> However, that did not stop academic researchers to study homogenous catalysts for that transformation and since the first chapter of the thesis is dedicated to such an example, here are some highlights in the field to give the reader some perspective into the work presented at the time out the work presented was carried. More comprehensive reviews are available for the interested reader.<sup>74,75</sup>

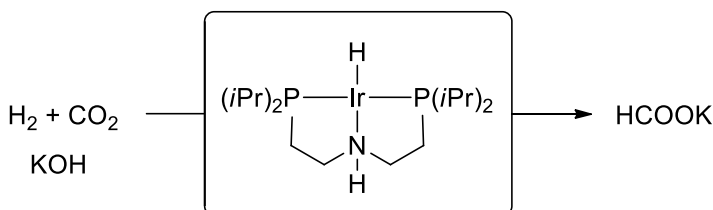
Even using transition metal catalysts, the reduction of CO<sub>2</sub> is not an easy task and often some “tricks” are required to obtain catalysis. Among the most interesting examples is the system reported by Guan *et al.* in 2010 using a nickel hydride pincer complex to promote CO<sub>2</sub> reduction.<sup>76</sup> They were able to promote the reduction to the methoxide using a hydroborane as a reductant. Boranes and silanes are quite reactive reducing agents and make the CO<sub>2</sub> reduction thermodynamically very favorable. Hence, it is a great way to get reactivity, but their utilization to produce methanol is obviously not profitable since boranes and silanes are way more costly than methanol. In 2011 Hazari *et al.* were able to reduce CO<sub>2</sub> using molecular hydrogen, but only to formate, which they were able to trap with an inorganic base (KOH) in order to allow catalysis.<sup>77</sup> This system is interesting since they use an ambiphilic activation of CO<sub>2</sub> for the reduction, which will be described partly in Chapter 2. Some more catalysts were more recently reported for hydrogenation of CO<sub>2</sub> to methanol, including the report by Sanford

*et al.* using a combination of three catalyst.<sup>78</sup> Some other examples exist, but the reaction remains quite challenging.<sup>79</sup>

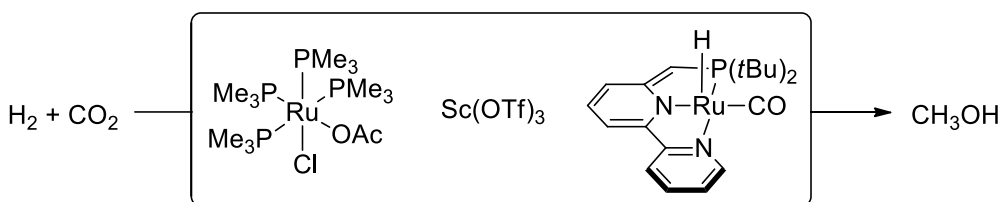
**Guan 2010**



**Hazari 2011**



**Sandford 2011**

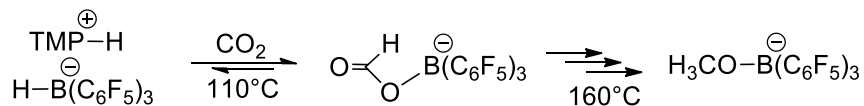


**Figure 8** Transition metal catalyzed reduction of  $\text{CO}_2$ .

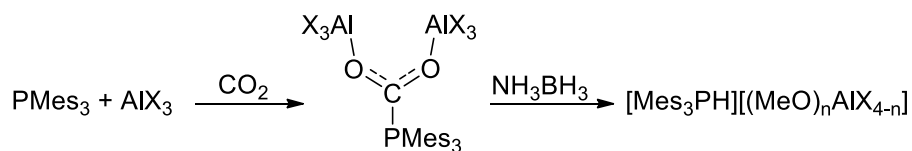
The examples from metal free chemistry are certainly more limited. Nevertheless some precedents existed. After few reports of  $\text{CO}_2$  adducts with FLPs,<sup>80</sup> Ashley *et al.* reported in 2009 the sub-stoichiometric reduction of  $\text{CO}_2$  to methoxy derivatives using the hydrogen adduct of TMP and BCF.<sup>81</sup> Not long after, Stephan *et al.* reported the stoichiometric reduction using ammonia borane and a phosphorus aluminum Lewis pair.<sup>82</sup> The first examples of catalytic reduction by metal-free processes, using silanes as reducing agents, were made by Piers in 2010 and Ying in 2009 using as catalysts the combination of TMP and BCF<sup>83</sup> and N-heterocyclic carbene<sup>84</sup>, respectively. However, in both cases the number of turn-overs was quite low and the rate very slow. Finally, in 2013, Fontaine *et al.* reported the catalytic hydroboration of  $\text{CO}_2$  using a phosphorus boron Lewis pair<sup>85</sup> and later showed that the active species was in fact a formaldehyde adduct of that Lewis pair.<sup>86</sup> What was surprising was the efficiency of the catalytic system, which exhibited TOF of  $973 \text{ h}^{-1}$ , surpassing the best metallic system for the hydroboration of  $\text{CO}_2$  at the time, which was the system reported by

Guan, as explained above. Since then several other metal-free processes have been developed using similar concepts, as it has been recently reviewed.<sup>75</sup>

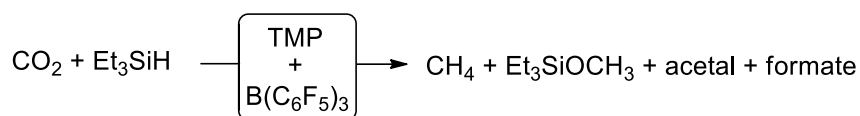
**Ashley 2009**



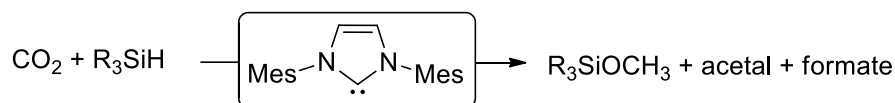
**Stephan 2010**



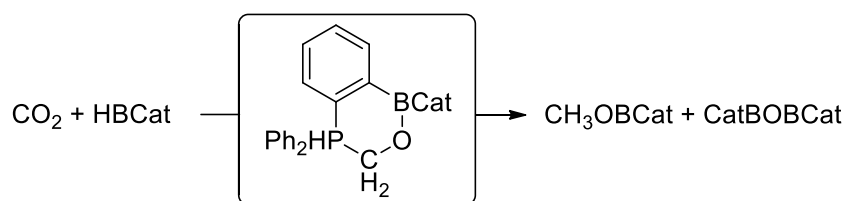
**Piers 2010**



**Ying 2009**



**Fontaine 2013**



**Figure 9** Metal-free reduction of CO<sub>2</sub>.

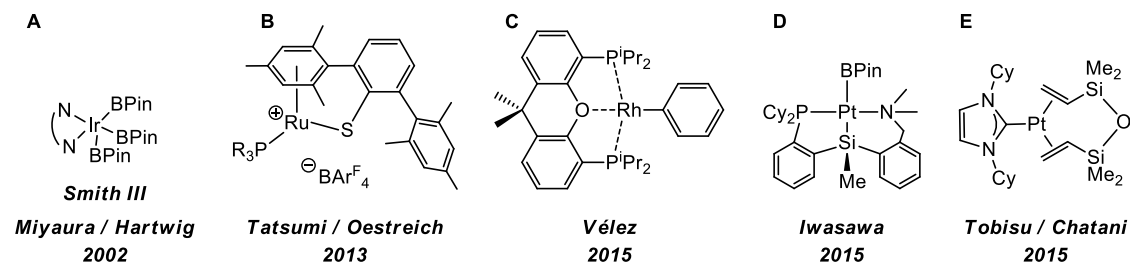
### *Csp<sup>2</sup>-H borylation*

C-H bonds are the most abundant bonds in molecules, but are also considered quite inert. This is strikingly reflected in the simplified representation of molecules, the type of drawing usually used in organic chemistry, in which the C-H bonds are simply omitted for clarity. Nevertheless, in the past decades many researchers have been interested in the functionalization of C-H bonds, which is now regarded as a sub-field of organic chemistry on which seminars and conferences are held. A plethora of types of functionalization can now be performed using C-H bonds, and describing them all is certainly out of the scope of this thesis, but yet highly reviewed.<sup>87</sup> One of them, the borylation of Csp<sup>2</sup>-H bonds, is particularly important to this thesis and deserves a short literature overview.

The C-H borylation reaction gets its importance from the versatility of boron compounds which can be used for many chemical transformations, including the very important Suzuki-Miyaura coupling reaction, allowing the formation of Csp<sup>2</sup>-Csp<sup>2</sup> bonds.<sup>15</sup> Moreover, the reaction is quite simple, is thermodynamically favorable, and usually only one borylation reagent is required (either a borane or a diborane). Boron has a relatively low electronegativity and boron compounds usually do not possess a free electron pair and are often Lewis acidic in nature. Thus, they will be poor ligands and will rarely interact with metal complexes. All these features make the borylation reaction a prime target as a catalytic reaction.

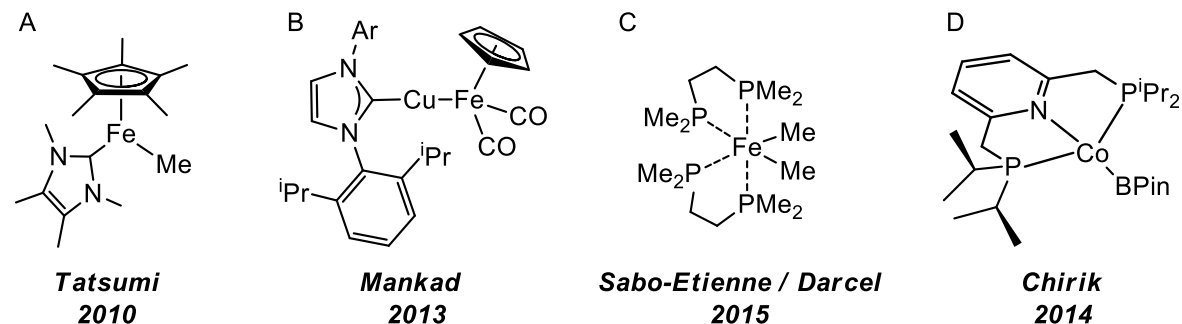
In that context, it is not surprising that many groups have been interested in the reaction and that quite diverse complexes have been reported to catalyze it. At the moment, the most performant system is certainly the one independently developed in 2002 by Smith III,<sup>88</sup> Hartwig and Miyaura<sup>89</sup> using iridium catalysts (**Figure 10A**). The reaction uses B<sub>2</sub>Pin<sub>2</sub> as a boron source, which is one of the most advantageous borane reagent, and more than 15 years after the initial discovery, it is used on large scale<sup>90</sup> using commercially available metal precursor (bis(1.5-cyclooctadiene) di-μ-methoxydiridium(I)) and ligand 2,2'-bipyridine. Its selectivity is mostly sterically driven, with the borylation usually occurring at the less hindered C-H bond. A more detailed description of its capability compared to the system we developed will be provided in Chapter 4. Other interesting systems for the Csp<sup>2</sup>-H bond borylation using second or third row transition metal catalysts include a ruthenium system reported in 2013 by Tatsumi, Oestreich *et al.* (**Figure 10B**),<sup>91</sup> which proceeds by a mechanism involving an electrophilic boryl intermediate. There is also a rhodium system reported by Vélez *et al.* in 2015 (**Figure 10C**),<sup>92</sup> which is among the most active using HBPin as a borylating agent. Platinum based systems were reported by Iwasawa *et al.*<sup>93</sup> and Tobisu, Chatani *et al.*<sup>94</sup> in 2015

(**Figure 10D-E**). The last last one being particularly interesting because of its capability to perform borylation at sterically congested sites.



**Figure 10** Selected 2<sup>nd</sup> or 3<sup>rd</sup> row transition metal catalysts for the Csp<sup>2</sup>-H bond borylation reaction.

In the past years, first row transition metals have also been investigated for the borylation reaction with some success. In 2010 Tasumi *et al.*<sup>95</sup> reported an iron catalyst able to borylate heteroarenes (**Figure 11A**), but the system requires the stepwise addition of HBPin and the presence of an alkene as additive to trap the molecular hydrogen side product that inhibits catalysis. Mankad *et al.* reported in 2013 a more active copper/iron catalyst able to borylate benzenic cycles, which requires light irradiation (**Figure 11B**).<sup>96</sup> A similar strategy was also employed by Sabo-Etienne, Darcel *et al.* in their simpler iron catalyzed system reported in 2015 (**Figure 11C**).<sup>97</sup> Finally, among first row metal catalysts for this transformation, the most performant system is certainly the cobalt pincer catalyst reported by Chirik *et al.* in 2014 (**Figure 11D**),<sup>98</sup> which is particularly selective for the borylation in *ortho* of fluorine atoms.<sup>99</sup>

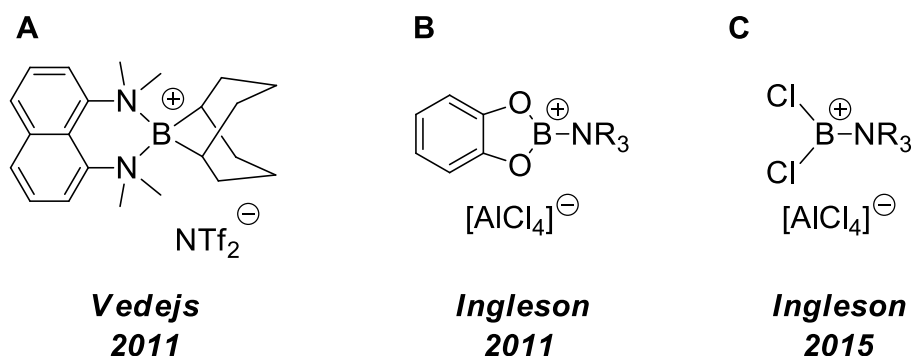


**Figure 11** Selected 1<sup>st</sup> row transition metal catalysts for the Csp<sup>2</sup>-H bond borylation reaction.

From the metal-free point of view, which is the main topic of this thesis, the borylation can be performed stoichiometrically using electrophilic boron species, such as borenium ions, an approach that has been successfully applied by the Vedejs and Ingelson groups first in 2011 (**Figure 12**),<sup>100,101</sup> but was since then refined.<sup>102</sup> However, such approach generally proceeds by halide abstraction from a reactive halogenated borane source to generate the borenium species. Moreover, the reactivity is

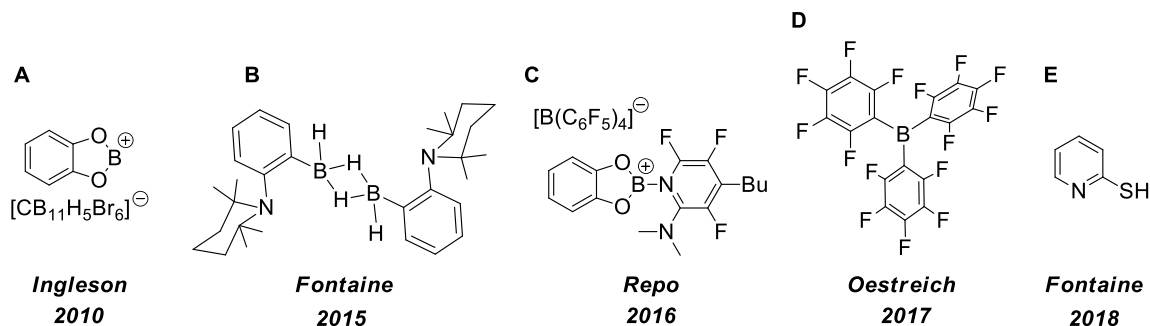


greatly influenced by the substituents on the boron, making the direct synthesis of pinacol derivatives more difficult.



**Figure 12** Selected stoichiometric metal-free borylation reagents.

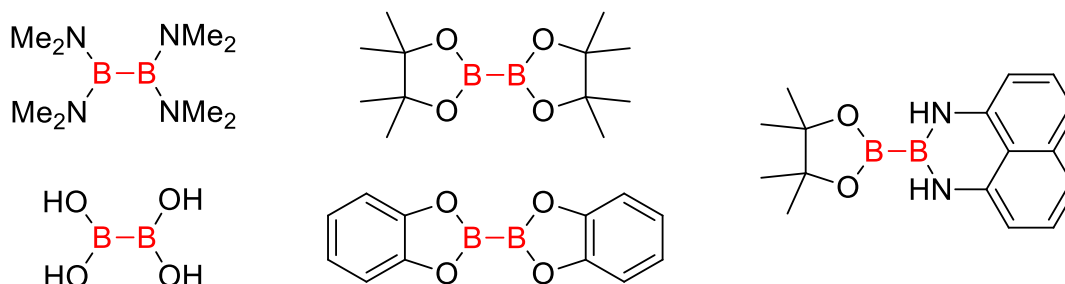
Metal-free catalysts for the borylation of Csp<sup>2</sup>-H bond exist, and some of them using a strategy involving the generation of a reactive electrophilic boron center. This is the case of the systems reported by Ingleson in 2010 (**Figure 13A**)<sup>103</sup> and Oestreich in 2017 (**Figure 13D**).<sup>104</sup> Others such as the one reported by Fontaine *et al.* in 2015 (**Figure 13B**), which will be described in detail in Chapter 4, use the combination of a Lewis acid and a Lewis base correctly arranged geometrically in order to perform the Csp<sup>2</sup>-H bond cleavage step. Finally, systems merging the two approaches have been reported by Repo *et al.* in 2016 ((**Figure 13C**)<sup>105</sup> and Fontaine *et al.* in 2018 (**Figure 13E**),<sup>106</sup> the latter will be described in more details in Chapter 7.



**Figure 13** Selected metal-free catalysts for the Csp<sup>2</sup>-H bond borylation reaction.

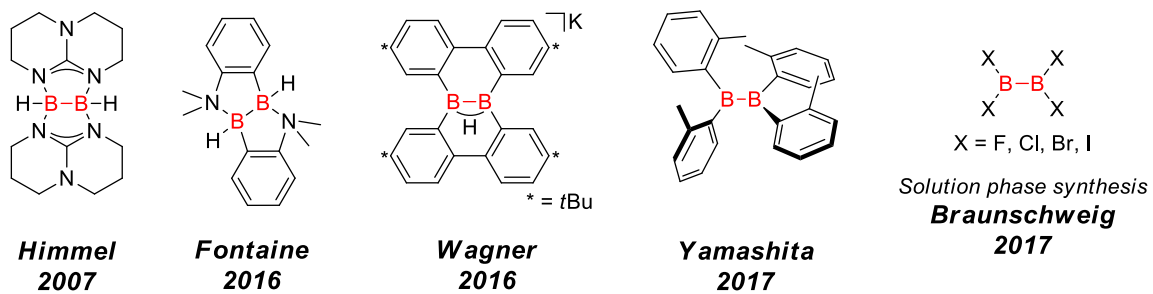
## Diboranes

Diboranes are species containing a single boron-boron bond. Few of them, such as  $B_2Pin_2$ , are commercially available on a large scale and are used in a variety of organic reactions such as borylations and diborations.<sup>107</sup> As mentioned in the previous section, in organic synthesis, boryl groups are almost always placed temporarily on molecules. From that perspective, research efforts are certainly better spent on developing new methodologies using existing diboranes to access products with scaffolds and substitution patterns of interest to the pharmaceutical or fine material industries, rather than on the development of new diboranes.



**Figure 14** Selected examples of commercially available diboranes.

However, other groups have been interested in diboranes for more fundamental reasons. Diboranes are quite interesting from a chemical bonding point of view because of the empty orbitals on both boron atoms that can be filled using Lewis bases or reductants, which can modify the electronic properties of the B-B bond.<sup>108</sup> Moreover, the B-B bond is quite weak and kinetically easy to break, making diboranes species quite reactive and thus useful to form metal-boron bonds. This chemistry has been mostly led by the Braunschweig group, which has been interested in multiple bonds between boron atoms. As such, he reported the lab scale synthesis of halodiboranes in 2017,<sup>109</sup> which can be precursors to many other diboron compounds. Fontaine *et al.* reported in 2016 the spontaneous formation of a diborane by heating an aminohydrobrane,<sup>110</sup> chemistry that will be detailed in Chapter 5. The work of the Himmel group on guanidinate bridged diboranes is probably the most similar that had been reported previously,<sup>111</sup> and later Wagner *et al.* reported another diborane synthesized using an analogous mechanism.<sup>112</sup> Finally, Yamashita *et al.* reported in 2017 that a tetraaryl diborane species could cleave molecular hydrogen.<sup>113</sup>



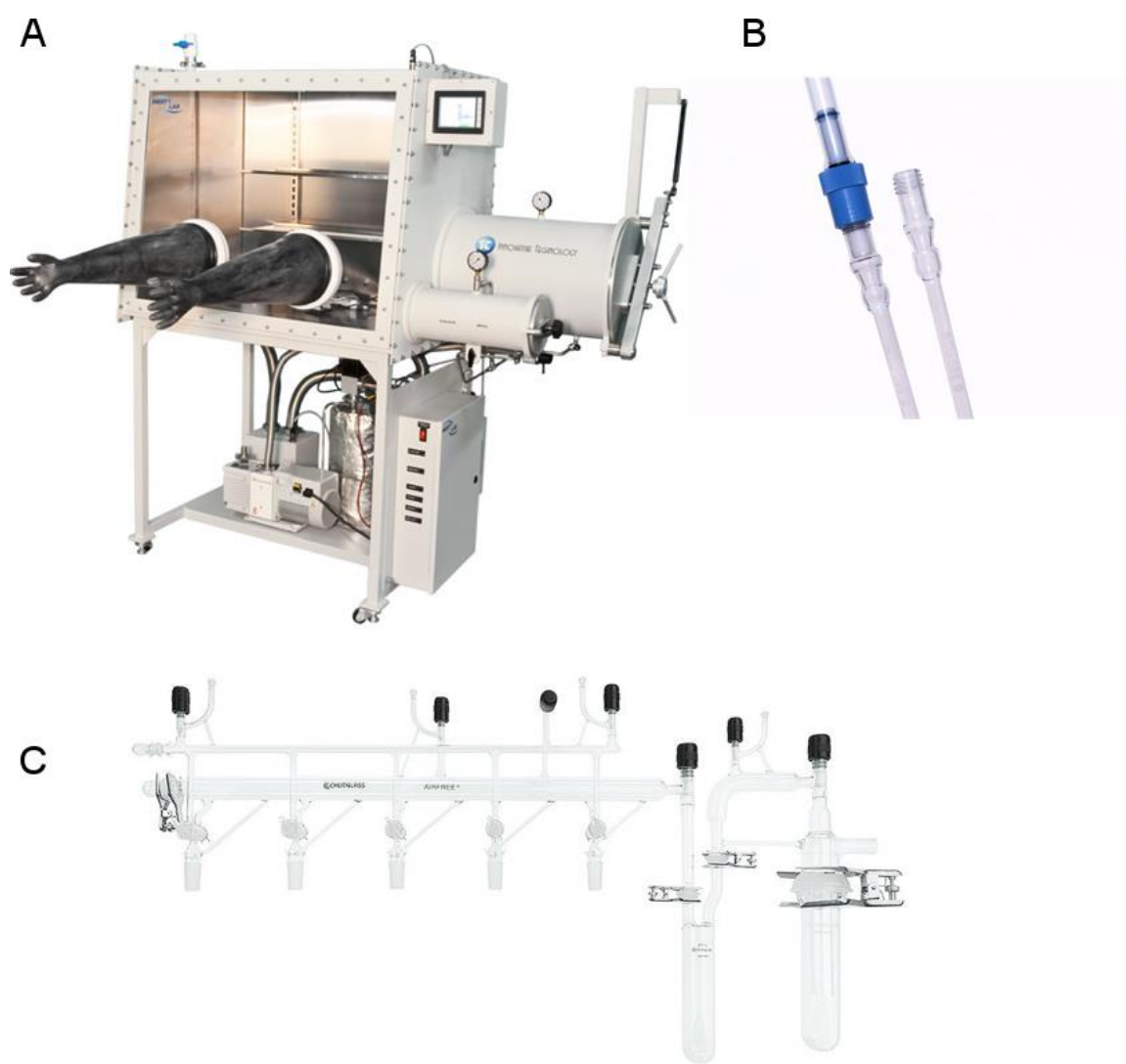
**Figure 15** Selected examples of diboranes reported in the literature.

## Chapter 1 Methodology

The chemistry I have been doing for the past five years may be best described as metal-free organometallic methodological development. It required the knowledge of many different skills and techniques. However, most of them (*e.g.* chemical synthesis, organic molecule characterization, etc.) are familiar to most chemists, are part of the general undergraduate chemistry curriculum and describing them all would certainly be useless for most, if not all readers. However, some of these techniques such as inert manipulations, gas transfer, more specific characterization techniques (*e.g.*  $^{11}\text{B}$  NMR spectroscopy) and computational chemistry (using density functional theory) are probably not as well-known, which justify a short explanation and/or discussion.

## 1.1 Inert synthetic methods

Inert synthetic methods, or air-free techniques, are a set of manipulations one can use to avoid contact with air, usually because an intermediate, a reagent, a catalyst or the product can react with the oxygen and/or the humidity contained in the atmosphere. They can mostly be classified in two types: glovebox techniques and Schlenk techniques (**Figure 16**). The use of J-Young tubes (sealed NMR tubes) is also very useful when dealing with the characterization of air-sensitive compounds and gas transfer.



**Figure 16** A) a glovebox B) a J-Young tube C) a Schlenk line.

A glovebox consists, as its name suggests, of a big box with gloves, fixed semi-permanently. The atmosphere of the box is filled with inert gas (usually nitrogen, but sometimes argon) and is kept at a slightly higher pressure than the atmospheric pressure in order to avoid air coming in. A constant feed of inert gas is connected to the box to compensate eventual slow gas leakage and meet the refilling need required by the glovebox utilization. Moreover, the atmosphere is constantly treated over a purifier of copper and molecular sieves in order to keep the oxygen and water level minimal. The user can place his hands in the gloves to perform manipulations inside the box and the materials (product, glassware etc.) can be brought in and out of the glovebox via an antechamber.

A Schlenk line is a piece of glassware with connections and manifolds designed to facilitate alternating between vacuum and inert gas the atmosphere of a vessel. This allows to effectively remove air from the reaction vessel and replace it with an inert gas at the beginning of the reaction setup. It also facilitates removal of volatiles (*e.g.* solvent) without exposition to air during the workup phase of the reaction. Because the pressure of the inert gas line is slightly higher than the atmospheric pressure, it is also relatively easy to transfer liquids from a flask to another and to perform filtration without exposing the reaction to air. Finally, it is also possible to perform air-free vacuum distillations and gas transfers on a Schlenk line. While it is possible to do gas transfer on larger scale using sealable reaction vessels, most reactions involving gas were performed using J-Young tubes in the course of my Ph. D., mostly because the goal was to develop new methodologies, and the reaction were usually performed on a small scale. J-Young tubes are a type of NMR tubes that are equipped with a special valve. This valve allows the user to seal the tube, isolating it from the atmosphere allowing NMR characterization of air-sensitive compounds without fear of degradation. It also allows heating of reaction performed in J-Young tubes at temperatures higher than the solvent boiling points. Finally the valve allows the user to connect the J-Young tube to a Schlenk line, enabling removal of the solvent, volatile reagents used in excess, or volatile side products, but also gas transfer enabling small scale reactions with gas such as CO<sub>2</sub>, H<sub>2</sub> or both at the same time.

The choice of the technique to use will depend of the acceptable limit of air exposure and the scale of the reaction. For example, a reaction requiring to use only one air-sensitive reagent to produce an air-stable product with a relatively complex workup at a relatively large scale do not require extremely strict anhydrous conditions and will usually be much more easily conducted outside a glovebox using a Schlenk line without affecting much the final result. On the other hand, a reaction using air-sensitive materials and reagents to form an air-sensitive product on a small scale, as often performed for the preparation of organometallic catalysts, will require very strict anhydrous conditions to be successful, and such reactions will usually be performed in a glovebox using solvents and reagents as dry as

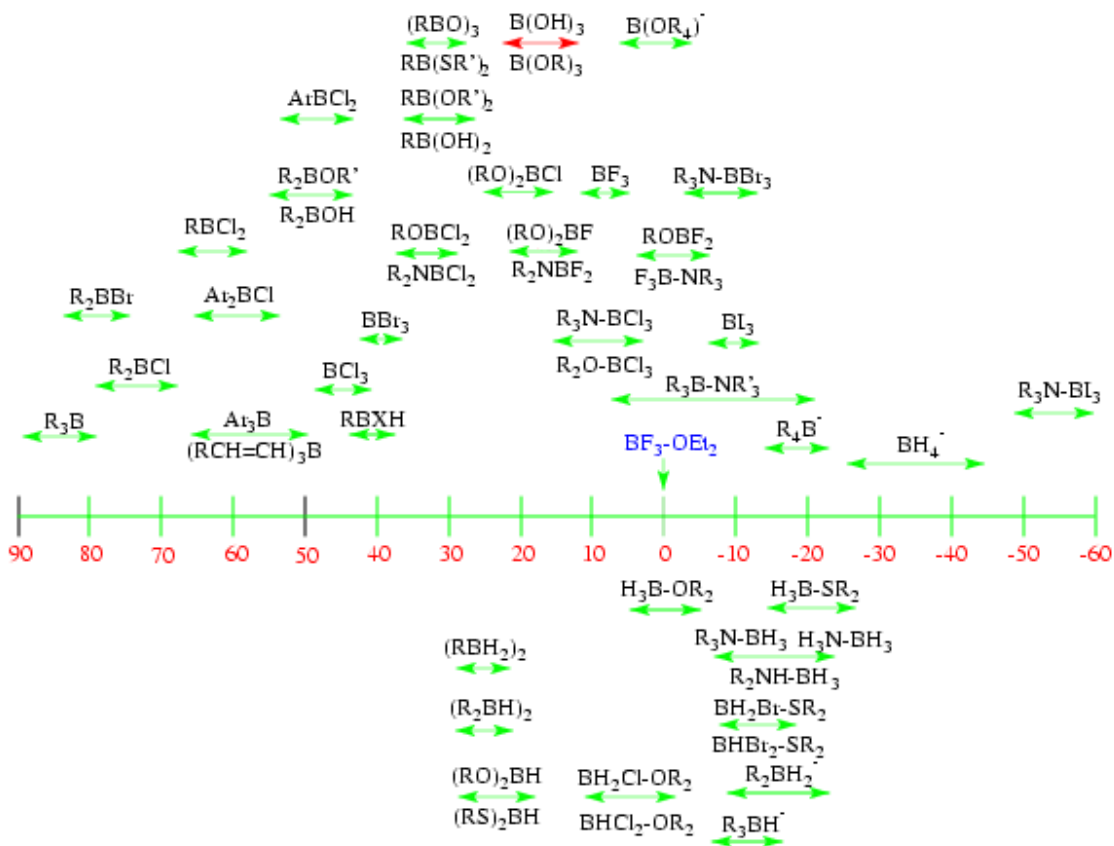
possible. Finally, small scale qualitative tests or reaction condition screenings are often more efficiently carried out in J-Young tubes.

## 1.2 $^{11}\text{B}$ NMR spectroscopy

Since most, if not all, of the compounds described in the thesis are formally organic molecules, classical organic characterization techniques are used in order to characterize them:  $^1\text{H}$  NMR,  $^{13}\text{C}$  NMR,  $^{19}\text{F}$  NMR, mass spectrometry, elemental analysis, infrared spectrometry, X-ray crystallography, etc. UV-Vis spectrometry and spectrofluorimetry were also used to characterize some colored and/or fluorescent molecules. Those techniques are probably well known to most readers and thus do not require presentation nor discussion. The only unusual characterization technique important to this thesis may be  $^{11}\text{B}$  NMR spectroscopy.  $^{11}\text{B}$  is a NMR active nucleus with a spin of 3/2 and a natural abundance of 81%.<sup>114</sup>  $^{11}\text{B}$  NMR spectroscopy is rarely used by most organic chemists, since most organic molecules do not contain a boron atom and when they do it is usually as a boronic acid or ester (in which cases  $^{11}\text{B}$  NMR spectroscopy gives very little information). However, in the work presented in the thesis, many molecules contain a boron atom in a variety of chemical environments.  $^{11}\text{B}$  NMR spectroscopy was thus an important characterization technique.  $^{11}\text{B}$  NMR shifts span from -60 to 90 ppm, with the 0 ppm reference being  $\text{BF}_3\text{-OEt}_2$ , and a lot of information on the boron chemical environment can be deduced (**Figure 17**). Of particular interest to frustrated Lewis pair (FLP) chemistry, the presence, or the absence, of a Lewis adduct will greatly influence the  $^{11}\text{B}$  NMR shift. Lewis adducts usually show around 0 ppm and trigonal boron at 20 ppm and higher chemical shifts, depending of the substituents (substituents with good  $\pi$  orbital overlap (O, N, F) shield the  $^{11}\text{B}$  nucleus). For intra-molecular FLP,  $^{11}\text{B}$  NMR spectroscopy can be used to provide information on the resting state of the molecule (monomeric, dimeric, intra-molecular adducts, etc.).



### <sup>11</sup>B NMR Chemical Shifts Relative to BF<sub>3</sub>·OEt<sub>2</sub>



**Figure 17** <sup>11</sup>B NMR shifts of various boron containing compounds.<sup>115</sup>

It is important to note that during the course of my Ph. D., the Université Laval NMR specialist (Pierre Audet) greatly improved the quality (a 10x increase in signal to noise ratio) and capabilities of <sup>11</sup>B NMR methods. It allowed to routinely perform good quality <sup>11</sup>B NMR and better characterize compounds containing B-H bonds, which are very important in the thesis. Among these new capabilities are <sup>1</sup>H{<sup>11</sup>B} NMR that allowed a better determination of the <sup>1</sup>H signals associated to the borohydrides. Because of its 3/2 spin, <sup>11</sup>B has a quadrupolar moment, complicating the NMR spectra. However, precisely predicting the effect of the quadrupolar moment on NMR spectra is difficult and it is thus used as a “black box” explanation for everything unusual observed doing NMR spectroscopy of boron containing compounds. Among those effects is coupling affected by the space group symmetry. As a result <sup>1</sup>H NMR borohydride signals can be either a very sharp quartet at low frequency (around -1 ppm) or a very broad and not so well define bump up to 5 ppm. In the latter case, and in other cases in which the broad <sup>1</sup>H NMR signal of the borohydride overlaps with others, <sup>1</sup>H{<sup>11</sup>B} NMR is often necessary to identify those key signals for the molecule characterization. B-H J<sup>1</sup> coupling can also be observed comparing <sup>11</sup>B{<sup>1</sup>H} and <sup>11</sup>B NMR spectra of a boron-hydrogen bond

containing compound. Sometimes, only small broadening of the signal is present, allowing only to confirm the presence of a borohydride. Other times, very well resolved multiplets are seen allowing the determination of the exact number of hydrides linked to the boron atom. In all cases, those methods, requiring only few minutes of NMR time, greatly accelerated the synthesis optimization, and ultimately the quality of the characterization of many compounds in the thesis. Finally,  $^{13}\text{C}$  NMR signals of carbon atoms directly linked to boron will be greatly broaden (especially in the case of  $\text{sp}^2$  carbon) to a point where they are usually not observed.

## 1.3 Density functional theory

### 1.3.1 Theoretical background

Density functional theory (DFT) is a category of computational quantum mechanical modeling methods. In that sense, it is more closely related to methods such as the Hartree-Fock than to molecular mechanics and is considered *ab initio* (from first principles), because the theory is indeed rooted in them. However, many of the most popular functionals are fitted to a training set of data and uses empirical fitting parameters which is not truly *ab initio*.

The key difference between DFT and other *ab initio* methods is that instead of using approximations to find a solution to the wave function (Schrödinger equation) DFT uses the electron density to describe the system. It is rooted in the Hohenberg and Kohn principles<sup>116</sup>

- 1- *The external potential (and hence the total energy), is a unique functional of the electron density.*
- 2- *The functional that delivers the ground state energy of the system gives the lowest energy if and only if the input density is the true ground state density.*

The advantage of using the electron density instead of the wave-function is that it is much less computationally costly to calculate. Thus, DFT can be used on system containing a larger number of atoms and electrons, with reasonable calculation time.

A DFT method usually consists of two parts, the functional and the basis set. The functional, which is a function of a function, is the actual mathematical framework in which the calculation is performed. However, for the calculation to run smoothly, the initial guess for the electronic density must be as close to the optimal density as possible. This is why a basis set, which is a set of functions describing the electronic density, is used.

### *1.3.2 Utilization of DFT in the work presented*

The use of DFT, and other computational methods, in chemistry is definitely gaining popularity. It transitioned from being accessible only to experts to being a commonly used technique. I think it will become soon a must-know technique used as broadly as NMR spectroscopy, which will certainly polarize discussions among researchers. First of all, DFT was the only computational tool I used, mostly because I worked on small molecules and wanted to calculate relative energies of intermediates and transition states. However, many other computational tools and methods exist to predict an always growing number of properties with varying accuracy and computational cost (time of the calculation), for systems going from single atoms to large macromolecules. Because DFT is the only computational tool I used, I tend to associate all others computational tools to it, especially in the debate of the place it should have in chemical research. Moreover, since I am far from being an expert in computational methods for chemistry nor in DFT, but rather an “experienced” user, I will speak from experience rather than from a fundamental understanding of the methods. Personally, I think all serious chemists should learn to use at least one type of computational methods, the most appropriate for his work.

DFT is far from as a magic solution to everything. It is a tool, a powerful tool, but only a tool. I consider it similarly to a characterization technique. It is good to get certain types of information, but does not give a complete picture of a problem. During the course of my Ph. D., I repeated many times, that I would never publish a scientific paper containing only computational work and I still think it is a very ethical commitment (at least in my field of study). However, most of the papers I contributed to (and all of those in which I am first author) contain some DFT calculations to support the experimental findings. It is easy and fast to get a tremendous amount of DFT data. However, when not backed by experimental data, DFT calculations have in my mind only little more value than an opinion. Carrying the DFT investigation of a mechanism is like conducting an interrogation, you control the question, but not the answers. Thus, you will not get answers to questions you do not ask, and if your questions are not guided by experimental evidences, they may not depict reality, but only your biased point of view. To sum it up, one has to be very careful when using computational calculations. It is extremely easy to forget to calculate adducts, dimeric forms or conformational isomers and that may result in wrongful predictions or explanations (the thesis will provide examples of such mistakes). However, I remain convinced that DFT is a great tool to compare much more objectively and precisely changes producing antagonist effects. For example, changing alkyl chains from methyl to ethyl on an amine will increase basicity and steric bulk making very hard to predict the overall effect of the change on a Lewis adduct strength using only classical molecular descriptors.

However, DFT can get reliable values to quantitatively and objectively evaluate the effect of such changes.

DFT was primarily used for two goals. First to design new potential catalysts or reactivity, and second to explain unexpected behaviors observed experimentally. The latter case is certainly more straightforward to discuss, since DFT is used to explain experimental evidences: molecule geometry, observed intermediate, reaction rate, etc. Examples of that include the spontaneous formation of a B-B bond presented in Chapter 4 and the cleavage of a Csp<sup>3</sup>-H bond and subsequent rearrangements, discussed in Chapter 5. The DFT brings plausible geometries for key transition states and allows the evaluation of the energy required to access them. Hence, DFT may help to support the plausibility of a mechanistic pathway versus another, something which can sometimes be very fastidious, or even impossible in some cases, to do experimentally. A “guide” often used while analyzing DFT results is presented in **Table 1**. It consists in a table containing the half-life time of reactions in function of the transition state energy at various temperature. I created it at the beginning of my Ph. D., inspired by a less precise version available on the web,<sup>117</sup> using basic kinetic equations. While it may seem very simple, the table is very useful to put DFT data in context, and essential when comparing these data to experimental results, ideally through kinetics analysis but most of the time through semi-quantitative kinetic observations. For example, if you are trying to explain a rearrangement observed at room temperature and only come up with pathways going through limiting transition states ( $\Delta G^\ddagger$ ) of over 30 kcal/mol, you should probably keep searching. Inversely, if a reaction needs elevated temperatures (*e.g.* 110 °C) to take place and your DFT supported mechanism predicts  $\Delta G^\ddagger$  of 20 kcal/mol, it is very likely you are missing a key intermediate, such as some kind of adduct, or reversible formation of an out-cycle species, and I would strongly advise going back to the lab to figure out what is going on before making claims. Nevertheless, doing explanatory DFT is easy and should be validated by experimental results.

Predictive DFT is a whole other story, but I think it is much more exciting and fun to do. You can let go your creativity even if most of the time the DFT results quickly bring you back to Earth. It allows exploring crazy ideas in only few minutes, or hours at most. DFT is like an experienced tutor, one that you always have access to, who can answer your questions and who you cannot really argue with because it gives you objective numbers.

**Table 1** Half-life reaction times function of the TS energy and of the temperature.

T (°C)	-78	0	25	40	60	80	100	110	150	200
$\Delta G^\ddagger$ (kcal/mol)	*Dry Ice	Ice	Room	DCM	Chloroform	Benzene	Water	Toluene	Bromobenzene	
12	4.7 s									
13	61.6 s	3 ms								
14	13.5 min	19 ms	2 ms							
15	3 h	122 ms	11 ms	3 ms						
16	39 h	771 ms	60 ms	16 ms	3 ms					
17	12.8 j	4.9 s	322 ms	78 ms	14 ms	3.1 ms				
18		30.7 s	1.7 s	387 ms	64 ms	13 ms	3.1 ms			
19		3.2 min	9.4 s	1.9 s	290 ms	54 ms	12 ms	5.9 ms		
20		20.4 min	51 s	9.6 s	1.3 s	224 ms	46 ms	22 ms	1.7 ms	
21		2.1 h	4.6 min	48 s	6 s	0.93 s	177 ms	83 ms	5.5 ms	1.0 ms
22		13.5 h	25 min	4 min	27 s	3.9 s	684 ms	307 ms	18 ms	1.7 ms
23		3.6 j	2.2 h	20 min	2 min	16 s	2.6 s	1.1 s	59 ms	3.0 ms
24		22 j	<b>12.1 h</b>	1.6 h	9.2 min	67 s	10 s	4.2 s	195 ms	8.6 ms
25			2.7 j	<b>8 h</b>	42 min	4.6 min	39 s	15.8 s	641 ms	25 ms
26			15 j	1.7 j	3.1 h	19 min	2.5 min	59 s	2.1 s	72 ms
27				8 j	<b>14 h</b>	1.33 h	9.7 min	3.6 min	6.9 s	208 ms
28					2.7 j	<b>5.6 h</b>	37 min	13.5 min	23 s	602 ms
29					12 j	23 h	2.4 h	50 min	1.2 min	1.7 s
30						4 j	<b>9.2 h</b>	3.1 h	4 min	5.1 s
31						17 j	1.5 j	<b>11.6 h</b>	13 min	14.6 s
32							5.7 j	1.8 j	44 min	42.4 s
33							22 j	6.7 j	2.4 h	2 min
34								25 j	<b>8 h</b>	5.9 min
35									26 h	17.2 min

\*Conditions in which this temperature can be easily reached.

With some luck, you may eventually get an interesting “DFT lead”. It may be an accessible transition state for a new reaction or a potentially better new catalyst for a reaction you have been studying. Calculating potential intermediates that may be thermodynamic wells, dimeric forms, alternative conformations, potential decomposition pathways, etc. is sometimes fastidious, but most of the time it remains much faster, cheaper and greener than doing actual lab work. The bright side of DFT objectivity is that when you try to disprove an idea it will continue to give you objective numbers. Eventually, when you have exhausted ideas to disprove your hypothesis, it is likely that the experiments will either work as planned or give something else surprising, and often interesting, that you legitimately missed. Nevertheless, in my case DFT certainly helped to accelerate discoveries and examples can be found throughout the thesis. Finally, it is important to note that sometimes, a hypothesis can be very easily tested experimentally and when it was the case it was done before doing any DFT work. My goal in using DFT was always to accelerate my understanding and thus the development of new interesting chemistry. I do not think I can stress enough the fact that relying too much on DFT can end up doing exactly the opposite.

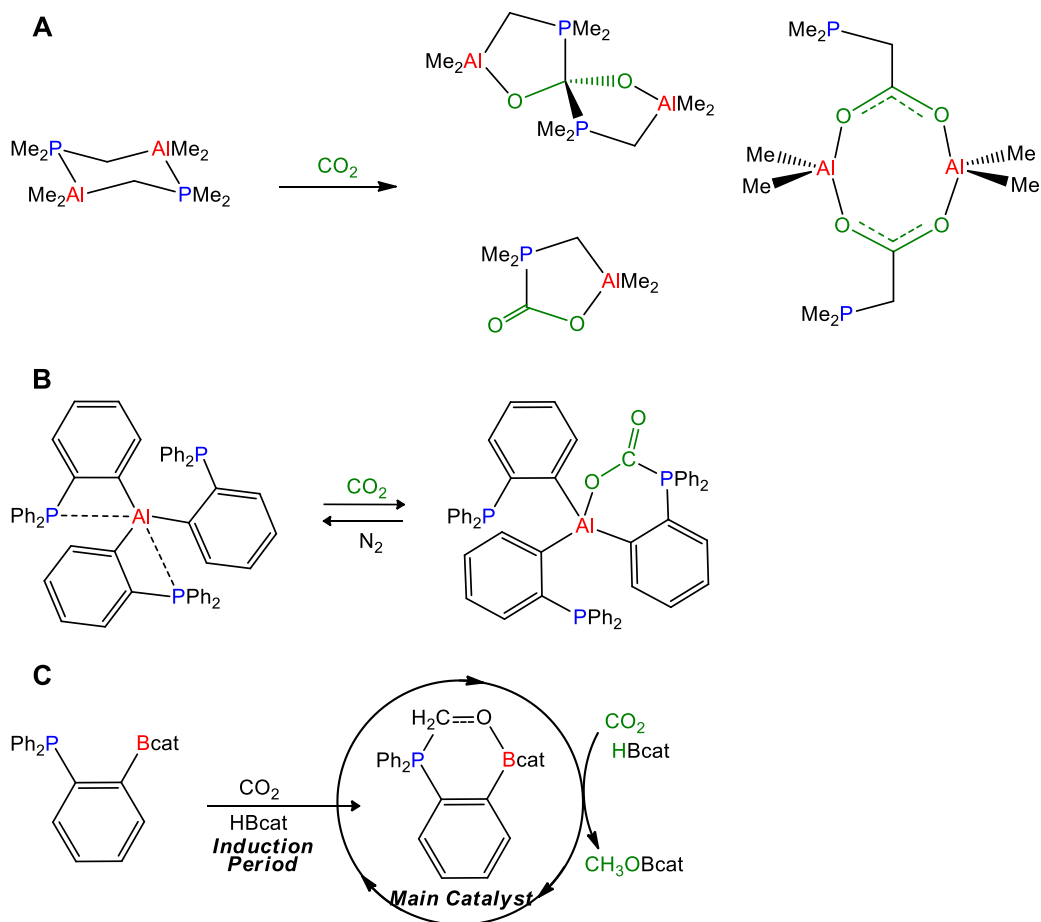
## Chapter 2 Metal-free reduction of CO<sub>2</sub>: from phosphinoboranes to aminoboranes

### 2.1 Previous work on phosphinoborane FLP catalyzed reduction of CO<sub>2</sub>

When I started in the Fontaine group in 2014, it already had some success in the field of frustrated Lewis pair (FLP) chemistry, in particular on the reactivity with CO<sub>2</sub>. The stoichiometric reactivity of aluminum/phosphorus Lewis pairs with CO<sub>2</sub> (**Figure 18A-B**)<sup>118,119</sup> did show “activation”, probably more accurately described as binding (that will be discussed shortly). Thus, the idea that frustration was not necessarily a requirement for accessing FLP reactivity was already quite present in the group mindset while searching for new reactivity or designing new compounds, or potential catalytic cycles, with ambiphilic molecules. The phosphorus/boron system for catalytic hydroboration of CO<sub>2</sub> (**Figure 18C**) had also already been discovered and the computational mechanistic studies as well as the synthesis of derivatives were well underway.<sup>85,86,120</sup>

For some reasons, the “active” lexicon (activation, activated, etc...) is generally overused, and often misused, in chemistry. I personally think it is because it sounds much more positive than the other often more appropriate options (functionalize, cleave, break, bind, etc...). The definition of bond activation used in the thesis is: *a bond is activated only if it is entirely transferred to a temporary state (the activated state) before being transferred to its final state*. In other words, the H-H bond is activated if and only if, when the H-H bond is cleaved to an H-A bond and an H-B (or two H-A bonds) that are not part of the final product are formed. That definition necessitates a complete transformation and a better mechanistic knowledge than just the initial and final products. Since the “active” lexicon is many things, but not static, I think it is only fair that its utilization reflects more than only static states.



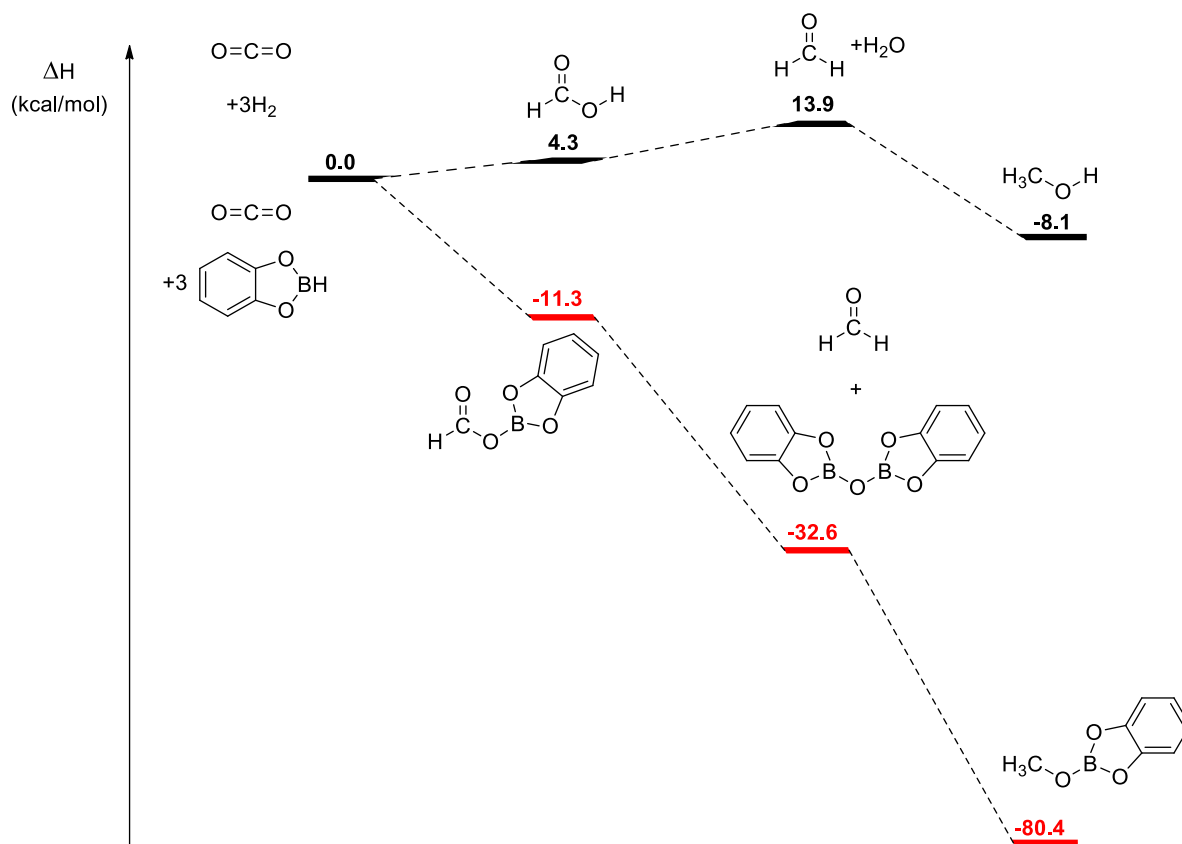


**Figure 18** Previous work on CO<sub>2</sub> reactivity and FLP.

The general mindset of the group at the time I arrived was that CO<sub>2</sub> hydroboration was, to say it politely, only useful to get fundamental knowledge on CO<sub>2</sub> reduction, but could not really lead to any useful application because of the high cost of hydroboranes. This led to the research project I was assigned: switching the reducing agent from hydroboranes to molecular hydrogen in the FLP catalyzed reduction of CO<sub>2</sub>. On that particular project I worked under the supervision of Marc-André Courtemanche.

Switching from boranes to H<sub>2</sub> may seem like a simple task; just replacing a reducing agent by another one. And when you know, or are told, that FLP can “activate” molecular hydrogen and CO<sub>2</sub>, they seem like perfect candidates. However, it turns out that there are challenges associated with that goal. First of all, by comparing the thermodynamics of both the hydroboration and hydrogenation of CO<sub>2</sub> reactions (**Figure 19**), it becomes evident that the huge thermodynamic gain at every step, which was certainly very useful in driving the hydroboration reaction forward, does not exist in the hydrogenation. The reaction is only slightly globally favored and much of that thermodynamic gain comes from the last step, the hydrogenation of formaldehyde. Moreover, the intermediate, side

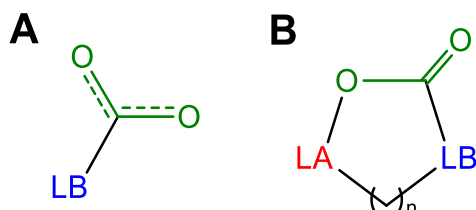
product and final product generated, in the case of the hydroboration reaction, boryl formate, acetal or methoxide were not problematic and often more easily reduced since they contain carbon atoms more electrophilic than CO<sub>2</sub>, again helping the reaction forward. In the case of the hydrogenation, formic acid, the first intermediate, has an acidic proton that can lead to catalyst decomposition pathways and is not an easy target for further reduction. The other products generated, such as formaldehyde, water and methanol, can also lead to catalyst decomposition.



**Figure 19** DFT calculated hydrogenation and the hydroboration of CO<sub>2</sub> using HBCat. Enthalpies reported in kcal/mol, calculations performed at the  $\omega$ B98XD/Def2TZVP level of theory.

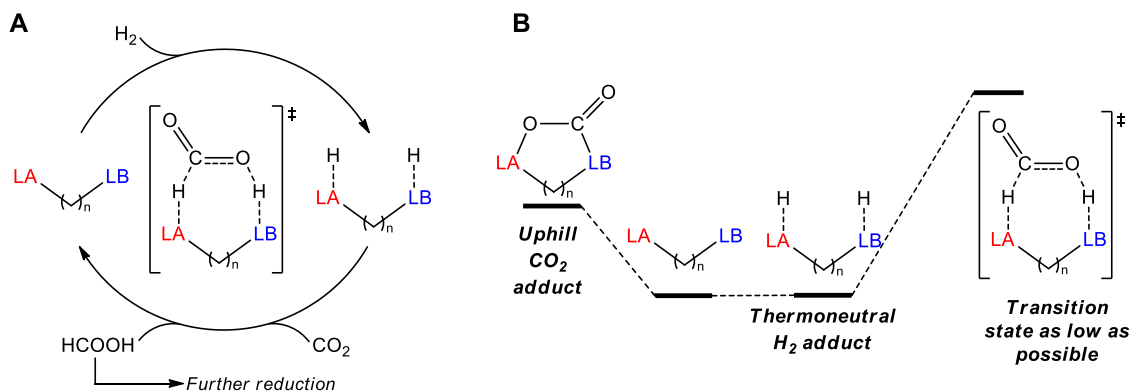
While thermodynamic consideration and potential decomposition pathways are certainly important, a catalytic cycle must also have a kinetically accessible pathway to run efficiently. Since the dominant reactive site of CO<sub>2</sub> is the electrophilic carbon atom, binding it with a Lewis base (**Figure 20**) often inhibits further reactivity. Therefore, to hydrogenate CO<sub>2</sub>, one must focus on having the reducing agent (in our case H<sub>2</sub>) kinetically transferable. This was one of the major conclusion of the mechanistic investigation on the previously presented CO<sub>2</sub> hydroboration system and also, after some debate, the conclusion of mechanistic investigations of the strong base, mostly N-heterocyclic carbenes, catalyzed hydrosilylation of CO<sub>2</sub>.<sup>84,121–123</sup> In the present case, since once again the dominant

reactive site of CO<sub>2</sub> is the electrophilic carbon atom, the generation of a nucleophilic hydride from H<sub>2</sub> is key to CO<sub>2</sub> hydrogenation. From previous studies, both in our lab and from others groups,<sup>124</sup> it was also known that the stabilization by a Lewis acid (even a weak one) of one oxygen atom of CO<sub>2</sub> during the hydride transfer is important to make the transition state more kinetically accessible. In the case of CO<sub>2</sub> hydrogenation, the proton generated from the heterolytic H<sub>2</sub> cleavage can play that role.



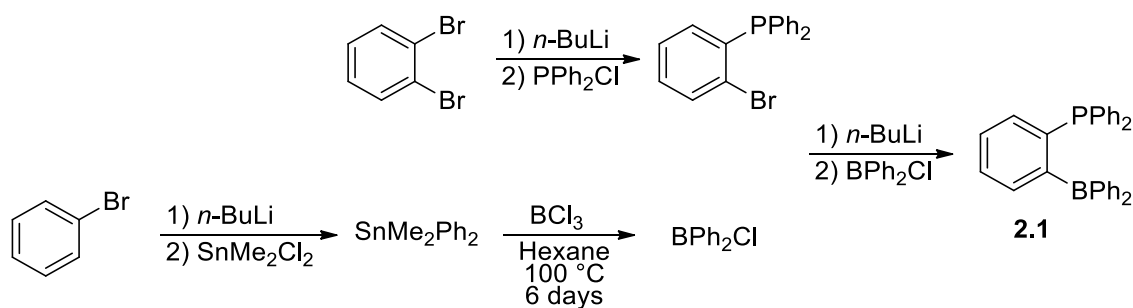
**Figure 20** Examples of a Lewis base CO<sub>2</sub> adduct (A) and a FLP CO<sub>2</sub> adduct (B).

With that in mind, we designed an optimal potential catalytic cycle (**Figure 21A**). The first step is the heterolytic cleavage of molecular hydrogen, the reaction that made the notoriety of FLP chemistry, followed by the simultaneous transfer of the hydride and proton from the FLP-H<sub>2</sub> adduct to the CO<sub>2</sub> molecule and regenerating the free FLP, which would be the key transition state for efficient catalysis. In order to favor that transition state, the goal was to use an intra-molecular system in which the FLP-H<sub>2</sub> adduct was as favorable as the separated form (FLP + H<sub>2</sub>), to avoid falling in a thermodynamic well. The hydride of the FLP-H<sub>2</sub> adduct requires to be nucleophilic to favor addition to the electrophilic carbon of CO<sub>2</sub>. Therefore, one would require the Lewis acid to be weak compared to commonly used boranes in FLP hydrogenation. That may seem quite logical, and even obvious, but at that time (and to some extent it is still true today) bulky and very Lewis acidic compounds such as B(C<sub>6</sub>F<sub>5</sub>)<sub>3</sub> and related derivatives were overwhelmingly dominant in FLP chemistry. That was so imbedded in the FLP community that the first reports of clear H<sub>2</sub> cleavage using strong Lewis bases and weak Lewis acids were named by the authors “inverse” FLP.<sup>125,126</sup> Finally, we should avoid a strong FLP-CO<sub>2</sub> adduct to prevent a thermodynamic sink.



**Figure 21** Proposed catalytic cycle for the hydrogenation of CO<sub>2</sub> (A) and ideal relative energy of different states in the mechanism (B).

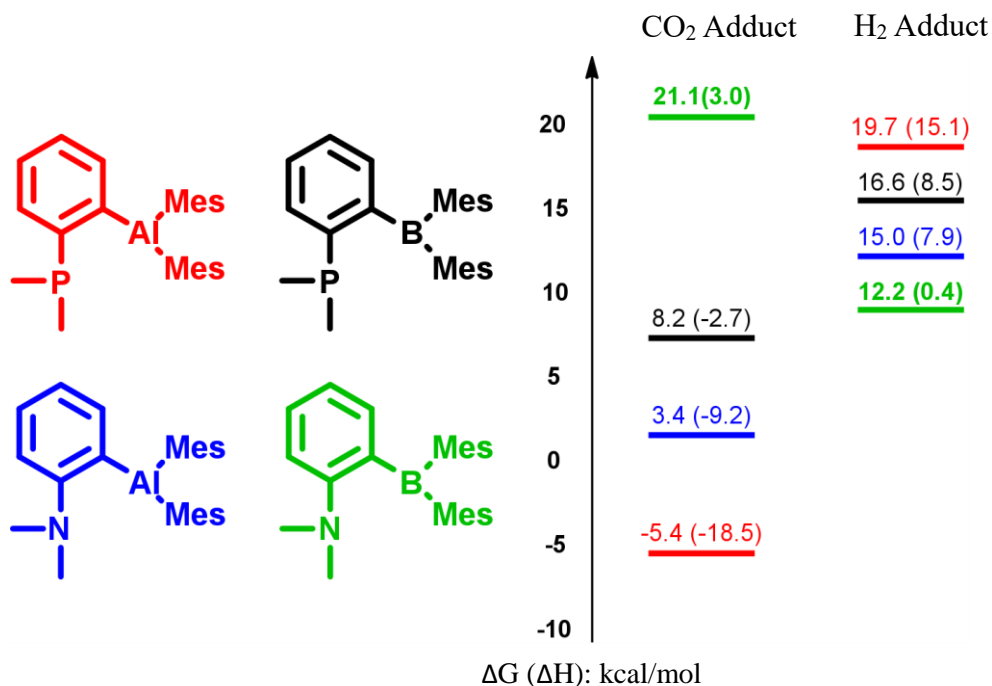
Based on those hypothesis, my first task was to synthesize PPh<sub>2</sub>-C<sub>6</sub>H<sub>4</sub>-BPh<sub>2</sub> (**2.1**) a compound that was thought to be ideal. The synthesis (**Scheme 1**) was relatively straight forward and based on literature precedents.<sup>127,128</sup> The first part, the synthesis of the *ortho*-brominated phosphine, had already been performed several times by my mentors. However, the synthesis of ClBPh<sub>2</sub> turned out to be more challenging. First of all, it necessitates the synthesis of a tin intermediate, with the safety risks associated. Furthermore, the metathesis between the tin analogue and BCl<sub>3</sub> requires harsh conditions (heating at elevated temperature in a closed vessel for a long time), but the real problem turned out to be the purification of the compound by sublimation, which turned out unsuccessful in our hands. In the end, we never isolated that compound. Partly because of bad initial results, but also because at the same time as I was trying the synthesis, I was taught to perform DFT computation and to use this powerful technique for catalyst design.



**Scheme 1** Planned and tried synthesis of compound **2.1**.

## 2.2 Aminoborane FLPs for the hydrogenation of CO<sub>2</sub>

When I started the computational work, a relatively anodyne question was asked by group members: why not using nitrogen instead of phosphorus? Although not convinced at first, the DFT results (Figure 22) motivated us to switch from phosphinoborane to aminoborane compounds.



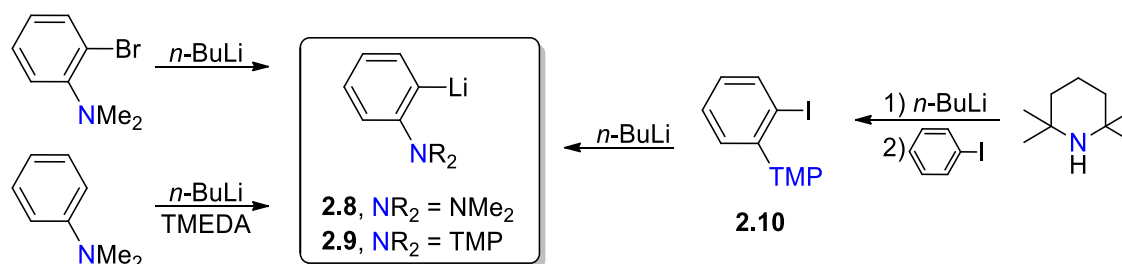
**Figure 22** DFT calculated CO<sub>2</sub> and H<sub>2</sub> adducts energy and enthalpy with different atom combinations (N, P, B, Al). Calculations performed at the  $\omega$ B97XD/6-31++G\*\* SMD solvent = benzene level of theory.

These results suggest that N/B compounds are much more interesting for catalysis than the other options tested at that time (P/B, N/Al and P/Al), which can be rationalize in many ways. First of all, aluminum is more oxophilic than boron and binds less favorably to a hydride. Adding that to the better stability toward air and moisture and better synthetic accessibility of the boron compounds, the choice of the Lewis acid atom was easy. For the Lewis base, the more localized electron pair of nitrogen apparently gives it better affinity for proton than for carbon electrophile compared to phosphorus. A shorter N-C bond compared to the P-C bond may also play a role in the CO<sub>2</sub> adduct stability. DFT clearly pointed us toward N/B compounds, the only type of FLP molecule that was predicted to favor H<sub>2</sub> cleavage over CO<sub>2</sub> binding.

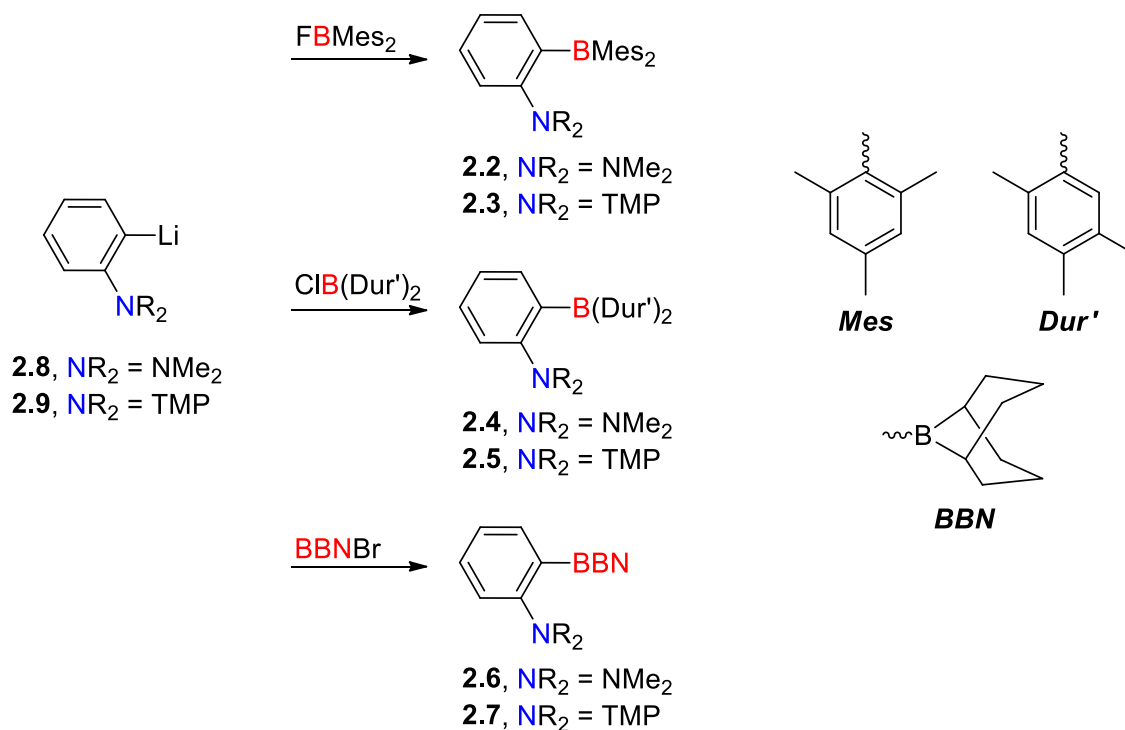
As synthetic target, both substituents on the Lewis base and the Lewis acid of the initial target were also switched from phenyl (PPh<sub>2</sub>) to methyl (NMe<sub>2</sub>) and from phenyl (BPh<sub>2</sub>) to mesityl (BMe<sub>2</sub>),

partly because of the better Lewis basicity of  $\text{NMe}_2$  compare to  $\text{NPh}_2$ , and to conserve the “frustration” with a bulkier Lewis acid, but mostly because of the synthetic accessibility. The synthesis of  $\text{NMe}_2\text{-C}_6\text{H}_4\text{-BMe}_2$  (**2.2**) and some other similar derivatives was already reported in the literature from fluorescence studies.<sup>129</sup> Analogs containing the more Lewis basic and more hindered 2,2,6,6-tetramethylpiperidine (TMP) as the Lewis base (**2.3**) and/or less hindered  $\text{B}(\text{2,4,5-trimethylphenyl})_2$  ( $\text{B}(\text{Dur}')_2$ ) (**2.4** and **2.5**) or 9-borabicyclo[3.3.1]nonane (BBN) as Lewis acid were also synthesized (**2.6** and **2.7**). See **Scheme 3** for details.

The reported synthesis,<sup>129</sup> that starts from 2-bromo-*N,N*-dimethylaniline to generate the corresponding methoxy boronic ester which is then reacted with 2-mesitylmagnesium bromide and followed by purification by chromatography on alumina, was not very successful. Instead, 2-lithio-*N,N*-dimethylaniline (**2.8**) was isolated and directly reacted with commercially available dimesitylboron fluoride, which proved to be a much more efficient synthesis. Eventually, it was realized that **2.8** could be readily isolated from the *ortho*-lithiation of *N,N*-dimethylaniline,<sup>130</sup> a much more affordable pathway that was preferred for further synthesis. A change that may seem very simple, but that ended up greatly facilitating the synthesis of many compounds that will be discussed in other chapters of the thesis. In the case of the  $\text{B}(\text{Dur}')_2$  analogue, a similar synthesis was adopted reacting **2.8** with  $\text{ClB}(\text{Dur}')_2$  that was previously synthesized using successfully the tin metathesis method that was previously discussed. The BBN derivatives were also synthesized with a similar procedure using the commercially available *B*-bromo-9-BBN solution. Finally, the TMP derivatives could also be made with an analogous method, using  $\text{TMP-C}_6\text{H}_4\text{-Li}$  (**2.9**) prepared from beforehand synthesized 2-iodo- $\text{C}_6\text{H}_4\text{-TMP}$  (**2.10**).<sup>131</sup>

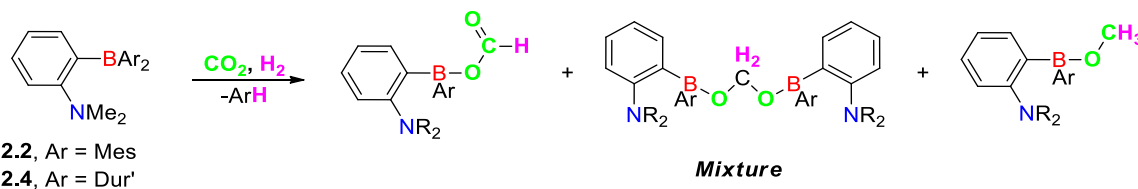


**Scheme 2** Synthesis of the lithiated precursors **2.8** and **2.9** for the synthesis of aminoboranes **2.2-2.7**.



**Scheme 3** Synthesis of the various N/B FLPs.

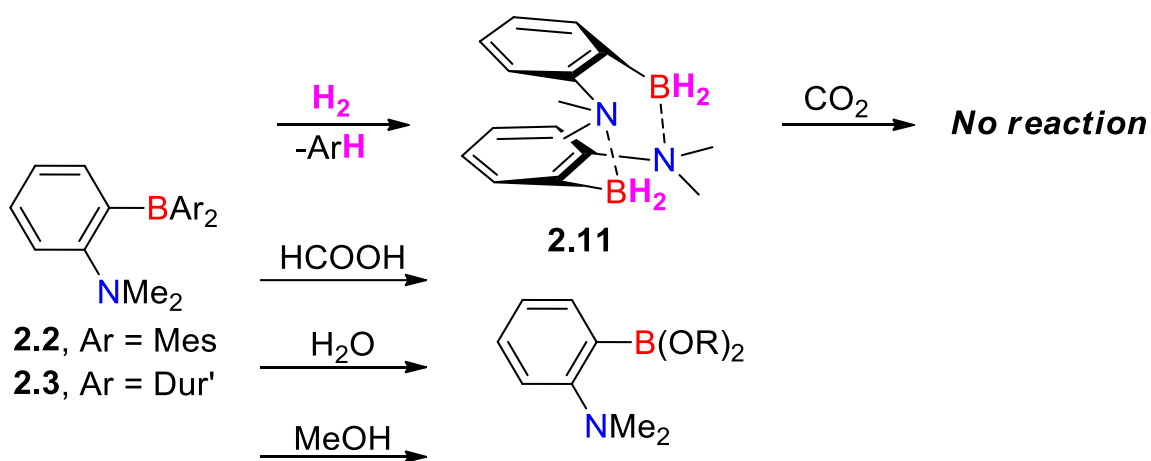
All of those compounds were eventually tested as catalysts for the  $\text{CO}_2$  hydrogenation and two of them (**2.2** and **2.4**) proved stoichiometrically competent (**Scheme 4**).<sup>132</sup> While these results, although interesting, might not seem relevant to the core of this thesis, it was inspirational and led to many important findings in C-H bond activation chemistry, as described in more details below.



**Scheme 4** Stoichiometric  $\text{CO}_2$  hydrogenation by **2.2** and **2.4**.

The first notable observation is that the aryl groups on the boron moiety are lost at some point. Understanding when, and eventually how, this group loss happens is very important in order to design other compounds that would avoid such decomposition pathways. A key question to answer was if the degradation was coming from  $\text{CO}_2$  reduction or if the  $\text{CO}_2$  reduction activity was coming from the degradation of the starting material, with or without the reagents. That was investigated first by heating a  $\text{C}_6\text{D}_6$  solution of the compounds in absence of any reagents for several hours at  $110\text{ }^\circ\text{C}$  which confirmed their thermal stability. Next, the compounds were heated in the presence of  $\text{H}_2$ , but in the absence of  $\text{CO}_2$ . In that case, free arene could be observed, as well as a new product

characterized by a  $^{11}\text{B}$  NMR signal at 2.5 ppm, a broad B-H signal that become sharper with  $^{11}\text{B}$  decoupling at 3.6 ppm and inequivalent *N*-methyl signals in the  $^1\text{H}$  NMR spectra. It was first associated to  $[\text{NMe}_2\text{-C}_6\text{H}_4\text{-BH}_2]_2$  (**2.11**), which was first thought to exist as a boat shape eight-membered ring. We will see in chapter Chapter 4 that this assignation, while making perfect sense with the information we had at that moment, was false. The resulting mixture was then exposed to  $\text{CO}_2$ , leading to no observable reaction. Exposure of the compounds to formic acid, water or methanol, the  $\text{CO}_2$  reduction products, also led to an aryl loss and formation of species analogous to those seen during the initial experiment (with  $\text{CO}_2$  and  $\text{H}_2$ ). In summary, the loss of the aryl group was either coming from the reactivity with  $\text{H}_2$  or with the  $\text{CO}_2$  reduction products, which does not answer our original question. Thus, we turned to DFT to get more insight.

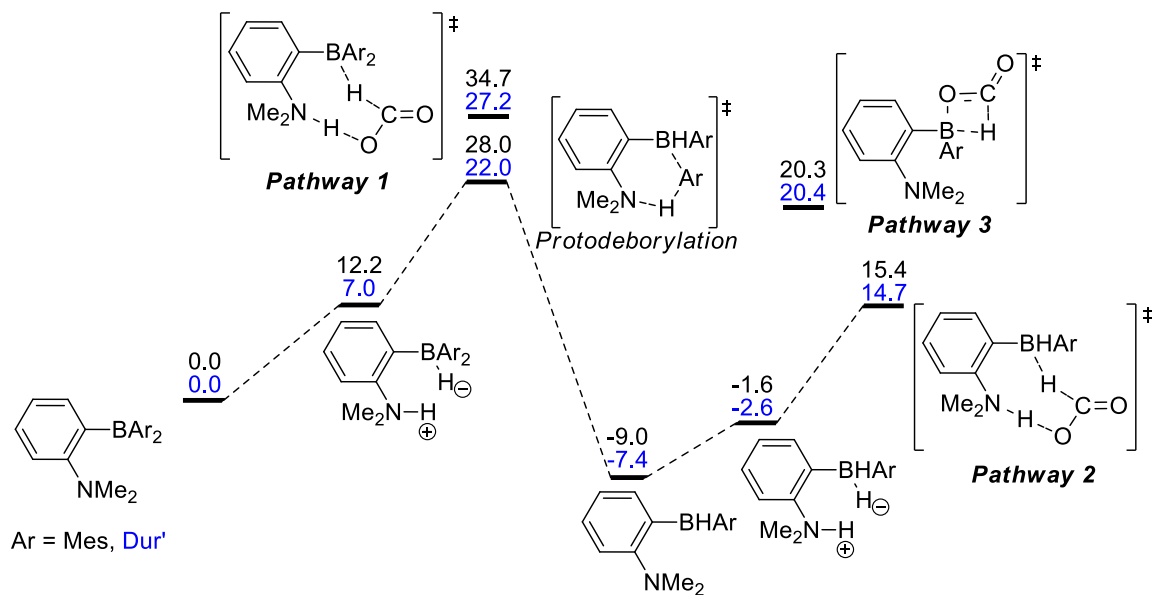


**Scheme 5** Summary of the experimental mechanistic investigation.

With the calculations, we discovered that a protodeborylation reaction was probably taking place, a reaction we realized had been recently proposed by the Repo and Pápai groups as a key step in the FLP reduction of internal alkynes using very similar molecules.<sup>133</sup> That also eventually led to the C-H activation system, the micro-reverse reaction, which will be discussed in Chapter 3. In the case of the first  $\text{CO}_2$  reduction event, three options were considered. A simultaneous  $\text{H}^-$  and  $\text{H}^+$  transfer following an  $\text{H}_2$  cleavage from the starting compounds (**Figure 23** pathway 1), or after a first protodeborylation event (**Figure 23** pathway 2), and direct  $\text{CO}_2$  reduction from the mono protodeborylated intermediate (**Figure 23** pathway 3). As the compound formed after a second protodeborylation event has been shown inactive toward  $\text{CO}_2$ , it was neglected in the computational study. In the end, the second option, a simultaneous  $\text{H}^-$  and  $\text{H}^+$  transfer following an  $\text{H}_2$  cleavage from the mono protodeborylated intermediate, turned out to be calculated the most energetically accessible pathway and our final proposition to explain the observations. However, other pathways are calculated relatively close in energy and some degree of contribution from them is certainly possible. A thorough kinetic



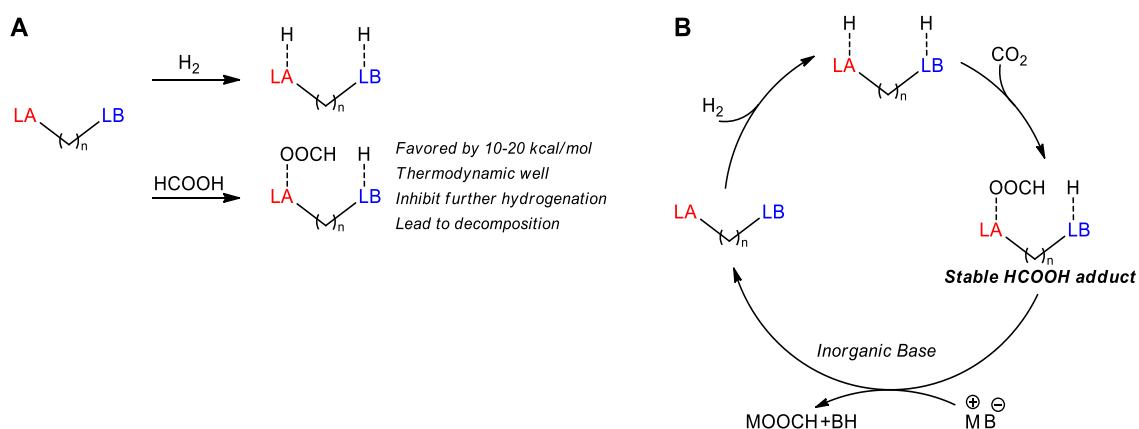
investigation of the system might have given more insights, but considering its complexity and general relevance, our efforts got oriented toward different projects.



**Figure 23** Summary of the DFT investigation of the aminoborane mediated CO<sub>2</sub> hydrogenation mechanism.  $\Delta G$  reported in kcal/mol, calculations performed at the  $\omega$ B97XD/6-31++G\*\* SMD solvent = benzene level of theory.

### 2.3 Aminoborane FLPs Exhibiting High Robustness and Reversible Formic Acid, Water and Methanol Cleavage

One of those different project was the design of more resistant FLP derivatives that would not deactivate with CO<sub>2</sub> reduction products, in particular formic acid. Here it might be pertinent to give some more details of our thought process. As I already mentioned, the catalytic hydrogenation of CO<sub>2</sub> is not a simple task. That means there is still some interest in being only partially successful. The stoichiometric reduction presented in the previous section is a good example of that. During that previous study, we came to realize that boron is quite oxophilic and formic acid is much easier to heterolytically cleave than hydrogen, while not being much bulkier. That means it would be practically impossible to design a catalyst, at least based on our amino-borane framework, which would make a thermoneutral adduct with hydrogen and not make a very favorable adduct with formic acid. Considering that, proceeding to further reduction steps to formaldehyde or methanol from that thermodynamic well would be extremely difficult. That left, among other, the possibility of focusing on that first reduction step and trying to remove the formic acid from the system, for example with an inorganic base. This strategy has been employed in some of the most successful transition metal catalyzed CO<sub>2</sub> hydrogenation systems.<sup>77,134</sup> However, doing that requires an amino-borane that would not degrade in the presence of formic acid, hence the goal of the side-project presented below.

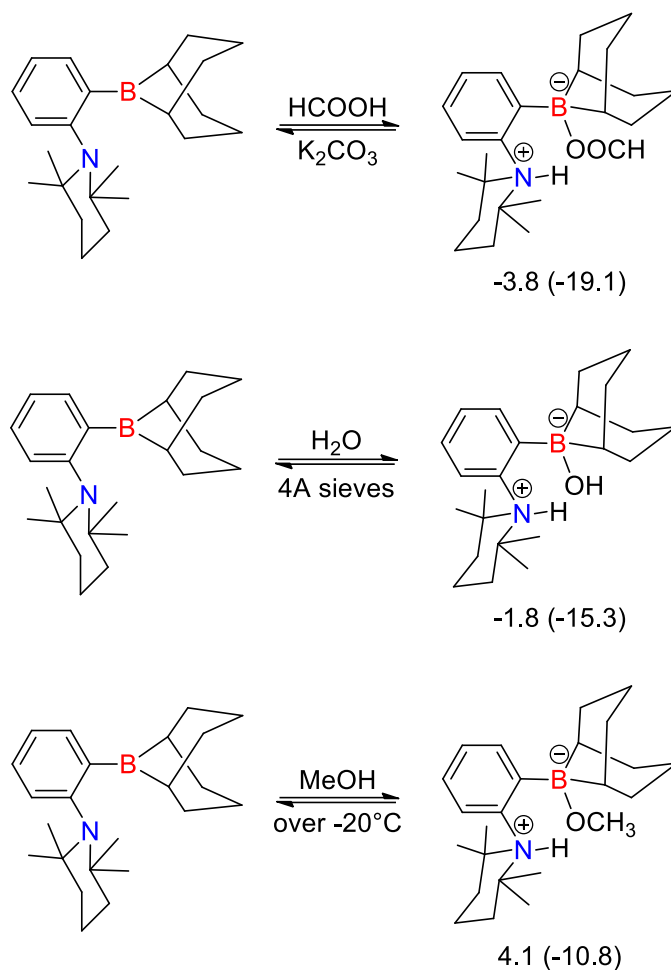


**Figure 24** Problem caused by formic acid, CO<sub>2</sub> first reduction product (A) and proposed solution, partial FLP catalyzed CO<sub>2</sub> hydrogenation.

The dominant decomposition pathway is protodeborylation. In order to occur, a nucleophilic carbon linked to boron must get close to the proton located on the nitrogen atom. Since sp<sup>3</sup> carbon atoms are much less nucleophilic, they usually do not protodeborylate. A bidentate group can also reduce the rate of the protodeborylation step because of geometric constraints or by favoring the reverse process. Finally, a more hindered environment around nitrogen also disfavors the proton transfer. It turned out

that the previously synthesized compound TMP-C<sub>6</sub>H<sub>4</sub>-BBN (**2.7**) corresponds to all those criteria and its reactivity toward CO<sub>2</sub> reduction products was thus investigated.<sup>135</sup>

Interestingly, it was possible to demonstrate reversible adduct formation of **2.7** with formic acid, water and methanol. In the case of formic acid, **2.7** proved quite resistant showing less than 5 % degradation when placed in presence of excess formic acid (10 equiv), even after heating at 80 °C for 24 h. The formic acid adduct could also be reverted back to free **2.7** simply by leaving a solution standing over K<sub>2</sub>CO<sub>3</sub>. Signs of hydrolysis could be observed when heating in the presence of excess water, but the **2.7** water adduct could be crystalized and also reverted back to free **2.7** by having a solution standing over 4 Å molecular sieves. Finally the methanol adduct proved thermally reversible. In fact, it could only be observed below -20 °C during NMR studies. DFT investigation of the adducts “strength” fits well with the experimental results and also allowed to evaluate the accessibility of the H<sub>2</sub> adduct. While those results are very encouraging in the quest for metal free catalytic CO<sub>2</sub> hydrogenation, despite all our efforts, mostly performing reactions at higher pressure and temperature, no signs of CO<sub>2</sub> hydrogenation catalysis could be obtained with **2.7**.

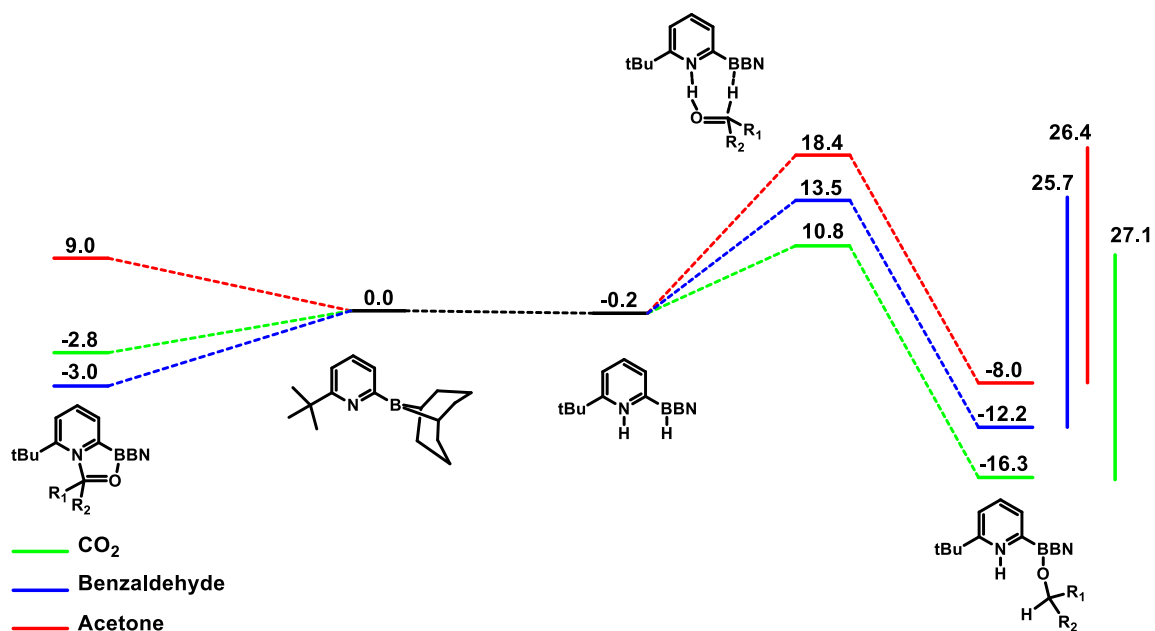


**Scheme 6** DFT calculations on the reversibility of the **2.7** adducts with various CO<sub>2</sub> reduction products, HCOOH, H<sub>2</sub>O and MeOH.  $\Delta G$  ( $\Delta H$ ) reported in kcal/mol, calculations performed at the  $\omega$ B97XD/6-31++G\*\* SMD solvent = benzene level of theory.

The interest for metal-free CO<sub>2</sub> reduction is mainly an intellectual quest. As discussed in the introduction, the interest in metal-free processes reside mostly in not having to deal with regulated metal impurities coming from the catalyst. In the case of CO<sub>2</sub> reduction, methanol is not made for human consumption and can easily be purified by distillation, thus trace metal impurities are not really a concern. Moreover, because starting materials and products can be heated at elevated temperature and because reaction selectivity is not a primary concern, heterogenous catalysts are more appropriate. This eventually made us shift our interest from CO<sub>2</sub> hydrogenation to aldehyde or ketone hydrogenation, a class of reaction broadly used in the pharmaceutical industry and that could benefit from selective and efficient metal-free catalysis.

Pushing the idea of using stronger nitrogen-based Lewis base and weaker boron-based Lewis acid further, we designed derivatives including phosphinimide or amidine as Lewis basic sites.

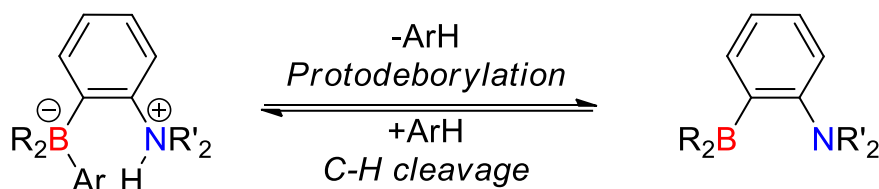
Geometrical effects were also considered and different spacers, notably 2-borylated pyridine, were investigated computationally giving very promising results (**Figure 25**). The presence of a bulky substituent at the 6 position in order to disfavor dimerization is noteworthy since, as described in the introduction, intramolecular FLPs, especially those with only one atom spacer, have a very high tendency to form stable 6-membered ring dimers. However, synthetic difficulties slowed down our efforts and eventually reports of the first examples of FLP catalyzed carbonyl hydrogenation using  $B(C_6F_5)_3$  in ethereal solvents<sup>136-140</sup> combined with the discovery of new interesting FLP reactivity patterns in our group took our efforts away from that project. Interestingly, it was recently reported that using a stronger base/weaker acid FLP approach can indeed lead to ketone hydrogenation.<sup>141</sup>



**Figure 25** DFT calculated intermediate and transition state free energies for the hydrogenation of  $CO_2$ , benzaldehyde and acetone using a pyridine based FLP.  $\Delta G$  reported in kcal/mol, calculations performed at the  $\omega B97XD/6-31+G^{**}$  level of theory.

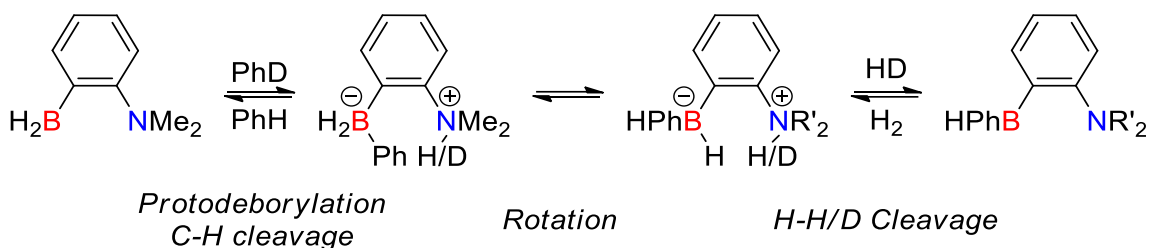
### Chapter 3 Metal-free Csp<sup>2</sup>-H borylation of heteroarenes

As noted in Chapter 2, protodeborylation and C-H bond cleavage are micro-reverse reactions (**Figure 26**). It means that in theory, if one of the reactions is kinetically feasible, the other one should also be possible by tuning the thermodynamics correctly. That initial thought really started the quest in our lab for the first example of FLP promoted Csp<sup>2</sup>-H bond cleavage. At that time, the cleavage of the terminal alkyne Csp-H bonds was already a known reactivity pattern of FLPs.<sup>69</sup> That project was initially led by Marc-André Légaré, before we rediscovered the protodeborylation reaction doing our CO<sub>2</sub> hydrogenation studies. Marc-André Courtemanche and I joined the effort, as the compound we made during our CO<sub>2</sub> studies were promising for such reactivity.



**Figure 26** Micro-reversibility of the protodeborylation and C-H cleavage functionalization.

The first approach taken was trying to observe H/D exchange between C<sub>6</sub>D<sub>6</sub> and H<sub>2</sub>, promoted by NMe<sub>2</sub>-C<sub>6</sub>H<sub>4</sub>-BH<sub>2</sub> (**2.11**) generated from NMe<sub>2</sub>-C<sub>6</sub>H<sub>4</sub>-BAr<sub>2</sub> (**2.2** or **2.4**). While the final goal was the development of a catalytic cycle for the functionalization of C-H bond, a proof of concept of Csp<sup>2</sup>-H bond cleavage would already be an important achievement. The small energy difference between the B-Ar and B-H bonds suggests that in conditions where protodeborylation is observed, which is at elevated temperature and in the presence of H<sub>2</sub>, an equilibrium should exist between **2.11**, Ar-H, and species of the type NMe<sub>2</sub>-C<sub>6</sub>H<sub>4</sub>-BHA<sub>r</sub>. While the equilibrium is expected to favor the free arene, doing the reaction in C<sub>6</sub>D<sub>6</sub> should entropically help accessing the transition state and in the presence of H<sub>2</sub>, it should lead to scrambling, giving indirect evidence that Csp<sup>2</sup>-H bond cleavage is happening. However, that experiment proved unsuccessful. Later, the discovery that the final product of the reaction between **2.2** and H<sub>2</sub> is not **2.11**, but **4.1** as detailed in Chapter 4 explained the observation.

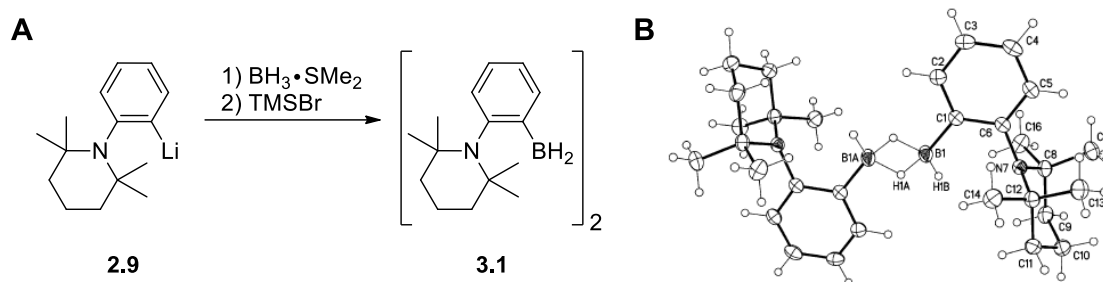


**Scheme 7** Proposed sequence for the **2.11** catalyzed H/D scrambling between C<sub>6</sub>D<sub>6</sub> and H<sub>2</sub>.

Nevertheless, interesting design features of a possible C-H functionalization catalyst came out of our DFT studies. First of all, a small boron moiety makes the transition state of C-H cleavage more accessible. Reducing the steric bulk around the reactive center may seem an obvious way to favor reactivity, but as mentioned earlier, highly hindered Lewis acids are usually the norm in the field of FLP chemistry. The boron acidity is also another important factor in accessing the C-H bond cleavage transition state and in the resulting equilibrium balance. For equivalent steric hindrance, the most acidic boron will have the lowest transition state. Those two principles, and the possibility of favoring the equilibrium entropically by the loss of H<sub>2</sub>, brought the BH<sub>2</sub> moiety at the top of the list of potential Lewis acid candidates. As for the substrate to be activated, it should contain a relatively nucleophilic carbon such as those observed in five-membered heterocycles like, thiophene, furan, pyrrole and indole. However, despite predicting many accessible transition states, the experimental results were not conclusive.

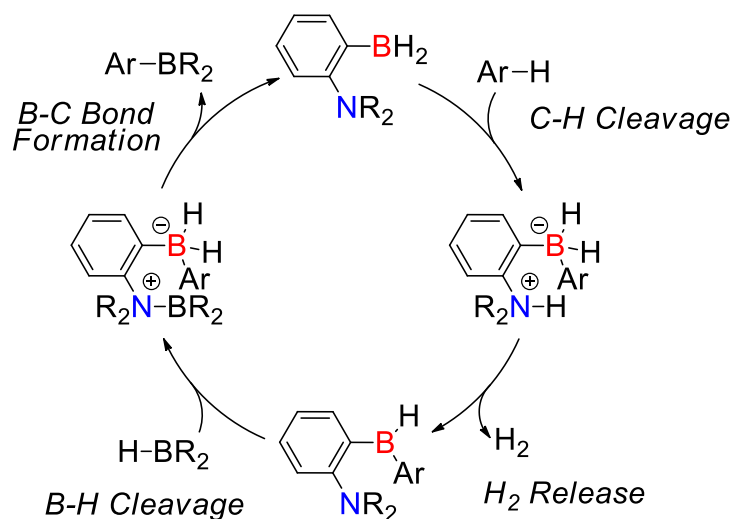
While we were doing that research, the Repo group published an article on the reactivity between H<sub>2</sub> and [TMP-C<sub>6</sub>H<sub>4</sub>-BH<sub>2</sub>]<sub>2</sub> (**3.1**).<sup>142</sup> This result made us realize that we had neglected the possibility of a dimeric form, which is around 7 kcal/mol more stable than the monomer, in our computational studies. It also provided a relatively simple synthetic method for the preparation of a compound that we had calculated to possess all the characteristic required to promote Csp<sup>2</sup>-H bond cleavage. After

publishing the work presented in that chapter, the Repo group reported that the cleavage of the C-H bonds of arenes is a general reactivity of aminoboranes.<sup>105</sup>



**Figure 27** Selected results concerning **3.1** reported by the Repo group A) Synthesis B) Crystallographic structure.

Having compounds **2.3**, **2.5**, and some synthetic intermediates in hand to synthesize **3.1**, the investigation of its potential activity toward Csp<sup>2</sup>-H bond cleavage started. The targeted transformation was the catalytic borylation of C-H bonds via a C-H bond cleavage/H<sub>2</sub> release/B-H bond cleavage/B-C bond formation mechanistic sequence (**Figure 28**).



**Figure 28** Initial mechanistic hypothesis for the catalytic borylation of C-H bonds.

In the initial test run, **2.3** and **2.5** showed some, but limited, activity for the borylation of *N*-methylpyrrole using BH<sub>3</sub>·SMe<sub>2</sub> as a borylating agent. However, **3.1** proved to be an efficient catalyst for the borylation of *N*-methylpyrrole using HBPIn as borylating agent. We rapidly recognized the importance of this finding and Marc-André Légaré, Marc-André Courtemanche and I worked collaboratively and intensively with daily updates and discussions since we had the feeling

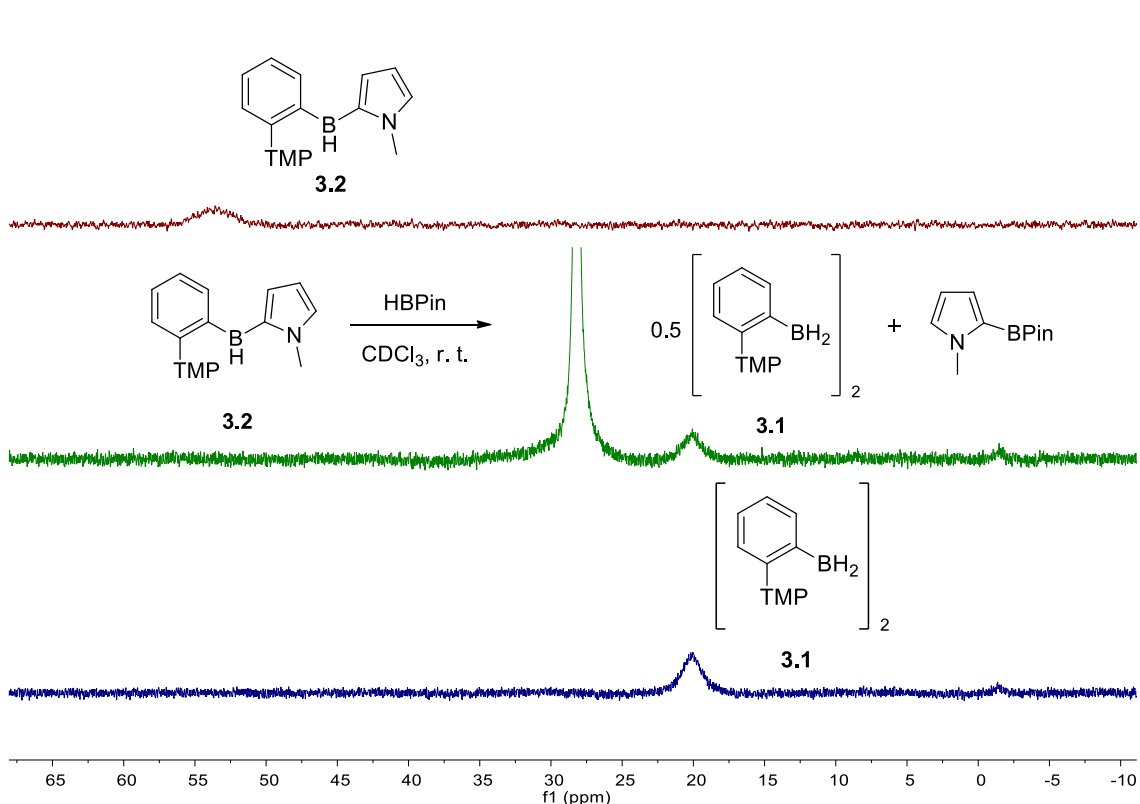


that sitting on those results for too long was probably not in our best interest. To maximize efficiency, Marc-André Légaré, who made the initial discovery, took charge of the kinetic isotope effect measurements, of screening the conditions for the different substrates as well as performing the isolation of the products. For that last part, he had important help from Marc-André Courtemanche who also took care of the functional group tolerance study. I was charged with the synthesis of sufficient amount of the catalyst and some substrates, the isolation of intermediates in the catalytic cycle, and of the DFT investigation of the mechanism.

The goals of the study were first to clearly demonstrate that the observed reactivity was indeed coming from our metal-free catalyst through careful experimental and computational mechanistic investigations, and second to assess the scope and limitations of the catalyst. This may seem totally obvious, but the catalyst you put in is not necessarily the species doing catalysis, and many examples of wrongfully assigned catalytic activity coming from decomposition products, impurities or nanoparticles have been reported.<sup>143</sup> That is particularly true in the fields of base metal and metal-free catalysis in which precious metal impurities came from contaminations from flasks, spatula, and even entire gloveboxes. The best way to minimize the chances of wrongfully assigning the catalytically relevant species is mechanistic investigation: isolation of intermediates, kinetic measurements, DFT studies, etc. Getting orthogonal reactivity, a different activity trend among substrates, or a different selectivity than the other known catalysts, especially if it can be explained or predicted, are also very convincing evidences.

As in many cases, the mechanistic investigation started with attempts to observe and isolate intermediates. This is usually not an easy task as the “Halpern’s rule” suggests: “If you can isolate it, it is probably not the catalyst”.<sup>144</sup> This statement emphasizes the fact that most in-cycle states of the active species are very reactive and only exist in low concentration. Isolated species are often off-cycle, degradation products, or some stabilized state of an active species. The dimeric resting state of **3.1** is a good example of that. However, in our mechanism, because H<sub>2</sub> is released, which prevents the reversibility of the reaction, there was hope to isolate intermediates. After a quick optimization of the conditions, the reaction of **3.1** with a small excess of *N*-methylpyrrole at 80 °C for 5 h in toluene allowed the isolation of a new species. Despite our efforts, a crystallographic structure could not be obtained, but multi-nuclear analysis of the compound allowed its assignation as TMP-C<sub>6</sub>H<sub>4</sub>-B(H)(*N*-methylpyrrole) (**3.2**) (see **Figure 29**). The <sup>11</sup>B{<sup>1</sup>H} NMR signal of **3.1** in the BHAr<sub>2</sub> range at 20 ppm shifted at 54 ppm. The comparison of the integration between the phenylene and pyrrole moieties in the <sup>1</sup>H NMR spectrum confirmed that only one *N*-methylpyrrole was linked to the boron atom. At that time, the methodology to observe <sup>1</sup>H coupling in <sup>11</sup>B NMR or perform <sup>11</sup>B decoupling in <sup>1</sup>H NMR

had not yet been developed at Université Laval. As shown on **Figure 29**, the signal to noise ratio was also sub-optimal and has been substantially improved since and better spectra are presented in the other chapters of the thesis. **3.2** was then reacted with HBPIn at room temperature and converted back to **3.1** in 5-10 min, suggesting that the transfer of the *N*-methylpyrrole moiety from the catalyst to the borylating agent is fast and probably not limiting in the catalytic cycle.

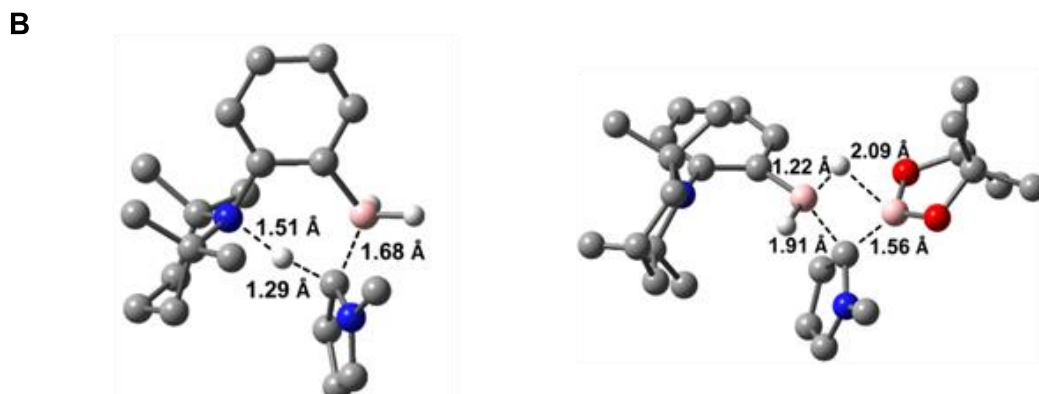
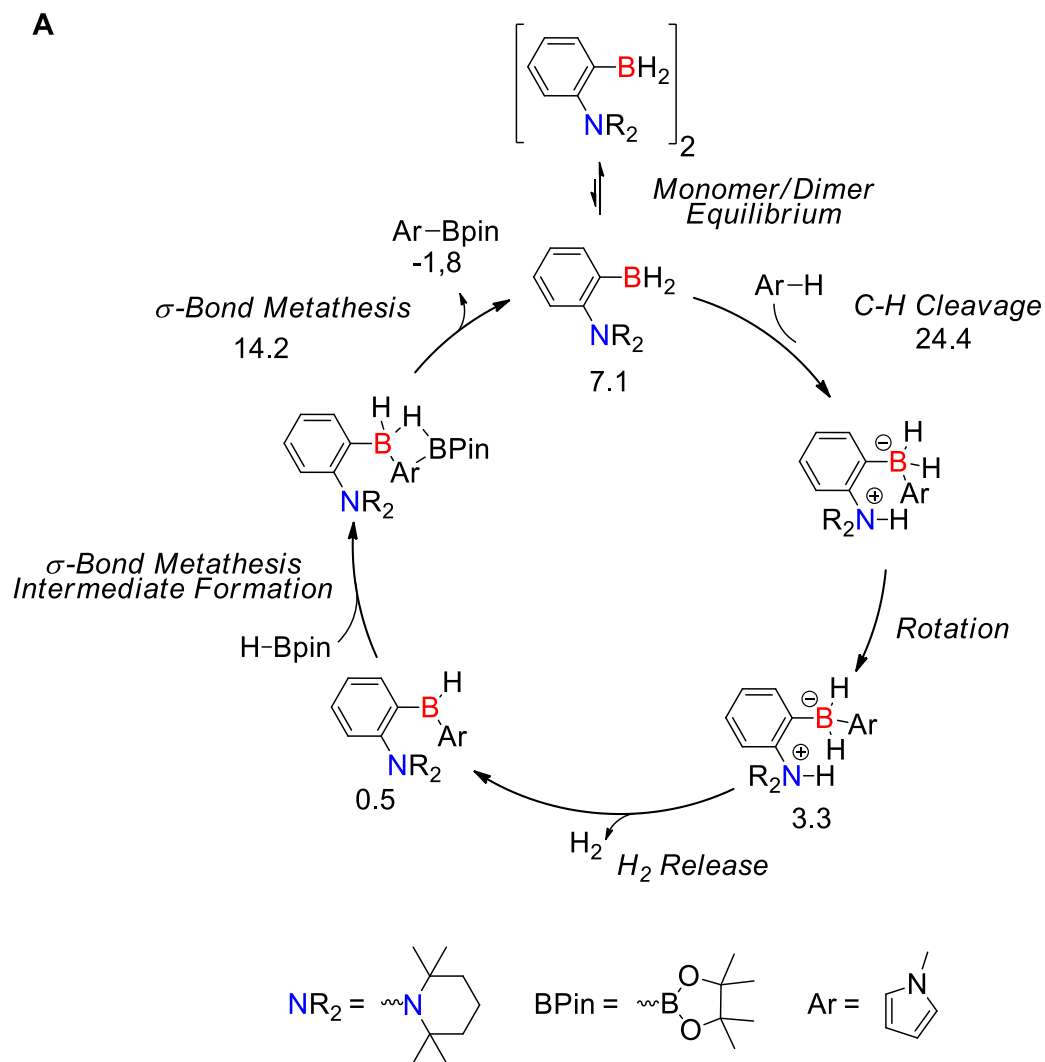


**Figure 29**  $^{11}\text{B}\{^1\text{H}\}$  NMR spectra of **3.2** (top), the reaction of **3.2** and HBPIn (middle) and of **3.1** (bottom).

Quick laboratory experiments like those are often enough to guide a more thorough DFT investigation of a mechanism and the information obtained often help in the design of informative experiments. From the experimental evidence, the mechanism could be separated in two parts: the C-H functionalization to get **3.2** and regenerating **3.1** from the borylation agent. Our proposition for the first part was first the dissociation of the dimer, followed by C-H bond cleavage, rotation around the phenylene-boron bond, in order to place the hydride in front of the proton, and finally  $\text{H}_2$  release. The intermediates formed in each of those steps were calculated at reasonable energies, under 5 kcal/mol, and a transition state for the concerted cleavage of the C-H bond was calculated at 24.4 kcal/mol, in

good agreement with the observed experimental activity. The other transition states (dimer separation, rotation and H<sub>2</sub> release) were neglected in that study.

For the second part of the mechanism, our first hypothesis as presented earlier in **Figure 28**, was the cleavage of a B-H bond of the reducing agent followed by rotation and formation of the C-B bond. However, the intermediates calculated were very crowded and the pathway seemed unreasonable with the speed of the reaction observed experimentally. Another simpler pathway, involving a  $\sigma$ -bond metathesis between the catalyst intermediate and HBPIn was proposed. This transformation seemed more reasonable with a transition state energy calculated of 14.2 kcal/mol, coherent with a fast reaction at room temperature. It is important to note that an intermediate with a 3-center 2-electron bond, which is very similar and very close in energy to the transition state, exists and can complicate the calculation. Indeed, when the energy surface is flat and many minima and saddle points are close to one another, transition states are harder to locate. However, since that step is clearly not limiting, it was neglected for clarity in the initial report. A more detailed mechanism is presented in **Figure 30** and the importance of the  $\sigma$ -bond metathesis step will be discussed in more details later in this chapter and in Chapter 6.

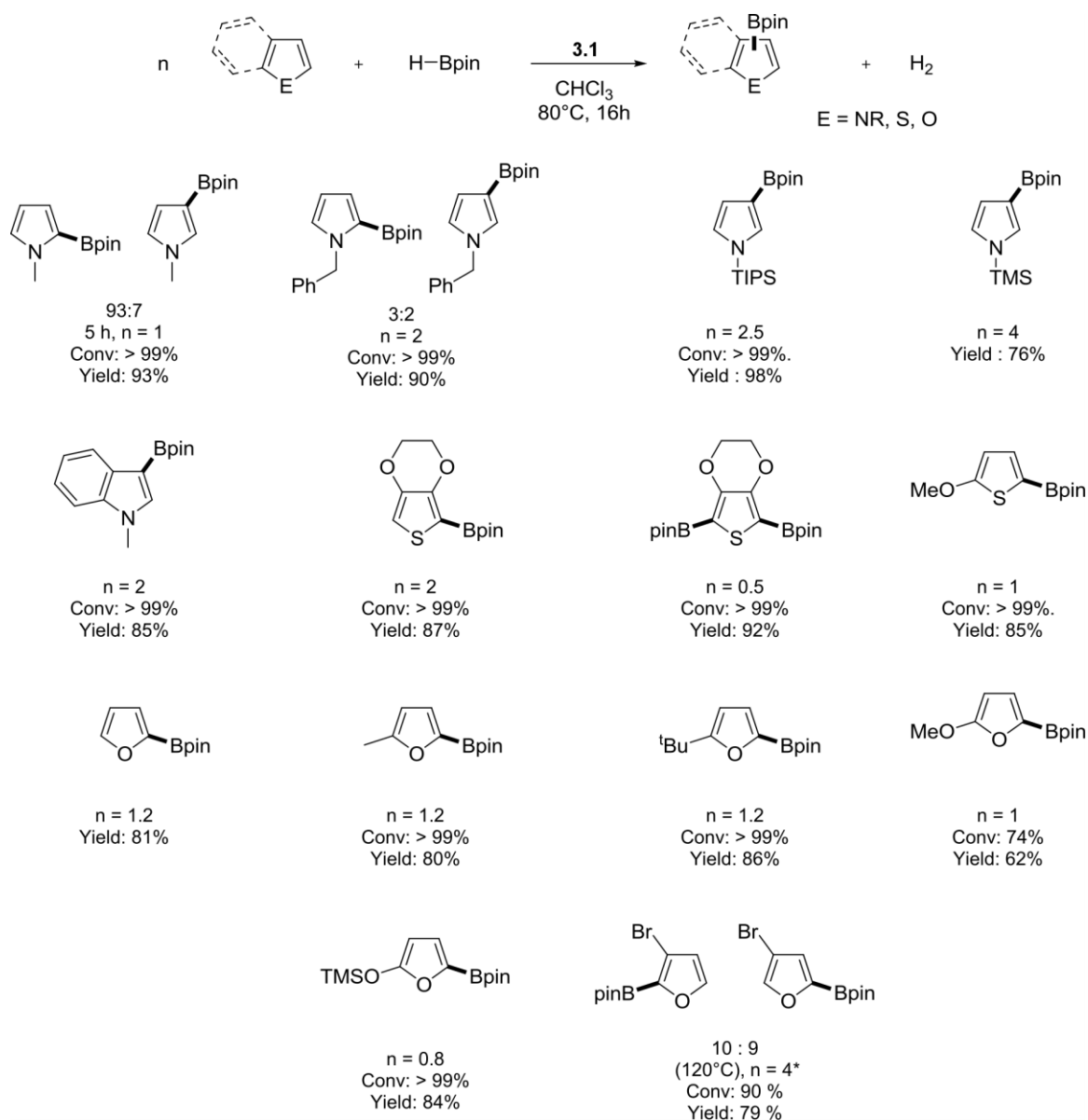


**Figure 30** A) DFT studies of **3.1** mediated catalytic C-H bond borylation of *N*-methylpyrrole. B) Optimized transition states geometries.  $\Delta G$  reported in kcal/mol, calculations performed at the  $\omega$ B97XD/6-31++G\*\* SMD solvent = chloroform level of theory.

As the DFT and preliminary experimental observations suggested that the limiting step is the cleavage of a C-H bond, it was decided to carry kinetic isotope effect (KIE) measurement studies to confirm it. To do those measurements, both stoichiometric and catalytic competitive experiments were carried out with a 1:1 ratio of *N*-methylpyrrole and *N*-methylpyrrole-*d*<sup>4</sup> to compare the respective conversion at the end of the reaction. In retrospective, this may not have been an ideal experiment. *N*-methylpyrrole was chosen as a substrate for comparison with the initial experiments and the DFT work. However, even though less than 7% of the C-H cleavage occurs at the C3 position, this side-reaction increases measurements uncertainty. Moreover, a perfect 1:1 ratio is very hard to obtain and an initial spectrum had to be taken to adjust for the real ratio. The use of *N*-methylpyrrole-*d*<sup>1</sup> (deuterated at the 2 position) would have assured a correct ratio all the time, but the volatility of *N*-methylpyrrole (boiling point = 112 °C) makes difficult the preparation of this deuterated analogue while *N*-methylpyrrole-*d*<sup>4</sup> is commercially available. More importantly, by taking the measurement at the end of the reaction, we neglected the possibility of an equilibrium, and the concentration change during the reaction, which happens when a compound is more reactive than the other, thus underestimating the KIE. Finally, using a more sensitive method such as HPLC-MS or GC-MS in the first 10 % of the reaction, rather than using <sup>1</sup>H NMR spectroscopy, which is not an ideal method for quantitative analysis, or simply doing complete kinetics would have been more precise. In the end, limited equipment access and the volatility of the compound made the use of NMR spectroscopy more convenient in our case. We measured similar KIE of 1.8 and 1.9 at 80 °C for the stoichiometric and catalytic reactions, respectively. While clearly unneglectable and suggesting that the cleavage of the C-H bond is the limiting step of the catalytic cycle, the KIE values were surprisingly low. Usually, KIE of 5-6 are expected from the linear cleavage of a C-H bond, such as via deprotonation, with the maximum theoretical value being 8.<sup>145,146</sup> However, systems in which the cleavage of the C-H bond is not linear usually have lower KIE values. For example, the Co catalyzed C-H borylation of pyridine has a KIE of 2.9(6) at 80 °C<sup>147</sup> and the Ir catalyzed borylation of 1,2-dichlorobenzene exhibits a KIE of 3.3(6) at 25 °C.<sup>148</sup> Interestingly, the mechanistic investigation of the Pd C-C coupling via concerted metalation deprotonation, having a transition state very similar to the one we propose, has shown a similarly low KIE of only 2.1 at 100 °C.<sup>149</sup> Simply comparing our observed values to other similar systems is certainly comforting, but it does not bring any logical explanation. As discussed earlier, the measurements method might have slightly underestimated the KIE value. The observed KIE value might also indicate that the C-H bond is highly bent during its cleavage, which would suggest that the formation of the C-B bond is a very important component of the transition state. Indeed, in the DFT optimized transition state, the B-C distance is quite short (1.68 Å), the boron is pyramidalized to some extent, but most importantly, the C-H bond being cleaved is bent out of the *N*-methylpyrrole

plane by approximately 75°. We should note that a KIE can also come from the release of H<sub>2</sub>. However, the magnitude of a KIE for H<sub>2</sub> release still is debated in literature. This subject will be discussed in more details in Chapter 4. Finally, attempts to get more insight by predicting the expected KIE value from the DFT calculated transition state sadly led to inconclusive results.

The next unavoidable step when developing a new reaction or studying a novel catalyst is the investigation of the substrate scope. Not only can it be very informative on the transformation mechanism, for example giving information on the importance of steric versus electronic effects, but it is also necessary to promote the generality of your chemistry. In the case of our study, substrates were targeted according to several factors. First, the commercial availability or ease of synthesis was a primary criterion, as we did not want to lose time synthesizing substrates. The diversity is also an important criterion. While the probability of successful reactions was obviously considered, especially in the first selection of substrates, more risky substrates were tried as the study progressed. Finally, especially for the final selection of substrates on which isolated yields were obtained, the volatility of the substrates was an important criterion to facilitate the isolation. It may not be obvious when quickly looking at the substrate scope table, but the number of equivalents of substrate was optimized for each molecule by running preliminary small-scale reactions. In many cases the optimal conditions required a small excess of substrate, which is quite logical considering that the expected limiting step is the C-H bond cleavage which would be dependent on substrate concentration. Moreover, because the final borylated compounds are somewhat sensitive to moisture and silica gel, the isolation was not always easy. Having substrates that could be removed under vacuum allowed purification by a simple short and fast silica pad to remove the catalyst followed only by evaporation (at high vacuum in some cases), streamlining the procedure. In the end, the reaction works on pyrrole, indole, thiophene and furan derivatives that can be decorated by functional groups such as alkyls, alkoxides, halogens (Br in particular), protected using functions such as silylated alcohols or alkylated, benzylated or silylated at the *N* position, in the case of pyrroles and indoles.

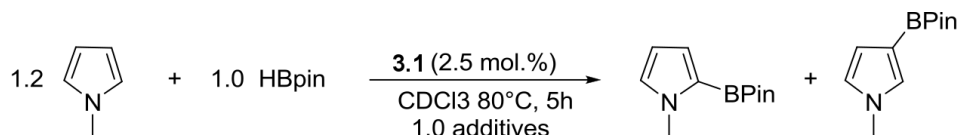


**Figure 31** Substrate scope of the borylation using **3.1** as catalyst. Standard reaction conditions: **3.1** 2.5 mol %, HBPin 1 equiv., substrate n equiv. in 5 mL of CHCl<sub>3</sub> at 80 °C, 16 h. \* **3.1** 5 mol %, 36 h.

Finally, the investigation of the functional group tolerance was pushed a little further. Since decorating substrates with different functional groups can be really fastidious, the approach taken was to add one equivalent of molecules containing various functional groups to see the impact on the yield of a working reaction. This approach had been previously reported by the Grubbs group in the context of the catalytic silylation of heteroarenes<sup>150</sup> and allows a faster and often more complete screening of the impact of different functional groups on the catalytic system. However, this method does not guarantee that all substrates with one or more of the compatible functional groups will work in the catalytic system. Functional groups induce electronic and steric effects and the test reaction chosen

is often one that works best, which in our case was the borylation of *N*-methylpyrrole. If the functional group induces slow degradation of the catalyst, the relative rate of the desired reaction can be faster in the screening test, but slower for an actual substrate of interest containing that function. Since the method allows to get information rapidly, I think it counterbalances its slight imprecision. The functionalities that were tolerated in that test are aromatic and aliphatic halides, hindered tertiary amines, and ethers. Protecting groups such as Boc, acetal, as well as epoxides, nitro groups and less hindered tertiary amines inhibited the reaction, but did not completely shut it down. Finally, alkenes, alkynes secondary amines, carbonyl, and cyano groups completely shut down catalysis. The test also showed that the incompatibility of thiophene was not coming from catalyst inhibition, but that the incompatibility of benzofuran was. These observations are not surprising considering the catalyst bears a  $\text{-BH}_2$  moiety. This functional group is sensitive to protic groups, to hydroboration, and can interact with a small Lewis base.





Additive	Yield(%)	Entry	Additive	Yield(%)
-	95	12		48
	4	13		88
Ph—C≡C—Ph	0	14	THF	98
PhF	>99	15	DMF	0
PhCl	93	16		12
	90	17		31
Br-(C) <sub>10</sub> -Br	88	18		68
Ph <sub>3</sub> N	92	19		64
Ph <sub>2</sub> NH	0	20	PhCF <sub>3</sub>	94
	0	21	HMPA	87
	0	22	TMEDA	24

**Figure 32** Functional group tolerance study results for the borylation of *N*-methylpyrrole using **3.1** as catalyst.

This new catalytic C-H borylation system was certainly fundamentally interesting, bringing new concepts into the FLP reactivity, and more broadly to the field of metal-free catalysis. However, it was only the first stage of development and suffered from important drawbacks compared to metal catalyzed C-H borylation systems. C-H functionalization can be particularly interesting at two steps of chemical production, with different criteria for a good catalyst. First, it can be used to rapidly expand the diversity of compounds in the discovery phase. At the same time, it can cut down the

number of steps in synthesis optimization for larger scale production. In the discovery phase, substrate scope and functional group tolerance is often a priority because the target molecules are diverse and highly functionalized. However, yield, cost, selectivity, and reaction conditions are not important factors. In process chemistry, yield and selectivity are very high on the list of criteria, while cost and practicability come close behind. On larger scale, two simple steps can be better than a complicated one and purification and waste management can cause more trouble than the transformation itself.

The substrate scope of our new FLP catalyst was very limited. Only protected pyrroles, indoles, furans and electron rich thiophenes can be borylated. Those heterocycles have some interest in metal-free transformations, in particular indole, which is an abundant heterocycle in biologically active molecules,<sup>151</sup> and thiophene derivatives that are broadly used in conjugated polymers.<sup>152</sup> In comparison, after now more than 15 years of development,<sup>89,153</sup> the most performant borylation system<sup>154,155</sup> based on iridium can borylate almost anything including benzenic cycles,<sup>156</sup> cyclopropanes,<sup>157</sup> pyridines<sup>158</sup> and other heterocycles<sup>159–161</sup> with TON up to 20 000<sup>162</sup> and usually with a sterically directed selectivity.<sup>90,163</sup> Using silyl or other directing groups, it can achieve selective borylation of indoles at the C3<sup>164</sup> or C7<sup>165</sup> positions, and *ortho* or *peri* selective borylation of phenol,<sup>166</sup> aniline<sup>167</sup> and other aryl derivatives.<sup>168,169</sup> In some specific cases, the borylation can even be done in an enantioselective fashion.<sup>170</sup> More recently developed base metal catalysts, notably using cobalt,<sup>98,147,171–173</sup> can also borylate a much broader range of substrates, being particularly efficient for fluorinated arenes.<sup>99,174</sup> As such, our new FLP catalyst is not very impressive and the only interesting functional groups tolerated are halides. While they are, with the exception of fluorine, problematic for most first row transition metal systems, the iridium catalysts usually tolerate them quite well.<sup>90</sup> In our case, selectivity has not been studied in detail yet, but it seems to be guided by electronic factors, with a preference for the carbon nucleophilicity, which could be an advantage in some cases when compared to the iridium catalysts whose selectivity is usually guided by steric factors when no directing groups are present. The cost of the catalyst is also hard to evaluate at this stage, but you would expect that a metal-free catalyst has the potential to be much cheaper than one based on a precious metal. Finally, metal based systems and **3.1** require moisture and oxygen free conditions during the course of the reaction, but air-stable precatalysts have been developed for both the cobalt and iridium systems to facilitate storage and reaction setup. In the case of the iridium system, the precatalyst and ligand are even commercially available. A lot of work and development was still to do before that newly reported FLP catalyzed C-H borylation system could be compared seriously with the best catalysts in the field. Some improvements of this catalytic system will be presented in the next section, which eventually led to the development of a new system that will be presented in the last chapter of the thesis.

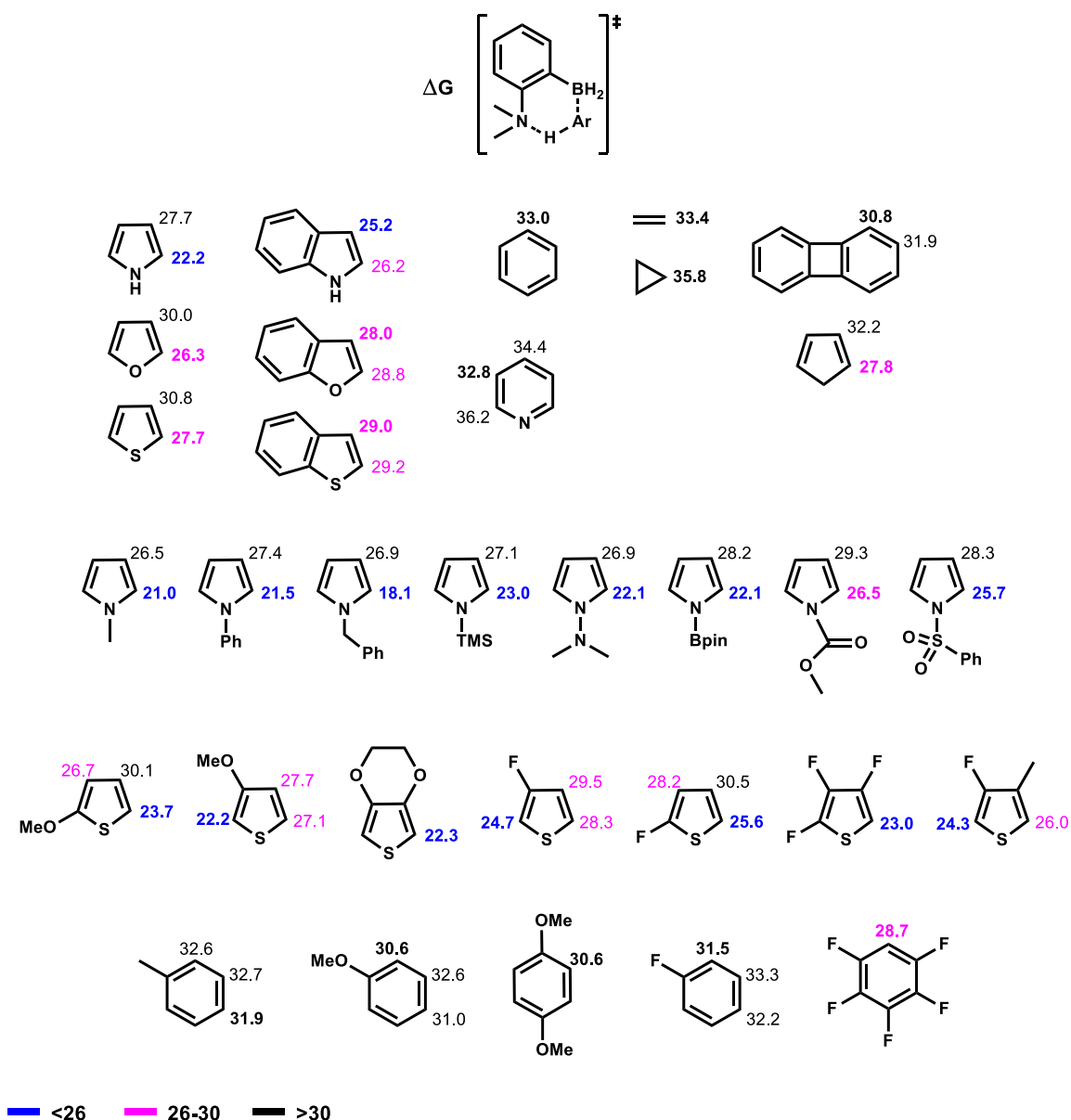
### 3.1 Improvements on the C-H borylation system

#### 3.1.1 Initial objectives and ideas

As noted at the end of the previous section, the initial report of a FLP catalyzed C-H borylation was only the beginning of the story. After our report, the two major objectives we set to improve the system were: 1) expanding the substrate scope and 2) improving the practicability of the system, notably by developing air-stable pre-catalysts and/or simpler catalysts.

Before going into details on how we thought and tried to improve the system, I think it would be advisable to define the targets more accurately, in particular concerning the substrate scope, the major improvement we were aiming. To qualitatively rank substrates according to the difficulty to cleave their C-H bonds, the transition state energies were calculated using DFT for a variety of arenes and heteroarenes (**Figure 33**). Obviously, more substrates were added over time and the figure presented is the product of the last update. The study was carried using  $[\text{NMe}_2\text{-C}_6\text{H}_4\text{-BH}_2]_2$  (**3.3**) as a model catalyst in order to reduce the computational time and minimize the effect of steric hindrance on the calculated transition state energy. Quite interesting results came out of this investigation. First, unsurprisingly, the substrates that gave the best experimental results, notably *N*-methylpyrrole and alkoxythiophenes, had amongst the most energetically accessible transition states (between 22 and 24 kcal/mol). Furans and indoles, other experimentally compatible substrates, were a little bit higher (25-26 kcal/mol) on the energy scale. Substrates that have transition state energies slightly too high to borylate include unsubstituted thiophene and benzene at 27.7 and 33.0 kcal/mol, respectively. Significant improvements of the system would be required for functionalization of these substrates to happen. However, the most interesting observation was certainly that electron donating (alkoxides in particular) and electron withdrawing groups (fluorine in particular) both tend to reduce the transition state energy, suggesting that both carbon nucleophilicity and C-H bond acidity are important factors in a substrate compatibility. Fluorinated thiophenes, heteroarenes of growing interest in organic electronics,<sup>175-177</sup> are calculated to have surprisingly accessible cleavable C-H bonds, I say surprisingly because we have never been able to functionalize these substrates. Retrospectively we

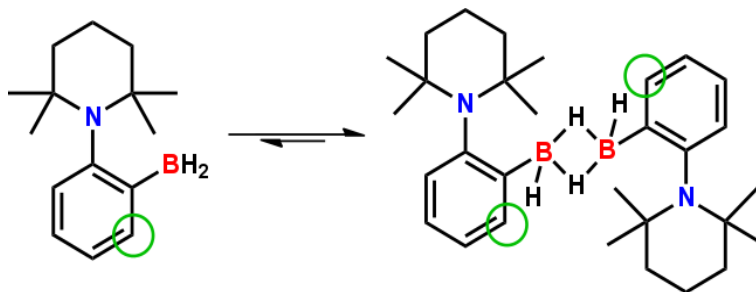
know that something else than C-H bond cleavage influence the borylation of these substrates, but it took more catalyst design to find the exact reason, which will be discussed later in the chapter.



**Figure 33**  $\Delta G$  (kcal/mol) for the C-H cleavage transition state between **3.3** and a variety of arenes and heteroarenes. Calculations performed at the  $\omega$ B97XD/6-31+G\*\* level of theory.

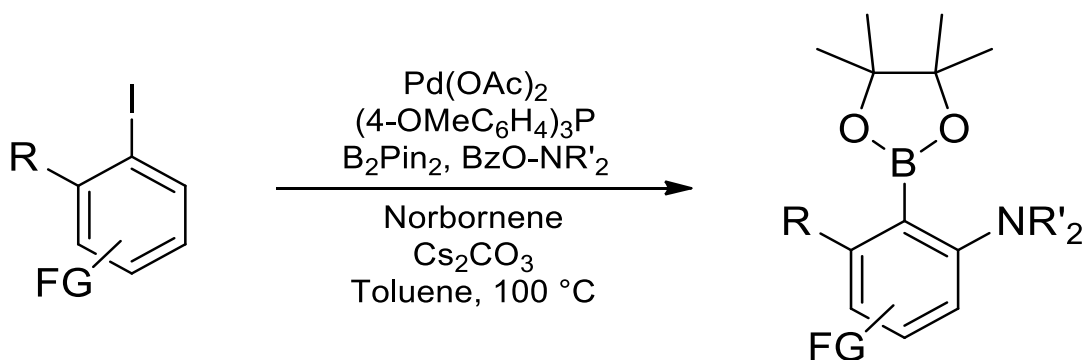
The first idea to improve the system was to find a way to destabilize the dimeric form of the catalyst and to favor the monomer. By doing so, we were hoping to make the C-H bond cleavage transition state, which was shown to be limiting in our mechanistic study of **3.1** catalyzed borylation of *N*-methylpyrrole, more accessible by about 7 kcal/mol, which is a huge kinetic gain. We thought that it would translate in a more active catalyst and a broader substrate scope for the borylation reaction.

Looking at the structure of the dimeric and monomeric forms suggested that the position *ortho* to the boron atom could potentially generate steric repulsions favoring the monomeric form (**Figure 34**). However, it looks much better on the two-dimension of paper than in reality.



**Figure 34** Potential of *ortho*-to-boron-substituted catalysts to favor the monomer.

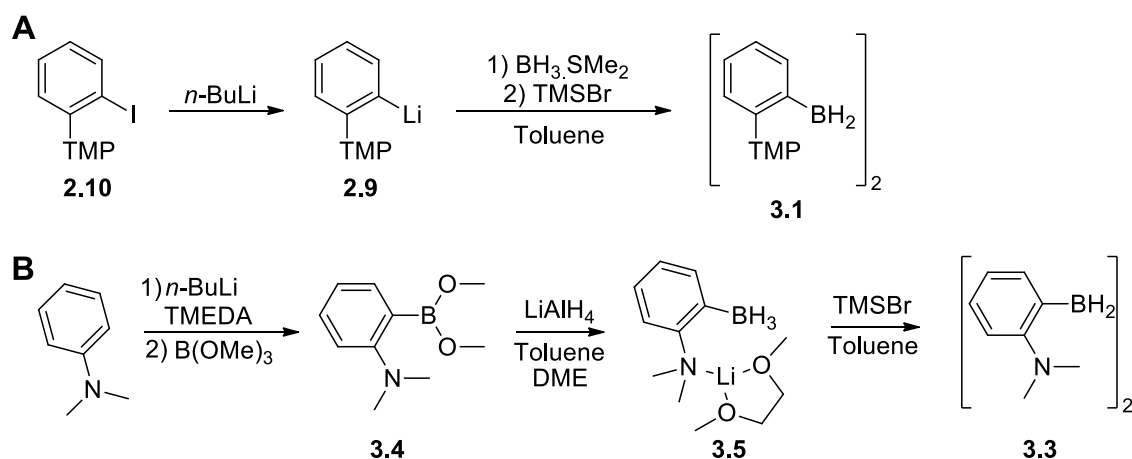
With surprisingly good timing, the Ritter group reported a straightforward way to synthesize this type of molecule using a one-step Catellani coupling<sup>178</sup> and it was decided to explore this avenue. Since, most of this chemistry was performed by Nicolas Bouchard, initially under the supervision of Marc-André Légaré, I will not go into much details on this project, but since I was solving the X-ray structures I ended collaborating on it.



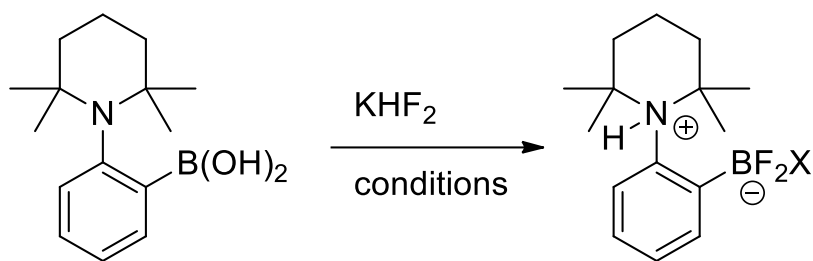
**Scheme 8** General aminoborane synthesis reported by the Ritter group.

### 3.1.2 Discovery of bench stable pre-catalysts

In addition to work on the C-H borylation reactivity with species  $[\text{TMP-C}_6\text{H}_4\text{-BH}_2]_2$  (**3.1**), I was using  $[\text{NMe}_2\text{-C}_6\text{H}_4\text{-BH}_2]_2$  (**3.3**) for alkyne hydrogenation studies, which will be discussed in Chapter 4. As already discussed, the synthesis of **3.1** goes by the direct reaction of  $\text{BH}_3\cdot\text{SMe}_2$  with **2.9** followed by the addition of  $\text{TMSBr}$ . The synthesis of **3.3** is somewhat different with as key step the reaction of  $\text{NMe}_2\text{-C}_6\text{H}_4\text{-B(OMe)}_2$  (**3.4**), a precursor that can be synthesized up to a 50 g scale, with  $\text{LiAlH}_4$  to form  $\text{NMe}_2\text{Li-C}_6\text{H}_4\text{-BH}_3\cdot\text{DME}$  (**3.5**), a reaction inspired by Wagner and coworkers.<sup>179</sup> However, in the *ortho*-to-boron-substituted catalyst project, only pinacol boronic esters could be made when using the Catellani coupling reaction (**Scheme 8**). This was problematic since the boronic esters are harder to convert to the active  $-\text{BH}_2$  form using  $\text{LiAlH}_4$ . We discovered at some point that it was possible to generate the trifluoroborate analogues from the boronate esters, which could then be activated with  $\text{HBPi}$  to generate active catalysts. Since the synthesis of aryl trifluoroborate salts is straightforward (**Scheme 10**), to be rigorous I decided to synthesize the trifluoroborate analogues of our initial C-H borylation catalyst and test if those species can be active precatalysts.

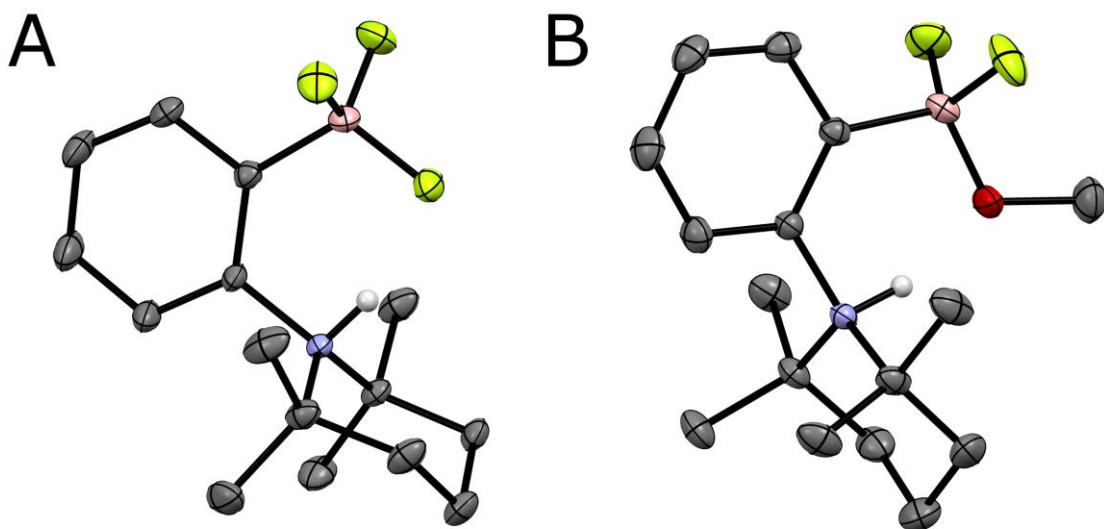


**Scheme 9** **3.1** Synthesis (A) vs **3.3** synthesis (B).



- 3.6**, X = F: THF/H<sub>2</sub>O, 60°C; Yield : 92%  
**3.7**, X = OMe: MeOH, HCl<sub>(aq)</sub> r. t.; Yield : 90%  
**3.8**, X = OH: THF/H<sub>2</sub>O, r. t.; Yield : 87%

**Scheme 10** Synthesis of **3.6-3.8**, fluoroborate analogue of **3.1**.



**Figure 35** A) Crystal structure of **3.6**. B) Crystal structure of **3.7**. Ellipsoids drawn at 50% probability level. Hydrogen atoms linked to carbon were omitted for clarity. Grey = C, blue = N, pink = B, Yellow = F, Red = O, White = H.

As previously stated, the synthesis of aryl trifluoroborate salts is straightforward by treating the corresponding boronic acid or ester with excess KHF<sub>2</sub> in aqueous or alcoholic solvents. The solubility of the product in polar organic solvents, such as chloroform or acetone, is usually sufficient to separate the desired products from the inorganic side-products and unreacted KHF<sub>2</sub>. The only down side of this transformation is the fact that KHF<sub>2</sub> can etch the glassware. While successful, the synthesis of the desired derivatives did not go exactly as planned. First, we obtained the protonated amine instead of the potassium salt (**3.6**). More importantly, depending on the conditions, analogous methoxy (**3.7**) or hydroxy (**3.8**) derivatives were obtained instead of the trifluoroborate derivatives. In addition to the <sup>1</sup>H NMR signal associated to the methoxy or hydroxy moieties, those species can easily be

differentiated from the trifluoroborate derivative by looking at the  $^{11}\text{B}$  NMR spectra, which exhibit a triplet for **3.7** and **3.8** and a quartet for **3.6**, because of the B-F coupling. These species were also characterized by mass spectrometry and in some cases by X-ray crystallography. This change in reactivity is attributed to the FLP nature of the  $\text{TMP-C}_6\text{H}_4\text{-BF}_2$  intermediate that can form adducts with alcohol or water, as discussed in Chapter 2 in the case of  $\text{TMP-C}_6\text{H}_4\text{-BBN}$  (**2.7**). These adducts can be viewed as the kinetic products of the reaction. Simply heating at 60 °C is enough to make the reaction go to the trifluoroborate derivative, which is the thermodynamic product. This was further supported by DFT calculations on the stability of those adducts (**Table 2**) which shows that indeed, the HF adduct should be thermodynamically more stable than the methanol or water adducts.


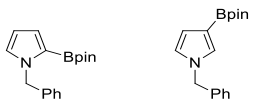
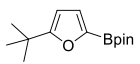
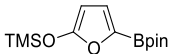
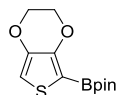
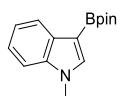
**Table 2** Computed binding energies of small molecules by a  $\text{TMP-C}_6\text{H}_4\text{-BF}_2$  FLP. Calculations performed at the  $\omega\text{B97XD/6-31++G**}$  SMD solvent = chloroform level of theory.

Species	$\Delta\text{H}$ (kcal/mol)	$\Delta\text{G}$ (kcal/mol)
$\text{TMPBF}_2$	0	0
$\text{TMPBF}_2 + \text{HF}$ ( <b>3.6</b> )	-36.1	-26.5
$\text{TMPBF}_2 + \text{MeOH}$ ( <b>3.7</b> )	-31.4	-18.4
$\text{TMPBF}_2 + \text{H}_2\text{O}$ ( <b>3.8</b> )	-28.0	-17.4

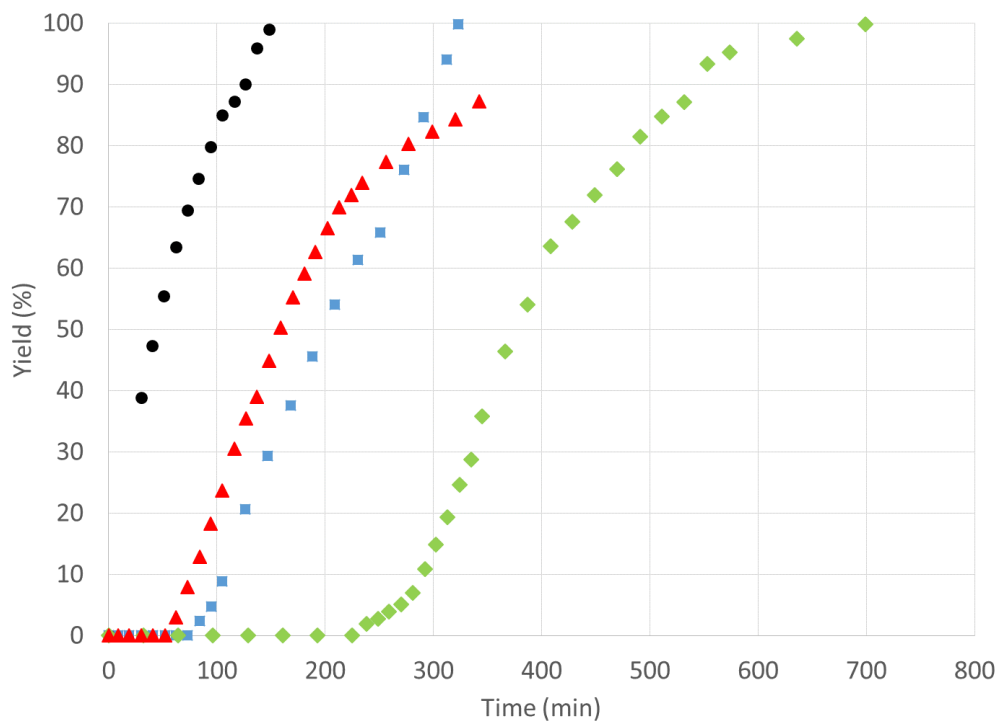
While these observations are trivial, the interesting part was that those three derivatives were competent air-stable precatalysts for the C-H borylation. After the initial proof of concept, further substrate scope and methodological studies were carried out with the help of Marc-André Légaré and Julien Légaré Lavergne, and it was demonstrated that the fluoroborate derivatives, **3.7** in particular, promote the C-H borylation reaction as well as **3.1** for a representative scope of substrates. However, the use of a glovebox was not required to store the precatalyst nor to setup the reaction.



**Table 3** Yield comparison for representative substrates using **3.1** and **3.7**.

Product	Yield <b>3.7</b> , (%)	Yield <b>3.1</b> (%)
 88:11	85	93
 3:2	78	90
	70	86
	94	84
	96	87
	81	85

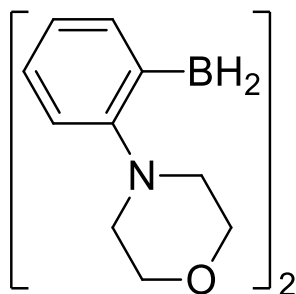
Some efforts were also oriented toward understanding the nature and formation of the active species. Attempts at observing direct evidences of the formation of **3.1** from the reaction of **3.7** and HBPIn were tried by NMR spectroscopy, but were not very convincing because of overlapping signals and the presence of several intermediate species that could not be isolated and characterized. The most informative experiment was certainly the rate of product formation during a catalytic run (**Figure 36**). That experiment shows a clear induction period for the fluoroborate derivatives, highlighting their nature as precatalysts. Moreover, when the catalysis takes off, the rate is very similar to the one observed using **3.1**, suggesting that our initial assumption that the  $\text{-BH}_2$  derivative is the active species is reasonable. Finally, the longer induction period for the trifluoro derivative **3.6** compared to the methoxy and hydroxy derivatives **3.7** and **3.8** suggests that the first “deprotection” step is kinetically limiting. In the end, our attempts to determine a more precise picture for the deprotection, in particular for a concerted transition state, using DFT fell short and we settled on the reasonable hypothesis that a simple anionic abstraction by HBPIn was the first and limiting step of the deprotection.



**Figure 36**  $^1\text{H}$  NMR monitoring of the borylation reaction of 1-methylpyrrole catalyzed by amphiphilic fluoroborate salts using HBPIn. Conditions: The precatalyst (0.01 mmol) was mixed with HBPIn (0.195 mmol), 1-methylpyrrole (0.195 mmol) and hexamethylbenzene (internal standard) in 0.4 mL  $\text{CDCl}_3$  under a  $\text{N}_2$  atmosphere. The reaction mixture was introduced to a J-Young NMR tube and followed by  $^1\text{H}$  NMR (400 MHz) at 80  $^\circ\text{C}$ . Legend: 3.1 (●), 3.6 (◆), 3.7 (▲), 3.8 (■).

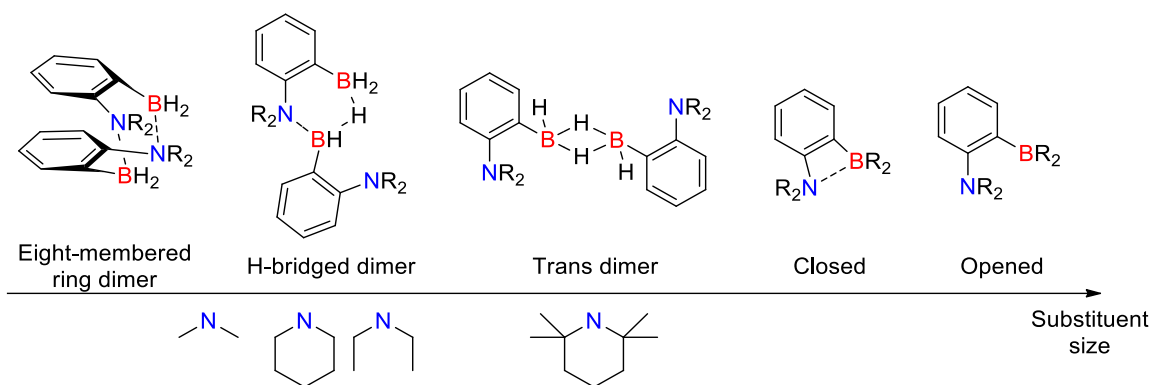
### 3.1.3 Derivatives comporting less hindered amino group

Those trifluoroborate protected precatalysts certainly helped the practicability of the system, but it did nothing to expand the activity and the substrate scope of the catalyst, which was our major goal. Some efforts had previously been made toward optimizing the amine substituent of the catalyst, but with very limited synthetic success. In fact, only the NMe<sub>2</sub> derivative (**3.3**) had been successfully synthesized and characterized, but was showing quite limited activity for C-H borylation. Most efforts, especially from Julien Légaré Lavergne, had been put toward the synthesis of a morpholino derivative (**Scheme 11**) in order to compare it to the *ortho*-substituted derivatives that were being synthesized using the powerful, but specific, Catellani reaction that was only working with morpholine substrates.



**Scheme 11** Structure of the targeted morpholino derivative.

However, the reaction to form the borohydride using LiAlH<sub>4</sub> did not work well with the morpholino derivatives. We later hypothesized that it could come from the ether function of the morpholino moiety that could coordinate the lithium or aluminum salts and complicate the purification. A lot of DFT work was being done on the *ortho*-substituted derivatives which predicted that they would be better catalysts, or at least better for the C-H bond cleavage step. However, at some point it became less clear to me that the increase reactivity was because of the *ortho*-substituent and not of the less hindered morpholino derivatives. It is fair to say that at that time my project (the Csp<sup>3</sup>-H bond cleavage that will be discussed in Chapter 5) was not giving a lot of interesting results and that I was easily distracted. This prompted me to reinvestigate the amine substituent size effect using DFT, which eventually led to **Figure 37** and **Table 4**.



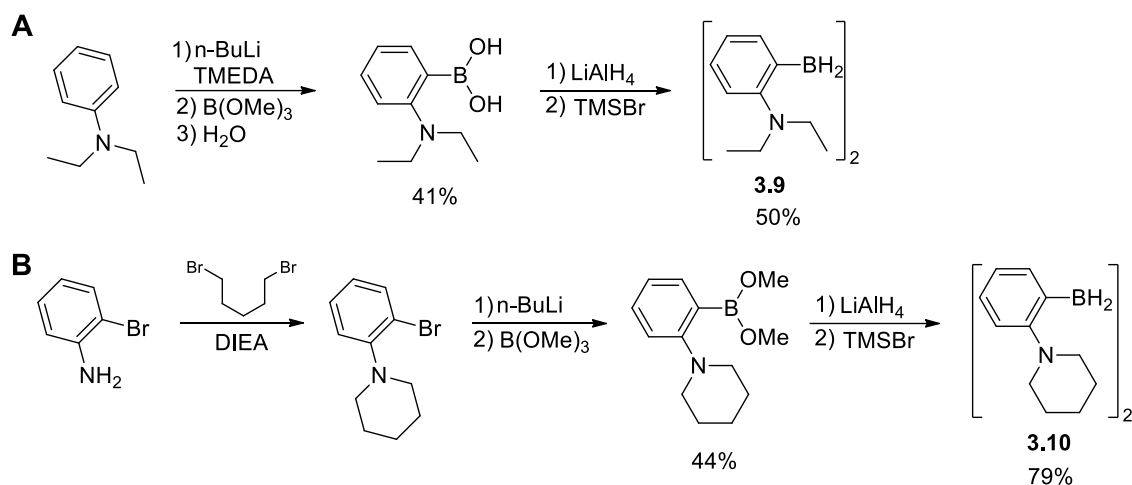
**Figure 37** Different possible dimeric forms of amino-hydroboranes.

**Table 4** DFT calculated  $\Delta G$  (kcal/mol) of amino-hydroboranes bearing different amine substituents in different dimeric form and  $\Delta G^\ddagger$  (kcal/mol) of the C-H bond cleavage transition state for *N*-methylpyrrole and thiophene. Calculations performed at the  $\omega$ B97XD/6-31+G\*\* (SMD, solvent = chloroform level of theory.

Amine	8-Membered Ring	H-Bridged	Trans	Closed	Opened	TS-Pyrrol	TS-Thio	
NMe <sub>2</sub>	1.2	<b>0</b>	6.2	4.2	10.7	21.1	26.8	
Piperidine	2.6	<b>0</b>	2.6	0.1	8.3	17.0	23.4	
NEt <sub>2</sub>	2.3	<b>0</b>	2.0	2.5	7.0	20.4	24.7	
TMP	nd	15.8	<b>0</b>	5.4	7.1	24.4	28.0	

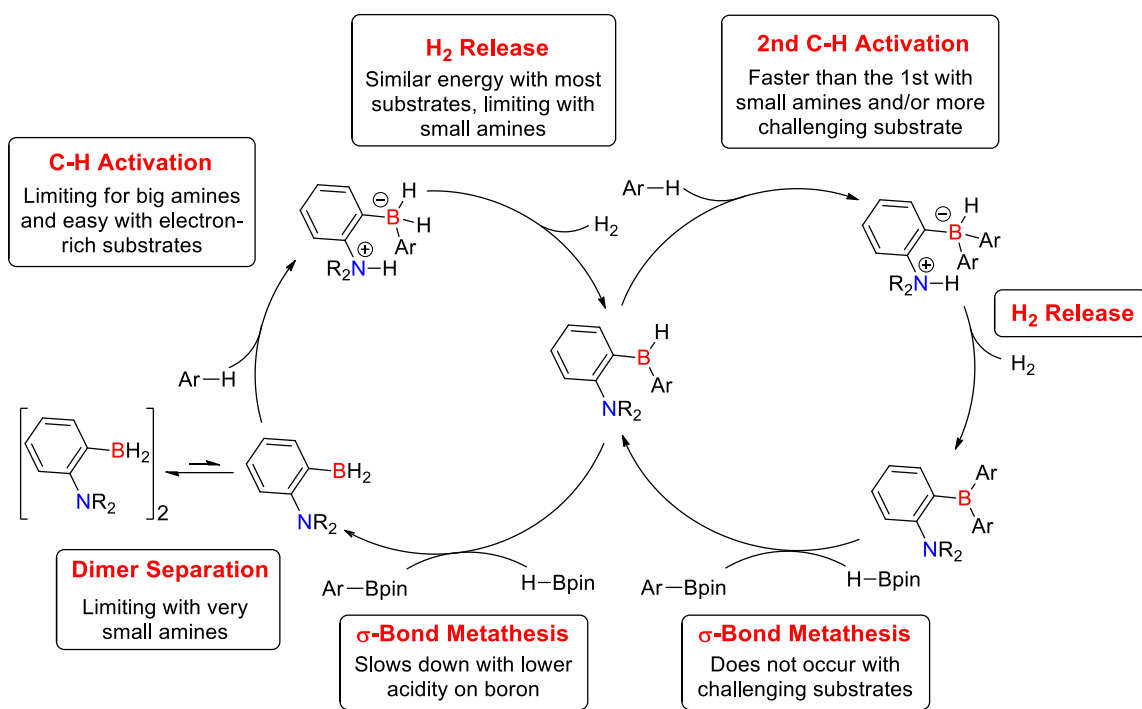
There is a lot of important information in these data. First, the data did show the most stable dimeric species for various  $[\text{NR}_2\text{-C}_6\text{H}_4\text{-BH}_2]_2$  species. In the case of the TMP derivative described earlier in this chapter, the most stable dimer contain two 3-center-2-electron bonds (or bridging hydrides). We refer to this dimer as *trans*, because of the *trans* arrangement of the phenyl spacer relative to the bridging hydrides, which was used to name this compound in the initial report from the Repo group.<sup>142</sup> As the steric hindrance around the amine moiety is reduced, a new unsymmetrical dimer containing one N-B bond and one bridging hydride (the H-bridged dimer) is usually the most stable species. Finally, with very small amines, a dimer containing two N-B bonds can also exist. All of those dimeric forms need to be taken into account when comparing derivatives with different amine moiety size. The two right columns of the table, with the calculated C-H cleavage transition state free energy for *N*-methylpyrrole and thiophene, contain the most important information. The C-H bond cleavage transition states are predicted to be more accessible for intermediate size amine derivatives (NEt<sub>2</sub> and piperidine). This is in large part what brought back the interest in making those derivatives. Another thing that sparked my interest was reading the paper on fluorescence studies that inspired the initial

aminoborane synthesis, which was reporting  $\text{NEt}_2$  derivatives made directly via an *ortho*-lithiation.<sup>129</sup> Trying their conditions proved successful and quite rapidly led to a working synthesis for  $[\text{NEt}_2\text{-C}_6\text{H}_4\text{-BH}_2]_2$  (**3.9**) that showed increased activity for the catalytic borylation of *N*-methylpyrrole. Encouraged by this success, the piperidine derivative  $[\text{Pip-C}_6\text{H}_4\text{-BH}_2]_2$  (**3.10**) was also synthesized, this time via the brominated analogue (**Scheme 12**), and also proved more efficient for the catalytic borylation of *N*-methylpyrrole. However, surprisingly, both analogues did not prove to be efficient for the borylation of thiophene despite clear evidence that the C-H bond cleavage was happening, strongly suggesting that another step of the mechanism was now limiting.



**Scheme 12** A) Synthesis of **3.9** B) synthesis of **3.10**.

After getting those proofs of concept, it was eventually decided to do an in-depth mechanistic study with those derivatives and because of my workload, my colleague Julien Légaré Lavergne worked on it. Thus, I will not discuss the conclusions in detail, but I will provide a brief summary of the results to facilitate understanding the efforts I made afterward to improve the system.



**Figure 38** Summary of the mechanistic investigation of the amino-hydroborane catalyzed C-H borylation of heteroarenes.

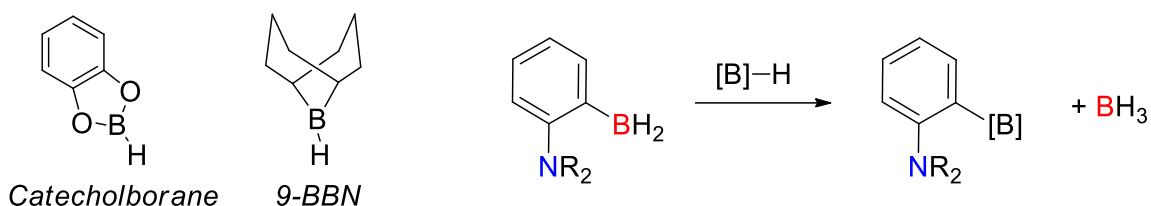
In brief, the mechanistic information summarized in **Figure 38**, mostly gathered by following the kinetics of the stoichiometric and catalytic transformations by NMR spectroscopy, shed light on three important things. First, for the derivative containing the most unhindered amine ( $[\text{NMe}_2\text{-C}_6\text{H}_4\text{-BH}_2]_2$ ), the dissociation of the dimer is kinetically limiting. Secondly, the metathesis step, somehow neglected in our initial study because it was very fast in the case of *N*-methylpyrrole, can be limiting in the case of more challenging substrates such as thiophene. This led to the last realization: a second cycle, starting from the intermediate still containing a B-H moiety, which was previously neglected, can be relevant to the overall activity and can also serve as a deactivation pathway with some substrates since  $\text{NR}_2\text{-C}_6\text{H}_4\text{-BAr}_2$  intermediates are less active for  $\sigma$ -bond metathesis, in part because of increased steric hindrance. This will be explored in more detail in Chapter 6 while discussing the borylation of S-H bonds.

In the end, our focus to improve the catalytic C-H borylation system had switched from improving the C-H cleavage step to improving the  $\sigma$ -bond metathesis step. This was probably the last nail in the coffin for the *ortho*-to-boron-substituted derivative project since having a substituent *ortho* to boron could only disfavor  $\sigma$ -bond metathesis because of increased steric hindrance. As you will see in the next pages, this was also the birth of other studies that unfortunately failed, with the exception of the work on the S-H borylation that will be presented in Chapter 6. Nevertheless, these studies provided

important information and was eventually part of the motivation leading to the development of a new system working via an alternative mechanism that will be presented in Chapter 7.

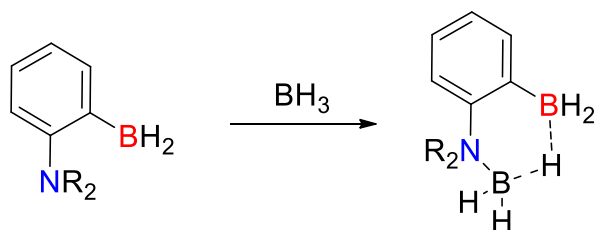
### 3.1.4 Final attempts at improving the system

The first, and probably most obvious, attempt to improve the metathesis step was to use boranes that are more “active” than pinacolborane, such as catecholborane or 9-BBN. While this is less interesting because those boranes are more expensive and the products less stable, it would be a nice way to demonstrate the possibility to perform metal-free C-H borylation of a larger scope of substrates. However, since the backbone of the catalyst is a phenylene moiety and the BH<sub>2</sub> moiety is unhindered, the metathesis with the backbone can happen leading to deactivation of the catalyst, as shown in **Scheme 13**.



**Scheme 13** Catalyst deactivation pathway while using more active hydroboranes as borylating reagent.

A quite clever, or at least that is what I thought, way to work around that problem would be to use BH<sub>3</sub> as the borylating agent. In that case, a metathesis with the backbone would not be deactivating since it would be a degenerative transformation. However, the less hindered catalysts can make strong adducts with the very small BH<sub>3</sub> molecule, which is deactivating them (**Scheme 14**), but not with the most hindered catalyst derivative **3.1**. In that case, some thiophene borylation, around 30 %, could be observed using BH<sub>3</sub> as the borylating agent, but some still unidentified decomposition pathways limit the conversion. Despite our optimization efforts, no conditions were found to significantly improve the conversion.

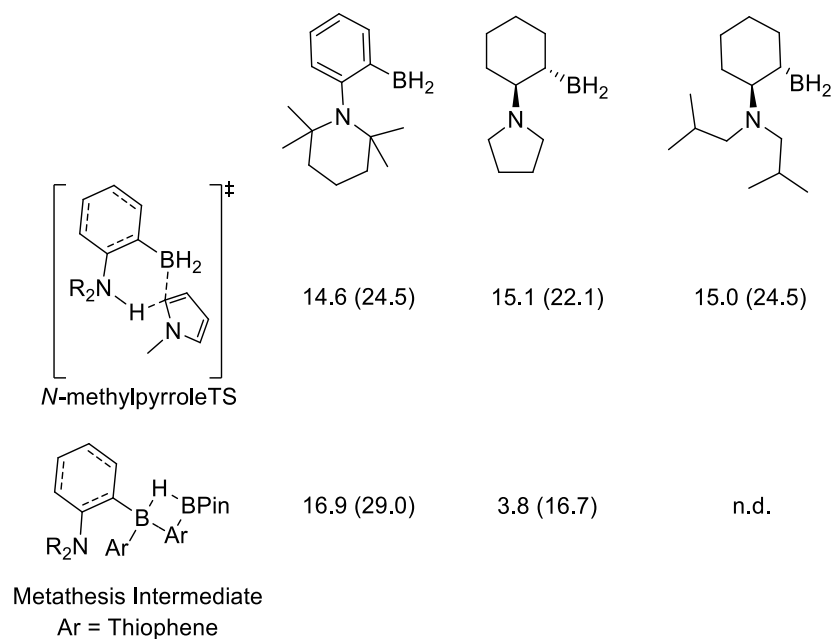


**Scheme 14** Deactivation pathway while using BH<sub>3</sub> as as borylating reagent.

Other efforts to unlock thiophene borylation included the synthesis of derivatives with saturated backbones. Csp<sup>3</sup>-B bonds do not usually participate in  $\sigma$ -bond metathesis, which could prevent the backbone metathesis decomposition pathway and allow the use of more active boranes. Moreover,



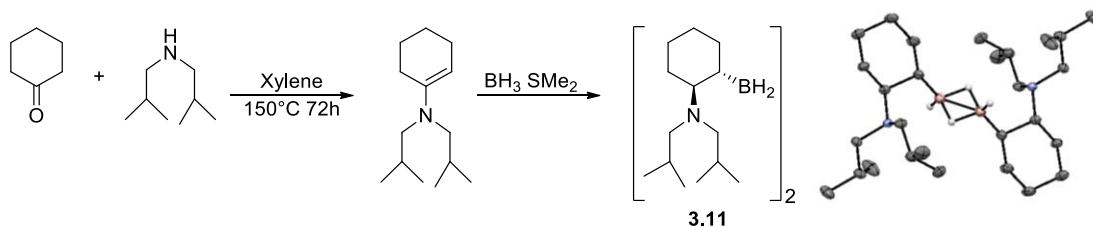
the initial DFT investigation of those derivatives predicted C-H bond cleavage transition states similarly accessible than for our previous catalysts based on a phenylene backbone, but with much more accessible metathesis intermediates (**Figure 39**). This trend is relatively hard to rationalize but may come from geometrical factors or reduced electron donation from the amine through an aliphatic backbone compared to an aromatic one, making the boron atom more acidic in the compounds with a saturated backbone. In all cases, that was enough motivation to synthesize some of those derivatives.



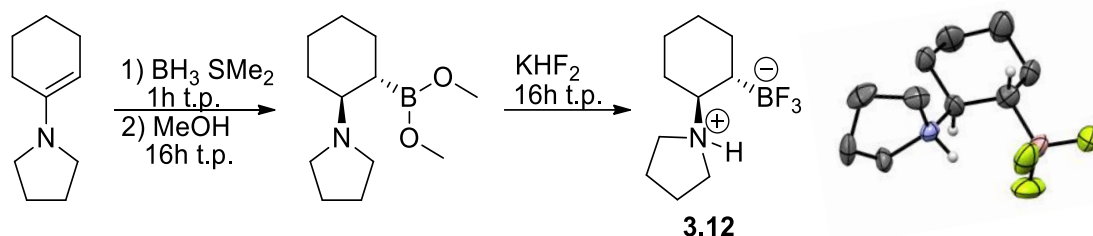
**Figure 39** DFT comparison of amino-hydroboranes catalysts with unsaturated and saturated backbones.  $\Delta G$  reported in kcal/mol, calculations performed at the  $\omega$ B97XD/6-31+G\*\* level of theory.

The planned synthesis of the compound is relatively straightforward. The key step is the hydroboration of an enamine. In some cases, the enamine is commercially available and in some others, it can be easily made by the condensation of the corresponding amine and ketone. The hydroboration of the enamine also worked well in all cases. However, depending on the steric hindrance of the amine substituent, the isolation of the aminohydroborane is not always easy. Indeed, as in the case of derivatives based on a phenylene backbone, different type of dimers can be obtained, which are mainly the *trans* and H-bridged dimers, previously described in **Figure 37**. The synthesis of those dimers present different challenges. Indeed, compounds forming the *trans* dimer usually crystallize well, probably because of its higher symmetry, making them relatively easy to obtain with a very good purity. This was indeed the case for the derivative with a di-*isobutyl*amine moiety (**3.11**) shown in **Scheme 15**. On the other hand, compounds forming the unsymmetrical H-bridged dimer were harder to crystallize. The pyrrolidino derivative was no exception and after some efforts, it was

decided to only synthesize the trifluoroborate analogue (**3.12**), see **Scheme 16**, to test it as a C-H borylation precatalyst, before spending more effort to isolate its active form. In the end however, those derivatives showed only very limited activity for the catalytic C-H borylation, a deception that was attributed to deactivation pathways, mostly via retro-hydroboration, and the project was eventually set aside.



**Scheme 15** Synthesis of  $[\text{NisoBu}_2\text{-C}_6\text{H}_{10}\text{-BH}_2]_2$  (**3.11**).

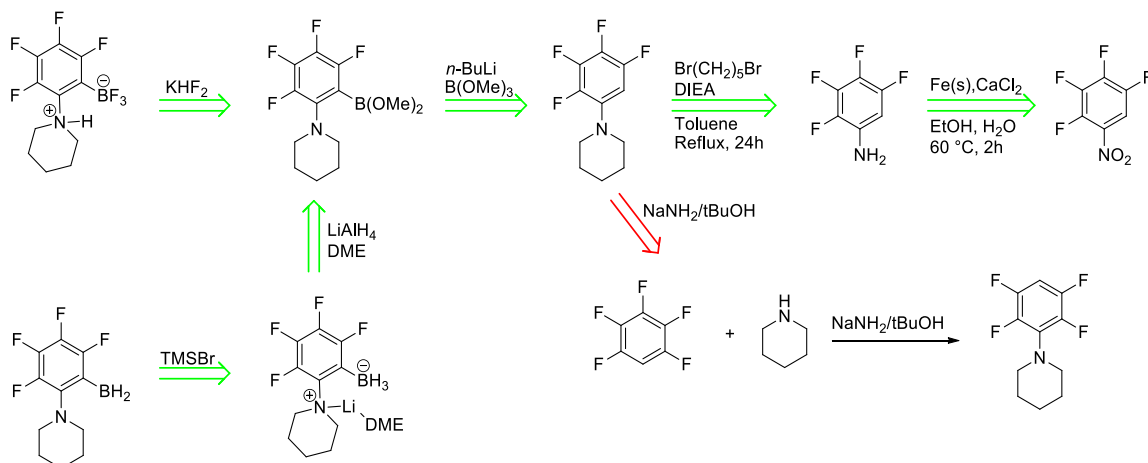


**Scheme 16** Synthesis of  $\text{N}(\text{pyrollidino})\text{H-C}_6\text{H}_{10}\text{-BF}_3$  (**3.12**).

Finally, the last, and quite desperate, attempt to improve the catalytic system came from a debate on the importance of the factors governing the accessibility of the  $\sigma$ -bond metathesis step, more precisely the boron acidity versus the carbon nucleophilicity. A very little difference in boron acidity is expected by changing its aryl substituent from *N*-methylpyrrole to thiophene and it is observed that *N*-methylpyrrole reacts very rapidly compared to thiophene, which points toward carbon nucleophilicity as the main factor governing the  $\sigma$ -bond metathesis step accessibility. Nevertheless, boron acidity was often pointed out as key factor during discussions. Maybe this is simply because, if the problem comes from the substrate, there is not much you can do to improve the substrate scope. Anyway, among the possibilities to increase boron acidity in the hope of accessing the  $\sigma$ -bond metathesis step with more substrates, making a derivative with a fully fluorinated phenylene backbone seemed quite attractive.

Having previously worked on the synthesis of aniline derivatives via benzyne generation using complex base (a mixture of  $\text{NaNH}_2$  and *t*BuOH), a method developed by Caubère<sup>180,181</sup>, I hoped to synthesize the key aniline intermediate using that method. However, it turned out to form another

regioisomer via a competing nucleophilic aromatic substitution mechanism (**Scheme 17**). Nevertheless, it was possible to synthesize that intermediate using a longer, more traditional, pathway starting from the nitro derivative, that can easily be made from 1,2,3,4-tetrafluorobenzene, via reduction and alkylation of the amine. The borylation can afterward be performed via *ortho*-lithiation using the method previously discussed (**Scheme 17**). In the end, this derivative did not show major improvement compared to its non-fluorinated analogue by being quite active for the borylation of *N*-methylpyrrole, but not for the borylation of thiophene.



**Scheme 17** Retrosynthesis of [N(piperidine)-C<sub>6</sub>F<sub>4</sub>-BH<sub>2</sub>]<sub>2</sub> and N(piperidine)(H)-C<sub>6</sub>F<sub>4</sub>-BF<sub>3</sub>.

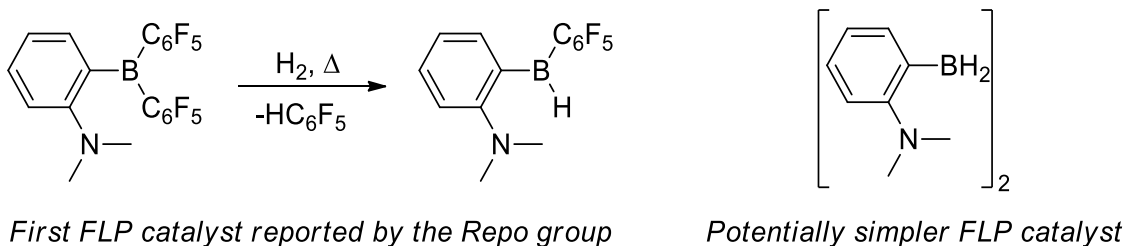
That last unsuccessful effort pretty much ended the attempts at improving the aminohydroborane catalyzed C-H bond borylation system, with the exception of the heterogeneization of the catalyst, a project in which I am not involved, which aims at improving the practicability of the system rather than the actual performance. All other avenues that we could envision to improve the catalytic system have been judged inefficient and abandoned. In the end, it was a nice run from the first evidence of proto-deborylation that inspired the first catalyst to the simpler and more easily synthesized fluoroborate salts and the derivatives containing less hindered amino groups. The kilogram scale-up of the reaction was eventually performed by my colleagues.<sup>182</sup> At this point, major changes are required in order to get significant improvement. A novel system will be described in Chapter 7, but the main project left some offsprings along the way. While I did not want to discuss those detours according to the chronology they happened in order to not over confuse the reader, the importance of those results justify their inclusion in the thesis. Thus, the next chapters will tell stories that happened during the development of the aminohydroborane catalyzed C-H bond borylation system, but I will clarify the literature background, timeline and mindset of these discoveries.

## Chapter 4 From alkyne hydrogenation to B-B bond formation

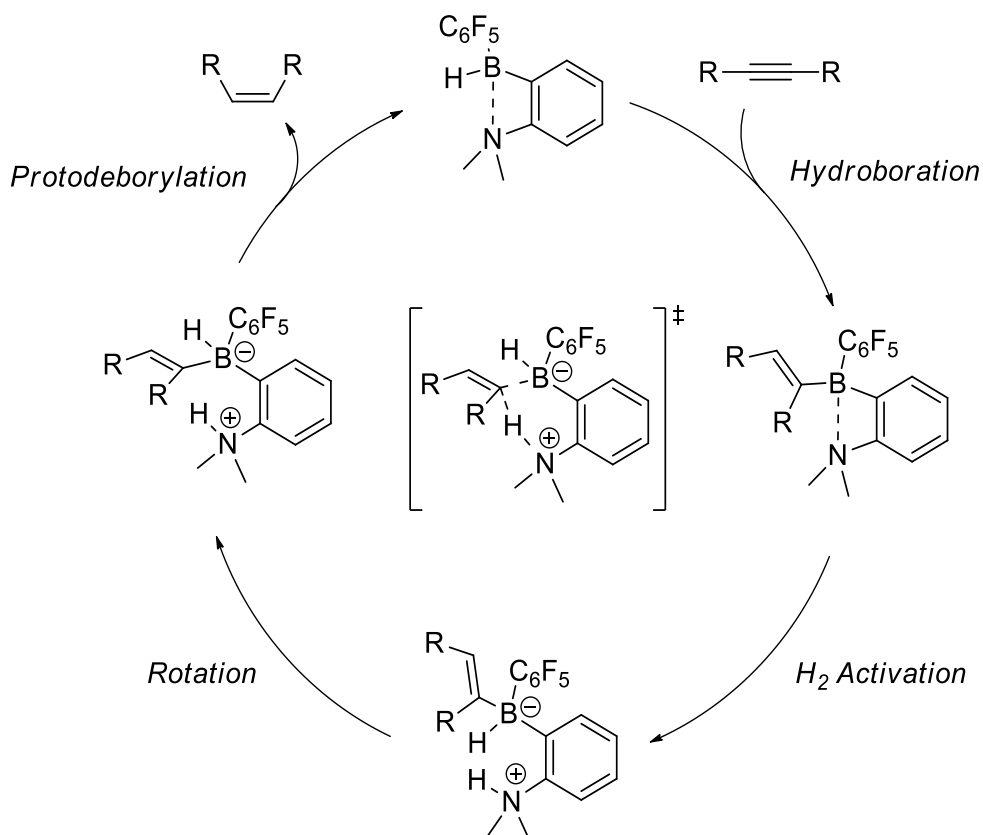
### 4.1 FLP catalyzed alkyne hydrogenation

As mentioned in Chapter 2, the CO<sub>2</sub> reduction project made us rediscover the protodeborylation reaction, which is key in the previously reported by the Repo group<sup>133</sup> FLP catalyzed alkyne hydrogenation. This was of course exploited in Chapter 3 to develop a FLP catalyzed Csp<sup>2</sup>-H borylation system. I also mentioned that at the time most FLP chemistry was carried out using B(C<sub>6</sub>F<sub>5</sub>)<sub>3</sub> or derivatives as Lewis acids and that those substituents, while very popular because they combine high Lewis acidity and steric bulk, are far from being the most practical synthetically. Because the C<sub>6</sub>F<sub>5</sub> group is not cheap, and there are already a lot of people working with it, and to demonstrate that FLP chemistry can be done without very bulky substituents, from its beginning in FLP chemistry, the Fontaine group always stayed away from using typical –B(C<sub>6</sub>F<sub>5</sub>)<sub>x</sub> Lewis acids in favor of simpler ones. Since the initial alkyne hydrogenation system was following the usual trend expected when using B(C<sub>6</sub>F<sub>5</sub>)<sub>3</sub> derivatives as the Lewis acid, we wondered if the same reaction could be performed using easier to synthesize aminohydroborane derivatives as Lewis acids, and **3.3** in particular (**Figure 40**).

### A) FLP Catalysts for alkyne hydrogenation



### B) Proposed mechanism



**Figure 40** A) Initial and potential FLP alkyne hydrogenation catalysts. B) Proposed mechanism for the FLP catalyzed alkyne hydrogenation as reported by Repo and Papai.<sup>133</sup>

In order to get easy access to greater quantities of **3.3**, a more practical synthesis than  $H_2$  induced protodeborylation of aryl groups had to be developed. As I mentioned earlier in Chapter 3, a synthetic pathway starting from *N,N*-dimethylaniline to form **2.8** via an *ortho*-lithiation, a reaction that can be performed on a multi-gram scale, followed by  $LiAlH_4$  addition was eventually developed (**Scheme 9 B**).

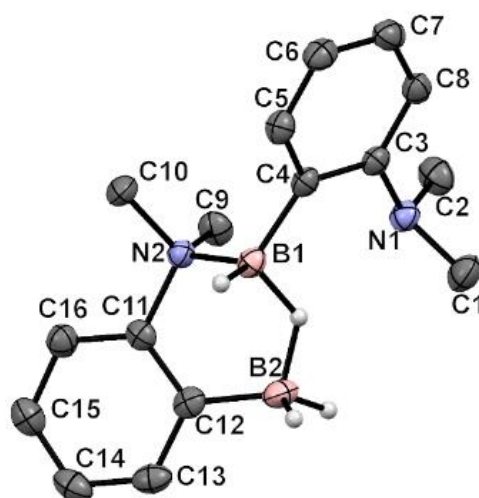
This synthetic pathway could be carried out on 1 g scale. At larger scale, yield and practicability diminish because of the very viscous reaction medium after the  $\text{LiAlH}_4$  reduction step, leading to the difficulty to remove the solids formed by filtration. The synthesis was also enabled by Schlenk-frit filtration illustrated in **Figure 41**, which allowed faster and more practical filtration under inert conditions and was more adapted than cannula filtration.



**Figure 41** Filtration apparatus used to synthesize **3.3**.

Another interesting choice that was made during the optimization of the reaction is the use of few equivalents of dimethoxyethane (DME) in toluene during the  $\text{LiAlH}_4$  reduction. Our initial reactions were performed in tetrahydrofuran (THF) and worked, but higher salt solubility in that solvent and the less defined coordinating behavior of THF produced more impurities and a product with a viscous aspect that was less practical to work with. A solvent change before the last step, which is the removal of the  $\text{LiH}$  adduct using  $\text{TMSBr}$ , was also required to avoid large amount of salt in the final product. When carried out in toluene only, the very low solubility of  $\text{LiAlH}_4$  inhibited the reaction. A comment made by Kathryn Preuss, while being an external evaluator during another group member thesis defense, on the better crystallinity of DME adducts compared to the THF ones prompted me to try exchanging THF by DME on an isolated batch of the intermediate in order to better characterize it, since obtaining quality crystals of the THF adduct proved very difficult. It worked very well and eventually led me to use few equivalents of DME directly during the synthesis.

The isolation of **3.3** using that new method allowed the first direct observation of a new type of an unsymmetrical dimer, which was dubbed the H-bridged dimer, that we had recently predicted using DFT. I quickly mentioned that type of dimer in Chapter 3 because its discovery was very important in the development of better C-H functionalization catalysts, allowing more accurate DFT predictions, because it is the resting state of most aminoborane derivatives. These unsymmetrical species are very characteristic by NMR spectroscopy. Two  $^{11}\text{B}$  NMR signals are observed at -3.3 and 10.4 ppm. In the  $^1\text{H}$  NMR spectrum, we observed eight resonances corresponding to the aromatic protons, a sharp  $\text{NMe}_2$  signal at 2.7 ppm corresponding to the uncoordinated  $\text{NMe}_2$ , and two broader signals at 2.8 and 3.1 ppm corresponding to the  $\text{NMe}_2$  linked to the boron atom. Eventually, good quality crystals could be obtained and X-ray crystallography confirmed the expected geometry of this species.



**Figure 42** Crystal structure of **3.3**. Gray = C, blue = N, pink = B and white = H. Ellipsoid drawn at 50% probability. Selected bond lengths (Å) and angles (°): N2-B1: 1.615(2), B1- $\mu\text{H}$ : 1.27(2), B2- $\mu\text{H}$ : 1.30(1), B2-C12: 1.584(3), C12-C11: 1.390(2), C11-N2: 1.494(2), C11-N2-B1: 108.7(1), N2-B1- $\mu\text{H}$ : 104.0(7), B1- $\mu\text{H}$ -B2: 123(1),  $\mu\text{H}$ -B2-C12: 108.7(7), B2-C12-C11: 121.9(2), C12-C11-N2: 115.7(1).

Interestingly, heating the species at 80 °C overnight led to the formation of a “new” compound, which we had previously observed from the decomposition of  $\text{NMe}_2\text{-C}_6\text{H}_4\text{-BMe}_2$  (**2.2**) under  $\text{H}_2$  and which had been assigned as a conformer of **3.3** in a symmetrical boat shaped 8-membered ring (**2.11**). For clarity, the 8-membered ring dimer will be named **3.3\*** from now on. At that moment, it was hypothesized that the H-bridged dimer was the kinetic product of the transformation and that heating allowed the formation of the 8-membered ring, the thermodynamic product. However, calculating the relative energy of both dimers using DFT sow doubt on this explanation, the H-bridged dimer being calculated to be slightly favored by 1.2 kcal/mol. Nevertheless, no big deal was made of these

computational results before carrying out the hydrogenation of alkynes since 1.2 kcal/mol is under the DFT accuracy generally accepted.

Early results on the alkyne hydrogenation were encouraging, as shown in **Table 5**. Using 5 mol% of **3.3**, full hydrogenation of diphenylacetylene could be obtained at 80 °C in 48 h using a relatively low H<sub>2</sub> pressure (3-4 atm). Those reactions were performed in a J-Young tube by freezing the tube in liquid nitrogen (77 K) during the H<sub>2</sub> addition. This operation required removing the nitrogen atmosphere of the tube without evaporating the solvent and using the perfect gas equation, a pressure of *ca* 4 atm is theoretically obtained once the tube warms back to room temperature (300 K). Other internal alkynes containing more donating alkyl substituents, such as 1-phenyl-1-propyne and 2-hexyne can also be hydrogenated, but with lower conversion. The terminal alkyne protected by the silyl group 1-phenyl-2-trimethylsilyl showed limited conversion. However, those activities are not impressive compared to the system previously reported by the Repo group, which is able to hydrogenate diphenylacetylene and 2-hexyne under similar conditions in 9 h and 3 h, respectively.<sup>133</sup> It is noteworthy that the substrate scope of the reaction does not include terminal alkynes.

**Table 5** Alkyne hydrogenation results.

Catalyst	Substrate	Time (h)	Conversion (%)
<b>3.3</b>	Diphenylacetylene	20	75
		48	100
<b>3.3</b>	1-Phenyl-1-propyne	18	39
		48	71
		72	80
<b>3.3</b>	2-Hexyne	18	26
		48	56
		72	70
<b>3.3</b>	1-Phenyl-2-trimethylsilylacetylene	18	12
		48	15
<b>3.3</b> LiH•DME <sup>#</sup>	Diphenylacetylene	48	67
<b>3.3</b> *	Diphenylacetylene	48	0
NMe <sub>2</sub> -C <sub>6</sub> H <sub>4</sub> -B(C <sub>6</sub> F <sub>5</sub> ) <sub>2</sub> <sup>‡</sup>	2-Hexyne	3	100
NMe <sub>2</sub> -C <sub>6</sub> H <sub>4</sub> -B(C <sub>6</sub> F <sub>5</sub> ) <sub>2</sub> <sup>‡</sup>	Diphenylacetylene	9	100

5 mol% of catalyst, CDCl<sub>3</sub>, Temperature: 80°C, H<sub>2</sub> Pressure: 3-4 atm

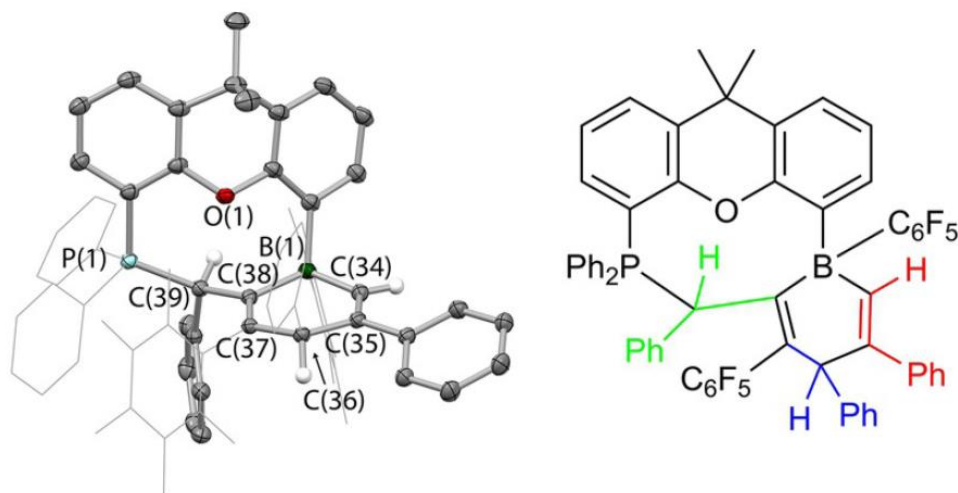
<sup>#</sup>Using 10 mol% NEt<sub>3</sub>•HCl as activator

<sup>‡</sup>Results reported by the Repo group in similar conditions<sup>133</sup>

The incompatibility of internal alkynes is relatively surprising, since all the proposed mechanistic steps should also be compatible with terminal alkynes. Thus, it must come from a degradation



pathway. The easiest to target is the Csp-H bond cleavage of terminal alkynes, a common reactivity pattern well known in FLP chemistry.<sup>69</sup> However, I do not think that it can explain the incompatibility of terminal alkynes in those systems. A Csp-H bond cleavage step, while certainly energetically accessible, is expected to be reversible, especially in presence of molecular hydrogen. Thus, such species could exist, but should not inhibit catalysis. In my opinion, another degradation pathway, probably implicating the insertion of an alkynyl or vinyl boron into an intermediate formed after a Csp-H bond cleavage step, leading to a thermodynamically more stable species, is more likely to be responsible for this incompatibility. Despite our efforts, no further evidence to support this hypothesis could be obtained. However, the behavior of FLP promoted terminal alkyne insertion was recently observed by Aldridge and coworkers as a decomposition pathway while studying alkyne hydroboration (**Figure 43**).<sup>183</sup>

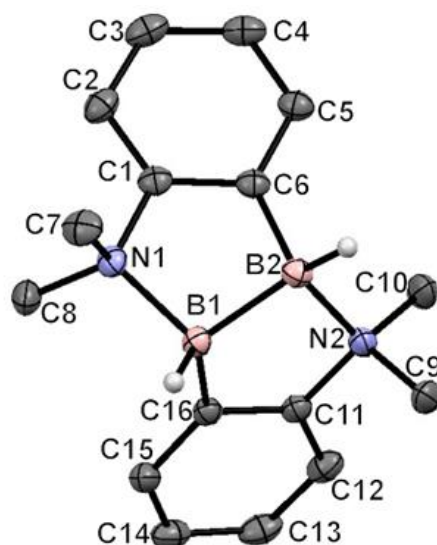


**Figure 43** Multi insertion product characterized by Aldridge *et al.*

Finally, the last comment worth mentioning concerning **Table 5** is that the synthetic intermediate **3.3** LiH•DME is also active for the internal alkyne hydrogenation when activated using the simple acid salt NEt<sub>3</sub>•HCl. This type of adduct, while not strictly air-stable, are more stable toward hydrolysis than the active aminohydroboranes, making them more reliable precursors after prolonged storage. Moreover, its crystallinity make the purification and handling easier. However, the species produced after heating **3.3**, assigned to another dimeric form (**3.3\***) is inactive toward alkyne hydrogenation, which is very surprising considering that both species were calculated by DFT to be very close energetically and that the initial hydroboration of the alkyne is considered a fast step in the catalytic cycle. Ethically, this observation had to be better understood before publishing those results, which in the end we never did, and efforts to get a good quality crystals of this species which had not been successful yet were increased.

## 4.2 The discovery of the diborane ( $\text{NMe}_2\text{-C}_6\text{H}_4\text{-BH}$ )<sub>2</sub>

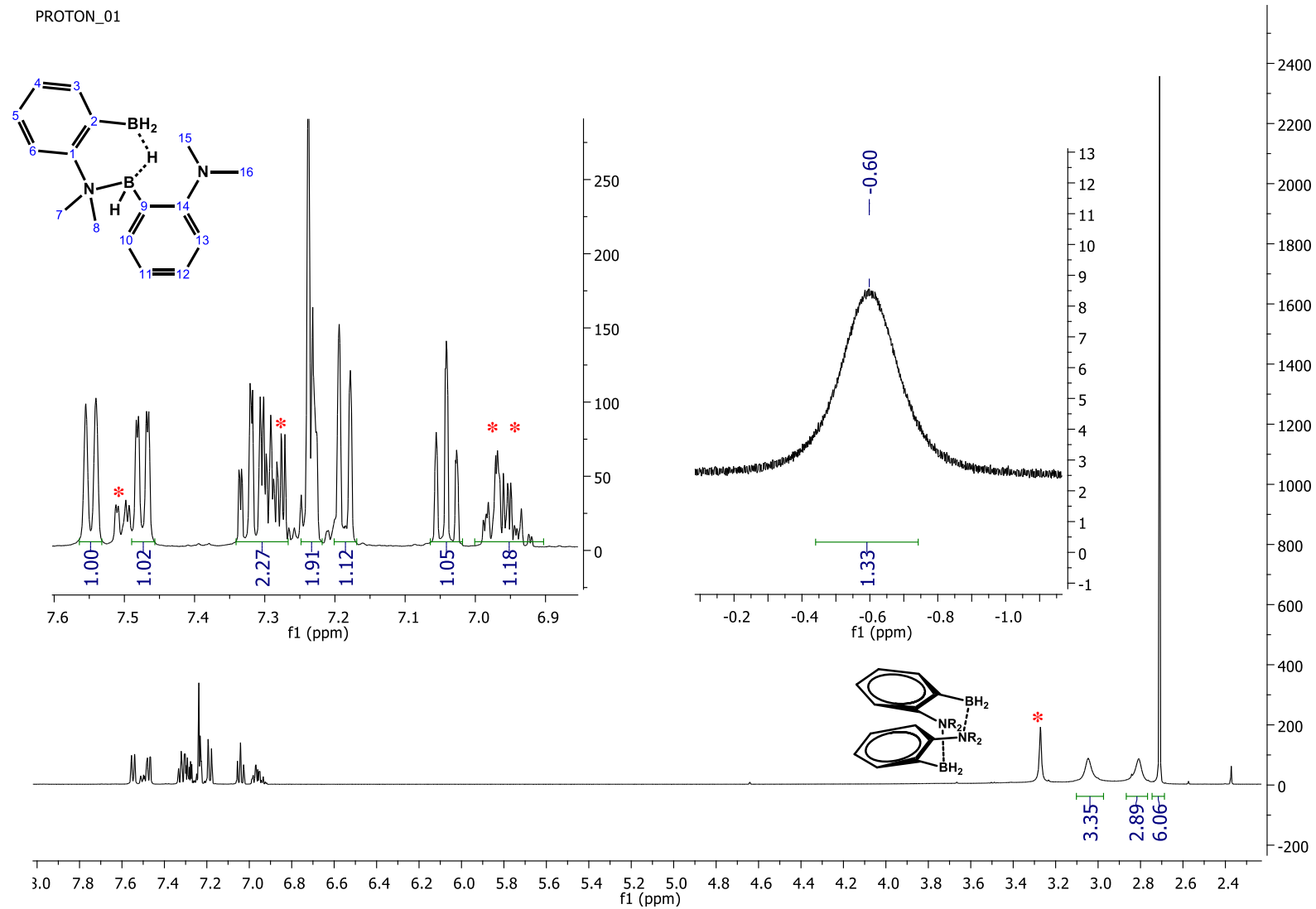
Eventually, small crystals could be obtained from a hexane/toluene mixture and initial crystallographic analysis revealed that they contained a toluene molecule in the unit cell, explaining why that mixture of solvent had to be used. The structure showed that the species produced by heating **3.3** is not the 8-membered dimer **3.3\***, but rather a very surprising molecule containing a B-B bond, ( $\text{NMe}_2\text{-C}_6\text{H}_4\text{-BH}$ )<sub>2</sub> (**4.1**). In order to get better quality data, the crystal was analyzed at the Université de Montréal, equipped with a much more sensitive X-ray diffractometer (equipped with a liquid jet gallium source), which confirmed our initial findings and provided publication level data (**Figure 44**).



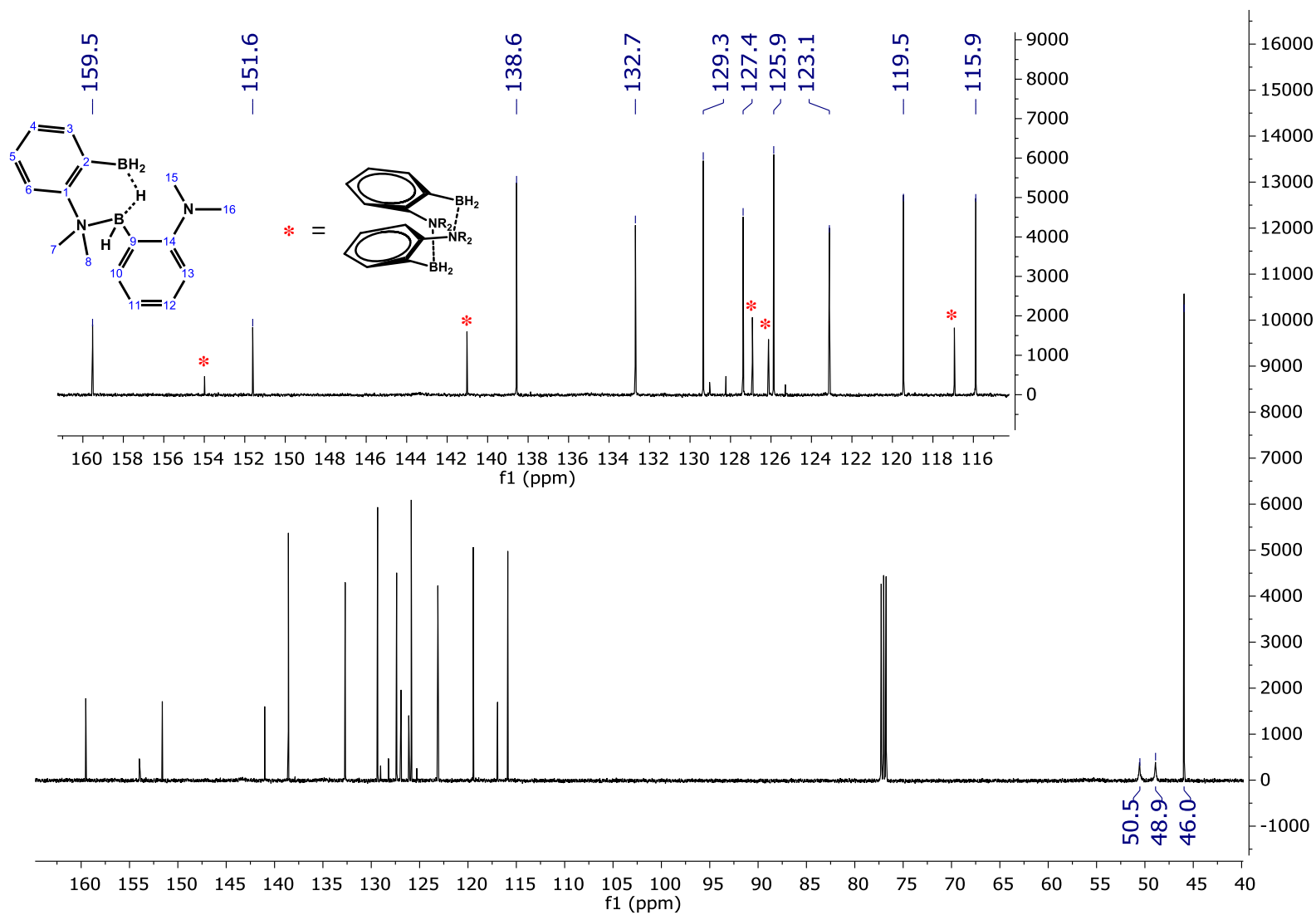
**Figure 44** Crystal structure of **4.1**. Gray = C, blue = N, pink = B and white = H. Ellipsoid drawn at 50% probability. H atom linked to carbon and co-crystallized solvent molecule are omitted for clarity. Selected bond lengths (Å) and angles (°): B1-B2: 1.740(2), N1-B1: 1.671(2), N2-B2: 1.677(1), N1-B1-B2: 101.42(8), B1-B2-N2: 101.20 (8).

Obviously, this discovery changed our understanding of aminohydroborane chemistry and explained many unexpected results observed and discussed previously. It also prompted us to reanalyze old data and revealed interesting things previously missed. The most interesting is the reinvestigation of the **3.3** NMR data (**Figure 45-Figure 47**), which revealed the presence of a previously missed impurity in a recrystallized sample, a compound that cannot be associated to the H-bridged dimer **3.3** nor the diborane **4.1**. With the previously discussed DFT data predicting a very small energy difference between **3.3** and **3.3\***, we hypothesized that the impurity might not be an impurity, but rather an equilibrium between both species. Careful analysis of the NMR data supported this hypothesis, since the signals of a species analogous to **3.3\*** were found on the <sup>1</sup>H, <sup>13</sup>C and <sup>11</sup>B NMR spectra.

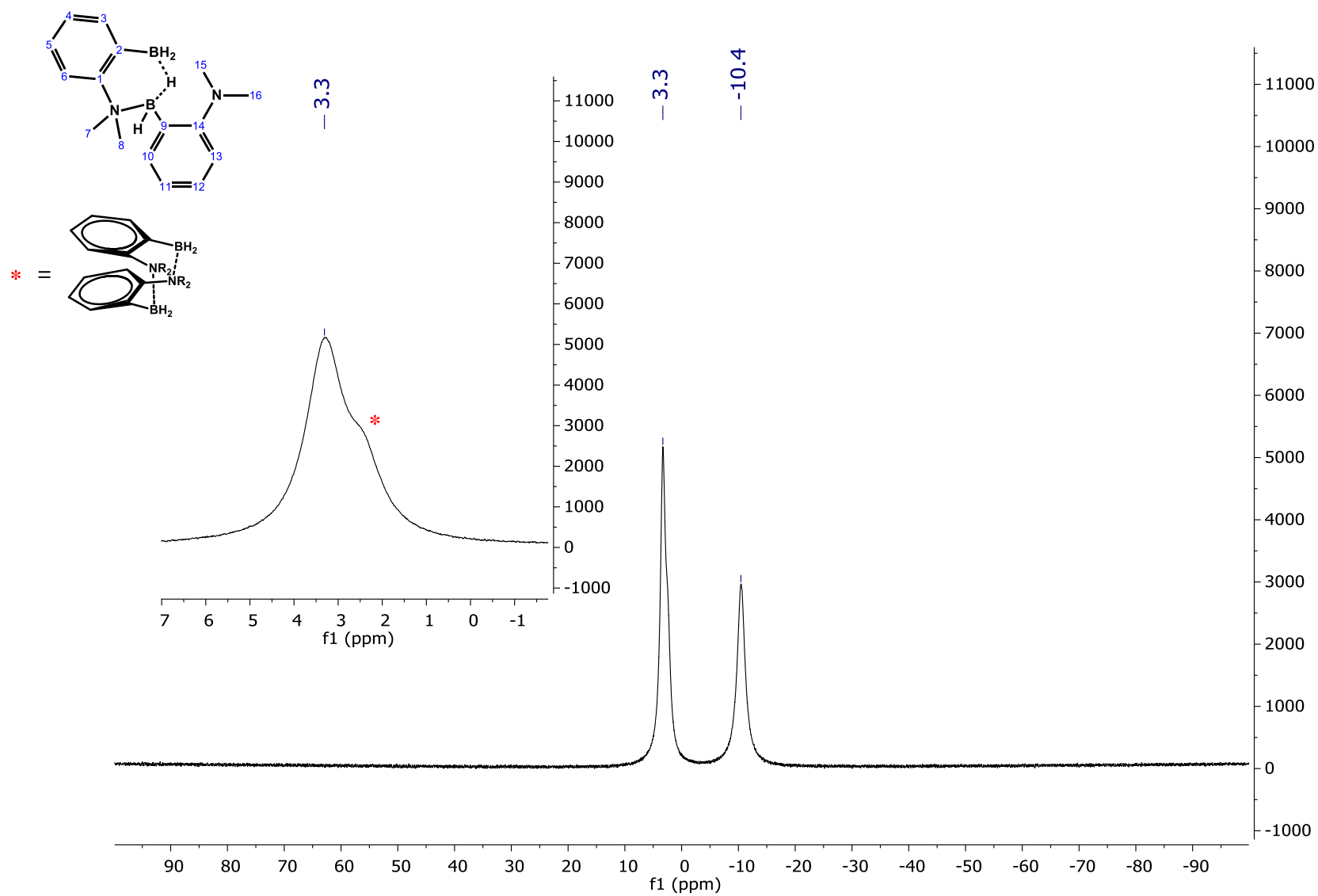
To help support that an equilibrium is taking place and that these NMR resonances were not caused by an unknown impurity, it was decided to conduct a  $^1\text{H}$  NMR analysis at varying temperature (VT  $^1\text{H}$  NMR) of **3.3**. While the two dimeric forms are very close in energy, the one containing two N-B bonds has a more limited degree of freedom compared to the other with only one N-B bond, and it is expected that the equilibrium would be influenced by the temperature. Indeed, the VT  $^1\text{H}$  NMR results, presented in **Table 6**, show an increase in the proportion of **3.3**, the dimeric form predicted to be entropically favored, with increasing temperature. Moreover, the temperature dependence of the ratio between the two species was plotted to extract the equilibrium thermodynamic parameters (**Figure 48**) and  $\Delta H$  and  $\Delta S$  of  $3.8 \pm 0.1$  kcal/mol and  $0.017 \pm 0.004$  kcal/mol\*K were respectively obtained, in good agreement with the DFT prediction.



**Figure 45**  $^1\text{H}$  NMR (500 MHz,  $\text{CDCl}_3$ ) of **3.3**.



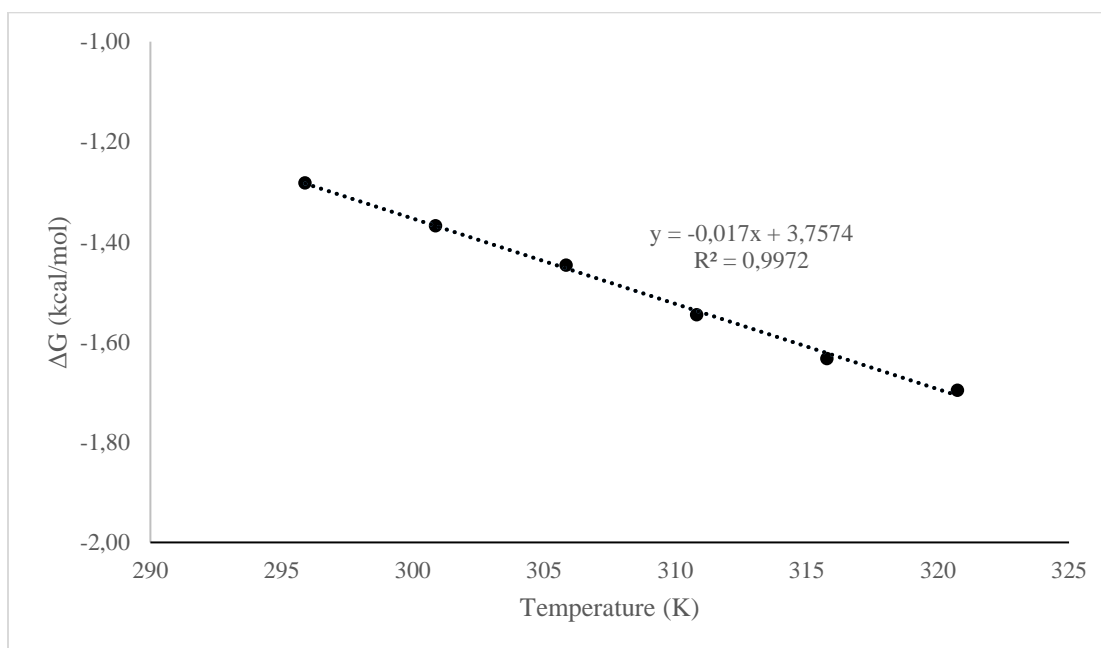
**Figure 46**  $^{13}\text{C}\{^1\text{H}\}$  NMR (126 MHz,  $\text{CDCl}_3$ ) of **3.3**.



**Figure 47**  $^{11}\text{B}\{^1\text{H}\}$  NMR (160 MHz,  $\text{CDCl}_3$ ) of **3.3**.

**Table 6** VT  $^1\text{H}$  NMR data of the equilibrium between **3.3** and **3.3\***.

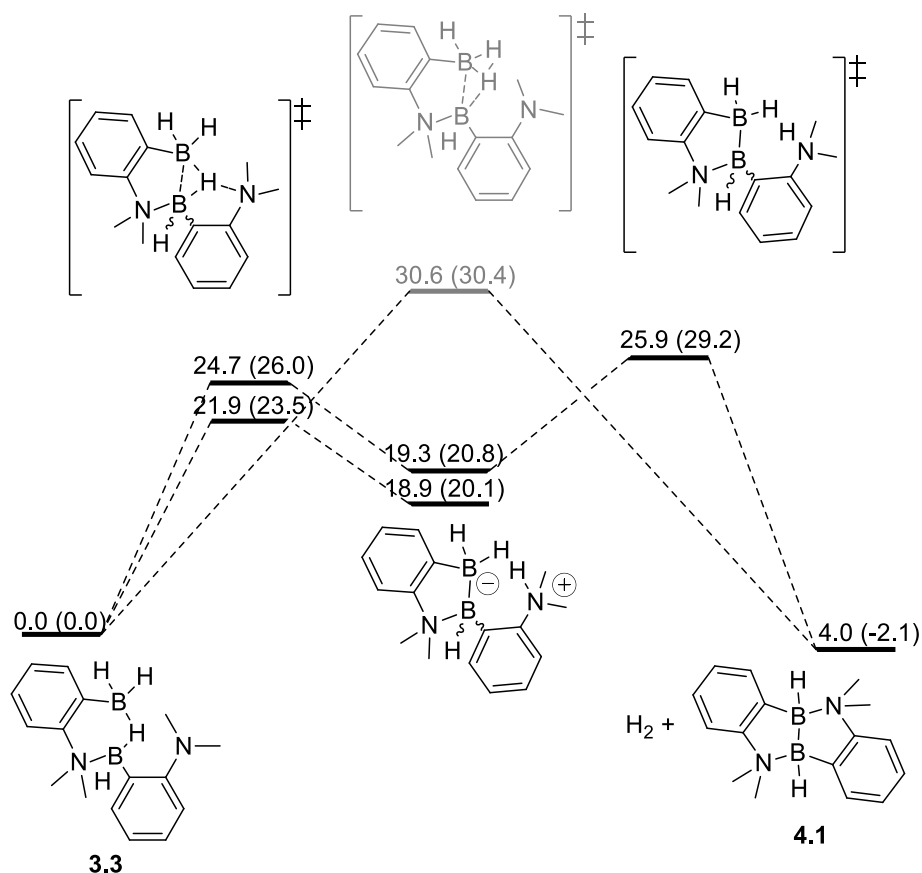
Set T	Corrected T	[ <b>3.3</b> ]	[ <b>3.3*</b> ]	$\ln$ (( <b>3.3*</b> )/( <b>3.3</b> ))	$\Delta G$
$^{\circ}\text{C}$	K	%	%		kcal/mol
25	295.90	89.8	10.2	-2.18	-1.28
30	300.87	90.8	9.2	-2.29	-1.37
35	305.84	91.5	8.5	-2.38	-1.45
40	310.81	92.4	7.6	-2.50	-1.55
45	315.78	93.1	6.9	-2.60	-1.63
50	320.76	93.5	6.5	-2.66	-1.70

**Figure 48**  $\Delta G$  in function of temperature for the equilibrium between **3.3** and **3.3\***.

Coming back to the main topic of this chapter, the mechanism for the formation of **4.1** was investigated using DFT. Preliminary experimental data, such as the X-ray crystallographic structures of the initial and final compounds as well as the observation of  $\text{H}_2$  as a reaction side product, which was confirmed while reanalyzing  $^1\text{H}$  NMR data of the transformation, were available and helped streamlining the DFT investigation. First, the general thermodynamic of the transformation was calculated and it was determined that the product formation was slightly favorable with a  $\Delta G$  of -2.1 kcal/mol. This suggests a potentially reversible reaction, a point that will be discussed later. With a  $\Delta H$  of reaction calculated at 4.0 kcal/mol, the reaction was predicted to be mostly entropy driven, which is not so surprising since the reaction releases  $\text{H}_2$ . Like with the other aminohydroborane transformations discussed in the thesis, that release of  $\text{H}_2$  can be considered the

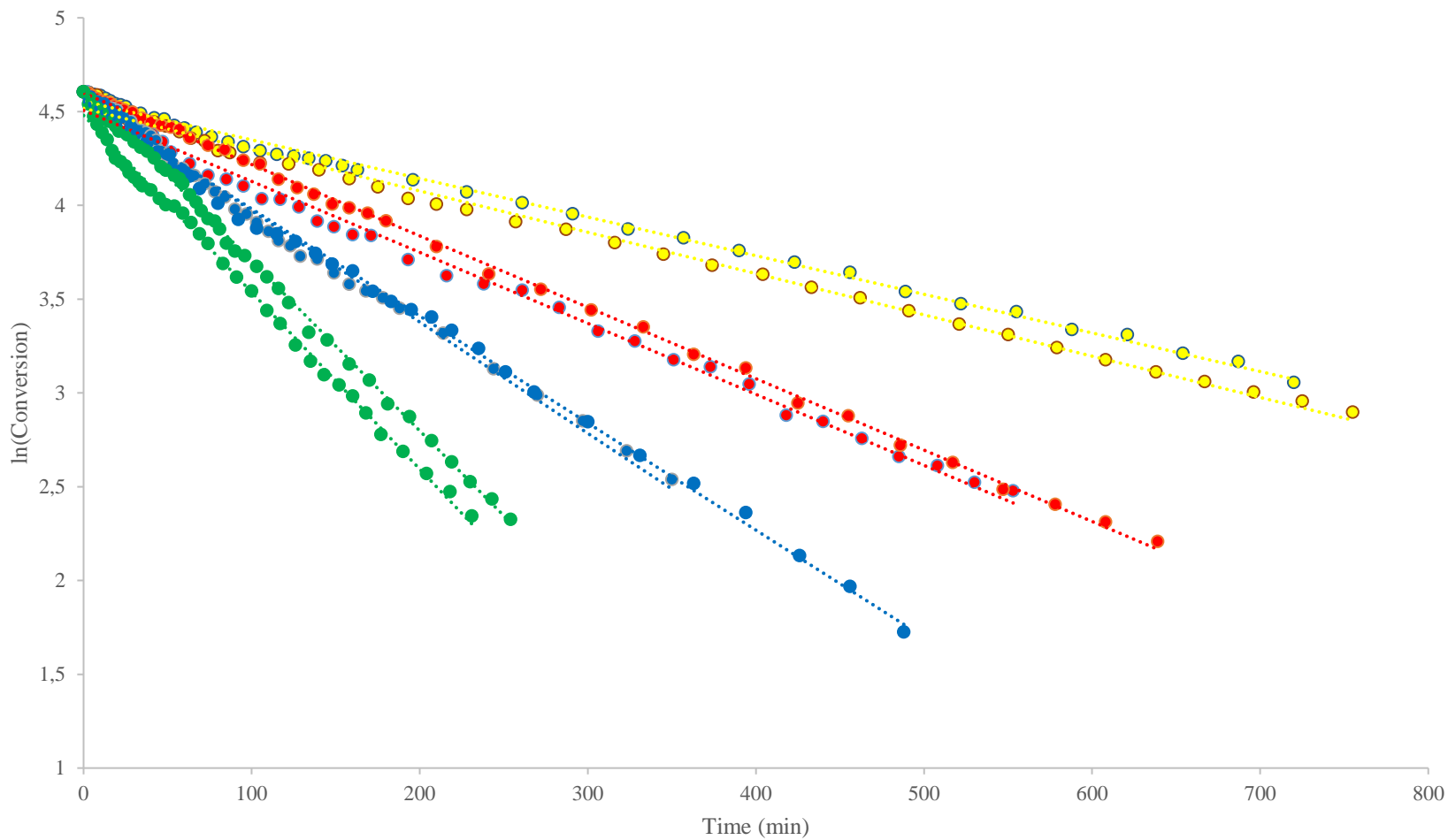
driving force of the reaction. That brings us to the most interesting part of a mechanistic investigation, the transition states. The first and most obvious possibility for generating **4.1** is a direct release of H<sub>2</sub>. It was calculated to have a  $\Delta H$  of 30.6 kcal/mol and a  $\Delta G$  of 30.4 kcal/mol. These values are a little high considering it is a reaction proceeding to completion in 24 h at 80 °C (see **Table 1**), but that could be considered acceptable considering the DFT precision for transition states. Nevertheless, that prompted us to consider other pathways, among which a deprotonation followed by a FLP release of H<sub>2</sub>. The deprotonation of a borohydride is quite unusual, especially using a weak base such as an amine, but in the case of the species of interest, the hydride is bridging between two boron atoms and the geometry of the dimeric form brings the amine very close in space. Moreover, the zwitterionic species resulting from such deprotonation could certainly release H<sub>2</sub>, a classical FLP reaction pattern. As I mentioned in the methodology section, one of the advantages of DFT is that it allows you to test objectively such unconventional ideas. Since the geometry of intermediates (minimum on the energy surface) is easier to optimize compared to transition states (saddle point on the energy surface) the zwitterionic intermediate was first calculated and was predicted to be quite high in energy with  $\Delta H = 18.9$  and  $\Delta G = 20.1$  kcal/mol, but accessible. Then the two transition states for the B-H deprotonation and the H<sub>2</sub> release were calculated to have  $\Delta H^\ddagger$  of 21.9 and 25.9 kcal/mol, respectively, and of  $\Delta G^\ddagger$  of 23.5 and 29.2 kcal/mol, respectively. It is good to note that conformational isomers exist and may influence the precision of the calculation. Attempts to calculate them were made, but full pathways could not be successfully calculated for each of them. The difference between both pathways remain in the DFT precision margin of error. However, the one going via B-H deprotonation followed by H<sub>2</sub> release is predicted to have a  $\Delta H$  for the limiting transition state 4.7 kcal/mol lower than the other pathway going via direct loss of H<sub>2</sub>, a difference that is at the limit of what can be called significant in DFT calculations.



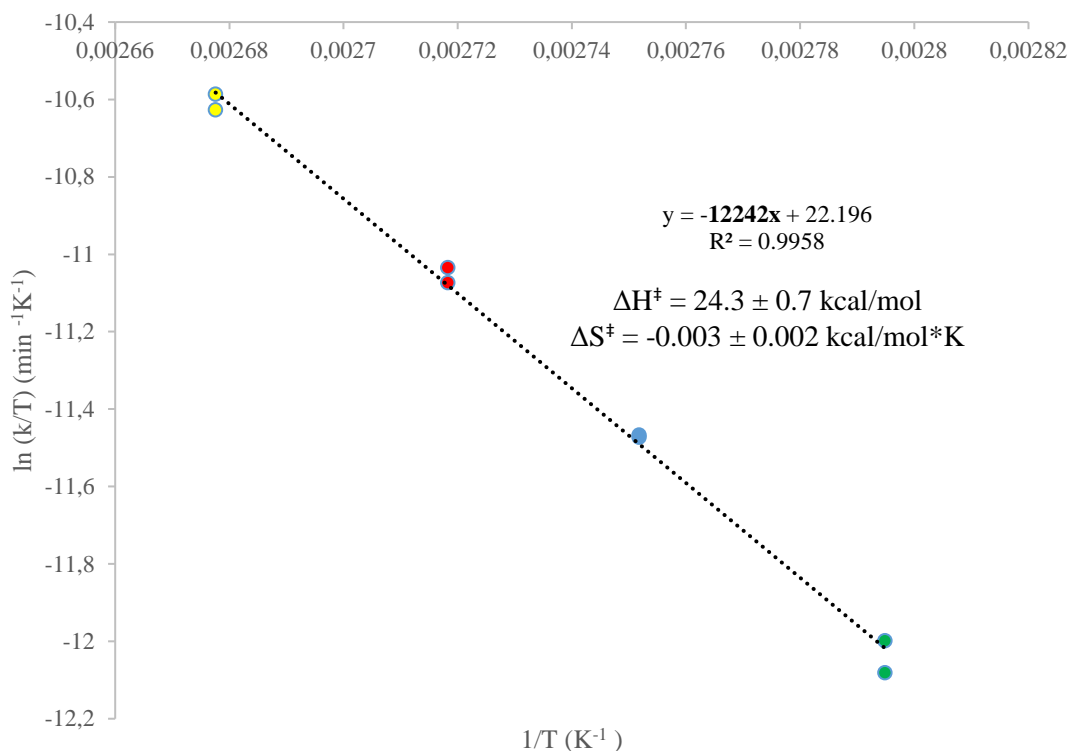


**Figure 49** DFT calculated mechanism for the formation of **4.1** from **3.3**,  $\Delta H$  ( $\Delta G$ ) reported in kcal/mol, calculations performed at the  $\omega$ B97XD/6-31++G\*\* SMD solvent = toluene level of theory.

This enthalpic difference between the pathways and the fact that experimental data are much more valuable prompted us to do a kinetic investigation of the transformation in order to get thorough kinetic data. The fact that the reaction is quite simple with only one starting compound and that the starting and final compounds have well defined  $^1H$  NMR  $NMe_2$  group signals facilitated the task. Most of the kinetic runs, a simple task that remains quite fastidious, were performed and analyzed by Nicolas Bouchard, under my supervision. The efforts gave the nice data in **Figure 50** and **Figure 51** that confirmed the expected first order of the reaction. The Eyring plot gave  $\Delta H^\ddagger$  and  $\Delta S^\ddagger$  values for the limiting step of the transformation at respectively  $24.3 \pm 0.7$  kcal/mol and  $-0.003 \pm 0.002$  kcal/mol\*K. The very low value for the  $\Delta S^\ddagger$  supports our hypothesis of an intramolecular reaction and the value of the  $\Delta H^\ddagger$  is in better accordance with the deprotonation of a B-H bond followed by the release of  $H_2$  in a FLP fashion, which ended up being our final proposed mechanism, even if we remained cautious of our claims.



**Figure 50** ln of the relative integration of **3.3** CH<sub>3</sub> signal at 2.35 ppm (conversion) over time at different temperature. ● 85 °C, ● 90 °C, ● 95 °C, ● 100 °C



**Figure 51** Eyring plot for the transformation of compound **3.3** in compound **4.1**.

To support our mechanistic proposition, other experiments were conducted. For example, a kinetic run was performed under 4 atm of H<sub>2</sub> and slowed down the reaction, which is consistent with a reversible H<sub>2</sub> release as the reaction limiting step. The final product containing the B-B bond was also heated under D<sub>2</sub> and the characteristic HD signal, meaning scrambling is happening, could be observed, confirming the reaction reversibility. Finally, the deuterated version of the starting compound was prepared by reacting **3.3** with D<sub>2</sub> and used to determine that the reaction have a KIE of  $2.0 \pm 0.4$ . This KIE value is quite low and no reliable literature reference value were found to support the mechanism. Indeed, the only mention I could find of a KIE in a FLP hydrogen cleavage is quite confusing and discussed of the absence of a KIE while reacting a N/B FLP with HD to form NH/BD and ND/BH. This phenomenon is more related to the transition state symmetry and is not a good way to probe the FLP hydrogen cleavage KIE in general.<sup>184</sup> Comparing the reaction rate of a FLP with H<sub>2</sub> and D<sub>2</sub> (the formation of the FLP-H<sub>2</sub>/D<sub>2</sub> adduct) in two independent vessels would be the method of choice, but since those reactions are usually quite fast at room temperature, it is not an easy task. Comparing the rate of hydrogenation of a compound using H<sub>2</sub> and D<sub>2</sub> for a transformation in which hydrogen cleavage is known to be the limiting step could be an easier way to indirectly probe such KIE. The low value we observed can be possible because the reaction proceeds via an

intermediate lying high in energy, if the deprotonation followed by H<sub>2</sub> release pathway is the right one. In very exothermic reactions where the transition state is similar to the starting materials, the change in the vibrational zero point energy ( $\Delta ZPE$ ) is very small between the ground state and the transition state, making the KIE small. Sadly, the absence of reference values limit the discussion on the mechanistic pathway discrimination.

While very interesting and consistent with our proposed mechanism, all those experiments did not allow us to differentiate unequivocally between the two proposed pathways. Attempts were made to predict the KIE value of the transformation using DFT in order to compare it to the one obtained experimentally but proved inconclusive. In the end, the comparison of the experimental and DFT calculated  $\Delta H^\ddagger$  values remain the strongest argument for the B-H deprotonation followed by release of H<sub>2</sub> in a FLP fashion pathway. Even if the deprotonation of a B-H bond is surprising because it is usually considered as an hydride, the only other study with an example of B-H deprotonation was the deprotonation of a carbene BH(CN)<sub>2</sub> adduct using the strong base KHDMS to form an isolable boryl anion, as reported by Bertrand<sup>185</sup>, which is quite remotely connected to our study. After our report, Wagner and coworkers reported a well-studied and reversible deprotonation of a bridging B-H bond to generate a B-B bond.<sup>112</sup>

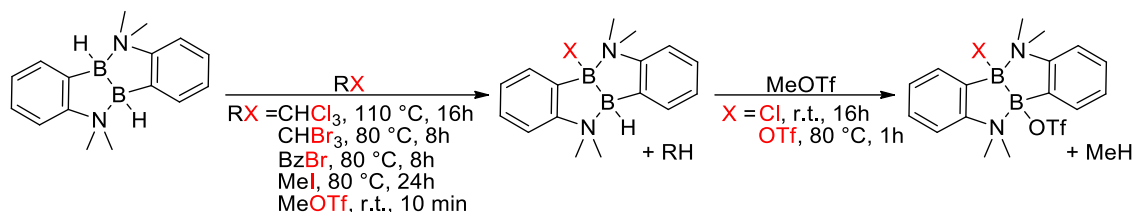
The synthesis and mechanistic investigation of **4.1** was a nice little story of interest for the boron chemistry community and was published on its own.<sup>110</sup> After that publication, most of my energy got diverted toward finishing other projects, notably the ones that will be presented in Chapter 5 and Chapter 6, but we also investigated the reactivity of **4.1**.

### 4.3 The reactivity of the diborane ( $NMe_2-C_6H_4-BH$ )<sub>2</sub>

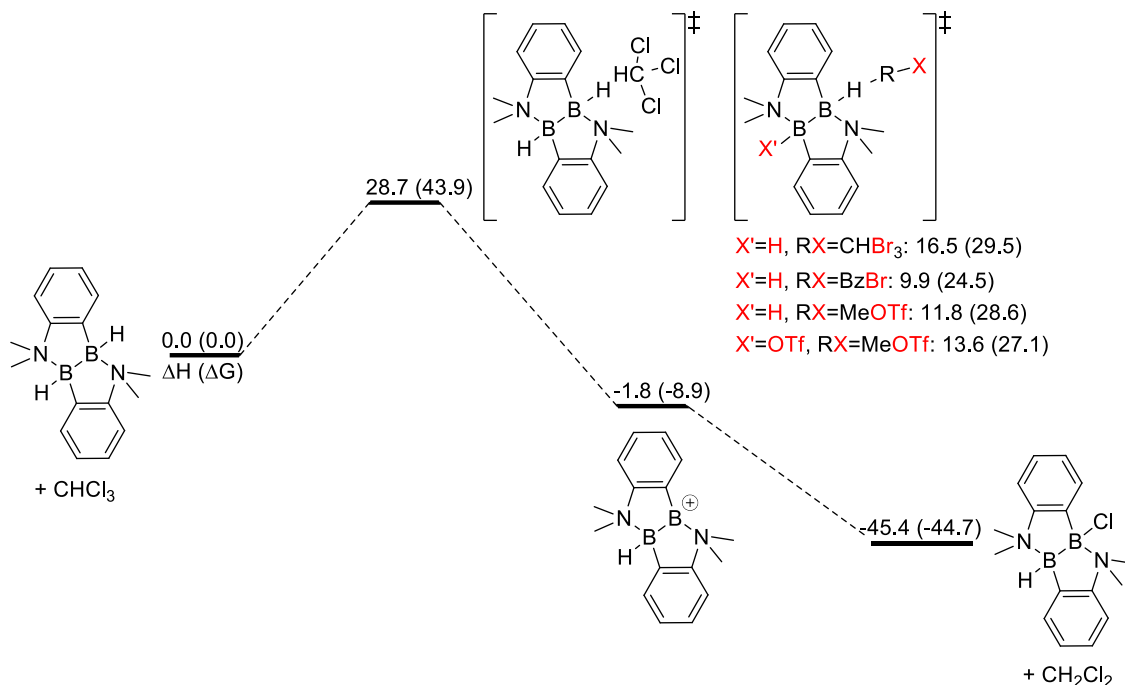
We are very interested in the development of new mechanistic paradigms in metal-free catalysis and the release of H<sub>2</sub> to form a B-B bond can be viewed as a formal reductive elimination, where B(III) is reduced to a B(II) species. A survey of **4.1** reactivity was started in order to determine if it was possible to take advantage of that elementary step for novel catalytic cycles. The reactivity study was encouraged by the observation that prolonged heating of **4.1** in a CDCl<sub>3</sub> solution led to the replacement of a borohydride by a chlorine atom and formation of CHDCl<sub>2</sub>. Initial attempts to use such reactivity to promote silane chlorination were promising, but a control experiment showed surprisingly that silane chlorination can occur at elevated temperature (110 °C) in CDCl<sub>3</sub> without requiring any catalyst. Despite that setback, the reactivity of **4.1** was pursued. A lot of the inspiration came from the work of the Himmel group who reported in more than 20 publications on the reactivity of similar species.<sup>111,186–206</sup>

Many potential reactive sites are present on molecule **4.1**. The B-H, B-B and B-N bonds can all potentially be cleaved in different reactions. That reactivity of the B-H bond toward chloroform, as mentioned above, puzzled us for a while and was studied using DFT, mostly looking for transition states implicating some sort of FLP behavior. All potential transition states optimized ended up being predicted at inaccessible energy (in the range of 70 kcal/mol). Finally, a simpler and realistic pathway was calculated, which is a simple S<sub>N</sub><sup>2</sup> reaction where the borohydride is the nucleophile. This pathway was calculated having a ΔH<sup>‡</sup> of 28.7 kcal/mol and a ΔG<sup>‡</sup> of 43.9 kcal/mol, which is very high even for a reaction requiring prolonged heating at 110 °C. However, weighing in the fact that the reaction was carried out in chloroform as the solvent, the DFT calculated entropy contribution to the transition state was probably overestimated. Since the reactivity trend of substrate for the S<sub>N</sub><sup>2</sup> reaction is well known and quite easy to test experimentally, we decided to attempt the reaction using different leaving groups. The reaction was tried with excess bromoform, benzylbromide, methyl iodide and methyl triflate, and all the substrates proved compatible forming primarily the mono-substitution product with the expected reactivity trend for an S<sub>N</sub><sup>2</sup> mechanism. In the case of methyl triflate, the *bis*-substitution product can also be obtained with mild heating. The experimental and the DFT results of the impact of the substrate on the transition state predicted enthalpy and free energy are presented in **Scheme 18** and **Figure 52**. However, it is fair to state that from all the DFT results presented in the thesis, those are probably the ones that fit less with the experimental observations. This may come from the fact that the substrates are very different from one another (containing very different atoms) and as mentioned before, the excess of substrate used in the reaction lead to some inaccuracy in the

entropy contribution. The formation of formally charged species can also be a factor reducing DFT accuracy.



**Scheme 18** Experimental results for the  $S_N^2$  reaction of **4.1** with different substrates.



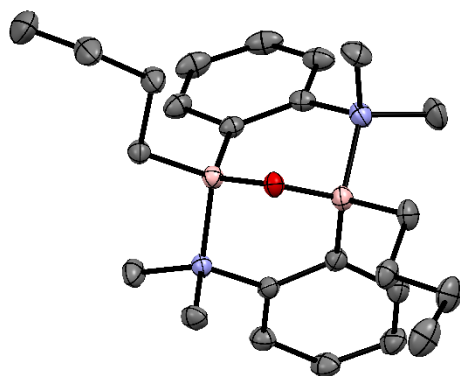
**Figure 52** DFT calculated transition states for the  $S_N^2$  reaction of **4.1** with different substrates.  $\Delta H$  ( $\Delta G$ ) reported in kcal/mol, calculations performed at the  $\omega$ B97XD/6-31++G\*\* SMD solvent = benzene level of theory.

The observation that the first nucleophilic substitution is faster than the second is quite interesting. This could allow the synthesis of unsymmetrical diboranes and suggest that the substitution at one boron influence the nucleophilicity of the second boron hydride. To support this hypothesis, the relative strength of the B-H bond was calculated using DFT for all species and are presented in Table 7. The results support our initial hypothesis. The substitution at one boron is predicted to increase the B-H bond strength, making the second bond harder to break in a  $S_N^2$  transition. Moreover, the effect seems to follow the expected trend of leaving group quality, varying in the order  $Cl < Br < I < OTf$ .

**Table 7** DFT calculated relative B-H bond strength.  $\Delta H$  reported in kcal/mol, calculations performed at the  $\omega$ B97XD/Def2TZVP level of theory.

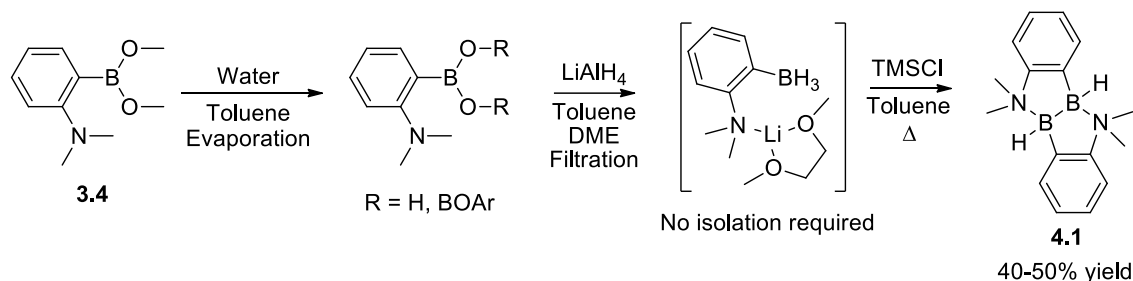
Substituents on the Boron atom	H, H	H, Cl	H, Br	H, I	H, OTf
Relative B-H bond strength (kcal/mol)	0	8.1	9.1	9.9	12.4

Finally, it was decided to perform the synthesis of many species on a preparative scale. However, as I previously mentioned, the synthesis used at that moment allowed only the preparation of at most 1 g of **4.1** because the filtration of larger batches after the  $\text{LiAlH}_4$  reduction was impractical and repeating the synthesis a tedious task. Thus, a second round of optimization was performed to allow a scalable synthesis. The initial idea was to start from the boronic acid instead of the methoxy boronic ester, in order to form less viscous and less soluble oxo aluminum species, facilitating the filtration. This idea came from the previously developed synthesis of **3.9**, which used the boronic acid  $\text{NET}_2\text{-C}_6\text{H}_4\text{-B(OH)}_2$  as starting material, since it is easier to synthesize than the methoxy boronic ester. While performing that synthesis, I observed that the filtration after the  $\text{LiAlH}_4$  reduction is more facile. However, the synthesis of  $\text{NMe}_2\text{-C}_6\text{H}_4\text{-B(OH)}_2$ , expected to be very straightforward since it is done by a simple hydrolysis of **3.4**, proved quite challenging and ill-defined mixtures were always obtained. That was quite surprising since the targeted compound had been previously reported in few literature articles.<sup>207–209</sup> After some time, the hypothesis that the small *ortho*-amine could promote dehydration of the boronic acid leading to a mixture of compounds containing B-O-B bonds was formulated. My colleague Hugo Boutin and I independently observed such phenomenon previously while involuntarily synthesizing and crystalizing a compound of the type  $[\text{NMe}_2\text{-C}_6\text{H}_4\text{-B(Bu)}]_2\text{-O}$  (**Figure 53**).



**Figure 53** Crystal structure of  $[\text{NMe}_2\text{-C}_6\text{H}_4\text{-B(Bu)}]_2\text{-O}$ . Gray = C, blue = N, pink = B, red = O and. Hydrogen atoms omitted for clarity, ellipsoid drawn at 50% probability.

Eventually, despite the absence of a convincing characterization of the hydrolysis product of **3.4**, the rest of the synthesis was pursued with the supposition that dehydration, if it was indeed the problem, should not interfere with the next steps. Finally, the rest of the synthesis worked as planned and the filtration step indeed proved to be much easier using that method. Other modifications to improve the synthesis include using out-of-the-bottle toluene as solvent, since the hydrolysis step is bringing more water than what is contained in the solvent and because LiAlH<sub>4</sub> can be considered a drying agent. Also, I replaced TMSBr by the cheaper analogue TMSCl and performed the removal of the LiH adduct and the thermally induced formation of the B-B bond in one pot. I should note that TMSBr was initially used because it is more reactive than TMSCl that requires heating and longer reaction time to completely react. This is problematic for the synthesis of [NR<sub>2</sub>-C<sub>6</sub>H<sub>4</sub>-BH<sub>2</sub>]<sub>2</sub> derivatives from which the synthesis of **4.1** was inspired because it often leads to degradation products and unreacted starting material. However, the synthesis of **4.1** requires prolonged heating so the use of TMSCl for bigger batches proved more practical.



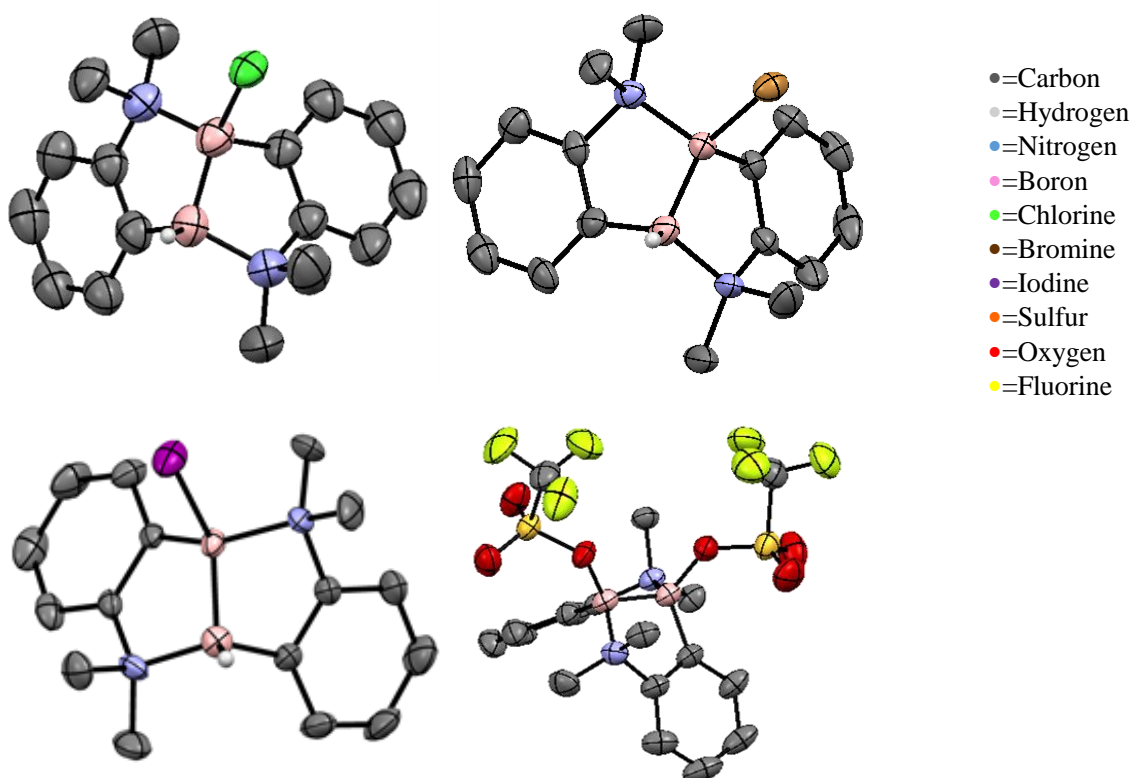
**Scheme 19** Re-optimized synthesis of **4.1**.

This optimized synthesis facilitated the isolation and characterization by multinuclear NMR and in some cases, X-ray crystallography of many **4.1** reaction products. However, the good selectivity between the *mono* and *bis* substitution products could not be reproduced on the preparative scale and during the crystallization, the *bis*-substituted product ratio tend to increase, probably because of differences in solubility. While this prevented the synthesis of pure products, it allowed the spectroscopic characterization of most species. The <sup>11</sup>B NMR shifts of some species are presented in **Table 8** and the X-ray crystallographic structures are presented in **Figure 54**. However, no interesting observation was made about those results, since all compounds adopt a geometry very similar to **4.1** in their crystalline form, the substitution of one H atom does not seem to significantly influence the B-B bond length, and the spectroscopic results are following the trend expected.



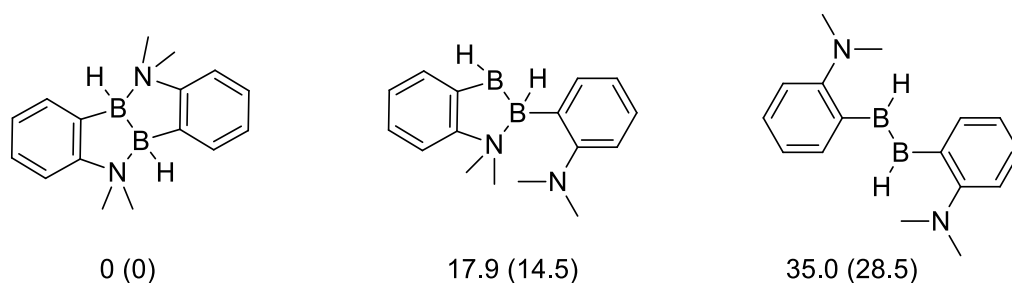
**Table 8** The  $^{11}\text{B}$  NMR shifts of the various diborane species synthesized.

Compound			$\delta^{11}\text{B}$ NMR		B-B Length
$X_1$	$X_2$	Number	(ppm)		(Å)
H	H	<b>4.1</b>	1.8		1.746(2)
Cl	H	<b>4.2</b>	11.1	-0.5	1.709(6)
Br	H	<b>4.3</b>	10.1	-0.2	1.71(1)
OTf	H	<b>4.4</b>	16.1	-0.4	
I	H	<b>4.5</b>	5.8	0.5	1.717(6)
Cl	Cl	<b>4.6</b>	6.8		
Br	Br	<b>4.7</b>	6.0		
I	I	<b>4.8</b>	2.4		
OTf	OTf	<b>4.9</b>	9.3		1.71(1)



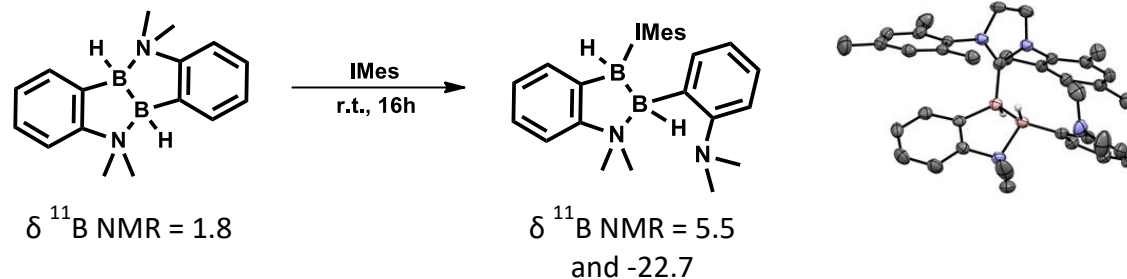
**Figure 54** Crystallographic structures of the various diborane species synthesized (**4.2**, **4.3**, **4.5** and **4.9**). Co-crystallized toluene and hydrogen atom linked to carbon are omitted for clarity. Ellipsoid drawn at 50% probability.

Other attempts at exploiting the B-H bond cleavage to form interesting species include the hydride abstraction using the strong Lewis acid  $B(C_6F_5)_3$  to form a formally cationic species, but ended up inconclusive, only a very complex mixture could be obtained. The formation of a similar species by chlorine abstraction from the chlorinated compound using  $AlCl_3$  was also attempted, but also proved inconclusive. Finally, our attention turned toward exploiting the other potential reactive moieties of the molecule. Since H/D exchange was observed during the investigation of the formation of **4.1**, it suggested the lability of one B-N bond, which was supported by DFT calculations (**Figure 55**). Thus, we sought further evidence of this behavior.



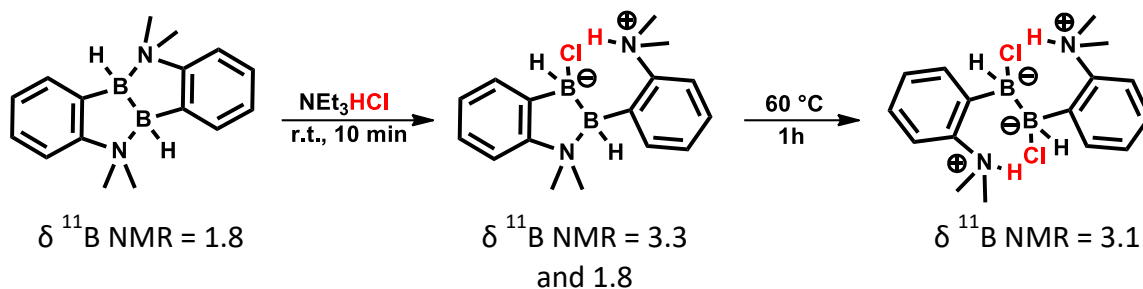
**Figure 55** DFT calculated potential lability of the B-N bond.  $\Delta H$  ( $\Delta G$ ) reported in kcal/mol, calculations performed at the  $\omega B97XD/Def2TZVP$  level of theory,

The displacement of the amine of B-N bond by another Lewis base was investigated. **4.1** was placed in presence of different Lewis bases, notably 4-dimethylaminopyridine (DMAP),  $PPh_3$  and 1,3-dimesitylimidazol-2-ylidene (IMes). At first, no reaction was observed, but after 16 h at room temperature the formation of a new species could be observed by NMR from the reaction between IMes and **4.1**. The reaction was performed on a preparative scale and crystal suitable for X-Ray diffraction analysis were obtained. The structure is interesting and present an inversion of configuration at the boron center bonded to the IMes moiety. In all previous crystal structures of similar diboranes (**Figure 44** and **Figure 54**) the B-H bonds are present in a *cis* fashion, while with **4.1**•IMes they are *trans* to each other. This behavior suggests an  $S_N1$  mechanism in which the B-N bond is broken as a first step and where the B-IMes bond is formed subsequently. Because the approach of the bulky IMes molecule is expected to be easier when the aryl moiety of the second bond is downward, this leads to the observed geometry. Probably because of the very high steric hindrance of IMes, displacing the second B-N bond was not possible.



**Scheme 20** Reaction of **4.1** with IMes and crystal structure of the compound formed.

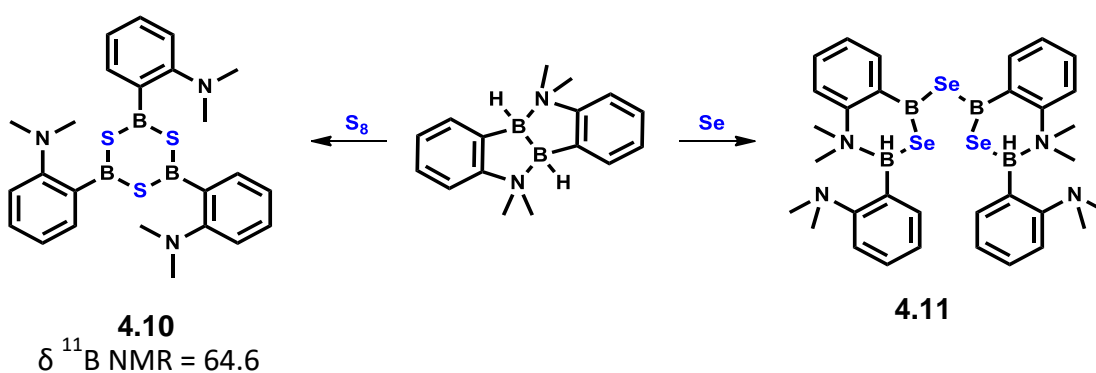
Our attention then turned to Brønsted acids and a similar reaction, using  $\text{NEt}_3 \cdot \text{HCl}$ , was observed, but this time it was very fast at room temperature. Moreover, mild heating allowed the cleavage of the second B-N bond. Surprisingly, no  $\text{H}_2$  generation could be observed. The preparation of the products on a preparative scale was performed, but surprisingly, evaporation of the  $\text{NEt}_3$ , expected to be produced as side product, was not possible. A possible explanation would be that  $\text{NEt}_3$  remain coordinated to the proton, something that could also explain the absence of  $\text{H}_2$  release. However attempts at crystalizing the molecule failed and that hypothesis could not be confirmed.



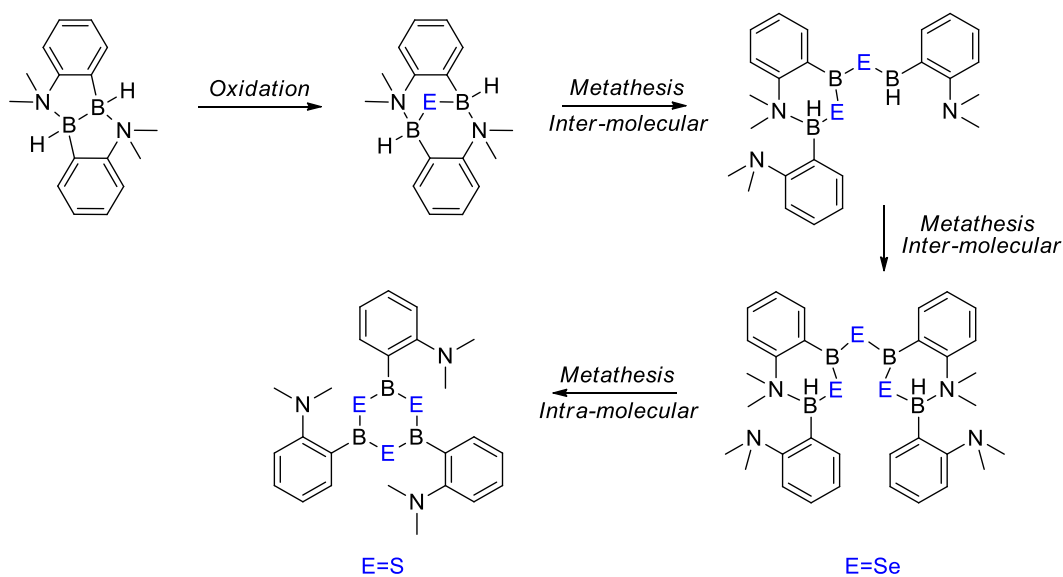
**Scheme 21** Proposed reaction of **4.1** with  $\text{NEt}_3 \cdot \text{HCl}$ .

Finally, the last, but not least, potential reactive site of **4.1** investigated was the B-B bond. As I mentioned before, the formation of **4.1** from **3.3** can formally be viewed as a reductive elimination of  $\text{H}_2$ . Thus, if the B-B bond can be somehow oxidized, mimicking another traditional elementary step of transition metal catalysis with metal-free species **4.1**, only another reduction step would be required, regenerating **3.3**, to close the equivalent of a metal-free reductive elimination/oxidative addition catalytic cycle. **4.1** was thus reacted with oxidants  $\text{O}_2$ , peroxide,  $\text{S}_8$  and  $\text{Se}_{(s)}$ . The reaction with oxygen based oxidants resulted in either the absence of reaction or the generation of a complex mixture. However, the reactions with  $\text{S}_8$  and  $\text{Se}_{(s)}$  were quite clean. Interestingly, both reactions do not produce analogous species. In the case of the reaction with  $\text{S}_8$ , the product formed is symmetrical with only one  $^{11}\text{B}$  NMR signal at 64.6 ppm and only one resonance corresponding to the  $\text{NMe}_2$  moiety in  $^1\text{H}$  NMR spectra. In the case of the reaction with  $\text{Se}_{(s)}$ , the product is unsymmetrical with two

$^{11}\text{B}$  NMR signals at 71.0 and 0.5 ppm, the latter suggesting a four coordinated boron atom with one of its substituent being an hydride because a  $J_{\text{B-H}}^1$  coupling could be observed. By  $^1\text{H}$  NMR spectroscopy, three signals associated to the  $\text{NMe}_2$  moiety could be observed, one integrating for 6 protons and two for 3 protons, consistent with an unsymmetrical molecule in which one of the amino group would be bonded to a boron atom, and with the other free. Eventually, the species presented in **Scheme 22** were determined the most likely products of the reactions and their formation explained by the pathway proposed in **Figure 56**. Unfortunately, once again the attempts at obtaining quality crystals to undoubtedly confirm the identity of the products by X-ray crystallography proved unsuccessful.

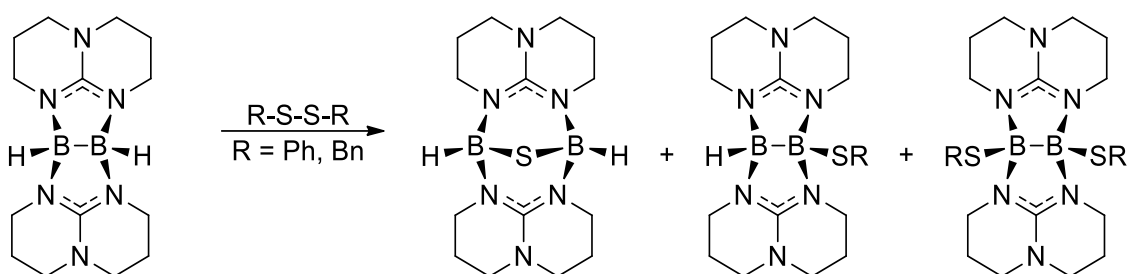


**Scheme 22** Proposed products from the reaction of **4.1** with  $\text{S}_8$  (**4.10**) and  $\text{Se}_{(s)}$  (**4.11**).



**Figure 56** Proposed pathway from the formation of the products observed in the reaction of **4.1** with  $\text{S}_8$  and  $\text{Se}_{(s)}$ .

Nevertheless, the observation of the B-B bond oxidation was very encouraging and attempts at closing a potential metal-free equivalent of a reductive elimination/oxidative addition catalytic cycle by using hydroboranes to regenerate **3.3** were made, but proved unsuccessful. The important steric hindrance coming from the aryl groups of the molecule, or the potential aromaticity of the thioboroxine reducing the boron acidity, might be responsible since the metathesis of B-S bonds is usually possible (results obtained before this study will be discussed in more details in Chapter 6). Finally, in order to generate a species more reactive toward metathesis, the oxidation of the B-B bond using disulfide species was attempted, a reactivity previously reported by the Himmel group using a related diborane (**Scheme 23**),<sup>205</sup> but **4.1** proved unreactive toward disulfide.



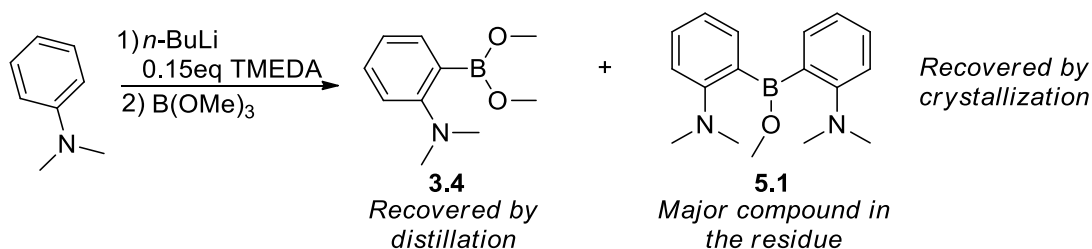
**Scheme 23** Reactivity of a diborane with disulfide reported by the Himmel group.<sup>205</sup>

Eventually, the project stopped there because no interesting catalytic behavior could be obtained, because getting publication quality characterization of the compounds proved challenging, and that my energy got oriented toward other potentially more interesting projects, notably the one that will be presented in the last chapter of the thesis. Nevertheless, considering the quantity of the results already obtained, it is possible that the project will be wrapped up and published by another student in the future.

## Chapter 5 FLP promoted intra-molecular Csp<sup>3</sup>-H bond cleavage and subsequent rearrangements

The previous chapters, with maybe the exception of the last part of Chapter 4, were either completed and submitted rapidly after the initial discovery or were abandoned quickly. The one presented in this chapter is different since it followed me during a long period of my Ph. D., sometimes at the top of my priority list and sometimes only in the background. It was a pivotal project since it was the first challenging one I had to manage on my own. Even though these results were published after the B-B bond formation project presented in Chapter 4, the Csp<sup>3</sup>-H bond cleavage project started way before. Contrarily to the former project where everything fell in place after obtaining a crystal structure, the latter project proved very challenging.

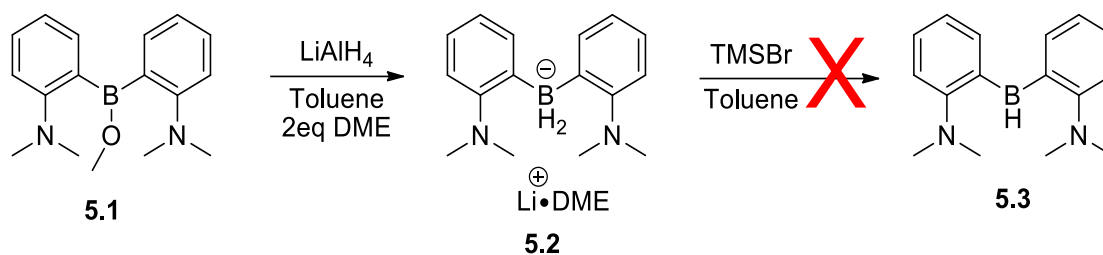
The Csp<sup>3</sup>-H bond cleavage project started in a fortuitous manner a little bit after the end of the project on FLP catalyzed Csp<sup>2</sup>-H bond borylation. As mentioned in Chapter 3, the focus of the group at that time was on the discovery of new, and potentially better, catalysts for C-H functionalization and one of the proposed ways to improve the catalyst activity was to prevent dimer formation. I also mentioned that the synthesis of **3.4** had been optimized and had been conducted several times on a multi-gram scale. What I did not mention in the previous chapters is that the major impurity formed during that synthesis is (NMe<sub>2</sub>-C<sub>6</sub>H<sub>4</sub>)<sub>2</sub>-BOMe (**5.1**) and that after the purification/removal of **3.4** by distillation it forms around 80% of the residue and can quite easily be recovered in analytically good purity by a simple crystallization from hexane (**Scheme 24**).



**Scheme 24** Synthesis of **5.1**.

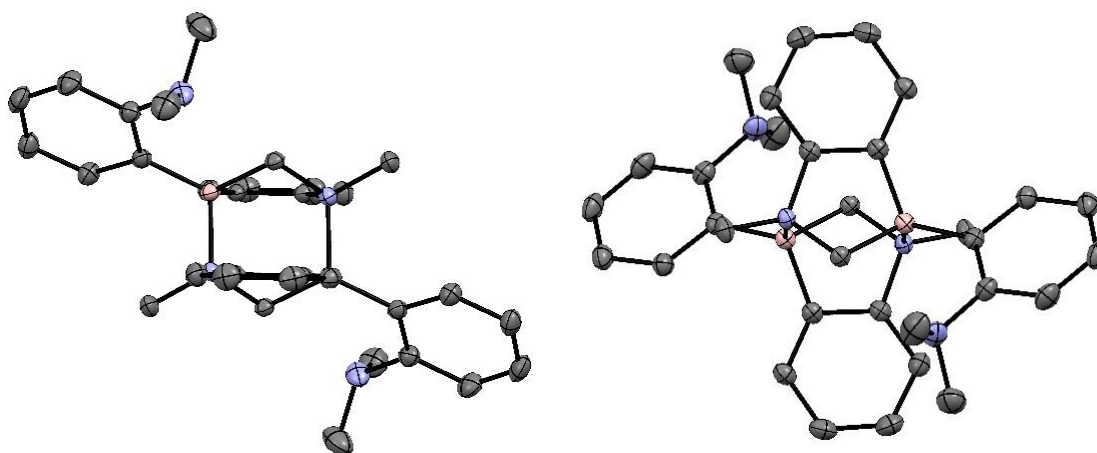
Having recovered few grams of **5.1** from previous batches of **3.4**, I eventually decided to try to convert it to its borohydride analogue to see if it was a Csp<sup>2</sup>-H borylation catalyst since many projects came to an end and I had some time on my hand. The first step of the synthesis, the reduction using LiAlH<sub>4</sub>, worked as usual giving relatively pure (NMe<sub>2</sub>-C<sub>6</sub>H<sub>4</sub>)<sub>2</sub>-BH<sub>2</sub>Li•DME (**5.2**) as product. However, the

last step, removing the LiH from **5.2** using TMSBr, surprisingly generated an extremely messy and unanalyzable mixture of compounds instead of the expected product (**5.3**) (**Scheme 25**).



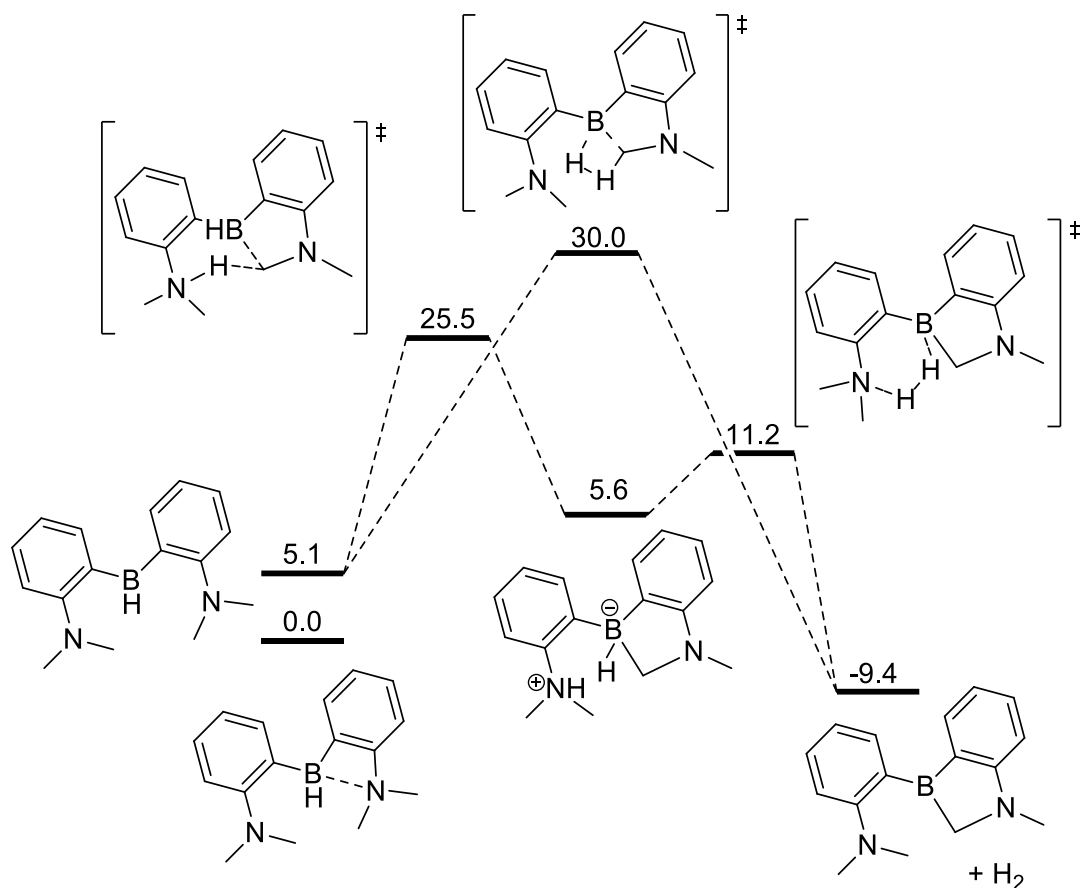
**Scheme 25** Attempted synthesis of **5.3**.

The mixture showed some unimpressive activity for the catalytic Csp<sup>2</sup>-H borylation. I washed the reaction vessel with hexane, put the vial in the freezer and hoped for some crystals to grow. Some free time on our diffractometer allowed me to run some crystals of the solution to give the structure presented in **Figure 57**, which puzzled me at first. After a moment, we realized that the structure was a dimeric form of a rearrangement product of **5.3**, the expected product, likely formed by the intramolecular Csp<sup>3</sup>-H bond cleavage of the C-H bond  $\alpha$  to the amine, followed by the release of an H<sub>2</sub> molecule (**5.4**).



**Figure 57** Crystal structure of **5.4**. Left, side view and right top view. Gray = C, blue = N, pink = B and white = H. H atoms linked to carbon are omitted for clarity. Ellipsoid drawn at 50% probability. A DFT investigation was done for a potential mechanism to explain such transformation. Two main pathways were explored, the direct loss of H<sub>2</sub> during the formation of the B-C bond, calculated to have a  $\Delta G^\ddagger$  at 30.0 kcal/mol, and the FLP promoted C-H bond cleavage followed by the classical FLP release of H<sub>2</sub>, calculated to have a  $\Delta G^\ddagger$  for the limiting step at 25.5 kcal/mol (**Figure 58**). A limiting step accessible at 25.5 kcal/mol can explain that partial rearrangement was observed during the

attempted synthesis of **5.3**, since mild heating is usually used to accelerate solvent evaporation, such as toluene, which was used in this case.



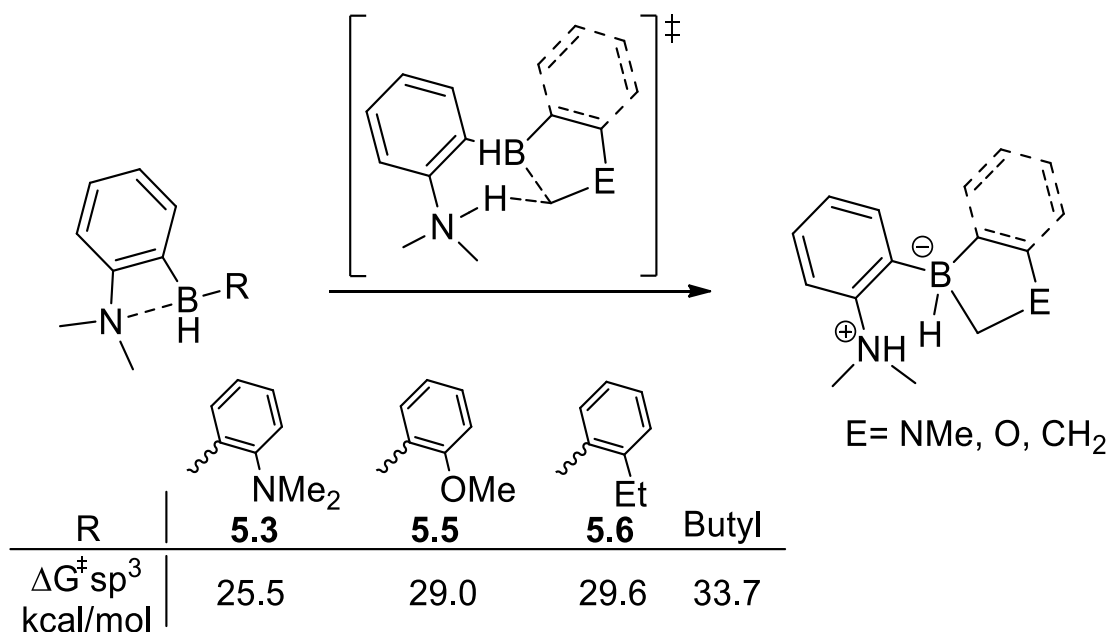
**Figure 58** DFT investigation of the rearrangement mechanism forming **5.4**.  $\Delta G$  reported in kcal/mol., calculations performed at the  $\omega$ B97XD/6-31++G\*\*, SMD solvent = benzene level of theory.

With that crystal structure and a DFT supported mechanism suggesting a FLP promoted Csp<sup>3</sup>-H bond cleavage, I had a serendipitous, but interesting, story in hand, but the synthesis of the precursor and the product of interest proved irreproducible and required a lot of work before publication. Moreover, I only had a crystal of that compound, which was gone, and no spectroscopic characterization and no easy way to get hand on the product. Since it was a stoichiometric reactivity, the synthesis of derivatives was hard to make without certitude that they would react as desired. Finally, the compound from which the rearrangement occurred had proven thermally too unstable to be isolated, meaning that a kinetic study would probably be quite complex to carry. Considering all those drawbacks, it is not so surprising that the project dragged for so long and was often pushed back in my priority list. Nevertheless, good description of such stoichiometric reaction is often the first step



in the development of catalytic systems and I believed that this work could be of some use for other researchers and was worth publishing. I am proud I eventually did, even if it dragged a long time.

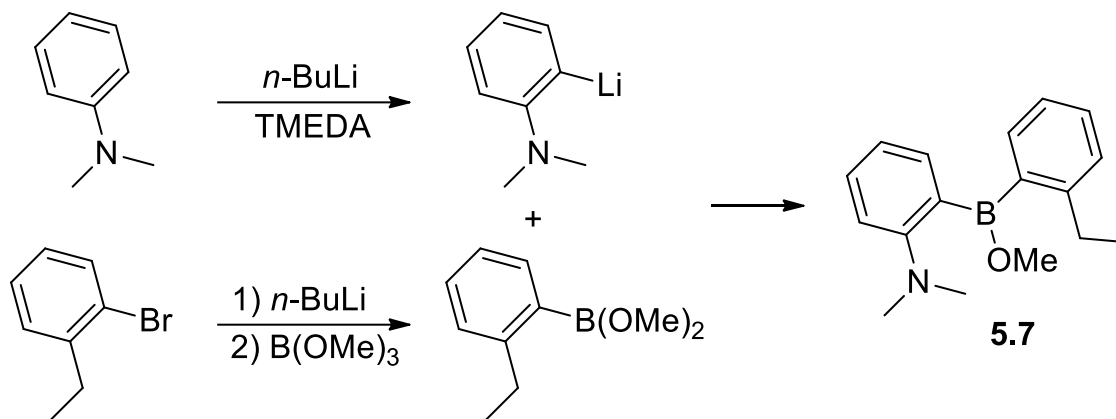
The first question I had concerned the importance of the  $\alpha$  nitrogen atom and of the geometry on the C-H bond cleavage. This was easily probed using DFT. The calculations suggested that the  $\alpha$  nitrogen atom is important to access the Csp<sup>3</sup>-H bond transition state, probably because it makes the carbon more nucleophilic, but that other derivatives, containing oxygen or carbon atoms could still have, while more energetically demanding, accessible Csp<sup>3</sup>-H bond cleavage transition states. However, the Csp<sup>3</sup>-H bond cleavage transition state for the simplest derivative, with only a butyl chain, was predicted to be too high energetically, suggesting that the geometry induced by the phenylene backbone was important.



**Figure 59** DFT investigation of the FLP promoted Csp<sup>3</sup>-H bond cleavage.  $\Delta G$  reported in kcal/mol, calculations performed at the  $\omega$ B97XD/6-31++G\*\*, SMD solvent = benzene level of theory.

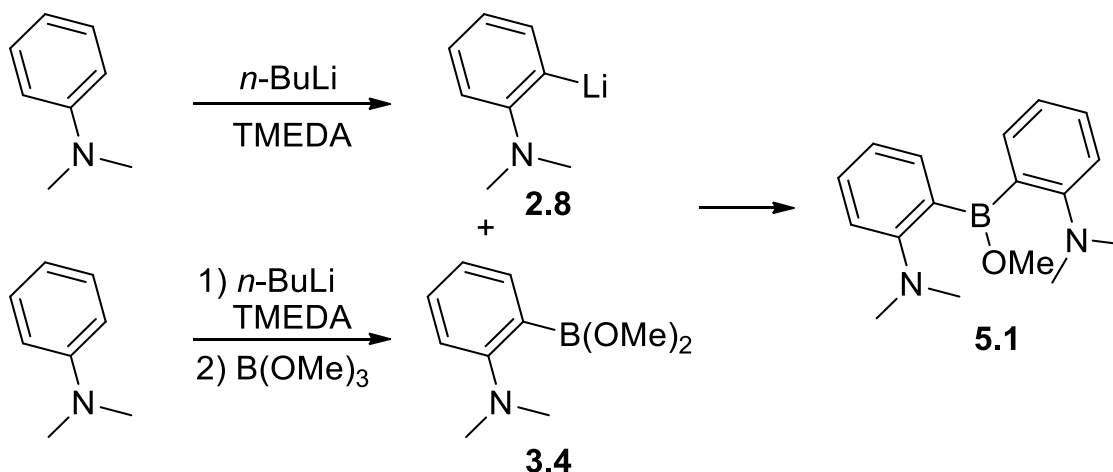
A lot of efforts were directed at the synthesis of the *ortho*-anisole (**5.5**) and eventually of the *ortho*-ethylbenzene (**5.6**) derivatives in order to get experimental proof of the DFT predictions. Moreover, their difficult Csp<sup>3</sup>-H bond cleavage transition states means that there is some hope in the isolation of the B-H derivatives, making an eventual kinetic study of the mechanism feasible. The synthesis of **5.5** proved difficult and after some time and because of evidence that the alkoxy substituent was problematic in the reaction with LiAlH<sub>4</sub>, most synthetic efforts were directed toward **5.6**. A reproducible synthesis of the boro-methoxy synthetic precursor (**5.7**) was achieved (**Scheme 26**). However, the synthesis is not practical, the yield is low, in particular because the final product needs

to be purified by a vacuum distillation at elevated temperature (*ca* 150 °C), a purification method leading to important product loss when performed on small scale. The next step in the synthetic pathway, the LiAlH<sub>4</sub> reduction, worked well, but the compound formed was inert toward TMSBr and acid salts such as NEt<sub>3</sub>•HCl and the targeted compound could never be obtained and this part of the Csp<sup>3</sup>-H bond cleavage project was eventually abandoned.



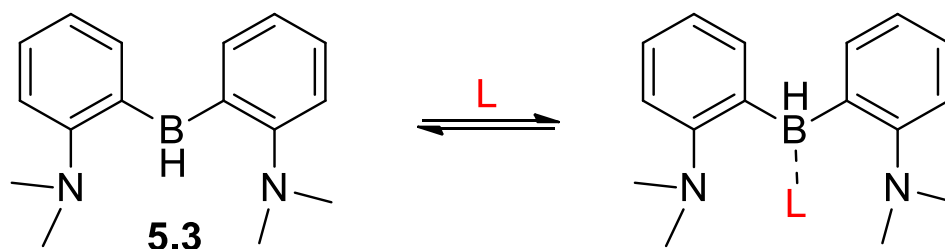
**Scheme 26** Synthesis of **5.7**.

A synthesis analogous to the one described previously for the *ortho*-ethylbenzene derivative could also be developed for **5.1** (**Scheme 27**), but was not very practical because of side reactions, which complicated the purification by crystallization and required a high temperature vacuum distillation. The same problematic reactivity pattern also prohibited a convenient synthesis by simply adjusting the number of B(OMe)<sub>3</sub> equivalents in the reaction with NMe-C<sub>6</sub>H<sub>4</sub>-Li (**2.8**). Since my colleague Hugo Boutin was synthesizing a lot of NMe-C<sub>6</sub>H<sub>4</sub>-B(OMe)<sub>2</sub> (**3.4**) for his own projects, most of the **5.1** used in my study was recovered from the crystallization of his distillation residues.



**Scheme 27** Alternative synthesis of **5.1**.

To isolate and observe the synthetic intermediate **5.3**, the strategy was to find a Lewis base that would stabilize it and allow its observation and eventually its isolation, but not too much to prevent reactivity. To determine suitable candidates, the stability of different Lewis base adducts with **5.3** was initially screened using DFT (**Figure 60**). The results suggested that PPh<sub>3</sub>, predicted to stabilize **5.3** by around 4 kcal/mol, would be an ideal candidate.



$$\Delta G(\text{kcal/mol}) \text{ for } L = \text{Pyridine: } -9.8$$

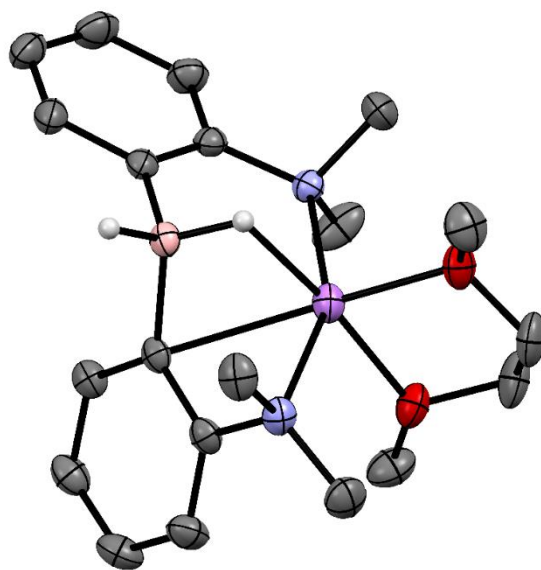
$$\text{PPh}_3: -3.9$$

$$\text{NEt}_3: 0.8$$

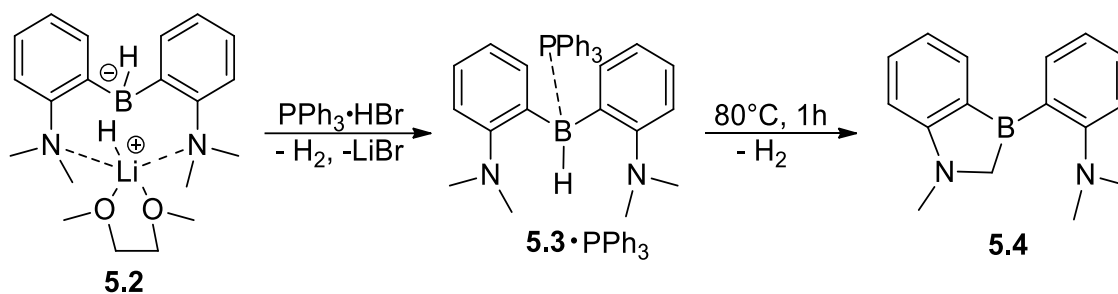
**Figure 60** Stability of the adducts between **5.3** with different Lewis bases calculated by DFT.  $\Delta G$  reported in kcal/mol calculations performed at the  $\omega$ B97XD/6-31++G\*\*, SMD solvent = benzene level of theory.

At the time, I was also investigating acid salts (PPh<sub>3</sub>•HBr and NEt<sub>3</sub>•HCl) as surrogates to TMSBr for the removal of LiH, which would always remain with our FLPs when using our usual synthetic methods. The method works well, but the number of equivalents of acid salts needs to be well measured in order to prevent further reactivity and that requires to know exactly the quantity of FLP•LiH used in the reaction. It can be problematic in one-pot syntheses and this is why we kept the TMSBr or TMSCl method. However, since I had well characterized and isolated **5.2** (**Figure 61**), I found that reacting it directly with PPh<sub>3</sub>•HBr in a J-Young tube was more practical than removing the LiH using TMSBr in presence of PPh<sub>3</sub>. First of all, it is more practical than adding PPh<sub>3</sub>, which is hard to remove and can lead to misleading stoichiometry. Moreover, TMSBr is usually required in a small excess and mild heating under vacuum to remove the excess can lead to degradation. The reaction of **5.2** with PPh<sub>3</sub>•HBr proved very successful and allowed the observation by multinuclear NMR spectroscopy of **5.3**•PPh<sub>3</sub>. Omitting the PPh<sub>3</sub> signals, **5.3**•PPh<sub>3</sub> features only 4 resonances in the aromatic region of the <sup>1</sup>H NMR spectrum, consistent with two equivalent phenylene rings. The aminomethyl groups are also all equivalent and a broad B-H signal is present at 5.1 ppm. The broad <sup>31</sup>P{<sup>1</sup>H} NMR signal is centered at -0.3 ppm and the <sup>11</sup>B NMR resonance appears as a broad singlet at 0.1 ppm, in line with a P-B interaction. Moreover, mild heating of the adduct led to its clean

conversion to the previously discussed and crystallized compound generated after the  $Csp^3-H$  bond cleavage and the release of  $H_2$  (**Scheme 28**). Interestingly, in solution, the  $^{11}B$  NMR shift at 65.3 ppm suggests that the compound is in a monomeric form.

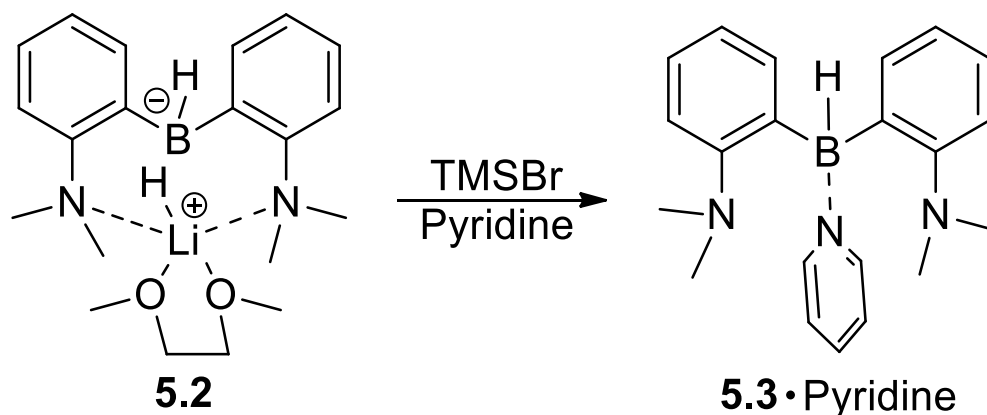


**Figure 61** Crystal structure of **5.2**. Gray = C, blue = N, pink = B, Purple = Li, Red = O and white = H. Hydrogen atoms linked to carbon are omitted for clarity. Ellipsoid drawn at 50% probability.



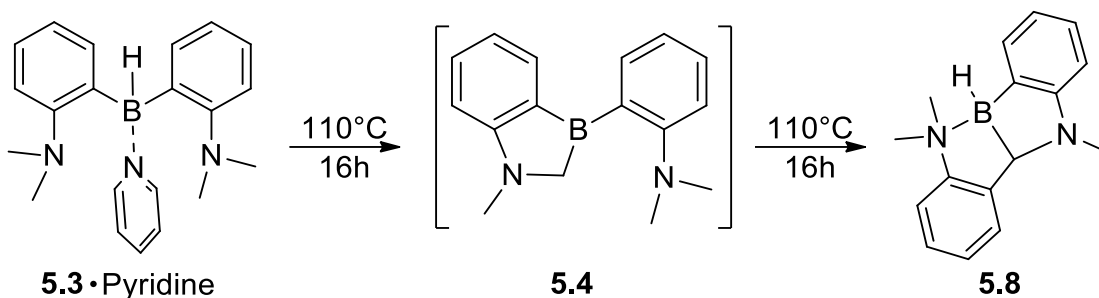
**Scheme 28** Reaction of **5.2** with  $PPh_3 \cdot HBr$  forming **5.3**· $PPh_3$  and **5.4** after mild heating.

Despite that success, the isolation of **5.3**· $PPh_3$  in good purity on a preparative scale proved difficult since it was thermally unstable. Moreover, the fact that  $PPh_3$  is very hard to remove from the reaction mixture prohibited the isolation of the rearrangement product (**5.4**) in a pure form. Those problems encouraged me to use pyridine as a Lewis base to stabilize **5.3**, since it is more volatile and predicted to be more coordinating. Thermal induction of the rearrangement from that adduct would be more difficult, but the isolation of an unreactive **5.3** Lewis base adduct would be easier. This time, because pyridine can be easily removed under reduce pressure, the synthesis was done between **5.2** and  $TMSBr$  in presence of an excess (5 equiv) of pyridine.



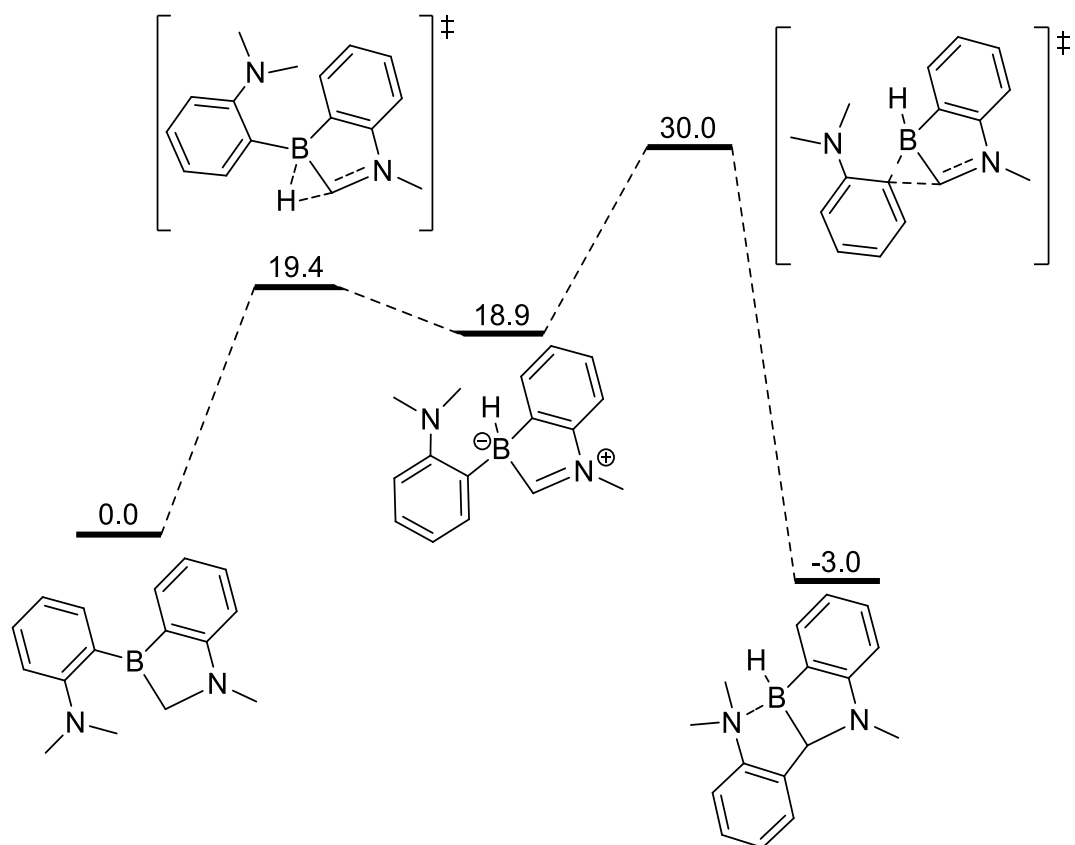
**Scheme 29** Synthesis of **5.3•Pyridine**.

The reaction was successful and allowed the isolation of pure **5.3•Pyridine**, which could be recrystallized in toluene and fully characterized by multi nuclear NMR spectroscopy and X-ray crystallography. As expected, attempting to thermally induce the rearrangement from this adduct was more challenging. Heating at 110 °C showed some signs of the formation of the expected compound, but after 16 h the reaction had converged to a previously unobserved compound, **5.8**. The multi-nuclear characterization of that compound allowed us to propose a reasonable structure. First, eight signals in the aromatic region of the  $^1\text{H}$  NMR spectrum, consisting of four doublets and four triplets, with two overlapping ones resolved by the  $^{13}\text{C}$ - $^1\text{H}$  HSQC, suggested that the molecule was formed of two inequivalent *ortho*-substituted phenylene moieties. Other important signals in the  $^1\text{H}$  NMR spectrum are three distinctive singlets between 2 and 3 ppm, each corresponding to N-Me groups, a doublet around 3.9 ppm integrating for only one proton confirmed to be a CH group by  $^{13}\text{C}$ - $^1\text{H}$  HSQC, and a B-H signal that was better seen using  $^1\text{H}\{^{11}\text{B}\}$  NMR spectroscopy. In addition, the  $^{13}\text{C}$  NMR suggested that the CH group was linked to a boron atom, its signal being very broad, which is distinctive of aliphatic carbons linked to a boron atom. Finally, the  $^{11}\text{B}$  NMR and  $^{11}\text{B}\{^1\text{H}\}$  NMR analysis confirmed the presence of a B-H bond with a  $J^{\text{B-H}}$  coupling that was clearly observed. The chemical shift of 6.8 ppm suggested a four-coordinated boron center, probably because of the presence of an  $\text{NMe}_2\text{-B}$  bond, which would be consistent with the observation of the inequivalency of the N-Me groups. Combining all this evidence and the knowledge of the initial structure led to the proposition in **Scheme 30** and **Figure 62** to explain the nature and the formation of the final product.

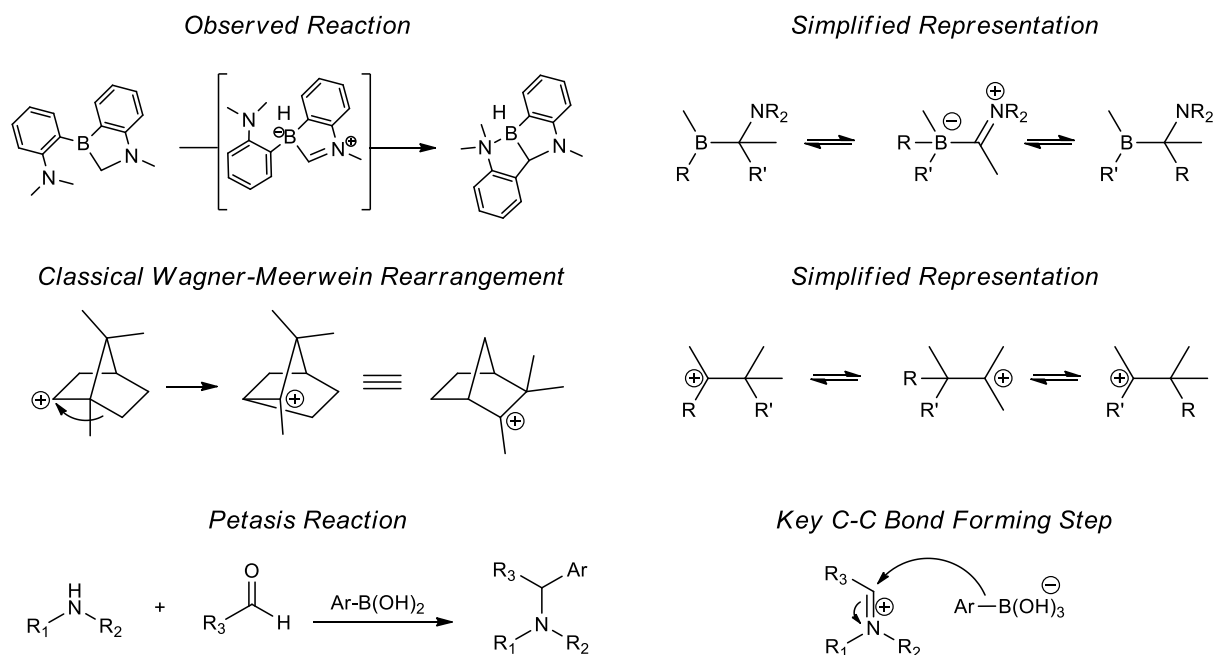


**Scheme 30** Reactivity of **5.3·Pyridine** upon heating.

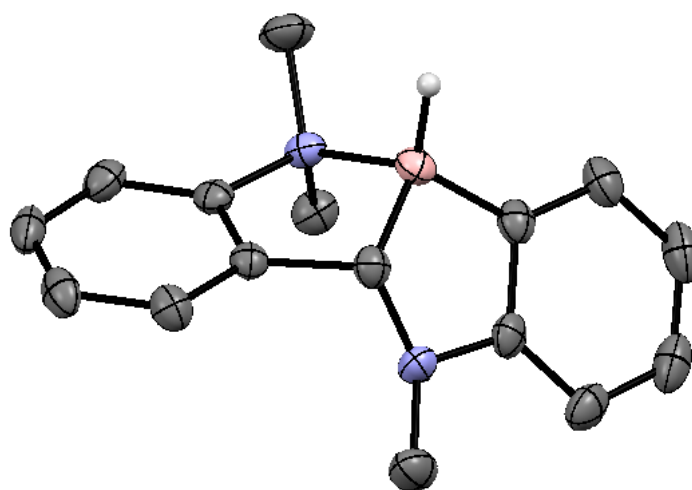
As usual, the mechanism of that transformation was investigated using DFT (**Figure 62**). The only reasonable pathway consisted in the migration of an hydride from the bridging  $\text{CH}_2$  group between the boron and nitrogen atom in the  $\text{Csp}^3\text{-H}$  bond cleavage product (**5.4**) to form a zwitterionic iminium hydroborate as an uphill, but accessible, intermediate. From this intermediate, the aryl moiety can migrate toward the electrophilic carbon atom of the iminium, forming the observed compound which is stabilized by an intra-molecular N-B bond forming a five-membered ring. The reaction can be viewed as analogous to the Wagner-Meerwein rearrangement<sup>210</sup>, which consists of the migration of alkyl groups to a carbocation, where the empty orbital of the carbocation is replaced by the one of a boron atom. Another similar, and maybe less known, reaction is the Petasis reaction to synthesize substituted amines,<sup>211,212</sup> which exploits the addition of an aryl group from a boron precursor to an iminium carbon formed in-situ by the condensation of an amine and a carbonyl group (**Figure 63**). Overall, a  $\Delta G^\ddagger$  of 30 kcal/mol for the limiting step of the DFT supported rearrangement was calculated, which is consistent with a reaction requiring several hours of heating at 110 °C to be complete. Finally, after preparing the compound on a preparative scale, suitable crystals for X-ray crystallography could be obtained and the structure of the compound determined unambiguously (**Figure 64**).



**Figure 62** DFT investigation to explain the formation of **5.8**.  $\Delta G$  reported in kcal/mol, calculations performed at the  $\omega$ B97XD/6-31++G\*\*, SMD solvent = benzene level of theory.



**Figure 63** Comparison between the observed rearrangement, the Wagner-Meerwein rearrangement and the Petasis reaction.



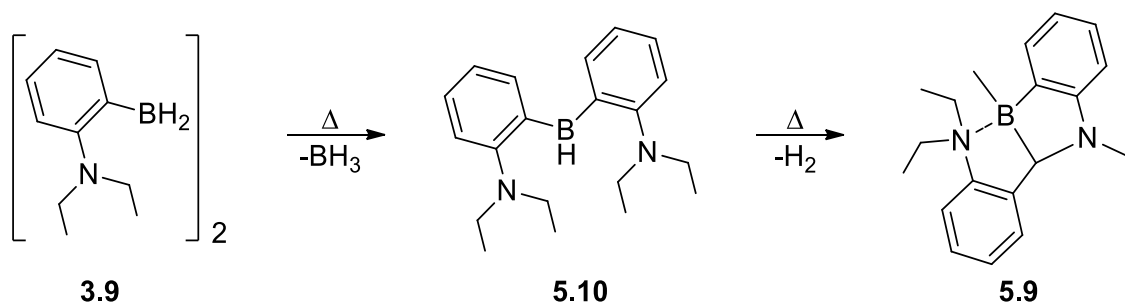
**Figure 64** Crystal structure of **5.8**. Gray = C, blue = N, pink = B, and white = H. Hydrogen atoms linked to carbon are omitted for clarity. Ellipsoid drawn at 50% probability.

After several detours, the initial results that had put us on the track of the FLP promoted Csp<sup>3</sup>-H bond cleavage were finally supported by a reproducible syntheses, which included the reactivity of a Lewis base stabilized form of **5.3**, as well as reliable spectroscopic evidences and DFT results, including the



finding of a further rearrangement reaction. Finally, those results were combined and published, even if the stoichiometric reaction could not be successfully exploited for catalysis.

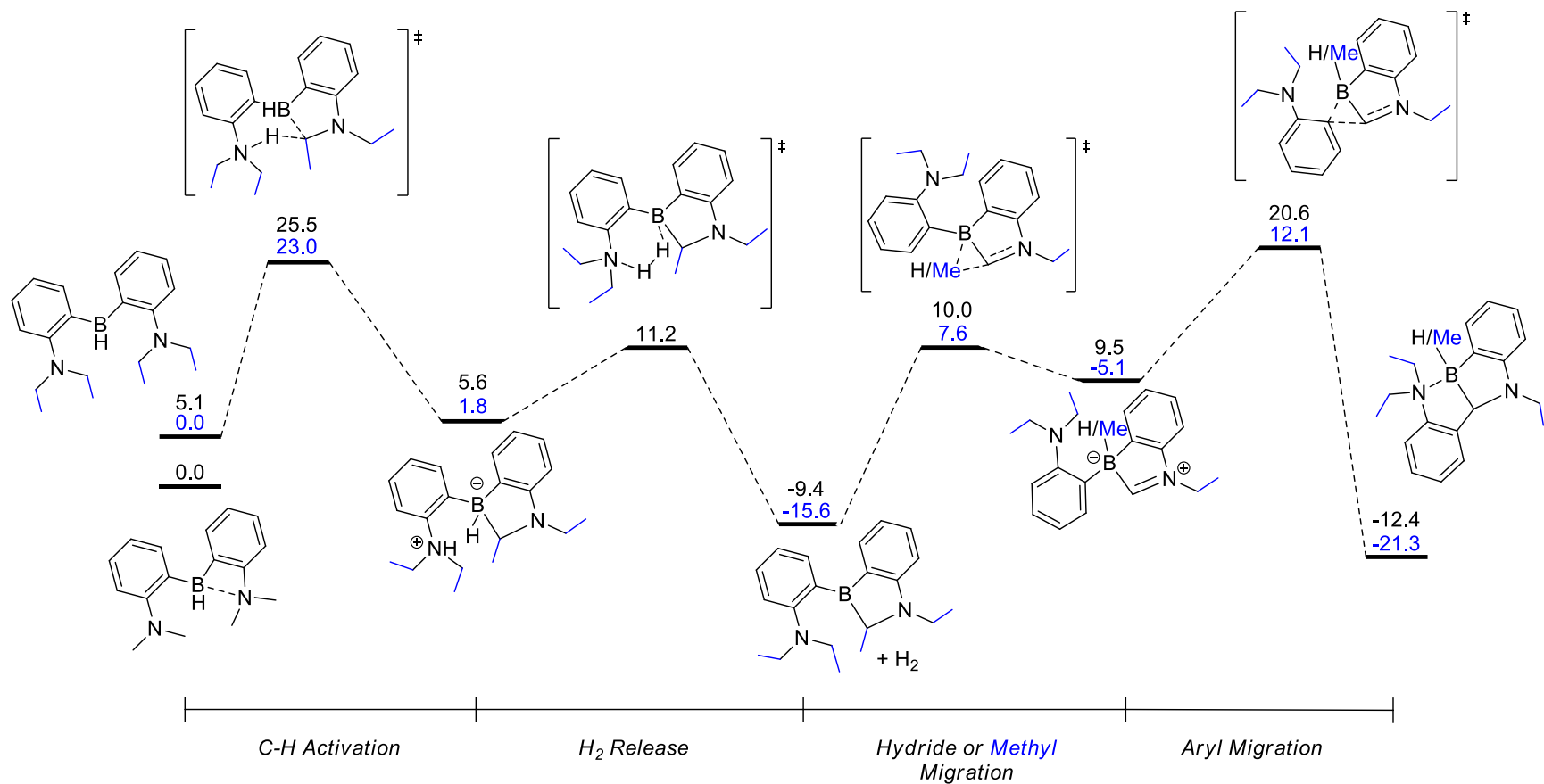
Several months after this report, while studying the thermal stability of other  $\text{NR}_2\text{-C}_6\text{H}_4\text{-BH}_2$  analogues, an interesting and related behavior was observed for compounds in which  $\text{R}=\text{Et}$ . I had previously observed that heating  $\text{NEt}_2\text{-C}_6\text{H}_4\text{-BH}_2$  (**3.9**) at  $110\text{ }^\circ\text{C}$  overnight leads to the clean formation of a new compound (**5.9**), but it could not be identified at the time. At one point, I decided to explore again that reaction, this time performing a complete multi-nuclear NMR characterization. Analyzing those NMR spectra, important features were detected. First, signals for two inequivalent *ortho*-substituted phenylene moieties can be seen in the  $^1\text{H}$  NMR spectrum, as well as signals corresponding to three inequivalent ethyl chains (three triplets for the  $-\text{CH}_3$  and the  $\text{CH}_2$  groups were also assigned using  $^{13}\text{C}\text{-}^1\text{H}$  HSQC). More importantly, a singlet corresponding to a  $\text{CH}_3$  group and a singlet corresponding to a  $\text{CH}$  group could be detected at 0.4 and 3.7 ppm, respectively. Using the  $^{13}\text{C}\text{-}^1\text{H}$  HSQC in combination to the  $^{13}\text{C}$  NMR data showed that these groups were probably linked to a boron atom, which appeared as a broad signal in the  $^{13}\text{C}$  NMR spectrum. In the aromatic region of the  $^{13}\text{C}$  NMR, three less intense and sharp signals that could not be found on the  $^{13}\text{C}\text{-}^1\text{H}$  HSQC, thus assigned to a quaternary carbon, can be observed at 143, 150 and 160 ppm, suggesting only one  $\text{Csp}^2\text{-B}$  bond in the molecule, since  $\text{Csp}^2\text{-B}$  are not usually observed in  $^{13}\text{C}$  NMR. Finally, the  $^{11}\text{B}$  NMR is constituted of only one major signal at 12.8 ppm, suggesting a tetra-coordinated boron, and no sign of a  $\text{B-H}$  bond could be observed in either the  $^{11}\text{B}$  or the  $^1\text{H}$  NMR spectra. Combining all this information suggested that a very similar compound as the one observed in the second rearrangement of the  $\text{Csp}^3\text{-H}$  bond cleavage project is produced while heating **3.9** at  $110\text{ }^\circ\text{C}$  for a prolonged period (**Scheme 31**).



**Scheme 31** Formation of species **5.9** from **3.9**.

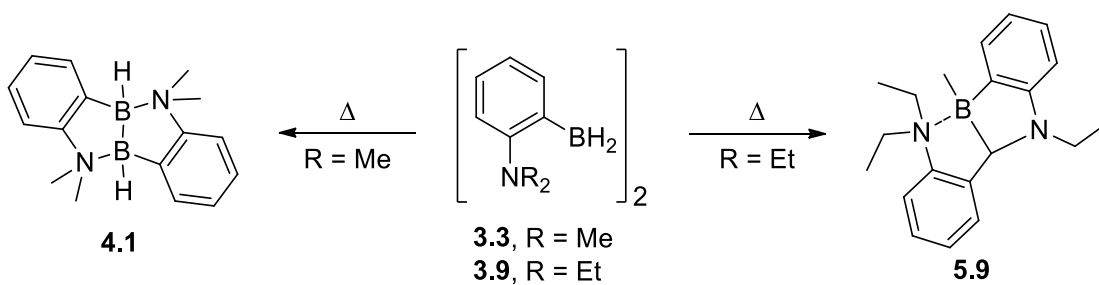
It might not be obvious since the  $\text{Csp}^3\text{-H}$  bond cleavage concerned molecules containing two aryl backbones when **3.9** has only one, but metathesis between the  $\text{BH}_2$  moiety of one molecule and the backbone of another molecule of **3.9** can occur. Once **5.10** is generated, a mechanism analogous to the one presented earlier (**Figure 58** and **Figure 62**) was calculated using DFT for (**Figure 65**). The

most important change is that a methyl group is migrating instead of a hydride to form the iminium zwitterion. Another important fact to consider is that in the case of the  $\text{NEt}_2$  derivative, the first step of the mechanism, the cleavage of the  $\text{Csp}^3\text{-H}$  bond, occurs at the carbon  $\alpha$  to the nitrogen atom preferentially compared to the less hindered terminal  $\text{CH}_3$  group. This supports experimentally the DFT prediction that the  $\alpha$  nitrogen atom has a positive impact on the  $\text{Csp}^3\text{-H}$  bond cleavage transition state accessibility.



**Figure 65** Comparison of the DFT investigation of the reorganization of **3.3** and **3.9**.  $\Delta G$  reported in kcal/mol, calculations performed at the  $\omega$ B97XD/6-31++G\*\*, SMD solvent = benzene level of theory for the NMe<sub>2</sub> derivative and at the  $\omega$ B97XD/Def2TZVP level of theory for the NEt<sub>2</sub> derivative.

The results of this chapter need to be put in the broader context of the thesis. First, the  $\text{LiAlH}_4$  reduction can be applied to synthesize many borohydride; however, this method is far from being general and seems problematic for derivatives containing alkoxy functional groups, probably because of their coordinating ability. Moreover, removing  $\text{LiH}$  from an aminoborane FLP using  $\text{TMSBr}$ , a method previously thought to be broadly applicable, might also be problematic in some cases. While no general trend can be deduced from this work, steric hindrance can certainly play an important role in the reactivity and should certainly be considered carefully in the synthetic design of such derivatives. I also think that this chapter emphasizes a general impression that certainly comes out of the thesis: even if structurally simple, aminohydroboranes are very reactive molecules and their reactivity can be hard to predict. In the previous chapters, the numerous dimers for these species have been discussed. In the last two chapters, it was also possible to compare very similar derivatives and observe that their behavior under thermal conditions can be very different. Indeed, in Chapter 4, I discussed the surprising formation of a B-B bond by simply heating **3.3**, and in this one, a completely different behavior is obtained changing the alkyl chains on the nitrogen atom from methyl to ethyl. It induced metathesis followed by  $\text{Csp}^3\text{-H}$  bond cleavage and other rearrangements, the reactivity that is also observed from a “*bis*-backbone”  $\text{NMe}_2$  analogue. Finally, if one is only interested in developing the metal-free  $\text{NR}_2\text{-C}_6\text{H}_4\text{-BH}_2$  catalyzed C-H borylation of heteroarenes, both of those reactivity patterns can be considered as potential decomposition pathways of the catalyst and taking them into account certainly complicates the task of rationally designing new catalysts based on that framework.



**Scheme 32** Small changes, divergent outcome.

## Chapter 6 S-H bond borylation and the $\sigma$ -bond metathesis

In the previous chapters, I discussed the reactivity of  $\text{NR}_2\text{-C}_6\text{H}_4\text{-BH}_2$  mostly with non-polar bonds, (i.e H-H and C-H), which are usually challenging to cleave and tend to generate reactive entities. However, the reactivity of  $\text{NR}_2\text{-C}_6\text{H}_4\text{-BH}_2$ , and similar derivatives, toward polarized bonds was only slightly discussed in the first chapter in the context of  $\text{CO}_2$  reduction and mostly considered in the context of their impact on catalyst deactivation. After publication of the work presented in the previous chapter, my mindset was mostly focused on finding anything that could be of some interest around  $\text{NR}_2\text{-C}_6\text{H}_4\text{-BH}_2$  chemistry and it is what made me investigate their reactivity with E-H bonds (E = OR,  $\text{NR}_2$ , SR), which are usually more reactive compared to C-H bonds and were thus almost guaranteed to react. This work turned out to be more interesting than I initially suspected and led to interesting chemistry in the context of catalysis.

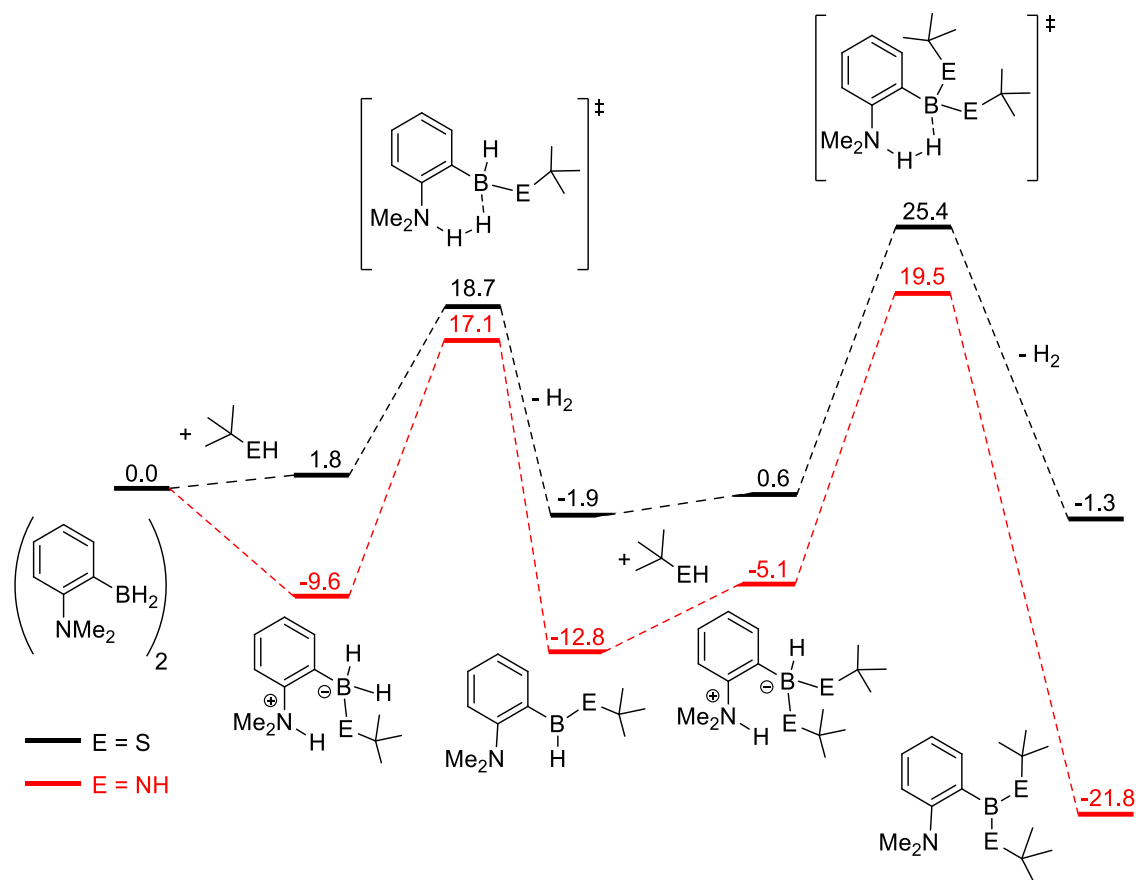
I think it is fair to say that because they are much more reactive, breaking E-H bonds is not of much interest and this is probably why most of FLP reactivity with polarized bonds, which is often stoichiometric, is mostly the formation of adducts. While those reactions are sometimes surprising, they rarely translate into concepts applicable to catalysis. On the other hand, if breaking an E-H bond is not interesting by itself, because it is an easy reaction, it could certainly play a role in a catalytic system and allow to take advantage of other more challenging steps. Hydroaddition reactions such as the hydroamination is certainly a good example of that. In the context of FLP chemistry, and of our C-H borylation system in particular, the realization that the  $\sigma$  bond metathesis step could be the limiting one with some substrates led to question which parameters are important, and if it can be replaced with other steps in a catalytic cycle to promote other reactions than borylation.

Moreover, maybe because it is not a very useful reaction and imply the use of odoriferous compounds to form air sensitive products, less than a handful of publications are reported on the dehydrogenative borylation of thiols. One by Bertrand *et al.*<sup>213</sup> discuss the uncatalysed borylation of alcohols, amines and thiols, but in the case of thiol borylation using HBPIn that reaction requires days of heating at 120 °C, which is often not very practical. Other reports include the description of a Ru catalyzed dehydrogenative borylation of thiols by Nolan *et al.* and the use of a very similar system by Fernández, Westcott and Bo to synthesize borylated thiols in a study of their reactivity.<sup>214,215</sup> Thus there was some place for improvement in the field, especially for metal-free catalysts, since the major interest in borylated thiols is their ability to react without requiring a metal catalyst. Moreover, thiols are often regarded as poisons for transition metal catalysts and are thus less studied in that field, but from the point of view of main group catalysis, especially boron based since the B-S bond is quite

weak and reactive, they are very interesting, especially in the quest for a better understanding of main group catalysis principles and its orthogonal reactivity compared to transition metal catalysis.

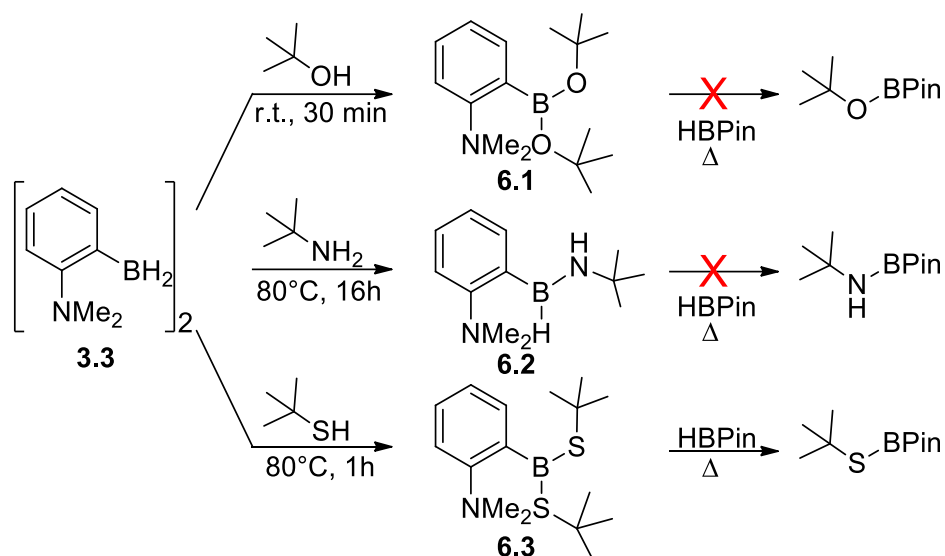
To compare the reactivity of the different E-H bonds, an excess of *tert*-butyl substituted alcohol, amine and thiol was reacted with **3.3**. The molecules were chosen to facilitate the NMR analysis of the reactions and because the reagents are sufficiently volatile to be easily removed under vacuum, but not too much so that they can be handled easily. Unsurprisingly, all molecules reacted with **3.3**. The alcohol was the most reactive, forming the *bis*-substituted product rapidly at room temperature. Such reactivity was expected as alcohols usually react with hydroboranes quite rapidly, even in absence of a catalyst.<sup>213</sup> The dehydrogenative borylation of amines can also be performed at room temperature using pinacolborane, but usually requires longer reaction times, on the hour scale. Moreover, in the case of primary amines, *mono*-borylation products are usually observed, suggesting that the N-B bond makes the second N-H bond less reactive. Such reactivity is also observed in the reaction between **3.3** and *t*Bu-NH<sub>2</sub>. The *mono*-aminated product, characteristic by its doublet at 36.5 ppm in the <sup>11</sup>B NMR spectrum, could be observed after minutes at room temperature, but no sign of the *bis*-aminated product could be observed, even after several hours of heating at 80 °C. Finally, in the case of *t*Bu-SH, the *bis*-thiolated product was observed after 1 h at 80 °C, again consistent with the results reported by Bertrand *et al.* suggesting that S-H bonds are more difficult to borylate.

The difference in the reactivity between *t*Bu-NH<sub>2</sub> and *t*Bu-SH with **3.3** was investigated by DFT (**Figure 66**) and supported the experimental observations. Indeed, in the case of the reaction with *t*Bu-SH, the first thiolation step and the release of H<sub>2</sub> are almost thermoneutral and the newly formed B-S bond seems to have very little impact on the boron acidity. The formation of the first and second FLP/*t*Bu-SH adducts are endothermic by 1.8 and 2.5 kcal/mol, respectively. Kinetically, the second thiolation reaction is significantly more difficult, probably because of steric factors, but is still accessible. However, in the case of the reaction with *t*Bu-NH<sub>2</sub>, the first amination reaction and the release of hydrogen are quite exothermic. The acidity of the boron also seems much more affected by the formation of a B-N bond. Indeed, the formation of the second FLP/*t*Bu-NH<sub>2</sub> adduct is endothermic by 7.7 kcal/mol, while the formation of the first one is exothermic by 9.6 kcal/mol. A striking difference when compared to the reactivity with *t*Bu-SH. Overall, the calculated  $\Delta G^\ddagger$  of the second amination reaction at 32.3 kcal/mol supports the observed absence of reactivity.



**Figure 66** DFT investigation of the borylation of *tert*-butylamine and *tert*-butylthiol. ΔG reported in kcal.mol<sup>-1</sup>, calculation performed at the ωB97XD/6-31+G\*\*, SMD solvent = chloroform level of theory.

Finally, it was attempted to react those products with HBPIn to know if the B-E bonds could enter in σ-bond metathesis. The product containing a B-S bond was the only one for which a reaction was observed, a behavior rationalized by the weaker π overlap in the B-S bond compared to the B-N and B-O bonds, making the boron atom of the B-S bond more Lewis acidic and the sulfur of the B-S bond more nucleophilic. A summary of the reactivity of **3.3** with the different *t*Bu-EH compounds and of those products with HBPIn is presented in **Scheme 33**



**Scheme 33** Stoichiometric reactions between **3.3** and *tert*-butanol, *tert*-butylamine and *tert*-butylthiol.

Since the cleavage of the S-H bond followed by the  $\sigma$  bond metathesis with HBPIn close a potential S-H borylation catalytic cycle, the catalytic reaction was attempted. It was found that **3.3** can catalyze the borylation of thiophenol in relatively mild conditions, using HBPIn as borylating agent. The reaction optimization was presented in **Table 9**.

**Table 9** Optimization of the borylation of thiophenol catalyzed by **3.3**

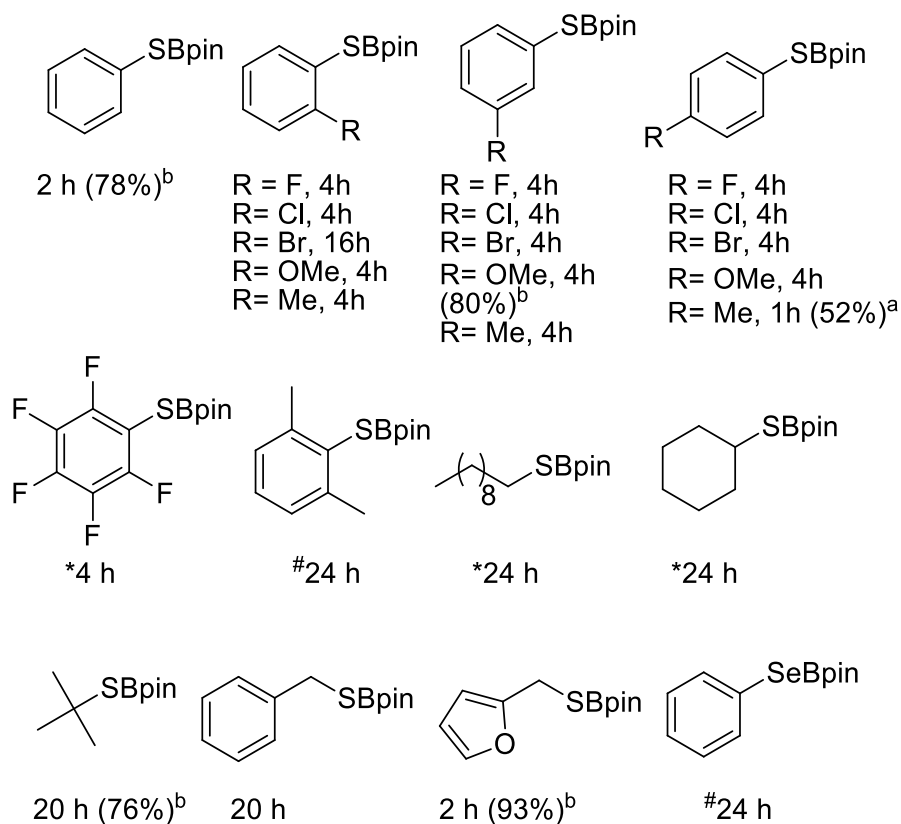
Entry	Catalyst loading mol%	Temperature °C	Solvent	Time h	Conversion %
1	0	80	CDCl <sub>3</sub>	48	31
2	0.5	80	CDCl <sub>3</sub>	2	>95
3	2.5	80	CDCl <sub>3</sub>	1	>95
4	2.5	60	CDCl <sub>3</sub>	2	>95
5	2.5	40	CDCl <sub>3</sub>	8	>95
6	2.5	20	CDCl <sub>3</sub>	24	>95
7	2.5	80	C <sub>6</sub> D <sub>6</sub>	1	>95
8	2.5	80	THF- <i>d</i> <sub>8</sub>	1	>95

As I mentioned before, the borylation of thiols can be performed without a catalyst, but requires elevated temperatures and prolonged reaction time. This is evident in the optimization table, where the borylation of thiophenol in absence of a catalyst produced 31% conversion of borylated thiophenol



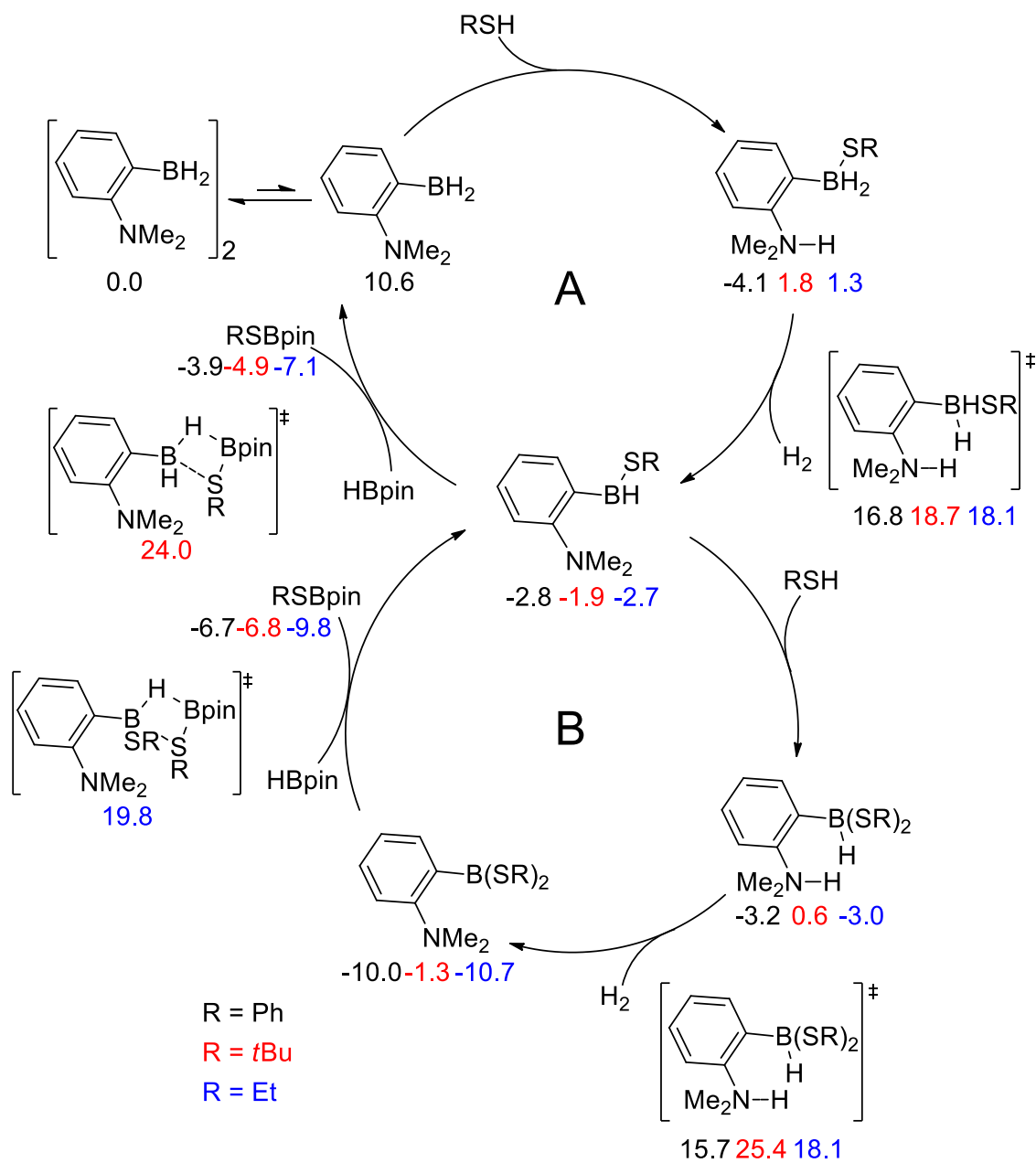
after 48 h at 80 °C. However, at the same temperature, the reaction reaches full conversion in only 2 h using a catalyst loading of only 0.5 mol% of **3.3**. The rest of the results follow the expected trend, with lower temperatures leading to longer reaction times to reach full conversion. The reaction can also be performed in aprotic and non-polar solvents such as chloroform, aromatic hydrocarbons and THF.

This prompted us to study the substrate scope of the **3.3** catalyzed borylation of thiol using HBPin as boron source. Most of those manipulations were performed by Hugo Boutin, a master student in the lab at the time, under my supervision. The reaction is compatible with alkyl, alkoxyde and halogen substituted thiophenols, as well as aliphatic and benzylic thiols. Unsurprisingly, hindered thiophenols, notably 2,6-dimethylthiophenol and 2-bromothiophenol, react more slowly, but surprisingly, this is not the case for bulky aliphatic thiols. Looking carefully at the substrate scope, one can note that *t*Bu-SH reaches full conversion in 20 h in the standard conditions while decanethiol and cyclohexanethiol required 24 h at a higher temperature with a higher catalyst loading (*vide infra*). Finally the reaction is also compatible with selenophenol, but required higher temperature, higher catalyst loading and 2 equivalents of HBPin to reach full conversion in a reasonable time (24 h).



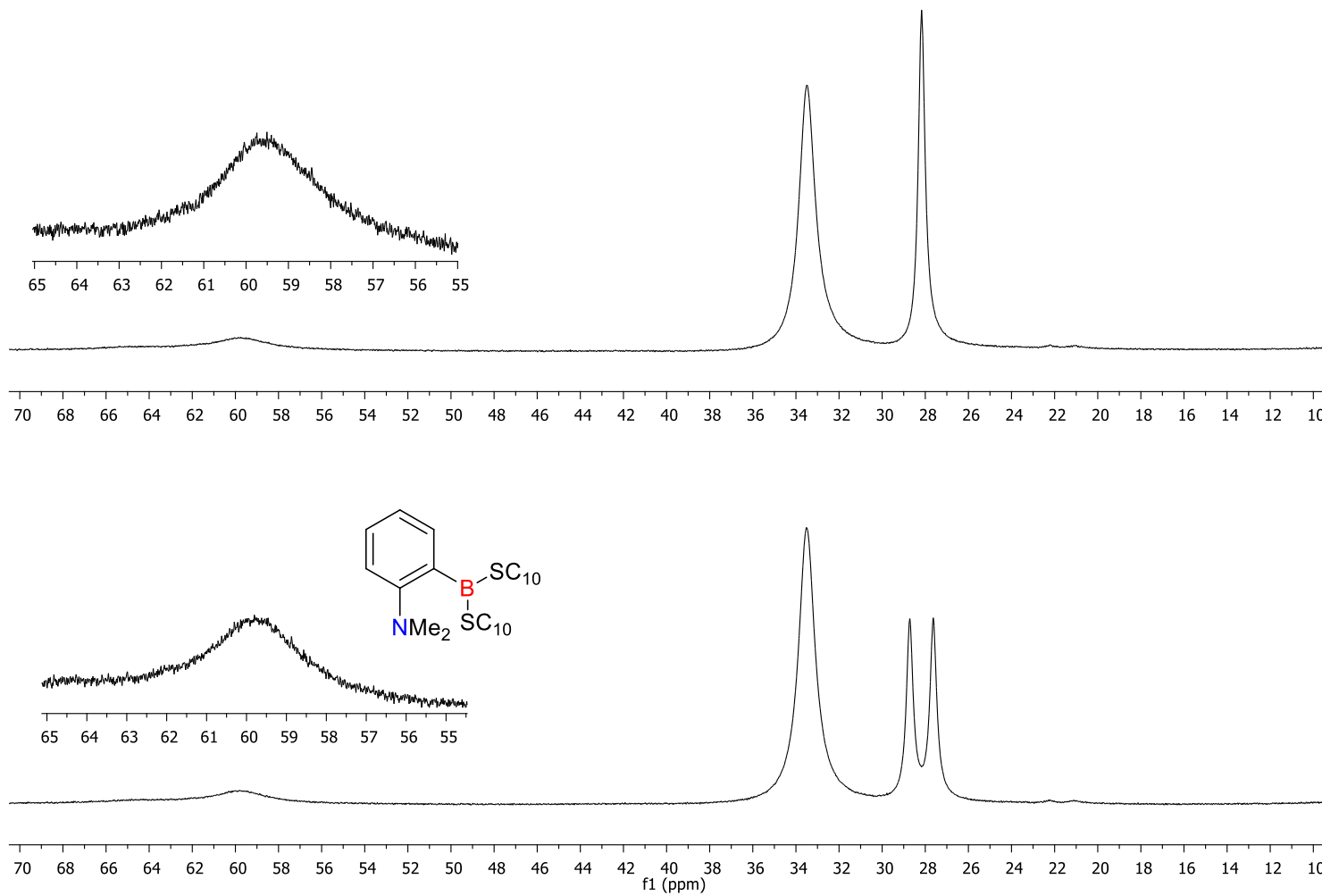
**Figure 67** Scope of the catalytic borylation of thiols and time required for full <sup>1</sup>H NMR conversion. Standard conditions: 2.5 mol% of **3.3**, 60 °C, CDCl<sub>3</sub>, 1.1 equiv HBPIn; \*10 mol% of **3.3**, 80 °C, CDCl<sub>3</sub>, 1.1 equiv HBPIn; #10 mol% of **3.3**, 80 °C, CDCl<sub>3</sub>, 2 equiv. HBPIn. Isolated yields are in parenthesis; <sup>a</sup>after recrystallization in hexane; <sup>b</sup>after vacuum distillation.

The difference in reactivity between the different substrates, decanethiol and *t*Bu-SH in particular, prompted us to investigate the reaction mechanism, using DFT and additional experiments. The DFT calculation suggests that a mechanism very similar to the one proposed for the borylation of C-H bond is also reasonable for the S-H bond borylation. In the case of the S-H borylation, the  $\sigma$  bond metathesis step is proposed to be the limiting one, making a second S-H bond cleavage possible and kinetically more facile for most substrates. In fact, the computational results suggest that cycle B on **Figure 68** can explain the higher reactivity of *t*Bu-SH compared to decanethiol (simplified as Et-SH in the computational study). Indeed, with *t*Bu-SH, the second S-H bond activation followed by the release of H<sub>2</sub> is predicted to be much more difficult than with Et-SH, probably because of steric hindrance. This means that cycle A is favored with *t*Bu-SH, but that cycle B is preferred with decanethiol. Since the intermediate entering the limiting  $\sigma$  bond metathesis is less hindered in cycle A, it would very well explain the observation that *t*Bu-SH reacts more rapidly.

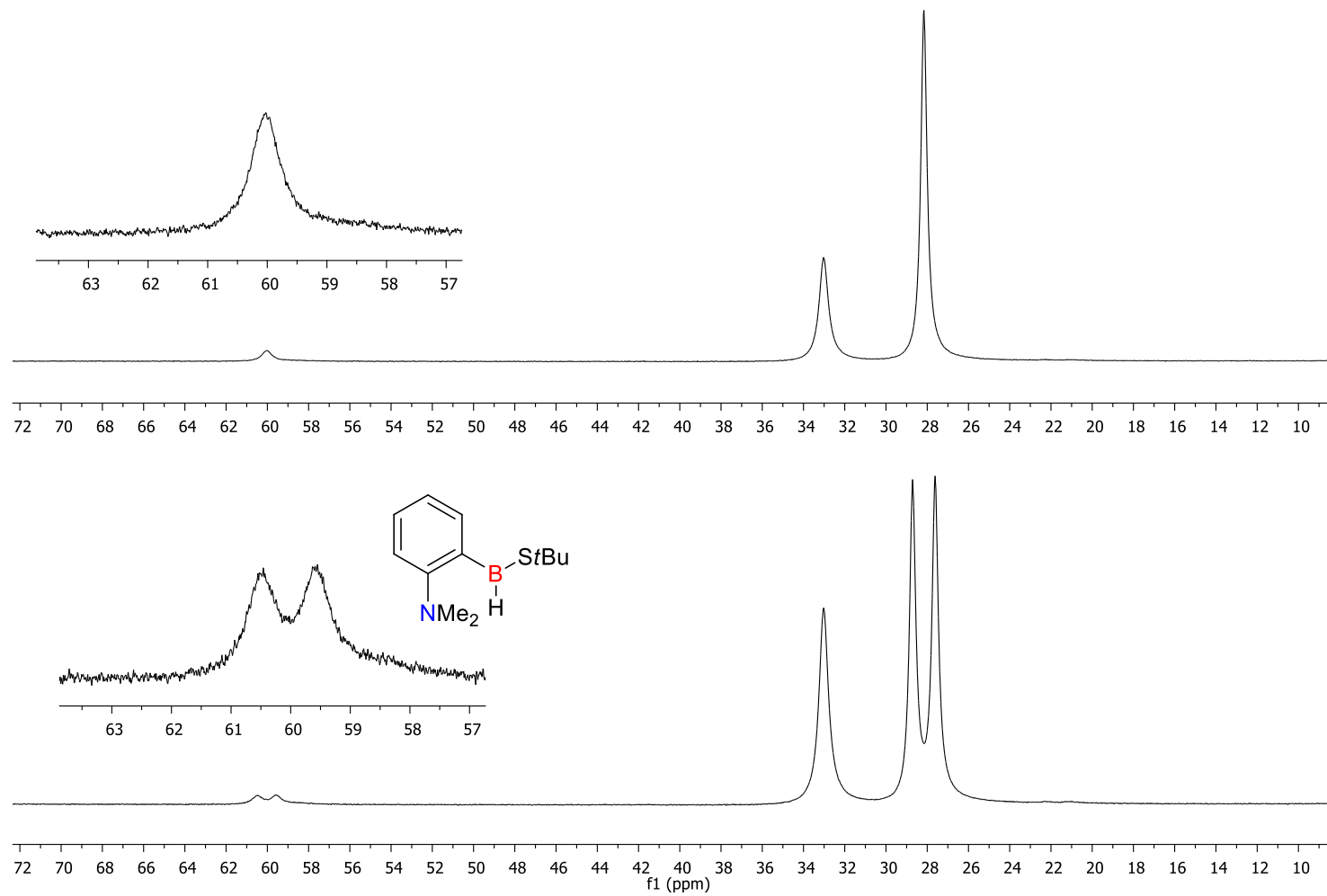


**Figure 68** Proposed mechanism for the FLP catalyzed borylation of thiol.  $\Delta G$  reported in kcal/mol, calculations performed at the  $\omega$ B97XD/6 31+G\*\*, SMD solvent = chloroform level of theory.

In order to support that proposition experimentally, we investigated the resting state of the catalyst in the reaction with both substrates using  $^{11}\text{B}$  NMR spectroscopy. The results are presented in **Figure 69** and **Figure 70** and support our hypothesis. Indeed, in the case of decanethiol, the resting state of the catalyst was found to be  $\text{NMe}_2\text{-C}_6\text{H}_4\text{-B(SR)}_2$  and with *t*Bu-SH,  $\text{NMe}_2\text{-C}_6\text{H}_4\text{-B(SR)(H)}$ , characterized by its very characteristic doublet signal in the  $^{11}\text{B}$  NMR spectrum (**Figure 70**).



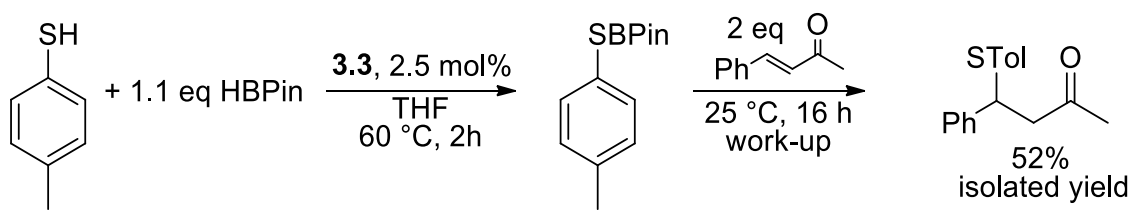
**Figure 69** Top:  $^{11}\text{B}\{^1\text{H}\}$  NMR (160 MHz,  $\text{CDCl}_3$ ) during the catalytic borylation of decanethiol. Bottom:  $^{11}\text{B}$  NMR (160 MHz,  $\text{CDCl}_3$ ) during the **3.3** catalyzed borylation of decanethiol.



**Figure 70** Top:  $^{11}\text{B}\{^1\text{H}\}$  NMR (160 MHz,  $\text{CDCl}_3$ ) during the catalytic borylation of *t*Bu-SH. Bottom:  $^{11}\text{B}$  NMR (160 MHz,  $\text{CDCl}_3$ ) during the **3.3** catalyzed borylation of *t*Bu-SH.

I mentioned many times now that the underlying goal of all the projects presented in this thesis is to better understand the basic principles of main group catalysis. It involves developing the stoichiometric reactions and use them as building blocks to promote useful catalytic reactions. Because of that, I consider the relevance of the previous results residing much more in the fact that they are insightful in the understanding of the  $\sigma$  bond metathesis reaction implicating boron centers rather than being useful in the development of the thioborylation reaction, which is a very niche reaction. That being said, as mentioned in the introduction of this chapter, the reactivity of borylated thiols and other related compounds has been and is still investigated by other research groups and they exhibit some interesting reactivity patterns.<sup>216</sup> Since one of the reaction intermediates of our proposed catalytic cycle is a borylated thiol, these reactivity patterns could potentially be used to replace the  $\sigma$  bond metathesis step in a catalytic cycle of a reaction potentially more useful than the thioborylation, thus deserving some attention.

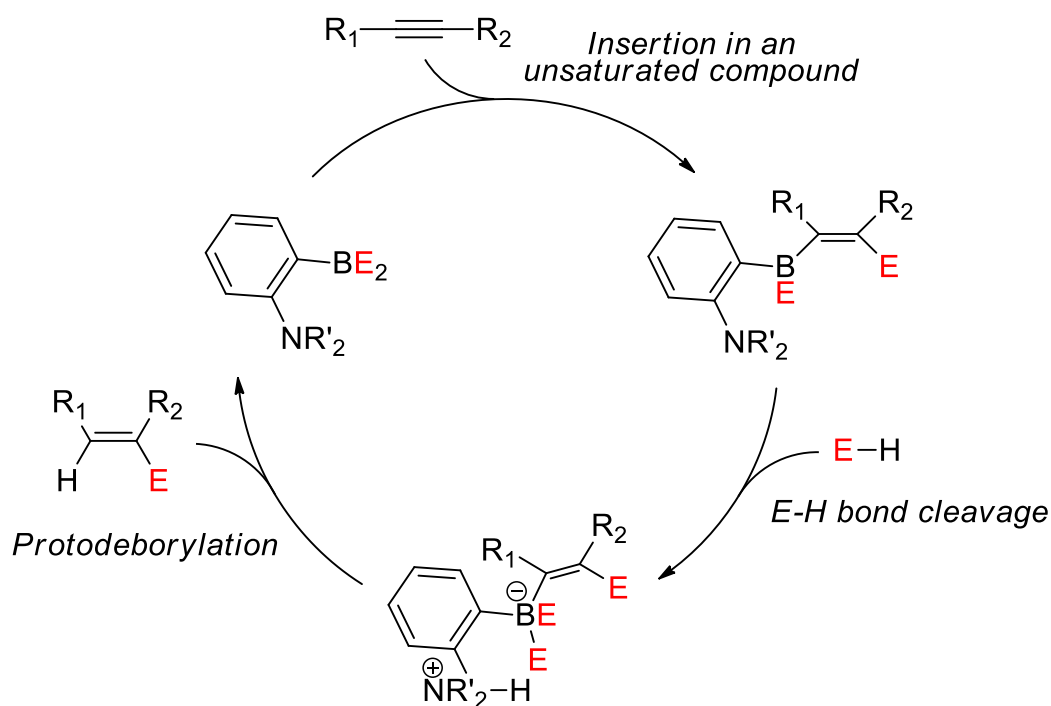
Fernández, Ito *et al.* recently reviewed the reactivity of B-E (E = O, N, S, Se) bonds containing compounds with organic molecules, putting emphasis on metal-free reactions and mechanistic insights.<sup>217</sup> Although I will not go in all the details of that chemistry, I want to emphasize on some aspects of the current state of development of B-E bond chemistry. First, the major reactivity pattern of B-E bonds is the stoichiometric addition to unsaturated compounds to form C-E bonds. The addition of borylated thiols to Michael acceptors such as  $\alpha,\beta$ -unsaturated ketones, a reaction we exploited to valorize our work on the catalytic borylation of thiols (**Scheme 34**), is a good example of that.



**Scheme 34** One-pot Michael addition of 4-methylthiophenol on 4-phenyl-3-buten-2-one through catalytic borylation.

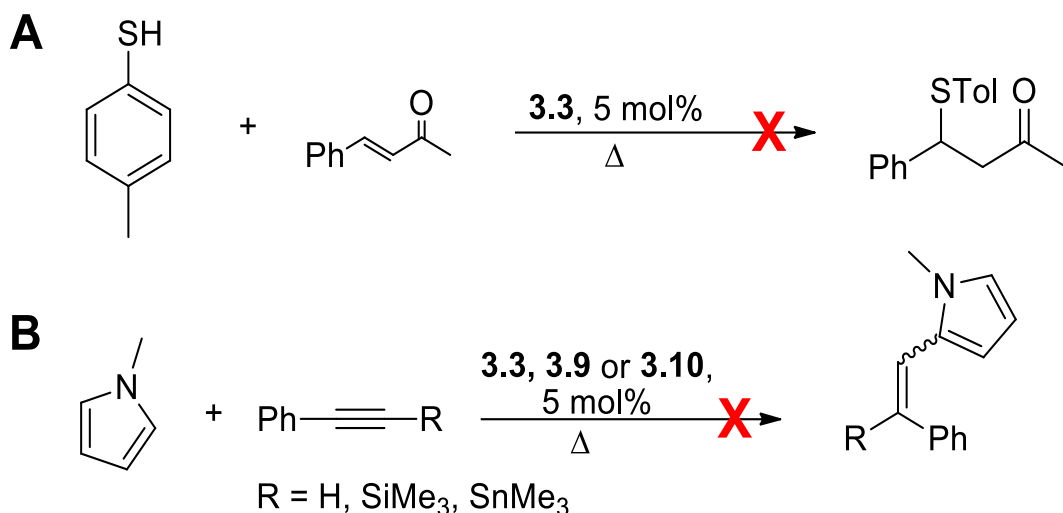
However, as most reactivity patterns of B-E bond containing compounds, the addition of borylated thiols to  $\alpha,\beta$ -unsaturated ketones consists of a stoichiometric reaction in which the B-E bond is sacrificed to form a C-E bond. Moreover, the compounds containing B-E bonds used in reactivity studies are overwhelmingly BPin derivatives, one of the least Lewis acidic boryl moiety available. This is certainly justifiable in a stoichiometric reaction because BPin compounds are usually cheaper and easier to synthesize, purify and handle, but it certainly also leads to a weaker reactivity of the

B-E bond compounds, thus limiting their use. Another aspect often neglected when reading B-E bond reactivity studies is that even if the B-E bond is formally added to a Michael acceptor, the isolated compound is usually the one formed after a protodeborylation step, certainly because the boron containing compounds, which are sensitive to hydrolysis, are harder to isolate. Combining all those observations, it is certainly easy to realize that generating transient B-E bonds using a metal-free catalyst could certainly be advantageous. First, the E-H species could be used directly, eliminating a step for the preparation of the B-E bond containing compound. Second, the boron containing waste would be eliminated. Finally, since the B-E bond containing species would not have to be handled directly but would only be an intermediate in the catalytic cycle, a more reactive borane, and reactive B-E species, could be used. A proposed potential catalytic cycle is presented in **Figure 71** as a general working hypothesis.



**Figure 71** Proposed potential catalytic cycle for a metal-free hydro-heteroelement addition reaction.

At the time of our study on the thioborylation reaction, performing catalytically the thioaddition on  $\alpha,\beta$ -unsaturated ketones was attempted. Unsurprisingly, the intermediate formed after the addition, which contains a B-O bond, proved unreactive in presence of thiols and the cycle did not turnover. Other similar reactions using a carboboration type addition were also attempted, but proved unsuccessful. In brief, the proposed catalytic cycle is still a working hypothesis and no working combination of substrates has been identified yet.



**Scheme 35** Attempted catalytic thioaddition on  $\alpha,\beta$ -unsaturated ketones (A) and carboboration (B).

To summarize, this work should not be seen as an effort to develop the borylation of thiols, but rather as an attempt to better understand FLP and main group catalysis by providing well defined examples and finding the important factors in  $\sigma$  bond metathesis with boron containing molecules. It is an important stepping stone in the development of metal-free catalyzed hydroaddition reactions.

This work is the last I did concerning  $\text{NR}_2\text{-C}_6\text{H}_4\text{-BH}_2$  chemistry and while it is fair to say that there is always more to find, I think that in research you should follow the scientific results and when everything points for major changes, it is certainly advisable to make some. In catalysis, and in particular in catalyst optimization, there is some undeniable clues that you are close to a “local minimum”. If every small changes made to the catalytic system result in a change of limiting step, it should ring a bell that small changes will not do it anymore and that it is the time for a bigger one. At that time, the  $\text{NR}_2\text{-C}_6\text{H}_4\text{-BH}_2$  catalyzed C-H borylation of heteroarenes could have as rate limiting step the dimer separation, the C-H bond cleavage or the  $\sigma$  bond metathesis step, according to the substrate and the R group on the amine. Another important call for a bigger change is when all your ideas for improving the catalyst would require increasingly complex synthesis. I mentioned in the introduction section that catalyst complexity is often overlooked in academia, but it is in fact of great importance if the catalytic system is to reach broader utilization. I believe that adding many steps to a ligand synthesis, or in our case to the catalyst synthesis, to improve its activity is rarely worth the trouble and probably a waste of time if it is only to improve slightly the reaction rate. I also want to emphasize that blindly doing mechanistic studies to only fine tune a catalyst, for example by changing ligands to optimize secondary interactions, is lacking perspective. A truly comprehensive mechanistic study should not only help to improve the catalytic system, but also simplify its utilization. At this point, I had milked this cow to a point where the fun of new discoveries was no more. However, I



wanted to use my knowledge gained on the  $\text{NR}_2\text{-C}_6\text{H}_4\text{-BH}_2$  chemistry to raise a new-born calf that would feed the next generation of students in Fontaine group, as you will see in the next chapter.

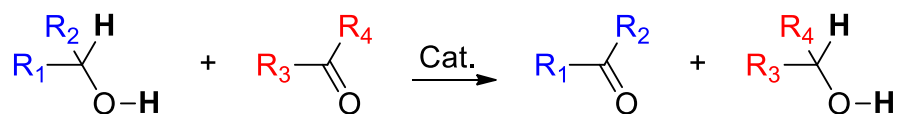
## Chapter 7 Transfer borylation: from N/B to N/S

Since we were getting to know very well the  $\text{NR}_2\text{-C}_6\text{H}_4\text{-BH}_2$  chemistry and very little surprises were occurring, it had an impact on my motivation. It was a good timing to experience working with a new research group, which I did during an internship with Prof. Paul Chirik at Princeton. In addition to bringing new learning experiences, it also helped the pursuit of my thesis. Although the chemistry I did during that internship, working on the borylation using cobalt catalysts, is not relevant to this thesis, that experience led me to the work presented herein.

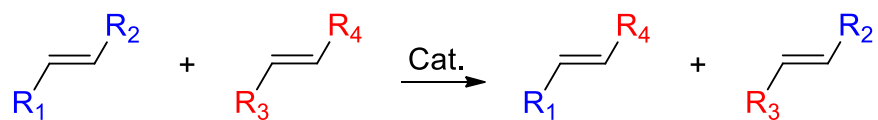
As many other metal catalyzed system for the C-H borylation reaction, the cobalt catalytic system uses  $\text{B}_2\text{Pin}_2$  as a convenient boron source. It is a commercially available solid that is considered being not very sensitive in ambient conditions. However, using it for the C-H borylation reaction will generate HBPIn as a side product, often wasting half of the boron atoms. Moreover, HBPIn is a good hydroboration reagent and its generation often limits the functional group tolerance. Finally, HBPIn may poison the catalyst limiting its activity, and in some cases the systems require the addition of a trapping agent, usually an alkene, to trap it from the reaction medium. These problems inspired me to use cheaper phenylboronic acid or esters as boron sources for the C-H borylation reaction. This reaction would be formally a transfer borylation, or isodesmic, reaction. In that system, an unreactive arene would be released, which could potentially improve the functional group tolerance since no reactive side-products, such as HBPIn, would be generated. This way, it would make possible using catalysts that would react either with HBPIn or  $\text{H}_2$ , the possible side-products of the reaction. Even if I was doubtful that such reaction could be performed by a metal-free catalyst, since breaking a C-B bond is mostly done via oxidative addition, I eventually proved myself wrong. However, before discussing of the actual results, I would like to introduce the concept of isodesmic reactions and the motivation behind the development of transfer borylation catalysts.

Isodesmic reactions have attractive features. In these chemical transformations, the type of chemical bonds cleaved in the reactants are the same as those formed in the reaction products.<sup>218</sup> Notable examples of such processes include transfer hydrogenation<sup>219</sup> and olefin metathesis<sup>220,221</sup> (**Scheme 36**). Using the same principle, Morandi and coworkers elegantly demonstrated that alkyl nitriles could be used as a replacement for highly toxic HCN to perform the hydrocyanation reaction.<sup>222</sup> In addition to enabling the use of cheaper, safer or more convenient reagents, isodesmic reactions often exhibit higher functional group tolerance, which is of importance for late stage functionalization reactions in drug synthesis.<sup>87</sup> However, quite surprisingly, isodesmic C-H functionalization transformations are extremely scarce.

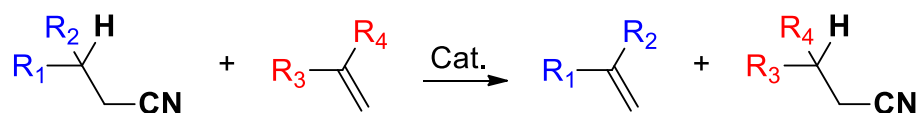
**A) Transfer hydrogenation**



**B) Olefin metathesis**



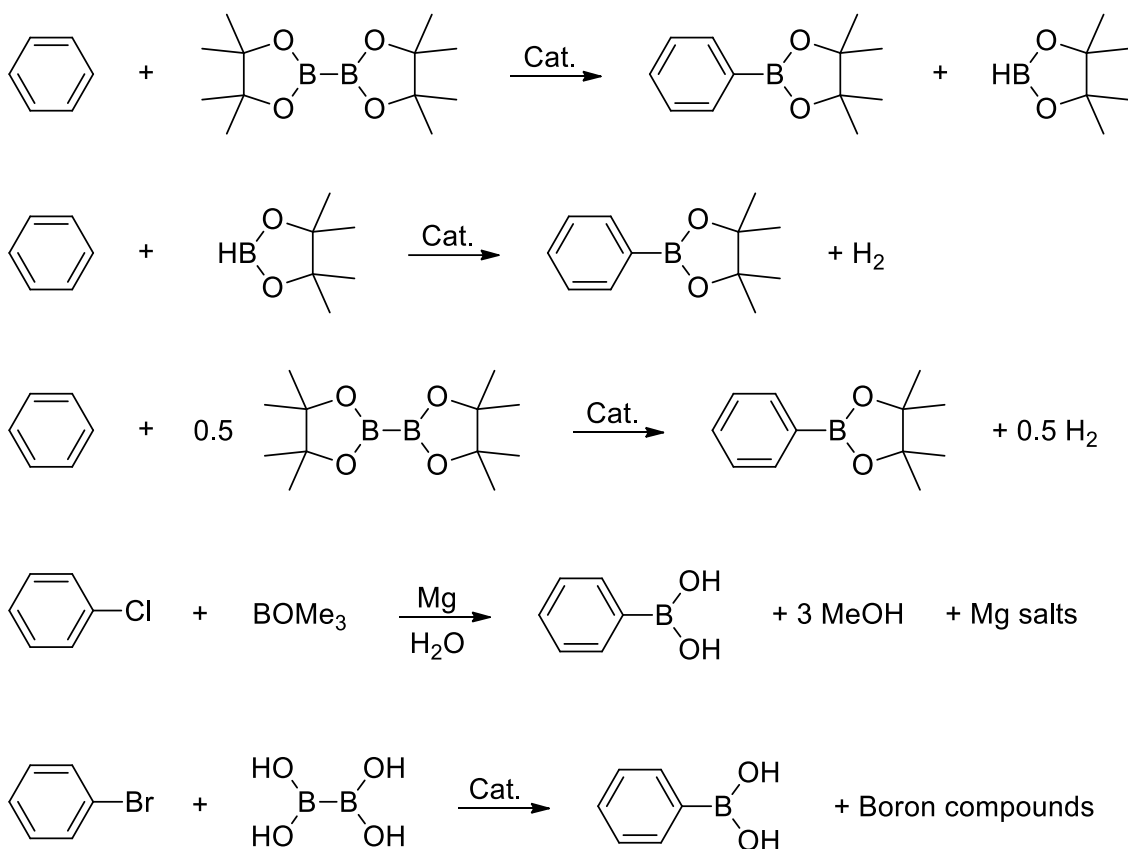
**C) Transfer hydrocyanation**



**Scheme 36** Examples of isodesmic reactions.

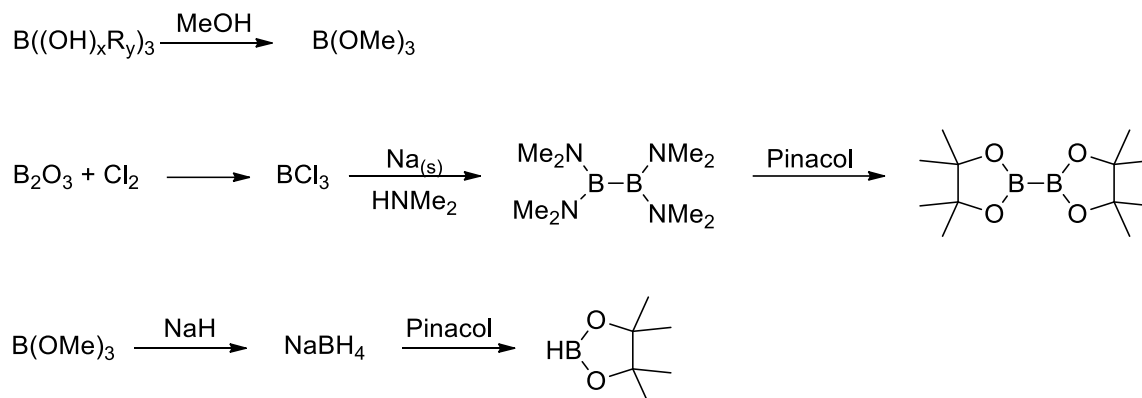
Before deepening the discussion on the application of an isodesmic methodology to the borylation reaction, I think it would be wise to discuss the borylation reaction in a green chemistry perspective. As I mentioned in the introduction, in academia a new methodology is often claimed green if it respects or improves one of the twelve aspects of green chemistry. This is in part because “green” is a buzzword, but also because in academia, the reactions are rarely put in the context of the large scale synthesis of a specific target, which is what the green chemistry principles were designed to improve. Thus, even though theoretically a reaction may seem “green”, it might not lead to a green process because it would require the use of protecting groups or a more complex workup. The inverse is also true, since a reaction seemingly wasteful may in reality improve the greenness of a chemical process by saving steps, being more selective, or simply because of easier workup. The borylation reactions, including but not exclusive to the C-H borylation reaction, are very good examples of that.

For example, the hydroboration of alkenes is a very selective reaction, which can be carried out in mild conditions with 100% atom economy. However, in the context of a full synthesis, the inserted boryl group will almost always end up as a waste limiting the apparent atom economy generated by such a step. Another factor is the waste generated when synthesizing borylation reagents. For example, there are many ways to perform the borylation of benzene and at first glance the greenest one seems to be C-H functionalization using HBPin, or even better half an equivalent of  $\text{B}_2\text{Pin}_2$ , generating only  $\text{H}_2$  as side-product. Another option is the formation of a Grignard reagent from chloro or bromo benzene, which will react stoichiometrically with  $\text{B}(\text{OMe})_3$  to form the same product but with a stoichiometric equivalent of magnesium salts,<sup>223</sup> which is seemingly more dirty.



**Scheme 37** Different synthesis of phenylboronic acid.

However, taking into account the complete synthesis can change the picture.  $\text{B}_2\text{Pin}_2$  is synthesized via the reduction of  $\text{BCl}_3$ , which itself is produced from the chlorination of boron oxide using  $\text{Cl}_2$ , using metallic sodium, generating stoichiometric equivalents of salt.<sup>224,225</sup> In the case of  $\text{HBPin}$ , the large scale synthesis process is less clear, but it is likely produced from either the reaction of pinacol with  $\text{BH}_3\text{SMe}_2$  or  $\text{NaBH}_4$ ,<sup>226</sup> itself coming from the reaction of  $\text{B(OMe)}_3$  with  $\text{NaH}$ , which is produced from the reaction of melted sodium and  $\text{H}_2$ , in a process that is also generating stoichiometric equivalents of salt. By taking the provenance of the reagents into account and their waste charge, the use of Grignard reagents certainly seems a less absurd option.

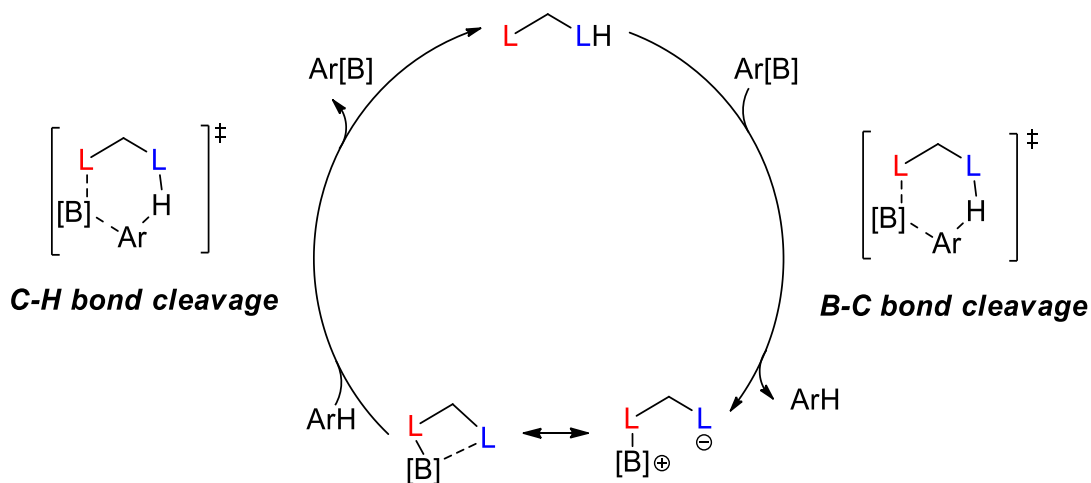


**Scheme 38** Synthesis of various borylating reagent.

Finally, the use of the final product is also important to consider. As discussed by Molander a few years ago, in the context of promoting the use of  $\text{B}_2(\text{OH})_4$  instead of  $\text{B}_2\text{Pin}_2$  for the Pd catalyzed borylation of aryl halides, most of the time the pinacol is a protecting group that will eventually become waste since the boronic acid is the active species.<sup>227</sup> While the borylation reaction, especially via C-H functionalization, may seem formidable because of its atom economy, the reality is that its usefulness resides in saving synthetic steps. In that context, practicability, selectivity, and functional group tolerance are probably the most important criteria to take into account for the development of useful C-H borylation reactions.

The transfer borylation reaction, while far from being perfect, presents some advantages compared to current borylation methodologies. First, the ideal methodology would use phenylboronic acid ( $\text{PhB}(\text{OH})_2$ ) as a boron source, since it is a cheaper boron source than  $\text{B}_2\text{Pin}_2$  and  $\text{HBPin}$ . As mentioned earlier, using  $\text{PhB}(\text{OH})_2$  as a boron source would generate an equivalent of benzene as a side product, which is a disadvantage from the atom economy point of view, but could prevent generating pinacol waste, thus being overall as atom efficient. However, as you will see below, the use of boronic acids in a C-H borylation system is unlikely to happen, since O-H bonds are generally cleaved much more rapidly than C-H bonds. That being said, contrarily to  $\text{B}_2(\text{OH})_4$ ,  $\text{PhB}(\text{OH})_2$  can form a boroxine by a dehydration reaction which is the equivalent of protecting the boronic acid by esterification, but without the waste associated. In brief, even if an equivalent of arene is generated in the transfer borylation reaction, fundamentally it could be as atom efficient as the current C-H borylation methodologies, but avoiding the use or generation of  $\text{HBPin}$  in the reaction, thus opening the way for functional groups sensitive to hydroboration, such as aldehydes, ketones, alkenes and alkynes.

When I came back at Université Laval after my internship with Prof. Chirik, I realized that the cleavage of a C-B bond could be promoted by the protodeborylation transition state using a molecule containing a Lewis base and Brønsted acid. Such reaction would generate an intermediate closely related to the molecules I studied and should be able to perform the C-H cleavage of heteroarenes, which would close a metal free transfer borylation catalytic cycle (**Figure 72**).



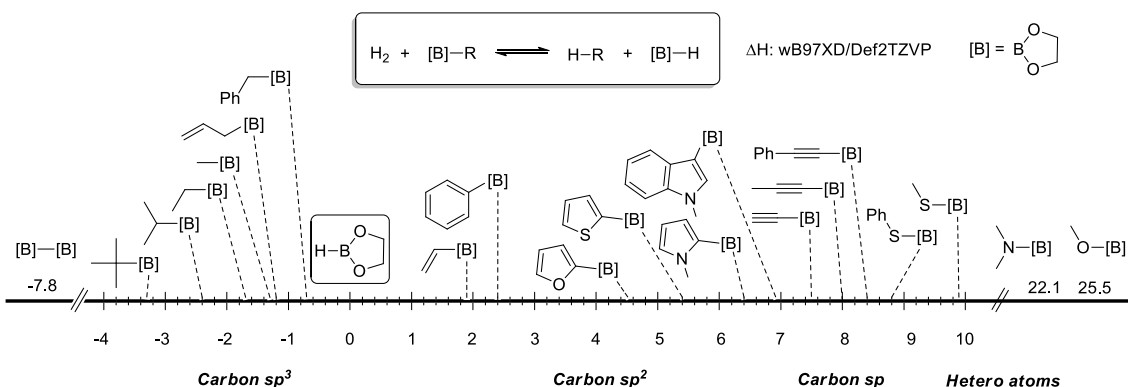
**Figure 72** Potential metal-free transfer borylation catalytic cycle.

I had investigated a few years back such an approach computationally to promote hydrogenation reactions using the combination of a pyrazole and a borane, but had not found a potential candidate because of the high tendency of FLPs to form six-membered ring when using a single atom spacer. Moreover, the Repo group had recently reported the use of a relatively complex protonated 2-aminopyridine derivatives to promote the C-H borylation of few heteroarenes using HBCat as the boron source, suggesting that this approach could certainly be applied to a catalytic transfer borylation system (**Figure 72**). However, the synthesis of that species is not trivial and charged molecules make the DFT computation less reliable. Knowing that B-S bonds are weak and had only little negative influence on the boron acidity, I decided instead to explore the potential of 2-mercaptopyridine (**7.1**) as a catalyst for this reaction. The initial DFT screening gave encouraging results and since **7.1** is commercially available and cheap (around 1 \$/g, or 0.11 \$/mmol),<sup>228</sup> it was rapidly tested.

The initial results were very encouraging, since the stoichiometric reaction between borylated *N*-methylpyrrole and **7.1** showed that the B-C bond was cleaved. Moreover, attempting the catalytic borylation of *N*-methylpyrrole using HBPin as a boron source also showed some conversion. Switching to HBCat, which has a more Lewis acidic boron center, improved the conversion. Finally,

among the boron sources tested for the transfer borylation reaction, 2-furylboronic catechol ester (**7.2**) was found to be competent.

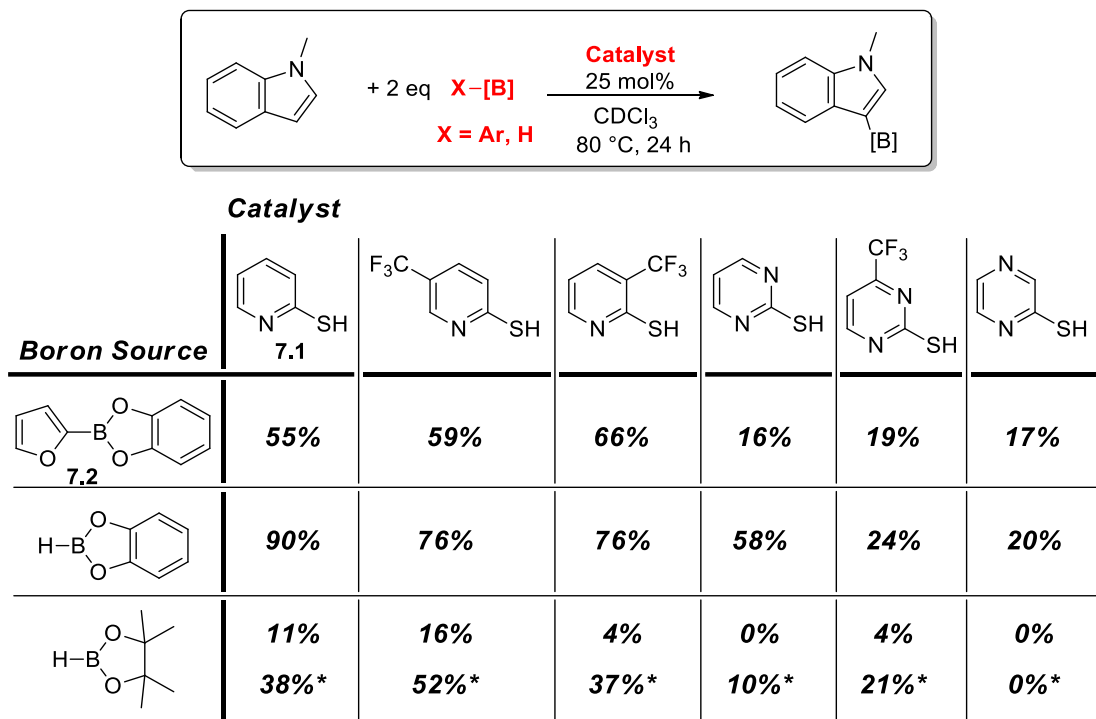
Having encouraging experimental results, I used DFT to try to improve the system. **Figure 73** shows the enthalpy difference between borylated molecules guiding the transfer borylation reaction. In short, under equilibrium, the boryl substituent would favorably end up on the substrate that is at the right of the other. HBPin has arbitrary been chosen as the zero of the scale. More importantly, **Figure 73** highlights that reagents containing a Csp<sup>3</sup>-B bond could favorably be used to form Csp<sup>2</sup>-B bond, and reagents containing a Csp<sup>2</sup>-B bond to form Csp-B bond or E-B bond (E = S, N, O). The calculations also suggest that among the Csp<sup>2</sup>-B region, phenylboryl compounds could be used to borylate heteroarenes and among the heteroarenes, furyl boryl compounds should be the favored borylating agents. Of course, those calculations comforted our choice of borylation reagent (**7.2**) and our proposed ideal boron source PhB(OR)<sub>2</sub>. Finally, it should be noted that the boiling point of benzene and furan are respectively 80 and 31 °C, which could eventually help to drive the reaction entropically.



**Figure 73** Thermodynamics of the transfer borylation reaction.  $\Delta H$  reported in kcal/mol, calculations performed at the  $\omega B97XD/Def2TZVP$  level of theory.

Among the many factors that were considered for an ideal catalyst, it included the effect of electron donating and withdrawing groups on the relative energy of the catalytically relevant intermediates, but also the effect of a second nitrogen atom in the catalyst “backbone”. Since the transfer of the boryl group to the catalyst can lead to an intermediate with loss of aromaticity, changes in the catalyst backbone could have a surprising impact on the C-B and C-H bond cleavage/forming transition state. In an ideal catalytic cycle, all intermediates are close to thermoneutrality and the transition states are as low as possible. The DFT calculations demonstrate that placing electron withdrawing groups on the backbone would be advantageous in order to favor the thermoneutrality between intermediates. Moreover, a backbone containing two nitrogen atoms (pyrazine and pyrimidine) are also predicted to

be advantageous, this time by reducing the transition state energetic barrier. With this information in hand, commercially available 2-mercaptopyridine and 2-mercaptopyrimidine derivatives containing CF<sub>3</sub> groups, and 2-mercaptopyrazine were purchased and tested as dehydrogenative and transfer borylation catalysts (**Figure 74**).

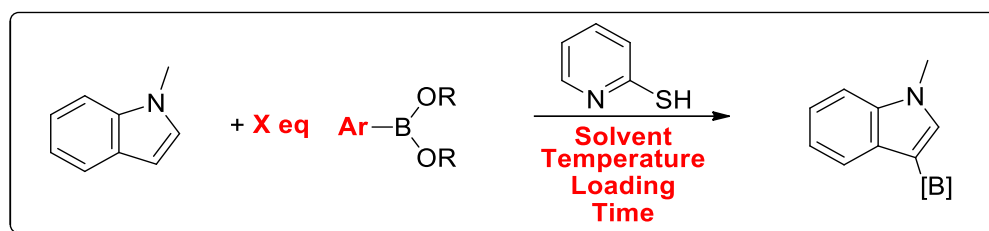


\* After an additional 24 h at 110 °C

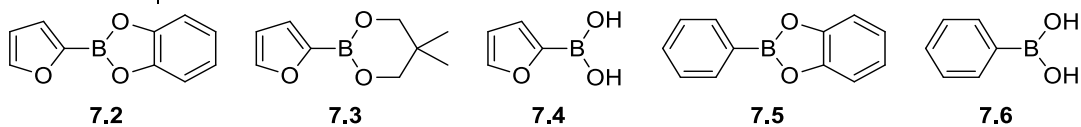
**Figure 74** Initial catalyst and boron source screening.

All derivatives showed some activity for the dehydrogenative and transfer borylation reaction. For simplicity, it was decided to continue the study with the unsubstituted 2-mercaptopyridine (**7.1**), the cheapest of all catalysts tested.



**Table 10** Condition screening of the C-H transfer borylation reaction.

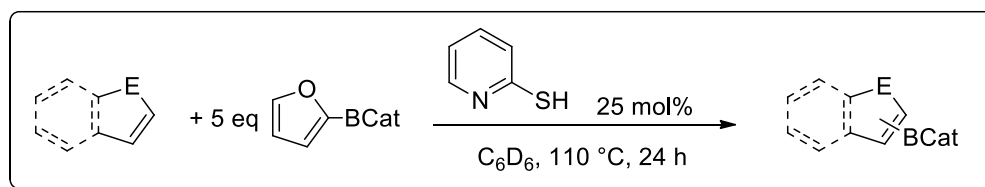
Entry	Temp. °C	Solvent	Boron Source	Equiv.	Catalyst Loading mol%	Time h	Conversion %
1	80	CDCl <sub>3</sub>	7.2	2	25	24	55
2	80	CDCl <sub>3</sub>	7.2	5	25	24	72
3	110	CDCl <sub>3</sub>	7.2	5	25	24	83
4	110	C <sub>6</sub> D <sub>6</sub>	7.3	5	25	24	0
5	110	C <sub>6</sub> D <sub>6</sub>	7.4	5	25	24	0
6	110	C <sub>6</sub> D <sub>6</sub>	7.5	5	25	24	0
7	110	C <sub>6</sub> D <sub>6</sub>	7.6	5	25	24	0
8	110	C <sub>6</sub> D <sub>6</sub>	7.2	5	25	1	57
9	110	C <sub>6</sub> D <sub>6</sub>	7.2	5	25	4	81
10	110	C <sub>6</sub> D <sub>6</sub>	7.2	5	25	8	90
<b>11</b>	<b>110</b>	<b>C<sub>6</sub>D<sub>6</sub></b>	<b>7.2</b>	<b>5</b>	<b>25</b>	<b>24</b>	<b>&gt;95</b>
12	110	C <sub>6</sub> D <sub>6</sub>	7.2	5	10	1	35
13	110	C <sub>6</sub> D <sub>6</sub>	7.2	5	10	4	57
14	110	C <sub>6</sub> D <sub>6</sub>	7.2	5	10	8	69
15	110	C <sub>6</sub> D <sub>6</sub>	7.2	5	10	24	87
16	110	C <sub>6</sub> D <sub>6</sub>	7.2	5	10	48	94
17	110	C <sub>6</sub> D <sub>6</sub>	7.2	5	-	24	0



In that second round of optimization (**Table 10**), it was found that benzene is more adequate for the reaction compared to chloroform. Although not clear at the moment, it is believed that the lower yields with chloroform might be due to decomposition pathways. Moreover, increasing the reaction temperature from 80 °C to 110 °C and the number of equivalents of the boron reagent from 2 to 5 allows for full conversion as judged by <sup>1</sup>H NMR monitoring. A relatively high catalyst loading (25 mol%) is required to get full conversion in reasonable conditions, but it was possible to obtain

high conversion (94 %) with a lower catalyst loading (10 mol%) and longer reaction time (48 h). Other potentially more interesting boron sources (7.3-7.6) were tested but did not yield any product in all cases. Finally, it is important to note that all the reactions were performed without taking any special precautions relative to inert atmosphere. Indeed, residual water in the solvent or reagents should not degrade the catalyst, but could consume some equivalent of borylating agent, which in our case is used in excess. Although it is not a problem on the preliminary scale, this problem should be kept in mind for future optimization of the reaction.

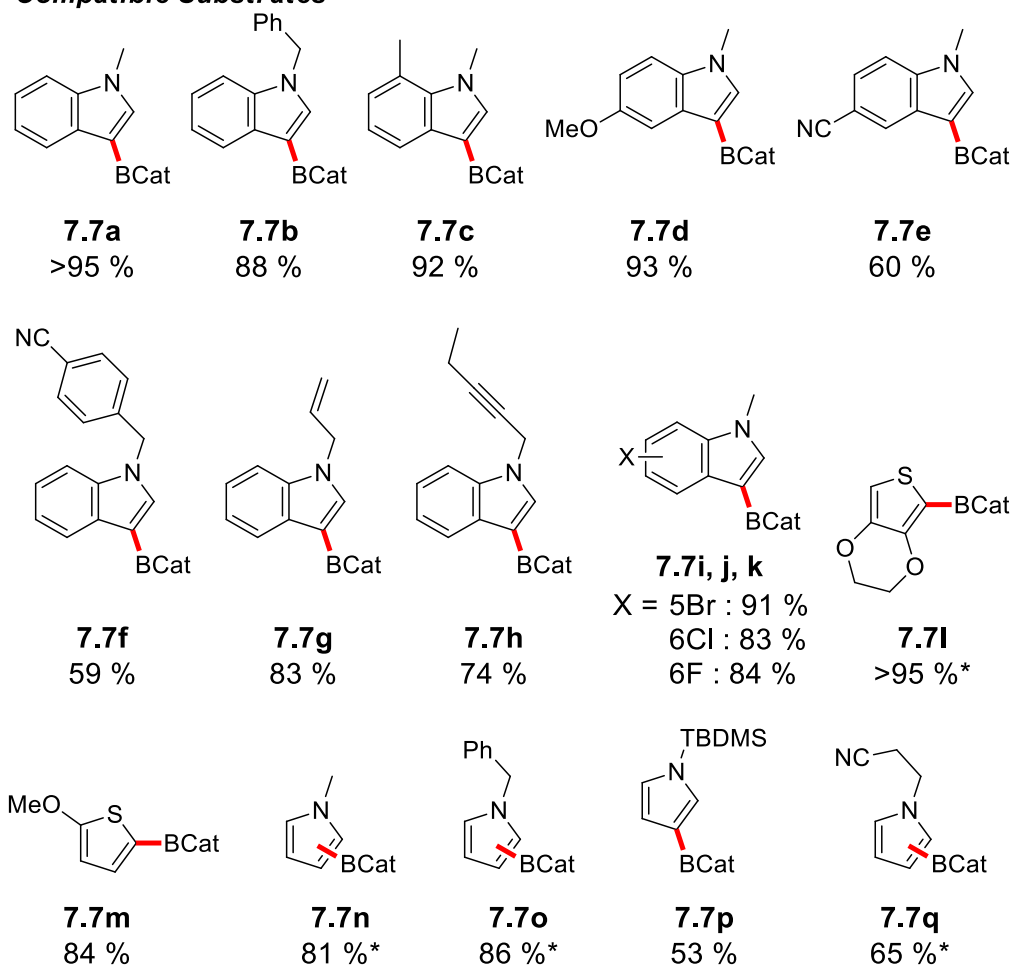
With conditions judged sufficiently good, the substrate scope of the reaction was investigated (**Figure 75**). All the reactions were performed in J-Young NMR tubes. The substrates have characteristic resonances in order to facilitate the determination of the conversion using  $^1\text{H}$  NMR spectroscopy. At the end of the reaction, the solution was quenched with excess pinacol and analyzed by GC-MS, in order to confirm that the conversion was indeed coming from the expected C-H borylation reaction and not from another unexpected process. Finally, it was attempted to get isolated yield, but the reactivity of the BCat derivatives and the excess pinacol required to convert them to BPin derivatives, which are also relatively sensitive to protodeborylation during chromatography, prevented us to obtain isolated yields. Since, the goal of this study was to get proof of concept of the borylation reaction before submitting my thesis, efforts were mostly directed toward getting the best understanding of the reaction instead of isolated yield of compounds that were in many cases already reported in the literature.



<sup>1</sup>H NMR conversion are reported

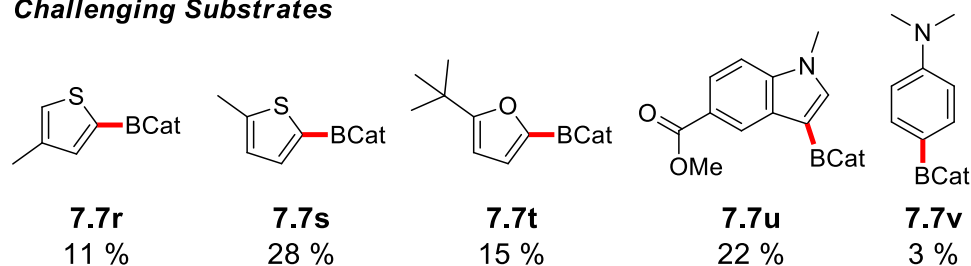
product formation also confirmed by GC-MS after conversion to the pinacol derivatives

### Compatible Substrates



\*Mixture of isomers and/or bis borylated product

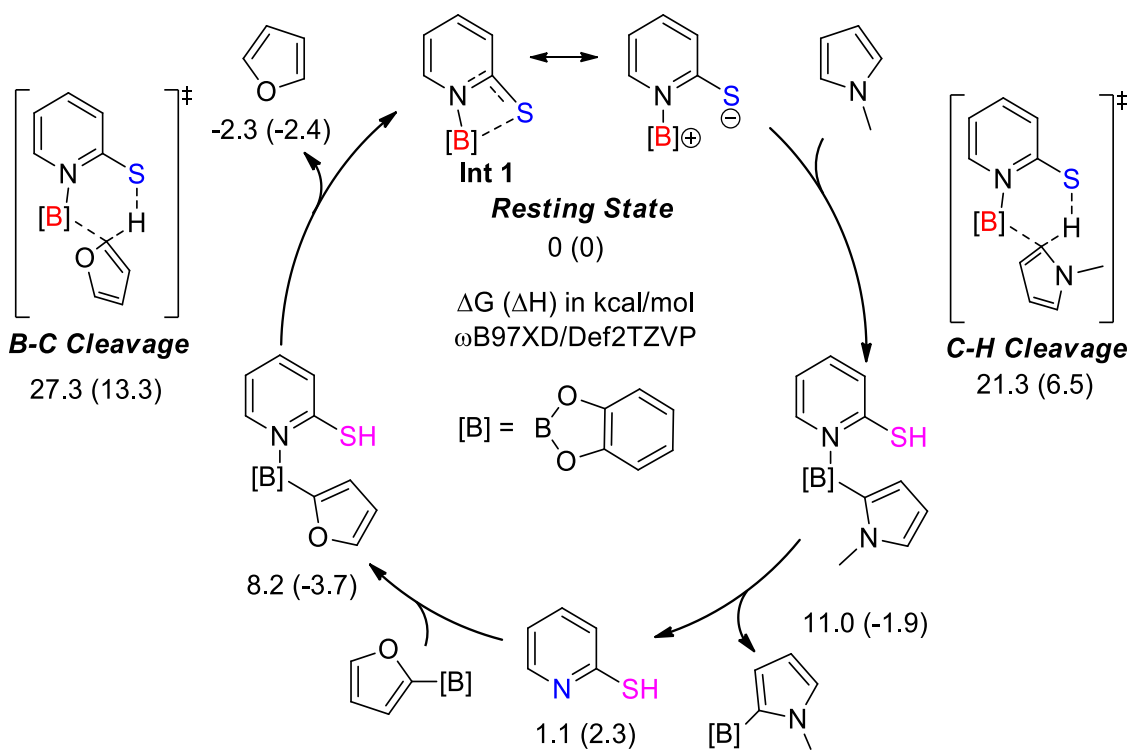
### Challenging Substrates



**Figure 75** Substrate scope of the **7.1** catalyzed transfer borylation.

The substrate scope includes alkyl, benzyl, silyl, halide, and alkoxy substituted indoles and pyrroles. More importantly, the system tolerates nitriles (**7.7e,f**), terminal alkenes (**7.7g**) and internal alkynes (**7.7h**), which are not tolerated by our  $\text{NR}_2\text{-C}_6\text{H}_4\text{-BH}_2$  catalysts nor by most other transition metal based catalysts. At the moment, carbonyl functionalities such as aldehydes and ketones remain problematic. Thiophene containing electron donating alkoxy groups can also be borylated efficiently, but in the case of methyl substituted thiophene, the conversion is lower. In summary, the activity of **7.1** for the C-H bond cleavage is similar as the  $\text{NR}_2\text{-C}_6\text{H}_4\text{-BH}_2$  framework; however, it has a better functional group tolerance, it is air-stable, commercially available, and the protocol does not require strictly anhydrous conditions, which is also a great improvement. Hopefully, future catalyst optimization will allow to further expand the substrate scope.

The full catalytic cycle has been calculated by DFT using *N*-methylpyrrole as model substrate and is presented in **Figure 76**. The proposed mechanism is going via similar transition states for the C-H and B-C bond cleavage states. The cleavage of **7.2** C-B bond is rate limiting with an energy of 27 kcal/mol, in the acceptable range of what is expected from the experimentally observed activity (95 % conversion in 24 h at 110 °C).



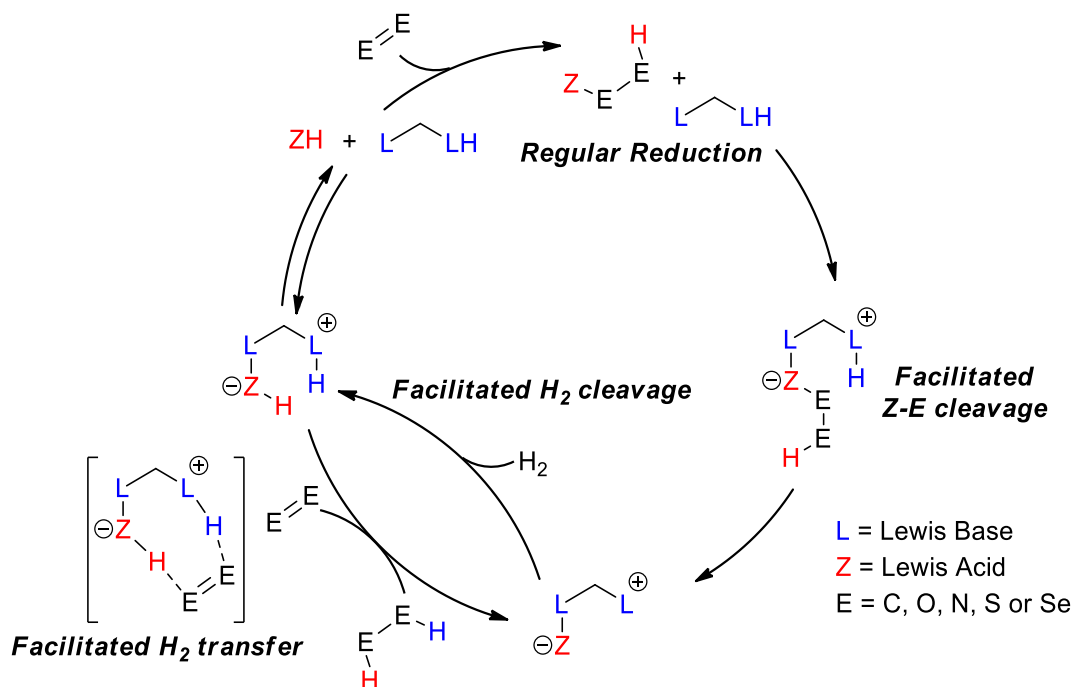
**Figure 76** Proposed catalytic cycle of the 2-mercaptopyridine catalyzed transfer borylation. Functions are emphasized with color: Lewis acid (red), Lewis base (blue), Brønsted acid (pink).  $\Delta G$  ( $\Delta H$ ) reported in kcal/mol, calculations performed at the  $\omega$ B97XD/Def2TZVP level of theory.

## Conclusion

### *Perspectives*

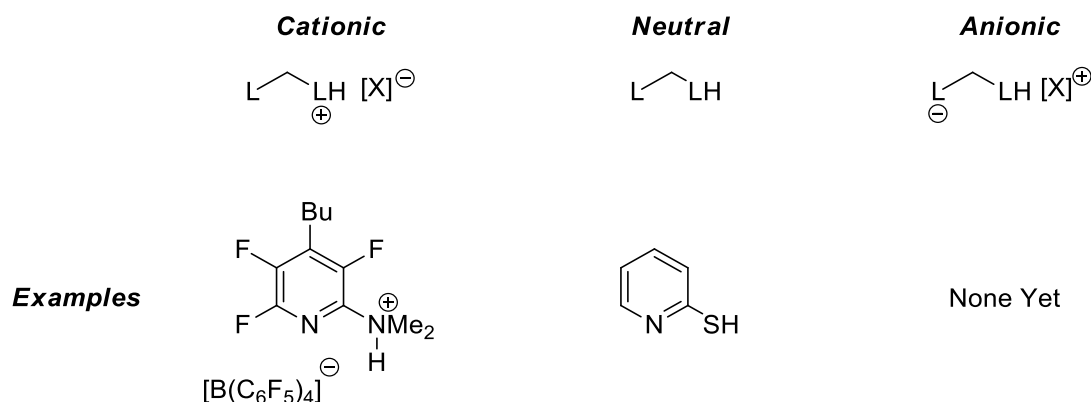
Along the thesis, many subjects were discussed, going from CO<sub>2</sub> hydrogenation to C-H borylation, and many surprising reactivity patterns were observed, such as the spontaneous formation of a B-B bond from an aminoborane molecule. This is what happens when one can freely follow the clues arising from mechanistic studies instead of being bonded to a restrictive project. It is certainly frustrating at times, pun intended, and certainly confusing for an outside observer since many ideas were not fully explored, sometimes because of a gut feeling or because another idea was more appealing. I certainly enjoyed sharing my work and points of view on those various topics and hope that it inspired the reader.

Before getting to the final conclusions, I think a discussion combining the knowledge assembled in the various chapters in the context of further development in FLP chemistry is in order. A very interesting and general FLP design principle that arose from the last chapter and that I briefly mentioned in the introduction, is the concept of auto-assembling FLPs, a type of FLP combining the advantages of inter-molecular and intra-molecular FLPs that would certainly gain to be investigated in more details. In theory, nothing would prevent using such principle to design very simple catalyst systems for more classical FLP reactions, such as the hydrogenation reaction. A potential catalytic cycle is presented in **Figure 77**. In addition to simplify some methodologies, this approach could also allow to unlock some of the few remaining substrates still resisting to the scope of FLP hydrogenation, such as terminal alkynes.



**Figure 77** Potential hydrogenation catalytic cycle using auto-assembling FLP.

Auto-assembling FLP can be as simple as Lewis base and a Brønsted acid correctly oriented in space, such as 2-mercaptopyridine as demonstrated in Chapter 7. One could imagine an almost infinite number of variations of such framework. In the context of the general borylation reaction, I think three main classes of potential catalysts could exist: cationic, neutral and anionic. The Repo group already showed that a protonated 2-aminopyridine catalyst could work<sup>105</sup> and I discussed a neutral analogue, but an anionic analogue such as a thiol thiolate combination could very well be imagined (**Figure 78**). I personally tend to favor neutral catalysts as they can be more easily and accurately calculated using DFT, are usually more soluble in organic solvents and do not require massive non-coordinating ion. Comparing charged analogues, the anionic ones probably have the advantage of having cheaper and more convenient non-coordinating ions, such as tetraalkylammonium, compared to the cationic ones that could use potentially reactive  $BF_4^-$  or  $PF_6^-$  anions or more expensive  $BAR_4^-$ . On the other hand, the cationic version can form a very Lewis acidic borenium center, which seems to be an important criteria for the reactivity.



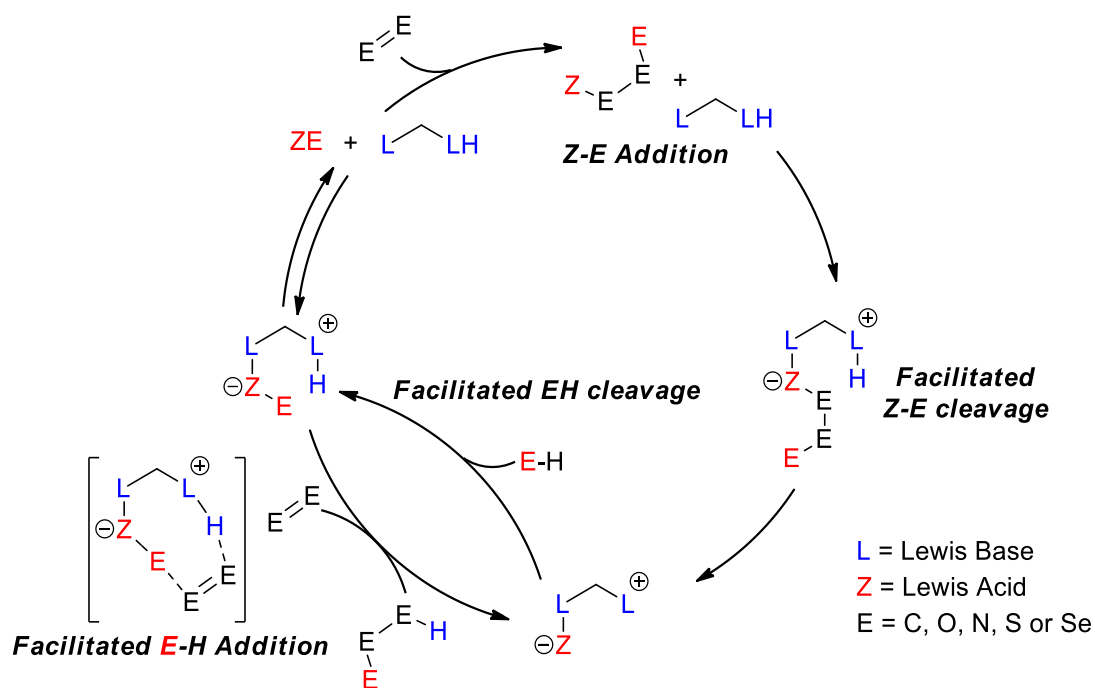
**Figure 78** Different type of potential C-H transfer borylation catalyst.

Another aspect to consider in future catalyst design that I have not discussed yet is the catalyst symmetry. It may seem futile, but since the proton, and to some extent the boron moiety, can be exchanged between Lewis bases, it is a very important factor since it will obviously end up where it is the most stable. Simply put, the C-H or C-B bond forming/cleavage transition state is favored with more basic Lewis bases and more acidic Lewis acids. However, in a very unbalanced catalyst, the initial proton will be on the strongest Lewis base, thus at its lowest reactivity, and after forming the intermediate the boron will also likely end up on that same strong Lewis base, again at its lowest reactivity. Thus, inserting the strong Lewis base on the catalyst would have been only detrimental. In that simplified view, a symmetric catalyst would be optimal since, wherever the proton or the boron end up, it will always be at its “maximal” reactivity. However, this is a very simplified view and in fact, thinking that the proton and boron affinity of a Lewis base are directly connected is an oversimplification. First of all, a boron moiety is much more hindered than a simple proton, but also the nature of the atom of the Lewis base making the bond can completely change the picture. A very close analogy of the discussion made in Chapter 2 to justify the change from P/B to N/B FLP in the CO<sub>2</sub> hydrogenation chemistry can be drawn here. In that case, replacing the phosphorus atom by a nitrogen atom in the FLP framework was favoring the H<sub>2</sub> adduct, but disfavoring CO<sub>2</sub> adduct. In the context of a Brønsted acid catalyst for the C-H transfer borylation, the picture is a bit more complex, but the underlying principle is the same. Simply put, as long as the proton and the boron atom do not end up on the same Lewis base, it should not be detrimental to the overall catalytic activity. Moreover, using unsymmetrical catalysts with different functions may end up advantageous and even a key design principle allowing easier tuning of the intermediate’s relative energies. After all, the two currently working catalysts classes are unsymmetrical.

Another area at the frontier of some chapters of the thesis is the hydroaddition reaction. The subject has been briefly discussed in Chapter 7, but in the light of new developments in the field of B-E

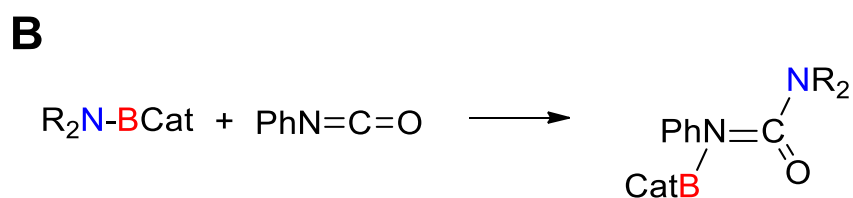
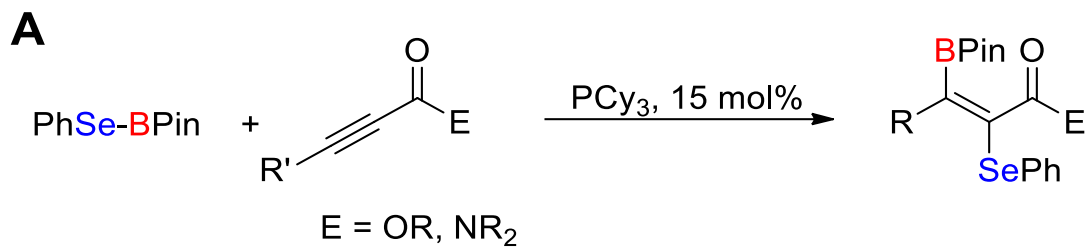


compounds, it could certainly benefit from a reinvestigation, especially from the point of view of auto-assembling FLPs. The development of those new reactions could be a great next step for FLP chemistry and metal-free catalysis in general. Again, a potential catalytic cycle, very similar to the hydrogenation one, is presented in **Figure 79**.



**Figure 79** Potential hydroaddition catalytic cycle using auto-assembling FLP.

The progression in the understanding of B-E bond reactivity could certainly lead to the development of catalytic additions. For example, a recent study concerning the addition of B-Se bond to ynone in the presence of a base suggests the formation of an addition product containing a B-Csp<sup>2</sup> bond,<sup>229</sup> a type of bond known to be competent in the protodeborylation reaction. Other potentially catalytic reactions include the hydroamination. Because the B-N and B-O bonds are of similar strength, a N-H containing compound could displace the B-O more easily than a thiol and metal-free addition of B-N containing compounds to isocyanates, isothiocyanates, carbodiimides and Michael acceptors have been described in the literature.<sup>217,230</sup>



**Scheme 39** A) Example of the reactivity of Se-B bond with ynone. B) Example of the reactivity of B-N bond with isocyanate.

## *Final conclusion*

In summary, I think the field of FLP chemistry still has a lot to offer. As shown in the thesis, a simple sub-class of FLP,  $\text{NR}_2\text{-C}_6\text{H}_4\text{-BH}_2$ , can lead to chemistry ranging from  $\text{CO}_2$  hydrogenation, C-H bond cleavage, B-B bond formation and catalytic C-H and S-H bond borylation. Considering all the variations that can be made concerning the Lewis acid and Lewis base nature, it is not hard to imagine that the basic FLP concept will lead to other interesting chemistry in the future. However, I also think that understanding the important mechanistic aspects governing the current catalytic cycles and stoichiometric reactions in FLP chemistry and in other related chemistries will be key in future development.

In that regard, I think the thesis presents interesting examples. First of all, it reiterates that the presence or absence of an adduct between a Lewis acid and a Lewis base is far from being directly related to its reactivity. I already mentioned that in the case of weak Lewis partners, adducts can be avoided with very minimal steric hindrance, but that using weak Lewis partners rarely translate into interesting chemistry, but that is just the most obvious example. On the other side of the spectrum, using very strong Lewis partners, very important steric hindrance is required to avoid adduct formation. However, that same steric hindrance, will also inhibit interactions with a substrate of interest. This is no coincidence that most of the FLP chemistry initially reported using this approach was with small molecules such as  $\text{H}_2$  and  $\text{CO}_2$ . From a catalytic point of view the “optimization of the frustration” is even more important. The demonstration that amines of intermediate hindrance are the most active in our C-H borylation system (Chapter 3.1.3) is certainly a great example of that. Using reagents in high energy states, or “activated” if you prefer, is a stoichiometric chemistry approach (see **Figure 4**), and it is exactly what using very strong and hindered Lewis partner is. It is great to discover new “elementary steps” for catalysis and describe them well, but when it comes to designing efficient catalytic cycles, using increasingly reactive reagents is probably not the best approach.

Another more subtle aspect addressed in the thesis is the importance of the geometry in transition state accessibility, and thus in catalyst design. Most of the time, a large part of the energy required to access a transition state comes from entropy and having correctly prearranged reactive sites can greatly reduce it. Moreover, it is one the aspect of a catalyst selectivity on which the designer has the more control. Enhancing or reducing the “strength” of functionalities can and often will make a transition state more accessible. However, in a catalytic context where there is often not one, but two, three or four transition states of interest, and it will often end up in borrowing from Peter to pay Paul. Playing on the geometry, on the other hand, can result in a net gain, especially when done carefully which is certainly easier using computational modelization. Geometry is more important for some

transition states than others, usually the most difficult to access, which are often the ones on which “catalyst designers” work the most. Thus, an optimal geometry is often seen as a rigid thing that should not change. A statement with which I do not completely agree. It is true that an optimal very static geometry will make a transition state of interest more easily accessed, but once again, in a complex catalytic cycle, with many steps, the optimal geometry for one might not be for the other, and having more flexibility can be the best way to go. The discussion of Chapter 7 on auto-assembling FLP is a good example of that, it also exemplify that having a better geometry does not necessarily means having more complex catalyst requiring complex synthesis.

Finally, if only one things needs to be remember from this thesis it is that the best way to improve a catalytic system is to understand it. When you know where it blocks, it is much easier to find a way to work around the problem. Or as Charles F. Kettering, one who certainly knows about problems, said: “*A problem well-stated is half-solved.*”

## Annexes – Experimental Section

### *Organization of the section*

The vast majority of the results presented in the thesis have been published, thus the characterization data of most compounds are already available on the web free of charge in the supplementary information files of those articles (see section details on the thesis content for the references). Consequently, for those compounds, I decided to only provide brief description of the synthesis and characterization data. In the case of unpublished compounds, more detailed descriptions, including spectra are provided. Some compounds have been numbered in the text in order to facilitate the reading, but have never been synthesized or fully characterized and will thus not be included in the following sections or will only be accompanied by partial characterization data.

The annexes, follow the same numeration as the main text and is divided into section corresponding to the main text chapters.

### *General experimental*

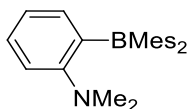
NMR spectra were recorded on Agilent Technologies NMR spectrometer at 500.00 MHz ( $^1\text{H}$ ), 125.757 MHz ( $^{13}\text{C}$ ), 160.46 MHz ( $^{11}\text{B}$ ) and 470.385 MHz ( $^{19}\text{F}$ ) or on Varian Inova NMR AS400 spectrometer, at 400.0 MHz ( $^1\text{H}$ ), 100.580 MHz ( $^{13}\text{C}$ ) and 376.29 ( $^{19}\text{F}$ ).  $^1\text{H}$  NMR and  $^{13}\text{C}\{^1\text{H}\}$  NMR chemical shifts are referenced respectively to the residual hydrogen and carbon atoms in the deuterated solvents.  $^{11}\text{B}\{^1\text{H}\}$  NMR calibration was performed using  $\text{F}_3\text{B}\cdot\text{OEt}_2$  as an external reference.  $^{19}\text{F}$  NMR was calibrated using  $\text{CFCl}_3$  as external standard. Multiplicities are reported as singlet (s), broad singlet (s, br) doublet (d), triplet (t), multiplet (m). Chemical shifts are reported in ppm. Coupling constants are reported in Hz.

Mass Spectrometry analyses were carried out on an Agilent 6210 LC Time of Flight Mass Spectrometer, using electrospray ionization (ESI) method or on an Thermo-Fisher Trace GC Ultra with a ITQ 900 MS, using electronic impact as an ionization source.

Elemental analyses for C, H, and N were carried out on a Thermo Scientific FLASH 2000 Series CHNS.

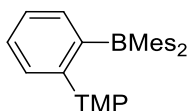
## Chapter 2

### Compound 2.2



This compound was synthesized with a slightly modified approach from a known procedure.<sup>231</sup> 1.5 g (5.5 mmol, 1.0 equiv) of dimesitylboron fluoride was dissolved in toluene and transferred to a  $-78\text{ }^{\circ}\text{C}$  solution of 700 mg (5.5 mmol, 1.0 equiv) of 2-(dimethylamino)phenyllithium in 10 mL of toluene. The resulting mixture was then left to warm to r.t. and stirred for 16 hours. Upon reaction completion the solution was bright, fluorescent green. The salts were left to separate without agitation and the solution was filtered via cannula. The residue was washed once with toluene (10 mL). The volatiles were then removed in vacuo. Upon cooling, 1.8 g of a green solid was recovered. Yield = 91 %. The compound can be further purified by recrystallization from a saturated hexane solution at  $-35\text{ }^{\circ}\text{C}$ . Using this method, 1.46 g of pure compound was recovered. Yield = 72 %. The characterization is identical to a previous report.<sup>129</sup>

### Compound 2.3

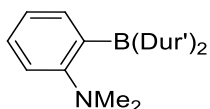


This compound was synthesized by a colleague (Marc-André Courtemanche) using the same method as compound 2.2.

$^1\text{H}$  NMR (500 MHz,  $\text{C}_6\text{D}_6$ )  $\delta$  7.68 (dd,  $J = 7.7, 1.8$  Hz, 1H), 7.44 (dd,  $J = 8.1, 1.0$  Hz, 1H), 7.19 – 7.14 (m, 3H), 7.02 – 6.97 (m 1H), 6.76 (s, 4H), 2.18 (s, 12H), 2.16 (s, 6H), 1.71 – 1.53 (m, 2H), 1.42 – 1.34 (m, 2H), 1.27 – 1.18 (m, 2H), 1.15 (s, 6H), 1.00 (s, 6H).

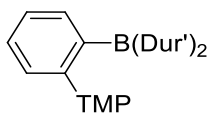
$^{13}\text{C}\{^1\text{H}\}$  NMR (126 MHz,  $\text{C}_6\text{D}_6$ )  $\delta$  154.63 (s), 141.56 (s), 138.53 (s), 137.81 (s), 132.77 (s), 129.59 (s), 129.13 (s), 124.57 (s), 55.58 (s), 39.61 (s), 33.67 (s), 29.81 (s), 24.65 (s), 20.80 (s), 18.42 (s). The carbons linked directly to boron were not observed.

### Compound 2.4



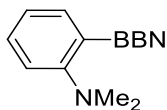
This compound was synthesized by a colleague (Marc-André Courtemanche) using the same method as compound 2.2 using 967 mg (1.0 equiv) of chlorobis(2,4,5-trimethylphenyl)borane and 432 mg (1.0 equiv) of (2-(dimethylamino)phenyl)lithium in 10 mL of toluene. 1.1 g of a sticky green solid was recovered. Yield = 88 %. The compound can be further purified by recrystallization from a saturated hexane solution at  $-35\text{ }^{\circ}\text{C}$ . Using this method, 807 mg of pure compound was recovered. Yield = 64 %. The characterization is identical to a previous report.<sup>129</sup>

### Compound 2.5



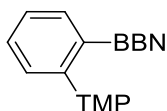
This compound was synthesized by a colleague (Marc-André Courtemanche) using the same method as compound **2.2**. The details of the synthesis could not be retrieved.

#### Compound **2.6**



This compound was synthesized by a collaborator from University of Toronto (Alexander P. Pulis) using a method analogous as the one used for compound **2.2**. The details of the synthesis could not be retrieved, neither could the NMR characterization at the exception of its  $^{11}\text{B}$  NMR:  $\delta$  29.

#### Compound **2.7**



917 mg of [2-(2,2,6,6-tetramethylpiperidin-1-yl)phenyl]lithium (4.1 mmol) were weighed into a Schlenk flask containing a Teflon coated magnetic stirring bar and dissolved in toluene (*ca.* 15 mL) and cooled down to *ca.*  $-80$  °C using a liquid nitrogen/acetone bath. In a separate Schlenk flask, 4.1 mL (4.1 mmol) of a 1.0 M solution of BBN-Br in dichloromethane was added and the solvent was removed *in vacuo* to be replaced with *ca.* 4 mL of toluene. The solution of BBN-Br was added dropwise to the cold solution of [2-(2,2,6,6-tetramethylpiperidin-1-yl)phenyl]lithium, which was stirred vigorously throughout the addition. The resulting mixture was left to warm to r.t. and left stirring overnight. The decanted solution was filtered to a separated Schlenk flask via cannula. The resulting solution was evaporated to dryness under reduced pressure and further dried at  $80$  °C under vacuum for 2 h. The residue was then dissolved in hexanes (*ca.* 5 mL). The resulting solution was left at  $-35$  °C for 72 h to allow complete precipitation of the title compound as a white powder (1.01 g, 73% yield). Crystals suitable for X-ray diffraction were grown by slow evaporation of a hexane solution.

$^1\text{H}$ -NMR 500MHz:  $\delta$  7.64 (dd,  $^3J_{\text{H-H}} = 7.2$  Hz,  $^4J_{\text{H-H}} = 2.0$  Hz, 1H); 7.39 (dd,  $^3J_{\text{H-H}} = 7.7$  Hz,  $^4J_{\text{H-H}} = 1.3$  Hz, 1H); 7.20 (td,  $^3J_{\text{H-H}} = 7.3$  Hz,  $^4J_{\text{H-H}} = 1.7$  Hz, 1H); 7.15 (td,  $^3J_{\text{H-H}} = 7.3$  Hz,  $^4J_{\text{H-H}} = 1.3$  Hz, 1H); 2.40 (s, 2H); 2.13–2.02 (m, 10H); 1.84–1.75 (m, 1H); 1.63 (ddd,  $^2J_{\text{H-H}} = 12.8$  Hz,  $^3J_{\text{H-H}} = 7.8$  Hz,  $^3J_{\text{H-H}} = 2.7$  Hz 2H); 1.56–1.50 (m, 2H); 1.50–1.43 (m, 1H); 1.41 (dt,  $^2J_{\text{H-H}} = 12.7$  Hz,  $^3J_{\text{H-H}} = 3.4$  Hz, 2H); 1.26 (s, 6H); 0.83 (s, 6H).

$^{13}\text{C}\{^1\text{H}\}$  (126 MHz):  $\delta$  150.4 (s); 133.0 (s); 131.3 (s); 129.2 (s); 125.0 (s); 54.7 (s); 41.4 (s); 35.0 (s); 34.1 (s); 32.5 (s, broad); 25.7 (s); 23.5 (s); 18.6 (s).

$^{11}\text{B}\{^1\text{H}\}$  (160 MHz):  $\delta$  83.4 (s).

$[\text{M} + \text{H}]^+$ , calculated 338.3019; found = 338.2852.

#### Compound **2.7**•H<sub>2</sub>O

**2.7**•H<sub>2</sub>O crystallized out of a solution of **2.7** exposed to air from hexane and the characterization was carried out on the few crystals obtained. However, attempts to form **2.7**•H<sub>2</sub>O in good yield from **2.7**

by adding stoichiometric equivalent of water gave a mixture of **2.7**•H<sub>2</sub>O and another product that was identified as [2-(2,2,6,6-tetramethylpiperidin-1-yl)phenyl]boronic acid.

<sup>1</sup>H-NMR 500MHz: δ 17.06 (s, 1H, N-H); 8.49 (d, <sup>3</sup>J<sub>H-H</sub> = 7.9 Hz, 1H); 7.25 (t, <sup>3</sup>J<sub>H-H</sub> = 7.5 Hz, 1H); 6.96 (t, <sup>3</sup>J<sub>H-H</sub> = 7.5 Hz, 1H); 6.80 (d, <sup>3</sup>J<sub>H-H</sub> = 8.2 Hz, 1H); 3.02–2.91 (m, 2H); 2.61–2.45 (m, 2H); 2.42–2.17 (m, 7H); 1.98 (dt, <sup>2</sup>J<sub>H-H</sub> = 13.4 Hz, <sup>3</sup>J<sub>H-H</sub> = 6.6 Hz 1H); 1.64 (s, 1H, O-H); 1.50 (td, <sup>2</sup>J<sub>H-H</sub> = 13.6 Hz, <sup>3</sup>J<sub>H-H</sub> = 3.1 Hz, 2H); 1.29 (dt, <sup>2</sup>J<sub>H-H</sub> = 13.5 Hz, <sup>3</sup>J<sub>H-H</sub> = 10.5 Hz, <sup>3</sup>J<sub>H-H</sub> = 3.2 Hz 1H); 1.17–1.02 (m, 3H); 1.06 (dt, <sup>2</sup>J<sub>H-H</sub> = 14.3 Hz, <sup>3</sup>J<sub>H-H</sub> = 3.1 Hz, 2H); 0.95 (s, 6H); 0.93 (s, 6H).

<sup>13</sup>C{<sup>1</sup>H} (126 MHz): δ 140.4 (s); 136.8 (s); 126.1 (s); 123.1 (s); 122.6 (s); 62.3 (s); 38.6 (s); 33.4 (s); 32.1 (s); 29.7 (s); 27.4 (s, broad 2C); 24.8 (s); 24.7 (s); 23.7 (s); 16.7 (s).

<sup>11</sup>B{<sup>1</sup>H} (160 MHz): δ 0.0 (s).

#### Compound **2.7**•HCOOH

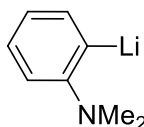
1.00 g of **2.7** (3.0 mmol) was dissolved in hexanes (*ca.* 15 mL) and 125 μL (1.1 equiv., 3.3 mmol) of formic acid were added provoking the precipitation of **2.7**•HCOOH. After filtration, the white solid was dried under vacuum and 435 mg of **2.7**•HCOOH (38% yield) were obtained.

<sup>1</sup>H-NMR 500MHz: δ 8.65 (s, 1H, COOH); 8.01 (dd, <sup>3</sup>J<sub>H-H</sub> = 7.7 Hz, <sup>4</sup>J<sub>H-H</sub> = 1.6 Hz, 1H); 7.55 (s, broad 1H, N-H); 7.10 (ddd, <sup>3</sup>J<sub>H-H</sub> = 7.7 Hz, <sup>3</sup>J<sub>H-H</sub> = 7.2 Hz, <sup>4</sup>J<sub>H-H</sub> = 1.1 Hz, 1H); 6.83 (ddd, <sup>3</sup>J<sub>H-H</sub> = 8.2 Hz, <sup>3</sup>J<sub>H-H</sub> = 7.2 Hz, <sup>4</sup>J<sub>H-H</sub> = 1.6 Hz, 1H); 6.60 (dd, <sup>3</sup>J<sub>H-H</sub> = 8.2 Hz, <sup>4</sup>J<sub>H-H</sub> = 1.0 Hz, 1H); 2.50–2.40 (m, 2H); 2.28 (m, 1H); 2.18–2.11 (m, 1H); 2.10–1.95 (m, 6H); 1.91 (td, <sup>2</sup>J<sub>H-H</sub> = 14.3 Hz, <sup>3</sup>J<sub>H-H</sub> = 7.4 Hz, 1H); 1.75–1.67 (m, 1H); 1.40 (s, 2H); 1.36 (s, 6H); 1.23–1.05 (m, 3H); 0.91–0.87 (m, 1H); 0.83 (dt, <sup>2</sup>J<sub>H-H</sub> = 15.0 Hz, <sup>3</sup>J<sub>H-H</sub> = 3.3 Hz 2H); 0.66 (s, 6H).

<sup>13</sup>C{<sup>1</sup>H} (126 MHz): δ 169.4 (s, COOH); 142.8 (s); 137.1 (s); 127.9 (s); 124.9 (s); 121.1 (s); 69.3 (s); 35.2 (s); 32.2 (s); 31.3 (s); 30.2 (s); 27.8 (s); 25.1 (s, broad); 24.5 (s); 23.3 (s); 14.8 (s).

[M-HCOO]<sup>+</sup>, calc = 338.3019, found = 338.2612.

#### Compound **2.8**

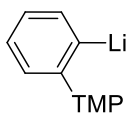


The compound was prepared following the protocol reported by Whitley *et al.*<sup>130</sup>

<sup>1</sup>H NMR (500 MHz, C<sub>6</sub>D<sub>6</sub>) δ 8.24 (s, broad 1H), 7.26 – 7.20 (m, 2H), 7.02 – 6.95 (m, 1H), 2.04 (s, broad 6H).

<sup>13</sup>C{<sup>1</sup>H} NMR (126 MHz, C<sub>6</sub>D<sub>6</sub>) δ 168.2 (s, broad), 165.8 (s), 139.8 (s), 125.8 (s), 118.6 (s), 46.5 (s, broad). One carbon atom was not observed, either because of solvent is overlapping or because of a broadening caused by the lithium atom.

#### Compound **2.9**



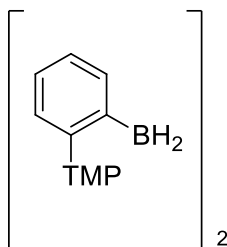
The compound was prepared following the protocol reported by Repo *et al.*<sup>231</sup>



$^1\text{H}$  NMR (400 MHz,  $\text{C}_6\text{D}_6$ )  $\delta$  8.35 (d,  $J = 6.6$  Hz, 1H), 7.43 (t,  $J = 6.7$  Hz, 1H), 7.35 – 7.25 (m, 2H), 1.71 – 1.58 (m, 3H), 1.57 – 1.50 (m, 2H), 1.44 – 1.37 (m, 1H), 1.28 (s, 6H), 0.94 (s, 6H).

## Chapter 3

### Compound 3.1



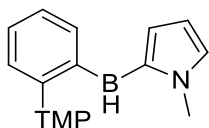
**3.1** was synthesized using the procedure reported by Repo and coworkers with minor modifications.<sup>142</sup> In a Schlenk tube, 4.2 g of [2-(2,2,6,6-tetramethylpiperidin-1-yl)phenyl]lithium (18.8 mmol) were suspended in *ca.* 90 mL of dry toluene and cooled to  $-80$  °C. Borane dimethyl sulfide complex (3.6 mL, 37.6 mmol, 2 equiv) was added via syringe in one portion. The reaction was stirred at  $-80$  °C for 2 h, then allowed to warm to room temperature within 1 h and stirred overnight. Trimethylsilyl bromide (2.6 mL, 19.7 mmol, 1.05 equiv) was added in one portion via syringe and the reaction was stirred for another 4 h at room temperature after which volatiles were removed in vacuum (1 mbar). The residue was dispersed in *ca.* 50 mL of hot hexane and was filtered hot. The filter cake was washed two times with additional *ca.* 25 mL of hot hexanes, and the combined liquors were left to crystallize at  $-35$  °C. After *ca.* 48 h the supernatant was removed by filtration and the crystals washed twice with cold hexanes (2 x 25 mL,  $-60$  °C). After evaporation of the volatiles *in vacuo*, 2.24 g (52% yield) of a white crystalline powder was obtained. Spectroscopic measurements corresponded to that of pure **3.1**.

$^1\text{H}$  NMR (500 MHz,  $\text{CDCl}_3$ )  $\delta$  7.71 (br. d,  $J = 7.3$  Hz, 2H), 7.43 – 7.32 (m, 4H), 7.25 (br. t,  $J = 7.1$  Hz, 2H), 5.10 (br, 1H, BH), 2.36 (br, 1H, BH), 1.96 – 1.83 (m, 2H, TMP), 1.67 – 1.52 (m, 10H, TMP), 1.33 (s, 12H,  $\text{TMP}(\text{Me}_2)$ ), 0.81 (s, 12H,  $\text{TMP}(\text{Me}_2)$ ).

$^{13}\text{C}\{^1\text{H}\}$  NMR (126 MHz,  $\text{CDCl}_3$ )  $\delta$  151.7, 134.6, 131.8, 129.1, 125.2, 55.4, 42.1, 32.9, 26.0, 18.8.

$^{11}\text{B}\{^1\text{H}\}$  NMR (160 MHz,  $\text{CDCl}_3$ ) :  $\delta$  20.0.

### Compound 3.2



In a glovebox, 300 mg (1.65 mmol) of **3.1** was dissolved in *ca.* 25 mL of toluene and placed into a Schlenk tube. 116  $\mu\text{L}$  (106 mg, 1.31 mmol) of 1-methylpyrrole was subsequently added by pipet. The reaction mixture was heated under nitrogen to  $80$  °C for 5 h and then evaporated to dryness *in vacuo*. The resulting thick orange oil proved to be difficult to handle and attempts to remove **3.2** from the small impurities (presumed to be the activation of 1-methylpyrrole at the 3 position and/or a double activation of 1-methylpyrrole). Instead, it was characterized as is and used without further

purification. The structure of the product could be unambiguously assigned as that of **3.2** by its  $^1\text{H}$  and  $^{13}\text{C}$  NMR signature.

$^1\text{H}$  NMR (500 MHz,  $\text{C}_6\text{D}_6$ )  $\delta$  7.85 (dd,  $J = 7.3, 1.8$  Hz, 1H,  $\text{C}_6\text{H}_4$ ), 7.37 (dd,  $J = 8.0, 1.1$  Hz, 1H,  $\text{C}_6\text{H}_4$ ), 7.27 (ddd,  $J = 8.0, 7.2, 1.9$  Hz, 1H,  $\text{C}_6\text{H}_4$ ), 7.19 (dt,  $J = 7.3, 1.1$  Hz, 1H,  $\text{C}_6\text{H}_4$ ), 7.17 (dd,  $J = 3.9, 1.5$  Hz, 1H,  $\text{NC}_4\text{H}_3$ ), 6.54 (t,  $J = 1.9$  Hz, 1H,  $\text{NC}_4\text{H}_3$ ), 6.25 (dd,  $J = 3.9, 2.3$  Hz, 1H,  $\text{NC}_4\text{H}_3$ ), 3.35 (s, 3H,  $\text{NCH}_3$ ), 1.30 (s, 6H,  $\text{TMP}(\text{Me}_2)$ ), 0.95 (s, 6H,  $\text{TMP}(\text{Me}_2)$ ), cyclic TMP signals were found as poorly resolved multiplets in the 2.0-0.9 area.

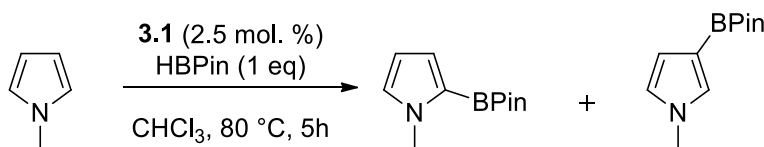
$^{13}\text{C}\{^1\text{H}\}$  NMR (126 MHz,  $\text{C}_6\text{D}_6$ )  $\delta$  152.8, 136.1, 132.2, 131.4, 129.7, 128.4, 125.2, 110.5, 55.4, 42.5, 34.6, 26.0, 19.1;

$^{11}\text{B}\{^1\text{H}\}$  NMR (160 MHz,  $\text{CDCl}_3$ ) :  $\delta$  54.3 (br).

### Borylation products in **Figure 31**

In a nitrogen-filled glovebox, a 0.0305 M stock solution of **3.1** in  $\text{CHCl}_3$  was prepared. 1 mL of this solution was introduced by pipet to a sealable 25 mL microwave vial equipped with a magnetic stirring bar and diluted in 4 mL additional  $\text{CHCl}_3$ . **Warning: using smaller vials may lead to hydrogen overpressure and explosion hazard.** To this was added HBPIn and the heteroaromatic substrate in the specified quantities. The vial was subsequently sealed and heated with stirring to 80  $^\circ\text{C}$  for 16 hours, after which the mixture was cooled down to room temperature and 60  $\mu\text{L}$  of p-xylene or mesitylene was added. An aliquot of the reaction mixture was analyzed by  $^1\text{H}$  NMR to determine the conversion, which was measured with regard to the resonance of the pinacol moieties. Heteroaromatic boronates were often found to be of dubious stability, especially in the case of furyl boronates. For this reason, the reaction mixture was purified by rapid passage through a *very short* pad of silica with vacuum suction along with  $\text{CH}_2\text{Cl}_2$  for rinsing. Such a treatment proved sufficient to remove the catalyst and yield the borylated product with good purity after vacuum evaporation of solvents and volatiles. Longer flash chromatography columns, on the other hand, tended to reduce the yields of obtained products.

### Borylation of 1-methylpyrrole



The general procedure was followed with the reaction time reduced to **5 hours**. 1-methylpyrrole (109  $\mu\text{L}$ , 99.1 mg, 1.22 mmol) was reacted with HBPIn (177  $\mu\text{L}$ , 156 mg, 1.22 mmol). Complete conversion was observed by NMR and 235 mg (93 %) of a 93:7 mixture of 1-methyl-2-(4,4,5,5-tetramethyl-1,3,2-dioxaborolan-2-yl)pyrrole and 1-methyl-3-(4,4,5,5-tetramethyl-1,3,2-dioxaborolan-2-yl)pyrrole was isolated as a white solid.

1-methyl-2-(4,4,5,5-tetramethyl-1,3,2-dioxaborolan-2-yl)pyrrole:  $^1\text{H}$  NMR (400 MHz,  $\text{CDCl}_3$ )  $\delta$  6.81 (m, 2H), 6.15 (m, 1H), 3.84 (s, 3H), 1.31 (s, 12H).

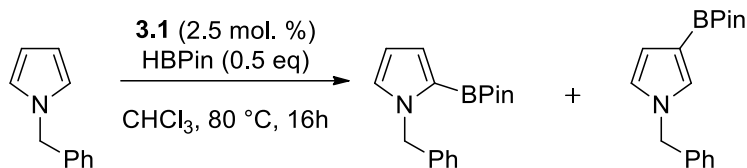
$^{13}\text{C}\{^1\text{H}\}$  NMR (101 MHz,  $\text{CDCl}_3$ ):  $\delta$  128.3, 122.0, 108.6, 83.2, 36.7, 25.0.

$^{11}\text{B}\{^1\text{H}\}$  NMR (160 MHz,  $\text{CDCl}_3$ ) :  $\delta$  28.1.

1-methyl-3-(4,4,5,5-tetramethyl-1,3,2-dioxaborolan-2-yl)pyrrole:  $^1\text{H}$  NMR (400 MHz,  $\text{CDCl}_3$ )  $\delta$  7.06 (m, 1H), 6.64 (m, 1H), 6.47 (m, 1H), 3.81 (s, 3H), 1.29 (s, 12H).

$M^+$ : 207.13 (calc.: 207.14).

### Borylation of 1-benzylpyrrole



The general procedure was followed with 1-benzylpyrrole (377  $\mu\text{L}$ , 384 mg, 2.44 mmol) and HBPin (177  $\mu\text{L}$ , 156 mg, 1.22 mmol). Complete conversion was observed by NMR and 311 mg (90 %) of a 3:2 mixture of 1-benzyl-2-(4,4,5,5-tetramethyl-1,3,2-dioxaborolan-2-yl)pyrrole and 1-benzyl-3-(4,4,5,5-tetramethyl-1,3,2-dioxaborolan-2-yl)pyrrole was obtained after thorough evaporation of volatiles as a colorless oil which rapidly became light pink. NMR characterization was conform to that of the reported compound for 1-benzyl-3-(4,4,5,5-tetramethyl-1,3,2-dioxaborolan-2-yl)pyrrole (34). 1-benzyl-2-(4,4,5,5-tetramethyl-1,3,2-dioxaborolan-2-yl)pyrrole is a new compound.

1-benzyl-2-(4,4,5,5-tetramethyl-1,3,2-dioxaborolan-2-yl)pyrrole:  $^1\text{H}$  NMR (400 MHz,  $\text{CDCl}_3$ )  $\delta$  7.30 – 7.17 (m, 3H), 7.12 – 7.06 (m, 2H), 6.89 (dd,  $J$  = 2.4, 1.6 Hz, 1H), 6.86 (dt,  $J$  = 3.6, 1.9 Hz, 1H), 6.23 – 6.19 (m, 1H), 5.39 (s, 2H), 1.24 – 1.21 (m, 13H)

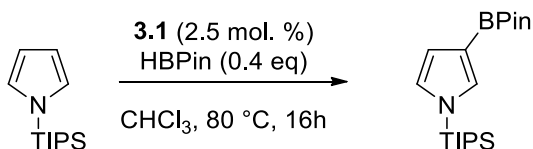
1-benzyl-3-(4,4,5,5-tetramethyl-1,3,2-dioxaborolan-2-yl)pyrrole:  $^1\text{H}$  NMR (400 MHz,  $\text{CDCl}_3$ )  $\delta$  7.36 – 7.26 (m, 3H), 7.17 – 7.12 (m, 3H), 6.73 – 6.68 (m, 1H), 6.51 (dd,  $J$  = 2.6, 1.7 Hz, 1H), 5.06 (s, 2H), 1.31 (s, 12H);

Mixture:  $^{13}\text{C}\{^1\text{H}\}$  NMR (126 MHz,  $\text{CDCl}_3$ )  $\delta$  139.8, 137.7, 130.4, 128.9, 128.5, 127.9, 127.7, 127.5, 127.2, 127.0, 122.4, 122.3, 114.6, 109.1, 83.3, 82.9, 53.5, 52.9, 25.0, 24.8.

$^{11}\text{B}\{^1\text{H}\}$  NMR (160 MHz,  $\text{CDCl}_3$ ):  $\delta$  27.8.

$M^+$ : 283.16 (calc.: 283.17).

### Borylation of 1-(triisopropylsilyl)pyrrole



The general procedure was followed with 1-(triisopropylsilyl)pyrrole (305  $\mu\text{L}$ , 321 mg, 2.44 mmol) and HBPin (177  $\mu\text{L}$ , 156 mg, 1.22 mmol). Complete conversion was observed by NMR and 342 mg (98 %) of 1-(triisopropylsilyl)-3-(4,4,5,5-tetramethyl-1,3,2-dioxaborolan-2-yl)pyrrole was obtained as a colorless solid after thorough evaporation of the volatile under vacuum.

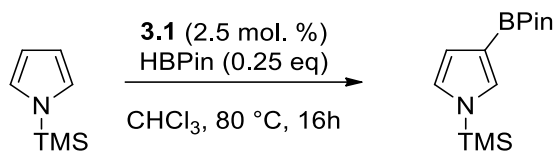
$^1\text{H}$  NMR (500 MHz,  $\text{CDCl}_3$ )  $\delta$  7.23 (br. s, 1H), 6.81 (m, 1H), 6.62 (m, 1H), 1.46 (sept,  $J$  = 7.3 Hz, 3H), 1.32 (s, 12H), 1.09 (d,  $J$  = 7.3 Hz, 18H).

$^{13}\text{C}\{^1\text{H}\}$  NMR  $\delta$  (126 MHz,  $\text{CDCl}_3$ )  $\delta$  133.8, 125.1, 115.7, 82.9, 25.0, 18.0, 11.8.

$^{11}\text{B}\{^1\text{H}\}$  NMR  $\delta$  (160 MHz,  $\text{CDCl}_3$ ): 30.0.

$M^+$ : 349.28 (calc.: 349.26).

### Borylation of 1-(trimethylsilyl)pyrrole



The general procedure was followed with 1-(trimethylsilyl)pyrrole (680 mg, 4.89 mmol) and HBPin (177  $\mu$ L, 156 mg, 1.22 mmol). A conversion of 75 % was observed by NMR and 342 mg (98 %) of 1-(trimethylsilyl)-3-(4,4,5,5-tetramethyl-1,3,2-dioxaborolan-2-yl)pyrrole was obtained as a colorless solid after thorough evaporation of the volatile under vacuum.

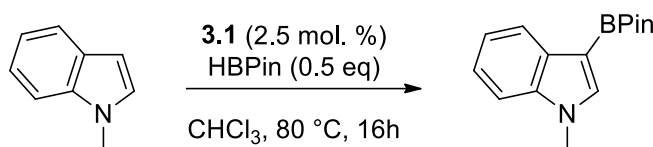
<sup>1</sup>H NMR (400 MHz, CDCl<sub>3</sub>)  $\delta$  7.28 (m, 1H), 6.83 (t, *J* = 2.2, 1H), 6.63 (m, 1H), 1.35 (s, 12H), 1.32 (s, 12H), 0.42 (9H).

<sup>13</sup>C{<sup>1</sup>H} NMR (126 MHz, CDCl<sub>3</sub>)  $\delta$  132.9, 124.0, 116.3, 83.0, 77.2, 25.0, -0.2.

<sup>11</sup>B{<sup>1</sup>H} NMR (160 MHz, CDCl<sub>3</sub>):  $\delta$  30.0.

M<sup>+</sup>: 365.12 (calc.: 265.17).

### Borylation of 1-methylindole



The general procedure was followed with 1-methylindole (305  $\mu$ L, 321 mg, 2.44 mmol) and HBPin (177  $\mu$ L, 156 mg, 1.22 mmol). Complete conversion was observed by NMR and 267 mg (85 %) of 1-methyl-3-(4,4,5,5-tetramethyl-1,3,2-dioxaborolan-2-yl)indole was obtained as pale yellow crystals.

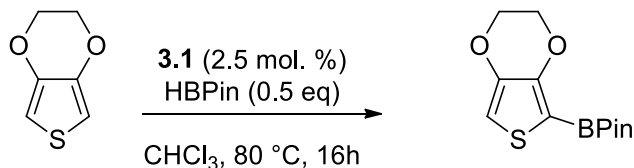
<sup>1</sup>H NMR (400 MHz, CDCl<sub>3</sub>)  $\delta$  8.04 (ddd, *J* = 7.7, 1.4, 0.8 Hz, 1H), 7.52 (s, 1H), 7.35 – 7.31 (m, 1H), 7.25 – 7.15 (m, 2H), 3.80 (s, 3H), 1.37 (s, 12H).

<sup>13</sup>C{<sup>1</sup>H} NMR (101 MHz, CDCl<sub>3</sub>):  $\delta$  138.6, 138.0, 132.6, 122.8, 121.9, 120.3, 109.3, 82.9, 33.1, 25.0.

<sup>11</sup>B{<sup>1</sup>H} NMR (160 MHz, CDCl<sub>3</sub>):  $\delta$  29.7.

M<sup>+</sup>: 257.16 (calc.: 257.16).

### Monoborylation of 3,4-ethylenedioxythiophene



The general procedure was followed with 3,4-ethylenedioxythiophene (261  $\mu$ L, 347 mg, 2.44 mmol) and HBPin (177  $\mu$ L, 156 mg, 1.22 mmol). Complete conversion was observed by NMR and 285 mg (87 %) of 2-(4,4,5,5-tetramethyl-1,3,2-dioxaborolan-2-yl)-3,4-ethylenedioxythiophene was obtained as a white crystalline solid. NMR characterization was conform to that of the reported product.<sup>232</sup>

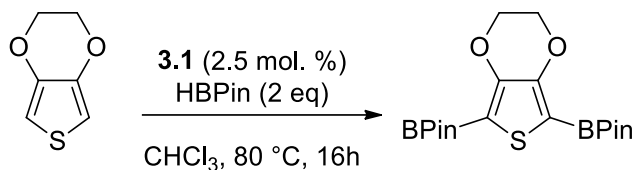
<sup>1</sup>H NMR (500 MHz, CDCl<sub>3</sub>)  $\delta$  6.63 (s, 1H), 4.31 – 4.28 (m, 2H), 4.19 – 4.17 (m, 2H), 1.34 (s, 12H).

$^{13}\text{C}\{^1\text{H}\}$  NMR (126 MHz,  $\text{CDCl}_3$ )  $\delta$  149.2, 142.5, 107.6, 84.0, 65.2, 64.4, 24.9.

$^{11}\text{B}\{^1\text{H}\}$  NMR (160 MHz,  $\text{CDCl}_3$ ):  $\delta$  28.2.

$M^+$ : 268.13 (calc.: 268.09).

### Diborylation of 3,4-ethylenedioxythiophene



The general procedure was followed with 3,4-ethylenedioxythiophene (65  $\mu\text{L}$ , 87 mg, 0.611 mmol) and HBPIn (177  $\mu\text{L}$ , 156 mg, 1.22 mmol). Complete conversion was observed by NMR and 443 mg (92 %) of 2-(4,4,5,5-tetramethyl-1,3,2-dioxaborolan-2-yl)-3,4-ethylenedioxythiophene was obtained as pale yellow crystalline solid.

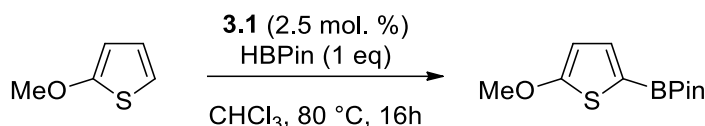
$^1\text{H}$  NMR (500 MHz,  $\text{CDCl}_3$ )  $\delta$  4.27 (s, 2H), 1.32 (s, 12H).

$^{13}\text{C}\{^1\text{H}\}$  NMR (101 MHz,  $\text{CDCl}_3$ )  $\delta$  149.0, 84.0, 64.8, 24.9.

$^{11}\text{B}\{^1\text{H}\}$  NMR (160 MHz,  $\text{CDCl}_3$ ).  $\delta$  28.4.

$M^+$ : 394.24 (calc.: 394.18).

### Borylation of 2-Methoxythiophene



The general procedure was followed with 2-methoxythiophene (123  $\mu\text{L}$ , 140 mg, 1.22 mmol) and HBPIn (177  $\mu\text{L}$ , 156 mg, 1.22 mmol). Complete conversion was measured by NMR and 249 mg (85 %) of 2-(4,4,5,5-tetramethyl-1,3,2-dioxaborolan-2-yl)-5-methoxythiophene was obtained as pale yellow oil.

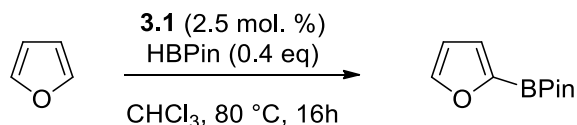
$^1\text{H}$  NMR (400 MHz,  $\text{CDCl}_3$ )  $\delta$  7.33 (d,  $J = 3.9$ , 1H), 6.30 (dd,  $J = 3.9$ , 1H), 3.92 (s, 3H), 1.32 (s, 12H).

$^{13}\text{C}\{^1\text{H}\}$  NMR (126 MHz,  $\text{CDCl}_3$ )  $\delta$  173.0, 136.6, 106.3, 83.9, 60.5, 24.9.

$^{11}\text{B}\{^1\text{H}\}$  NMR (160 MHz,  $\text{CDCl}_3$ ):  $\delta$  28.7.

$M^+$ : 240.10 (calc.: 240.13).

### Borylation of furan



The general procedure was followed with furan (222  $\mu\text{L}$ , 208 mg, 3.06 mmol) and HBPIn (177  $\mu\text{L}$ , 156 mg, 1.22 mmol). A conversion of 79 % conversion was measured by NMR after 36 hours and 203 mg (80 %) of 2-(4,4,5,5-tetramethyl-1,3,2-dioxaborolan-2-yl)methylfuran was obtained as pale yellow oil.

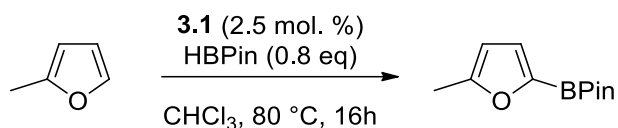
$^1\text{H}$  NMR (400 MHz,  $\text{CDCl}_3$ )  $\delta$  7.65 (dd,  $J = 1.7, 0.6$ , 1H), 7.07 (dd,  $J = 3.4, 0.6$ , 1H), 6.62 (dd,  $J = 3.4, 1.7$ , 1H), 1.35 (s, 12H).

$^{13}\text{C}\{^1\text{H}\}$  NMR (126 MHz,  $\text{CDCl}_3$ )  $\delta$  147.5, 123.4, 110.5, 84.4, 77.2, 24.9.

$^{11}\text{B}\{^1\text{H}\}$  NMR (160 MHz,  $\text{CDCl}_3$ ):  $\delta$  27.3.

$M^+$ : 194.08 (calc.: 194.11).

### Borylation of 2-methylfuran



The general procedure was followed with 2-methylfuran (132  $\mu\text{L}$ , 120 mg, 1.47 mmol) and HBPin (177  $\mu\text{L}$ , 156 mg, 1.22 mmol). Complete conversion was measured by NMR and 203 mg (80 %) of 2-(4,4,5,5-tetramethyl-1,3,2-dioxaborolan-2-yl)-5-methylfuran was obtained as pale yellow oil.

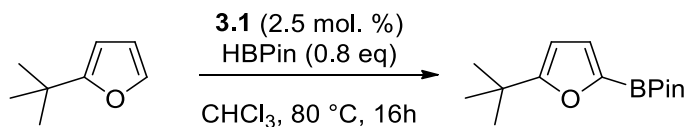
$^1\text{H}$  NMR (500 MHz,  $\text{CDCl}_3$ )  $\delta$  6.99 (dd,  $J = 3.2, 0.6$  Hz, 1H), 6.03 (dq,  $J = 3.2, 0.9$  Hz, 1H), 2.36 – 2.35 (br. s, 3H), 1.34 (s, 12H).

$^{13}\text{C}\{^1\text{H}\}$  NMR (101 MHz,  $\text{CDCl}_3$ )  $\delta$  157.9, 125.0, 107.0, 84.2, 24.9, 14.1.

$^{11}\text{B}\{^1\text{H}\}$  NMR (160 MHz,  $\text{CDCl}_3$ ):  $\delta$  27.1.

$M^+$ : 208.11 (calc.: 208.13).

### Borylation of 2-*tert*-butylfuran



The general procedure was followed with 2-*tert*-Butylfuran (209  $\mu\text{L}$ , 182 mg, 1.47 mmol) and HBPin (177  $\mu\text{L}$ , 156 mg, 1.22 mmol). Complete conversion was measured by NMR and 258 mg (86 %) of 2-(4,4,5,5-tetramethyl-1,3,2-dioxaborolan-2-yl)-5-*tert*-butylfuran was obtained as pale yellow oil.

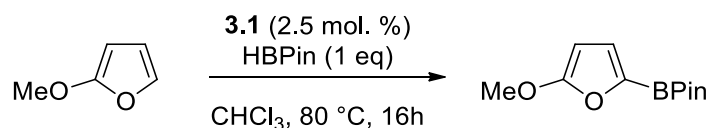
$^1\text{H}$  NMR (400 MHz,  $\text{CDCl}_3$ )  $\delta$  6.98 (d,  $J = 3.3$  Hz, 1H), 6.02 (d,  $J = 3.3$  Hz, 1H), 1.33 (s, 12H), 1.31 (s, 9H).

$^{13}\text{C}\{^1\text{H}\}$  NMR (101 MHz,  $\text{CDCl}_3$ )  $\delta$  169.9, 124.8, 103.3, 84.0, 77.2, 33.1, 29.3, 24.9.

$^{11}\text{B}\{^1\text{H}\}$  NMR (160 MHz,  $\text{CDCl}_3$ ):  $\delta$  27.4.

$M^+$ : 250.15 (calc.: 250.17).

### Borylation of 2-methoxyfuran



The general procedure was followed with 2-methoxyfuran (113  $\mu\text{L}$ , 120 mg, 1.22 mmol) and HBPin (177  $\mu\text{L}$ , 156 mg, 1.22 mmol). After 16 hours, a 74 % conversion was measured by NMR and 170 mg (62 %) of 2-(4,4,5,5-tetramethyl-1,3,2-dioxaborolan-2-yl)-5-methoxyfuran was obtained as pale

yellow oil. Although the product could be isolated and characterized, we found that it decomposed after a few hours at room temperature in  $\text{CDCl}_3$ . Its sensitivity presumably explains the lower yields obtained. The pure product can be kept for longer periods at low temperature in the dark.

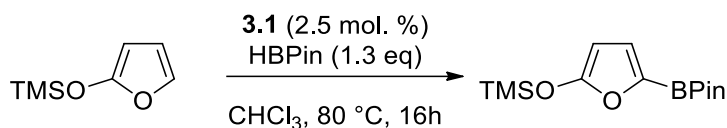
$^1\text{H}$  NMR (400 MHz,  $\text{CDCl}_3$ )  $\delta$  7.00 (d,  $J = 3.4$ , 1H), 5.22 (d,  $J = 3.4$ , 1H), 3.87 (s, 3H), 1.32 (s, 12H).

$^{13}\text{C}\{^1\text{H}\}$  NMR (126 MHz,  $\text{CDCl}_3$ )  $\delta$  126.5, 110.1, 84.0, 81.5, 58.0, 24.9.

$^{11}\text{B}\{^1\text{H}\}$  NMR (160 MHz,  $\text{CDCl}_3$ ):  $\delta$  26.9.

$M^+$ : 224.12 (calc.: 224.12).

### Borylation of 2-silyloxyfuran



The general procedure was followed on a smaller scale with 2-silyloxyfuran, (127.5 mg, 0.816 mmol) and HBPIn (177  $\mu\text{L}$ , 156 mg, 1.22 mmol) were added to 0.66 mL of the stock solution (0.0202 mmol of **1**). After 16 hours, a quantitative conversion was measured by NMR and 190 mg (84 %) of 2-(4,4,5,5-tetramethyl-1,3,2-dioxaborolan-2-yl)-5-silyloxyfuran was obtained as a yellow oil. Although the product could be isolated and characterized, we found that it tended to decompose under ambient conditions.

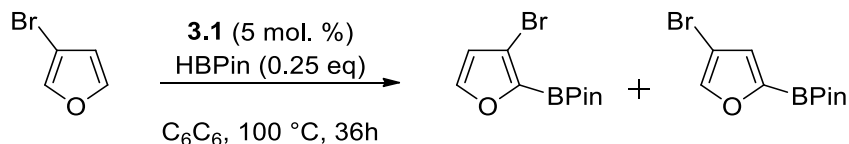
$^1\text{H}$  NMR (400 MHz,  $\text{CDCl}_3$ )  $\delta$  6.96 (d,  $J = 3.3$ , 1H), 5.18 (d,  $J = 3.3$ , 1H), 1.31 (s, 12H), 0.30 (s, 9H).

$^{13}\text{C}\{^1\text{H}\}$  NMR (101 MHz,  $\text{CDCl}_3$ )  $\delta$  126.4, 110.2, 85.5, 83.9, 24.9, -0.1.

$^{11}\text{B}\{^1\text{H}\}$  NMR (160 MHz,  $\text{CDCl}_3$ ):  $\delta$  26.7.

$M^+$ : 282.15 (calc.: 282.15).

### Borylation of 3-bromofuran



TMP- $\text{C}_6\text{H}_4\text{-BH}_2$  (2.1 mg, 0.045 mmol, 5 mol. %), 3-bromofuran (32.9  $\mu\text{L}$ , 53.9 mg, 0.367 mmol), hexamethylbenzene (1.4 mg, 0.0086 mmol) and HBPIn (12.8  $\mu\text{L}$ , 11.7 mg, 0.0916) were dissolved in  $\text{C}_6\text{D}_6$  (0.4 mL) and placed in a J-Young tube. This mixture was heated to 100  $^\circ\text{C}$  for 36 hours before being analyzed by  $^1\text{H}$  NMR to reveal a 90 % conversion. The contents of the tube were then passed through a short pad of silica and the volatiles of the filtrate were evaporated *in vacuo*. 26.4 mg of a yellow oil were thus collected, which contained the starting hexamethylbenzene. By subtracting the mass of starting hexamethylbenzene, we calculate a yield of 79 % (25.0 mg).

$^1\text{H}$  NMR (400 MHz,  $\text{CDCl}_3$ ) 7.54 (m, 1H), 6.50 (m, 1H), 1.36 (s, 12H).

$^1\text{H}$  NMR (400 MHz,  $\text{CDCl}_3$ )  $\delta$  7.61 (m, 1H), 7.05 (m, 1H), 1.34 (s, 12H).

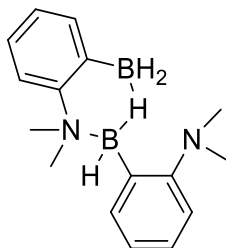
Mixture:

$^{13}\text{C}\{^1\text{H}\}$  NMR (101 MHz,  $\text{CDCl}_3$ )  $\delta$  147.8, 145.7, 126.0, 115.1, 110.1, 84.7, 84.6, 24.9, 24.9.

$^{11}\text{B}\{^1\text{H}\}$  NMR (160 MHz,  $\text{CDCl}_3$ ):  $\delta$  26.7.

M<sup>+</sup>: 272.05 (calc.: 272.02).

### Compound **3.3**



915 mg (6.49 mmol, 1 equiv) of **3.5** was dissolved in toluene and 0.95 mL (7.15 mmol, 1.1 equiv) of TMSBr was added. The reaction was stirred at room temperature for *ca* 4 h. The solution was separated from the precipitated salts by filtration and the volatile removed under vacuum to give 420 mg (98 % yield) of the title compound as a white powder. Single crystals were obtained from a toluene solution at -35°C.

#### *Alternate one-pot synthesis from 3.4*

4.00 g (20.7 mmol, 1 equiv) of **3.4** was dissolved in toluene, 790 mg of LiAlH<sub>4</sub> (20.7 mmol, 1 equiv according to Li) was added followed by 4.30 mL of DME (41.4 mmol, 2 equiv). The reaction was stirred for *ca* 1 h at room temperature, then the mixture was filtered and the volatile removed under vacuum until almost dryness. The oil was then dissolved in toluene and 3.00 mL (22.8 mmol, 1.1 eq) of TMSBr was added. The reaction was stirred at room temperature for *ca* 16 h. The solution was separated from the precipitated salts by filtration and the volatile removed under vacuum. Hexanes were added and then removed by filtration to obtain 1.34 g (49% yield) of a clean white powder dried over vacuum of the compound.

<sup>1</sup>H NMR (500 MHz, CDCl<sub>3</sub>) δ 7.55 (d, *J* = 7.2 Hz, 1H), 7.47 (dd, *J* = 7.3, 1.6 Hz, 1H), 7.35 – 7.26 (m, 2H), 7.26 – 7.22 (m, 2H), 7.21 – 7.17 (m, 1H), 7.08 – 7.01 (m, 1H), 3.05 (s, br, 3H, H7 or H8), 2.81 (s, br, 3H), 2.71 (s, 6H), -0.60 (s, br, 1H, BH).

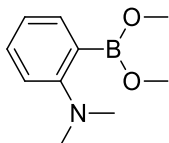
<sup>13</sup>C{<sup>1</sup>H} NMR (126 MHz, CDCl<sub>3</sub>) δ 159.5 (s), 151.6 (s), 138.6 (s), 132.7 (s), 129.3 (s), 127.4 (s), 125.9 (s), 123.1 (s), 119.5 (s), 115.9 (s), 50.6 (s), 48.9 (s), 46.0 (s).

<sup>11</sup>B{<sup>1</sup>H} NMR (160 MHz, CDCl<sub>3</sub>) δ 3.3 (s), -10.4 (s).

VT<sup>1</sup>H NMR analysis showed that compound **3.3** is at equilibrium with another dimeric form in which the phenyl rings are equivalent and the methyl equivalent only over 0 °C (**3.3\***). The equilibrium shifts toward **3.3** with increasing temperature. Those evidences suggest that the most probable dimeric form to be at equilibrium with compound **3.3** is a form with two N-B bonds forming an eight-membered cycle.

### Compound **3.4**





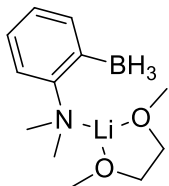
**3.4** was prepared using a method inspired from Kaufmann *et al.* and Whitley *et al.*<sup>129,130</sup> In a typical synthesis, 10.5 mL (82.5 mmol, 1 equiv) of N,N-dimethylaniline and 1.87 mL (12.4 mmol, 0.15 equiv) of tetramethylethylenediamine (TMEDA) were mixed in a Schlenk tube and 30.6 mL of a 2.7 M solution of *n*-BuLi in heptane (82.5 mmol, 1 equiv) was added at 0 °C. The reaction was then heated at 60 °C overnight (approximately 16 h) to form 1-NMe<sub>2</sub>-2-Li-C<sub>6</sub>H<sub>4</sub> that precipitate as a white solid. The reaction was then cooled at room temperature and *ca* 50 mL of dried toluene or diethylether was added to increase the solubility of 1-NMe<sub>2</sub>-2-Li-C<sub>6</sub>H<sub>4</sub>. The mixture was then cooled to -78 °C, 27.6 mL (165 mmol, 3 equiv) of B(OMe)<sub>3</sub> was added in one portion and the reaction warmed to room temperature. After *ca* 4 h at room temperature, the reaction is bright yellow-green and appreciable amount of salts precipitated. The salts were then removed by filtration and the volatile evaporated under vacuum. The title product was then purified by distillation under reduced pressure. The reaction gave 5 g to 7 g (31 % to 44 % yield) of the title compound as a colorless oil. A light green color is developing after several days when the product is stored at room temperature, so storage at -35 °C is recommended.

<sup>1</sup>H NMR (500 MHz, CDCl<sub>3</sub>) δ 7.32 – 7.25 (m, 2H), 6.91 – 6.85 (m, 2H), 3.64 (s, 6H), 2.87 (s, 6H).

<sup>13</sup>C{<sup>1</sup>H} NMR (126 MHz, CDCl<sub>3</sub>) δ 155.4 (s), 132.8 (s), 129.7 (s), 119.2 (s), 114.7 (s), 52.4 (s), 43.3 (s).

<sup>11</sup>B{<sup>1</sup>H} NMR (160 MHz, CDCl<sub>3</sub>) δ 30.5 (s).

#### Compound 3.5



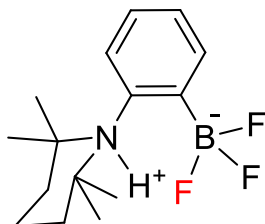
Synthesis based on the work of Wagner and coworkers.<sup>179</sup> 1.00 g (5.18 mmol, 1 equiv) of NMe<sub>2</sub>-C<sub>6</sub>H<sub>4</sub>-B(OMe)<sub>2</sub> was dissolved in toluene, 200 mg of LiAlH<sub>4</sub> (5.27 mmol, 1 equiv according to Li) was added followed by 1.10 mL of DME (10.4 mmol, 2 equiv). The reaction was stirred for *ca* 1 h at room temperature, then the mixture was filtered and the volatile removed under vacuum until almost dryness. The oil was then dissolved in hexanes and 0.55 mL (5.30 mmol, 1 equiv) of DME was added, which induced the precipitation of the title compound as a white powder. The liquid phase was removed by filtration through cannula and the solid dried under vacuum to yield 717 mg (60 % yield) of the title compound as a white powder. Single crystals were obtained from a toluene solution at -35 °C.

<sup>1</sup>H NMR (400 MHz, CDCl<sub>3</sub>) δ 7.59 (s, br, 1H), 7.12 – 6.97 (m, 3H), 3.69 (s, 4H), 3.48 (s, 6H), 2.65 (s, 6H), 1.17 (q, <sup>1</sup>J<sub>B-H</sub> = 79 Hz, 3H, BH<sub>3</sub>).

<sup>13</sup>C{<sup>1</sup>H} NMR (126 MHz, CDCl<sub>3</sub>) δ 155.8 (s), 150.1 (q, <sup>1</sup>J<sub>C-B</sub> = 50 Hz), 138.5 (s), 125.1 (s), 124.8 (s), 117.5 (s), 70.5 (s), 59.6 (s), 46.3 (s).

<sup>11</sup>B{<sup>1</sup>H} NMR (160 MHz, CDCl<sub>3</sub>) δ -29.3 (s).

### Compound 3.6



To a solution of TMP-C<sub>6</sub>H<sub>4</sub>-B(OH)<sub>2</sub> (250 mg, 0.95 mmol) in methanol (10 mL), were added KHF<sub>2</sub> (445 mg, 5.7 mmol) and 1 mL of a 2M HCl solution in water. The reaction mixture was sonicated for 30 min and stirred at 80 °C for 12 h. After evaporation of the volatiles *in vacuo*, a white solid was obtained and extracted three times with CHCl<sub>3</sub>. The combined organic fractions were dried to yield 250 mg (92 % yield) of the target compound.

A suitable single crystal for XRD were obtained by slow evaporation of an acetone solution at room temperature.

<sup>1</sup>H NMR 500 MHz: δ 9.7 (d, broad, J=12Hz, 1H, NH); 7.81 (d, <sup>3</sup>J<sub>H-H</sub>=7Hz, 1H); 7.41 (t, <sup>3</sup>J<sub>H-H</sub>=7Hz, 1H); 7.32-7.22 (m, 2H); 2.04-1.95 (m, 5H); 1.89-1.83 (m, 1H); 1.65 (s, 6H); 1.22 (s, 6H).

<sup>13</sup>C{<sup>1</sup>H} (126 MHz): δ 136.6 (s); 135.5 (s); 129.2 (s); 127.0 (s); 121.1 (s); 67.8 (s); 39.6 (s); 30.3 (s); 23.5 (s); 16.5 (s).

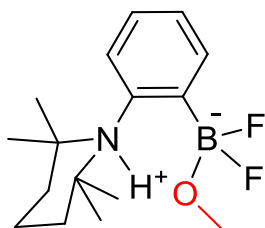
<sup>19</sup>F{<sup>1</sup>H} (470 MHz): δ -134.0 (m).

<sup>11</sup>B{<sup>1</sup>H} (160 MHz): δ 3.3 (m).

Elemental analysis calcd. for C<sub>15</sub>H<sub>23</sub>B<sub>1</sub>N<sub>1</sub>F<sub>3</sub>: C, 63.18; H, 8.13; N, 4.91%. Found: C, 63.02; H, 8.67; N, 4.98.

[M-H]<sup>-</sup> = 284.1810 (calc.: 284.1797)

### Compound 3.7



To solution of TMP-C<sub>6</sub>H<sub>4</sub>-B(OH)<sub>2</sub> (500 mg, 1.91 mmol) in methanol (10 mL), were added KHF<sub>2</sub> (445 mg, 5.7 mmol) and 1 mL of a 2 M HCl solution in water. The reaction mixture was sonicated for 5 min and stirred at room temperature for one hour. After evaporation of the volatiles *in vacuo*, a white solid was obtained and extracted three times with CHCl<sub>3</sub>. The organic fractions were combined and evaporated to give 514 mg (90% yield) of the target compound.

A suitable single crystal for XRD were obtained from a saturated toluene solution at -35 °C.

$^1\text{H}$  NMR 500MHz:  $\delta$  13.0 (s, broad, 1H, NH); 7.83 (d,  $^3J_{\text{H-H}}=7\text{Hz}$ , 1H); 7.37 (t,  $^3J_{\text{H-H}}=7\text{Hz}$ , 1H); 7.24-7.16 (m, 2H); 3.58 (s, 3H); 2.03-1.87 (m); 1.60 (s, 6H); 1.17 (s, 6H).

$^{13}\text{C}\{^1\text{H}\}$  (126 MHz):  $\delta$  137.7 (t,  $^3J_{\text{C-F}}=4\text{Hz}$ ); 137.7 (s); 135.2 (s); 128.8 (s); 121.4 (s); 65.5 (s); 47.1 (t,  $^3J_{\text{C-F}}=5\text{Hz}$ ); 39.5 (s); 29.8 (s); 23.8 (s); 16.8 (s).

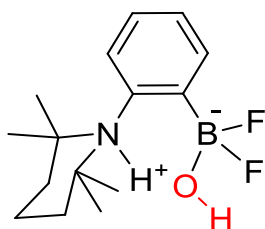
$^{19}\text{F}\{^1\text{H}\}$  (470 MHz):  $\delta$  -147.8 (q,  $^1J_{\text{F-B}}=58\text{Hz}$ ).

$^{11}\text{B}\{^1\text{H}\}$  (160 MHz):  $\delta$  3.4 (t,  $^1J_{\text{B-F}}=59\text{Hz}$ ).

Elemental analysis calcd. for  $\text{C}_{16}\text{H}_{26}\text{B}_1\text{N}_1\text{F}_2\text{O}_1$  : C, 64.66; H, 8.82; N, 4.71%. Found: C, 64.31; H, 9.21; N, 4.79.

$[\text{M-H}]^- = 296.2018$  (calc.: 296.1997)

### Compound 3.8



To solution of  $\text{TMP-C}_6\text{H}_4\text{-B(OH)}_2$  (500 mg, 1.91 mmol) in  $\text{THF:H}_2\text{O}$  (20 mL of a 5:1 mixture), was added  $\text{KHF}_2$  (445 mg, 5.7 mmol). The reaction mixture was stirred at room temperature for 15 minutes, then with  $\text{CHCl}_3$  (3 x 15 mL). After evaporation of the volatiles *in vacuo*, 470 mg (87 %) of a white solid was obtained, which was identified as the target compound.

$^1\text{H-NMR}$  500 MHz:  $\delta$  12.6 (s, broad, 1H, NH); 7.89 (d,  $^3J_{\text{H-H}}=7\text{Hz}$ , 1H); 7.41 (t,  $^3J_{\text{H-H}}=7\text{Hz}$ , 1H); 7.26-7.21 (m, 2H); 2.39 (s, broad, 1H, OH); 2.11-1.81 (m, 6H); 1.65 (s, 6H); 1.26 (s, 6H).

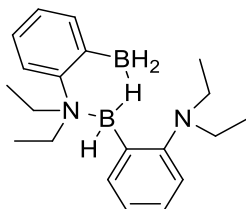
$^{13}\text{C}\{^1\text{H}\}$  (126 MHz):  $\delta$  137.6 (t,  $J=4\text{Hz}$ ); 135.4 (s); 129.0 (s); 126.4 (s); 121.3 (s); 66.2 (s); 39.2 (s); 30.0 (s); 23.8 (s); 16.8 (s).

$^{19}\text{F}\{^1\text{H}\}$  (470 MHz):  $\delta$  -133.9 (q,  $^1J_{\text{F-B}}=53\text{ Hz}$ ).

$^{11}\text{B}\{^1\text{H}\}$  (160 MHz):  $\delta$  3.5 (t,  $^1J_{\text{B-F}}=61\text{ Hz}$ ).

Elemental analysis calcd. for  $\text{C}_{15}\text{H}_{24}\text{B}_1\text{N}_1\text{F}_2\text{O}_1$  : C, 63.62; H, 8.54; N, 4.95 %. Found: C, 63.60; H, 8.84; N, 4.89.

### Compound 3.9



750 mg (2.89 mmol, 1 equiv) of 1-NEt<sub>2</sub>-2-BH<sub>3</sub>-C<sub>6</sub>H<sub>4</sub>•LiDME was dissolved in toluene and 0.57 mL (4.34 mmol, 1.5 equiv) of TMSBr was added. The reaction was stirred at room temperature for 12 hours. The solution was separated from the precipitated salts by filtration and the volatile removed under reduced pressure to give 140 mg (30 % yield) of the title compound as a white powder. Single crystals were obtained from a toluene solution at -35°C.

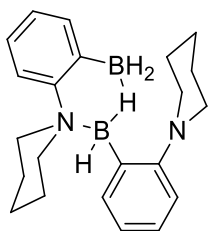
Alternative synthesis from 1-diethylamino-2-B(OH)<sub>2</sub>-C<sub>6</sub>H<sub>4</sub>: 2.75 g (14.2 mmol, 1 equiv) of 1-diethylamino-2-B(OH)<sub>2</sub>-C<sub>6</sub>H<sub>4</sub> was dissolved in toluene and cooled with an ice bath, 822 mg of LiAlH<sub>4</sub> (18.5 mmol, 1.3 equiv according to Li) was added followed by 3.5 mL of DME (24.4 mmol, 2 equiv). A certain amount of H<sub>2</sub> is liberated. The reaction was stirred for 1 hour at room temperature, then the mixture was filtered and the volatiles removed under reduced pressure. The remaining white oil was then dissolved in toluene and 2.42 mL (15.6 mmol, 1.1 equiv) of TMSBr was added. The reaction was stirred at room temperature for 12 hours. The solution was separated from the precipitated salts by filtration and the volatiles removed under reduced pressure to give 1.15 g (50% yield) of the compound as a white powder.

<sup>1</sup>H NMR (500 MHz, CDCl<sub>3</sub>) δ 7.55 (d, *J* = 6.7 Hz, 1H), 7.46 (dd, *J* = 7.4, 1.6 Hz, 1H), 7.29-7.24 (m, 2H), 7.20 (t, *J* = 7.0 Hz, 1H), 7.11 (d, *J* = 8.0 Hz, 1H), 7.03-6.97 (m, 2H), 3.49-3.33 (m, 2H), 3.12 (d, *J* = 5.1 Hz, 6H), 1.39-1.03 (m, 6H), 1.00 (t, *J* = 7.1 Hz, 6H), -0.69 (s, BH<sub>2</sub>).

<sup>13</sup>C{<sup>1</sup>H} NMR (126 MHz, CDCl<sub>3</sub>) δ 156.3 (s), 145.4 (br s), 144.3 (s), 138.1 (s), 136.5 (br s), 132.9 (s), 128.1 (s), 127.0 (s), 124.5 (s), 122.7 (s), 122.2 (s), 120.2 (s), 55.0 (br s), 50.0 (br s), 47.2 (s), 11.1 (s), 9.5 (br s).

<sup>11</sup>B{<sup>1</sup>H} NMR (160 MHz, CDCl<sub>3</sub>) δ 1.0 (s), -10.7 (s).

### Compound 3.10



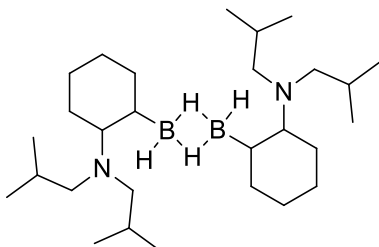
In a 100 mL Schlenk, 1.2 g (5.2 mmol, 1 equiv) of 1-piperidyl-2-B(OMe)<sub>2</sub>-C<sub>6</sub>H<sub>4</sub> was dissolved in toluene (60 mL), cooled in an ice bath, and 254 mg of LiAlH<sub>4</sub> (6.7 mmol, 1.3 equiv according to Li) was added, followed by 1.1 mL of DME (10.3 mmol, 2 equiv). A certain amount of H<sub>2</sub> is liberated. The reaction was stirred for 2 hours at room temperature, then the mixture was filtered on fritted glass and the volatiles were removed under reduced pressure. The remaining white oil was then dissolved in toluene (50 mL) and 0.8 mL (5.7 mmol, 1.1 equiv) of TMSBr was added. The reaction was stirred at room temperature for 16 hours. Afterwards, the solution was separated from the precipitated salts by filtration and the volatiles were removed under reduced pressure. This gave 0.7 g (79% yield) as a white powder. Single crystals were obtained from a toluene/hexanes solution at -35 °C. Since the product is extremely air-sensitive, no elemental analysis was performed.

<sup>1</sup>H NMR (500 MHz, benzene-*d*<sub>6</sub>): δ 7.79 (d, *J* = 6.5Hz, 1H), 7.19 (d, *J* = 9.0Hz, 1H), 7.15-7.08 (m, 2H), 7.01-6.96 (m, 2H), 6.76-6.69 (m, 2H), 4.84-3.64 (m, 3H, BH<sub>2</sub>), 3.59 (m, 1H), 3.07 (s, 2H), 2.84 (m, 1H), 2.75 (m, 1H), 2.65 (s, 2H), 2.40 (m, 1H), 2.08 (m, 2H), 1.68 (s, 2H), 1.53 (s, 2H), 1.41 (m, 2H), 1.19, (m, 1H), 1.10 (m, 1H), 0.92 (m, 1H), 0.79 (m, 1H), -0.95 (s, 1H, BH<sub>2</sub>).

$^{13}\text{C}\{^1\text{H}\}$  NMR (126 MHz, benzene- $d_6$ ):  $\delta$  159.6 (s), 152.4 (s), 135.6 (s), 133.7 (s), 128.7 (s), 127.3 (s), 125.5 (s), 122.7 (s), 119.0 (s), 117.0 (s), 61.7 (s), 54.4 (s), 26.7 (s), 24.5 (s), 22.3 (s), 22.0 (s), 20.3 (s). The carbon linked directly to boron was not observed.

$^{11}\text{B}\{^1\text{H}\}$  NMR (160 MHz, benzene- $d_6$ )  $\delta$  0.5 (s), -7.7 (s).

### Compound 3.11



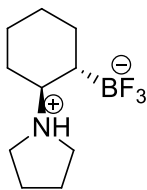
N,N-diisobutylcyclohex-1-enamine (1 g) was dissolved in THF and 450  $\mu\text{L}$  of  $\text{BH}_3\cdot\text{SMe}_2$  was added at 0  $^\circ\text{C}$ . After 1 h of reaction, the solvent was evaporated, 10 mL of hexanes were added and the reaction filtrated and placed at -35  $^\circ\text{C}$  overnight. The next day, white crystals had formed, the supernatant was removed and the crystals dried under vacuum. 420 mg, 39 % yield of **3.11** were recovered.

$^1\text{H}$  NMR (500 MHz,  $\text{CDCl}_3$ )  $\delta$  4.26 (s, broad, 2H), 2.66 – 2.52 (m, 1H), 2.31 – 2.22 (m, 2H), 2.18 – 2.06 (m, 2H), 2.01 – 1.91 (m, 1H), 1.91 – 1.70 (m, 5H), 1.62 – 1.40 (m, 2H), 1.29 – 1.11 (m, 3H), 1.09 (d,  $J = 6.5$  Hz, 6H), 0.95 (d,  $J = 6.7$  Hz, 6H).

$^{13}\text{C}\{^1\text{H}\}$  NMR (126 MHz,  $\text{CDCl}_3$ )  $\delta$  64.76 (s), 64.42 (s), 59.13 (s, broad), 32.29 (s), 32.02 (s, broad), 31.17 (s), 27.61 (s), 27.27 (s), 27.01 (s), 26.98 (s), 26.87 (s), 26.85 (s), 24.71 (s), 24.18 (s), 21.37 (s).

$^{11}\text{B}\{^1\text{H}\}$  NMR (160 MHz,  $\text{CDCl}_3$ )  $\delta$  23.1 (s).

### Compound 3.12



500 mg of pyrrolidino- $\text{C}_6\text{H}_{10}\text{-B}(\text{OMe})_2$  was dissolved in EtOH and 693 mg of  $\text{KHF}_2$  (4 equiv) were added along with 1.22 mL of 2 M HCl. The reaction was reacted at room temperature overnight. The next morning, the reaction was evaporated and the product recovered with acetone. Single crystal suitable for X-Ray diffraction were obtained by slow evaporation of an acetone solution.

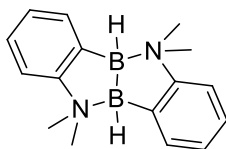
$^1\text{H}$  NMR (500 MHz,  $\text{CDCl}_3$ )  $\delta$  7.91 (s, broad, 1H), 3.92 – 3.78 (m, 1H), 3.56 (m, 1H), 3.31 – 3.21 (m, 1H), 3.17 – 3.02 (m, 2H), 2.30 – 2.06 (m, 2H), 2.04 – 1.85 (m, 5H), 1.72 – 1.62 (m, 1H), 1.38 – 1.02 (m, 4H), 0.64 – 0.50 (m, 1H).

$^{19}\text{F}\{^1\text{H}\}$  NMR (470 MHz,  $\text{CDCl}_3$ )  $\delta$  -145.0 (s).

$^{11}\text{B}\{^1\text{H}\}$  NMR (160 MHz,  $\text{CDCl}_3$ )  $\delta$  4.5 (s).

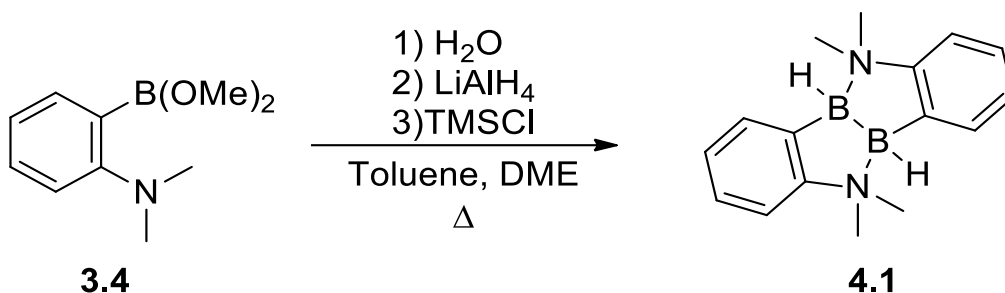
## Chapter 4

### Compound 4.1



250 mg of **3.3** was dissolved in toluene and heated at 90 °C overnight (*ca* 16 h). The reaction was then evaporated to give the title compound as a greenish powder in quantitative yield.

#### Large scale synthesis of compound 4.1



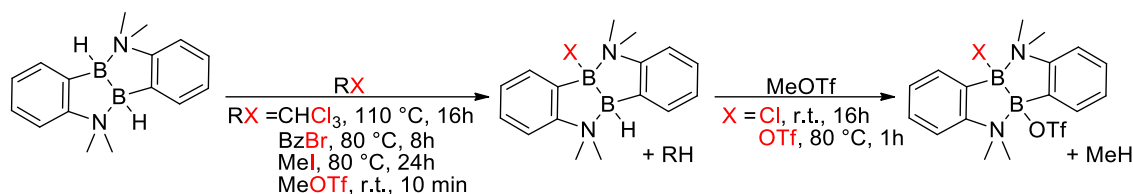
Starting from **3.4** that can be prepared on a multi-gram scale easily. 4.3 g of **3.4** was dissolved in toluene (undried) and few equivalents of water were added. The mixture was evaporated to dryness on the rotavap and the resulting white solid dissolved in undried toluene (around 100 mL) and transferred to a Schlenk tube. 1.06 g (1.25 equiv) of LiAlH<sub>4</sub> was then added at 0 °C followed by DME (4.6 mL, 2 equiv) which was added slowly to avoid intense bubbling and spilling over of the reaction. The ice bath was then removed and the reaction left to react at room temperature for approximately 1 h after which the reaction was filtered using a fritted glass filter (**Figure 41** of the thesis). 2.8 mL (1 equiv) of TMSCl were then added and the reaction heated at 90 °C overnight. The mixture was then filtered again and evaporated to dryness to give the title compound as a greenish solid. The product can be further washed with dry hexanes to make it more powdery and/or remove the colored impurity. Usually the synthesis give medium yield (30-70 %), around 1-2 g of product.

<sup>1</sup>H NMR (500 MHz, CDCl<sub>3</sub>) δ 7.69 (dd, *J* = 7.0, 1.8 Hz), 7.18 – 7.05 (m, 6H), 3.29 (s, 6H), 2.86 (s, 6H).

<sup>13</sup>C{<sup>1</sup>H} NMR (126 MHz, CDCl<sub>3</sub>) δ 157.4 (s), 136.8 (s), 126.5 (s), 126.4 (s), 116.6 (s), 59.6 (s), 49.0 (s).

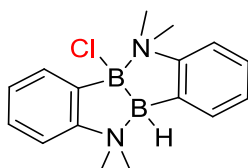
<sup>11</sup>B{<sup>1</sup>H} NMR (160 MHz, CDCl<sub>3</sub>) δ 1.79 (s).

### Reactivity of **4.1** as nucleophile in $S_N^2$ reactions



General procedure: Compound **4.1** was dissolved in toluene and the electrophile was added, the mixture was then heated for some time and then evaporated to dryness to give the various product. In most cases the electrophile is volatiles so the reaction were carried in sealed vessels. The volatility of the reactant also allows the use of excess electrophile which is removed during the evaporation. In other cases, such as benzyl bromide, excess electrophile can be removed by washing the product with dry hexane. The product can usually be crystallized at  $-30\text{ }^\circ C$  from a hexane/toluene solution, but toluene usually co-crystallize with them.

### Compound **4.2**



In that case, **4.1** was dissolved in dry  $CHCl_3$  and heated in a sealed vessel at  $110\text{ }^\circ C$  for 16 h.

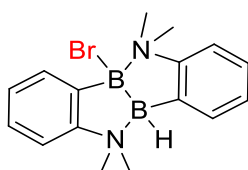
The characterization was made on a re-crystallized compound and contains significant amount of *bis* reacted product and of toluene.

$^1H$  NMR (500 MHz,  $C_6D_6$ )  $\delta$  7.68 (ddd,  $J = 7.4, 1.5, 0.5$  Hz, 1H), 7.58 – 7.53 (m, 1H), 7.12 – 6.96 (m, 2H), 6.90 – 6.79 (m, 2H), 6.50 (dd,  $J = 8.1, 0.4$  Hz, 1H), 6.47 – 6.43 (m, 1H), 2.75 (s,  $J = 1.9$  Hz, 3H), 2.66 (s, 3H), 2.63 (s, 3H), 2.59 (s, 3H). Signal overlap with residual toluene and *bis*-chlorinated impurity.

$^{13}C\{^1H\}$  NMR (126 MHz,  $C_6D_6$ )  $\delta$  157.2 (s), 156.8 (s), 136.2 (s), 134.3 (s), 127.1 (s), 126.7 (s), 126.6 (s), 116.4 (s), 116.3 (s), 58.2 (s), 57.2 (s), 47.8 (s), 44.0 (s). Some signal may not be observed because of overlapping with the  $C_6D_6$  signal.

$^{11}B\{^1H\}$  NMR (160 MHz,  $C_6D_6$ )  $\delta$  11.2 (s), -0.5 (s).

### Compound **4.3**



Following the general procedure, **4.1** was reacted with *ca.* 5 equiv. of benzyl bromide and heated at  $110\text{ }^\circ C$  for 8 h.

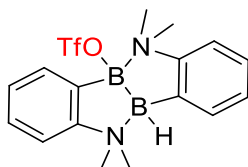
The characterization was made on a re-crystallized compound and contain significant amount of *bis* reacted product and of toluene.

$^1\text{H}$  NMR (500 MHz,  $\text{C}_6\text{D}_6$ )  $\delta$  7.69 (ddd,  $J = 7.5, 1.5, 0.5$  Hz, 1H), 7.55 – 7.51 (m, 1H), 7.06 – 6.93 (m, 2H), 6.89 – 6.82 (m, 2H), 6.46 (d,  $J = 8.1$  Hz, 1H), 6.40 (d,  $J = 8.1$  Hz, 1H), 2.78 (s, 3H), 2.72 (s, 3H), 2.67 (s, 3H), 2.55 (s, 3H). Signal overlap with residual toluene and *bis*-brominated impurity.

$^{13}\text{C}\{^1\text{H}\}$  NMR (126 MHz,  $\text{C}_6\text{D}_6$ )  $\delta$  156.9 (s), 156.2 (s), 136.1 (s), 134.8 (s), 134.5 (s), 127.1 (s), 126.7 (s), 126.6 (s), 116.5 (s), 116.3 (s), 58.8 (s), 57.5 (s), 48.1 (s), 44.6 (s).

$^{11}\text{B}\{^1\text{H}\}$  NMR (160 MHz,  $\text{C}_6\text{D}_6$ )  $\delta$  10.0 (s), -0.2 (s).

#### Compound 4.4



Following the general procedure, **4.1** was reacted with 1 equiv. of methyl triflate at room temperature. The product could be observed by NMR, but tentative isolation always lead to product containing significant amount of *bis* reacted product.

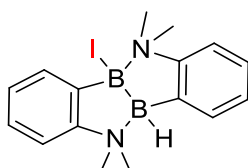
$^1\text{H}$  NMR (500 MHz,  $\text{C}_6\text{D}_6$ )  $\delta$  7.56 (dd,  $J = 7.5, 1.4$  Hz, 1H), 7.50 (dd,  $J = 7.4, 1.3$  Hz, 1H), 7.06 – 6.99 (m, 2H), 6.95 – 6.81 (m, 2H), 6.43 (d,  $J = 8.1$  Hz, 1H), 6.35 (d,  $J = 8.1$  Hz, 1H), 2.76 (s, 3H), 2.50 (s, 3H), 2.49 (s, 3H), 2.43 (s, 3H).

$^{13}\text{C}\{^1\text{H}\}$  NMR (126 MHz,  $\text{C}_6\text{D}_6$ )  $\delta$  158.5 (s), 155.6 (s), 137.1 (s), 133.6 (s), 129.0 (s), 127.1 (s), 127.1 (s), 126.9 (s), 117.1 (s), 116.2 (s), 58.7 (s), 56.0 (s), 48.3 (s), 45.1 (s).

$^{19}\text{F}$  NMR (470 MHz,  $\text{C}_6\text{D}_6$ )  $\delta$  -77.7 (s).

$^{11}\text{B}\{^1\text{H}\}$  NMR (160 MHz,  $\text{C}_6\text{D}_6$ )  $\delta$  16.1 (s), -2.5 (s).

#### Compound 4.5

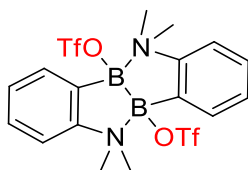


Following the general procedure, **4.1** was reacted with *ca.* 5 equiv. of methyl iodide and heated at 110 °C for 24 h. The NMR characterization was made on the reaction directly after evaporation.

$^1\text{H}$  NMR (500 MHz,  $\text{C}_6\text{D}_6$ )  $\delta$  7.74 – 7.70 (m, 1H), 7.50 (dd,  $J = 7.3, 1.1$  Hz, 1H), 7.04 – 6.94 (m, 2H), 6.87 – 6.78 (m, 2H), 6.59 (d,  $J = 7.9$  Hz, 1H), 6.45 (d,  $J = 8.1$  Hz, 1H), 6.35 (d,  $J = 8.2$  Hz, 1H), 2.82 (s, 3H), 2.78 (s, 3H), 2.72 (s, 3H), 2.51 (s, 3H).

$^{11}\text{B}\{^1\text{H}\}$  NMR (160 MHz,  $\text{C}_6\text{D}_6$ )  $\delta$  5.8 (s), 0.5 (s).

#### Compound 4.9





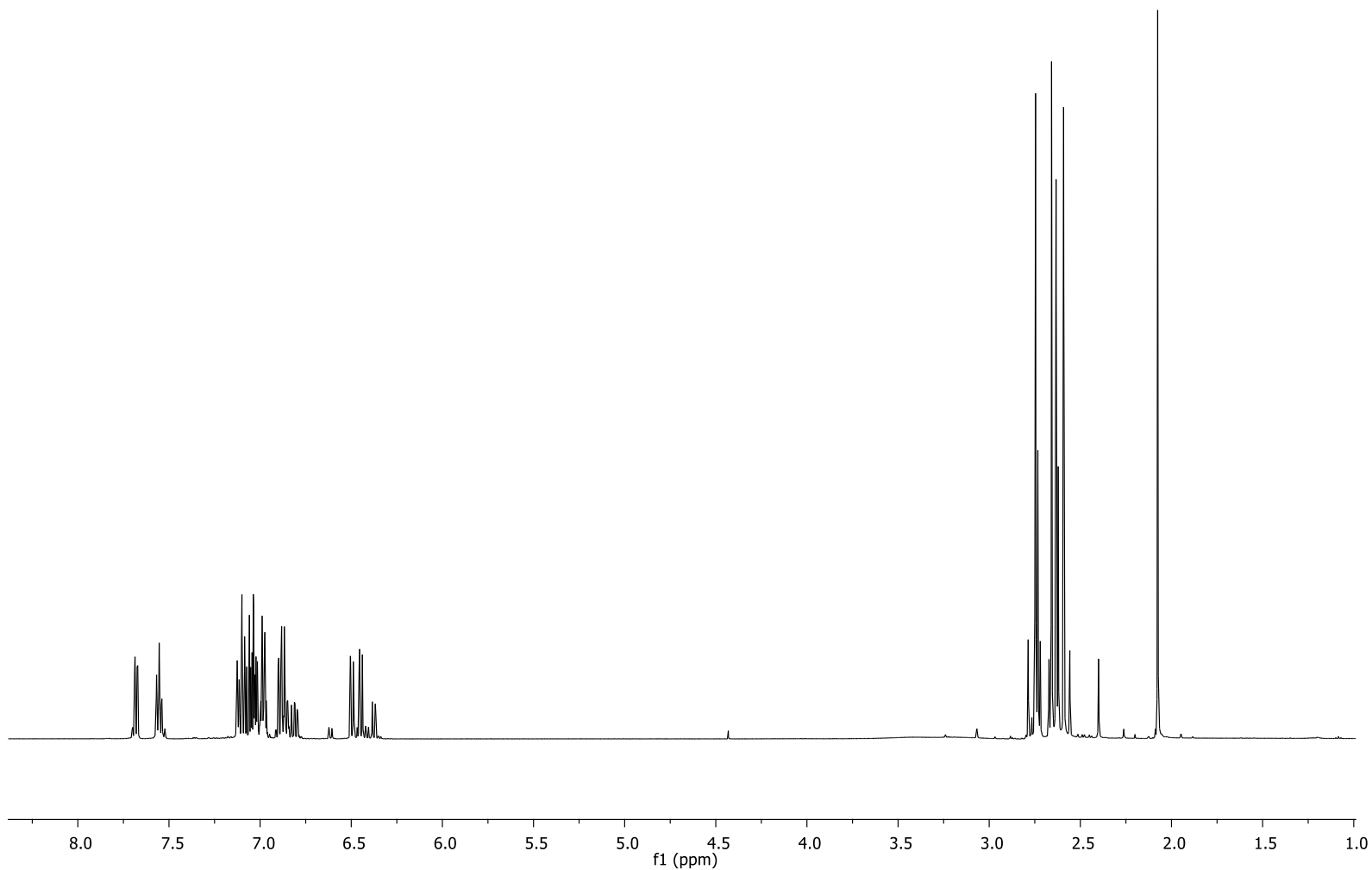
Following the general procedure, **4.1** was reacted with *ca.* 5 equiv. of methyl triflate and heated at 80 °C for 1 h. The characterization was made on a re-crystallized compound and contain significant amount of toluene.

$^1\text{H}$  NMR (500 MHz,  $\text{C}_6\text{D}_6$ )  $\delta$  7.66 (dd,  $J = 7.5, 1.4$  Hz, 1H), 6.92 (td,  $J = 7.4, 1.0$  Hz, 1H), 6.82 – 6.72 (m, 1H), 6.24 (d,  $J = 8.2$  Hz, 1H), 2.67 (s, 1H), 2.51 (s, 1H).

$^{13}\text{C}\{^1\text{H}\}$  NMR (126 MHz,  $\text{C}_6\text{D}_6$ )  $\delta$  156.2 (s), 135.0 (s), 130.0 (s), 116.6 (s), 55.2 (s), 45.6 (s).

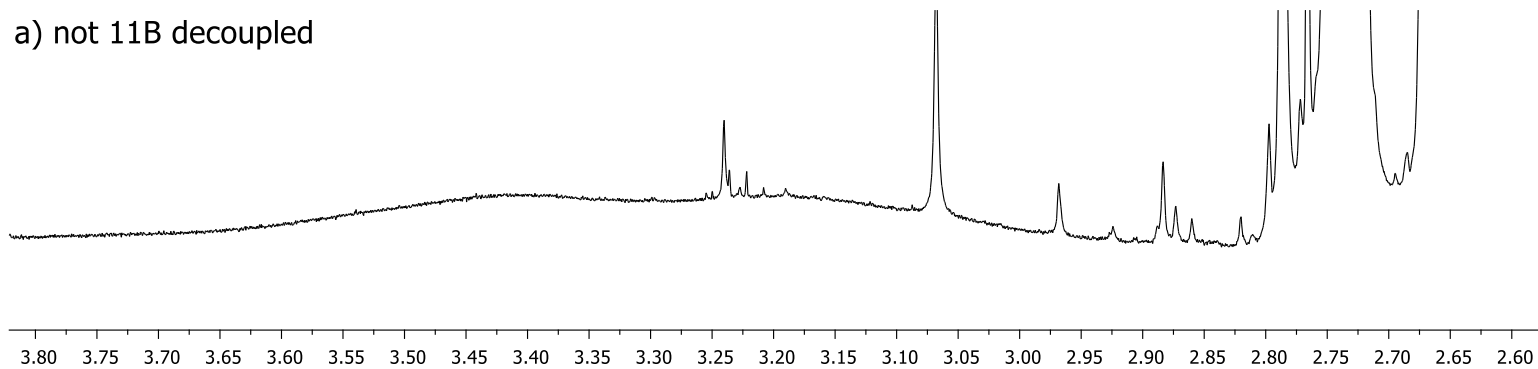
$^{19}\text{F}$  NMR (470 MHz,  $\text{C}_6\text{D}_6$ )  $\delta$  -77.7 (s).

$^{11}\text{B}\{^1\text{H}\}$  NMR (160 MHz,  $\text{C}_6\text{D}_6$ )  $\delta$  8.9 (s).

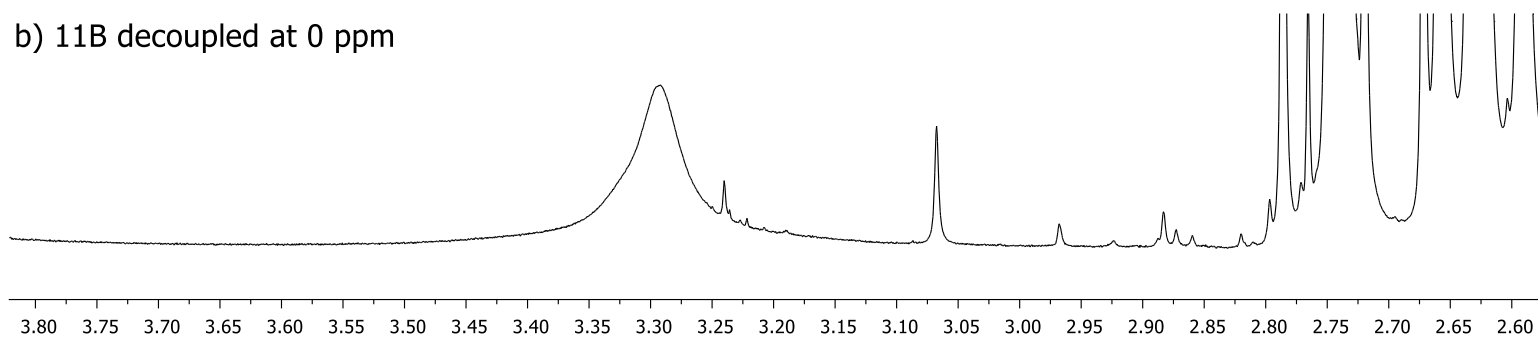


**Figure A1:**  $^1\text{H}$  NMR (500 MHz,  $\text{C}_6\text{D}_6$ ) of compound **4.2**.

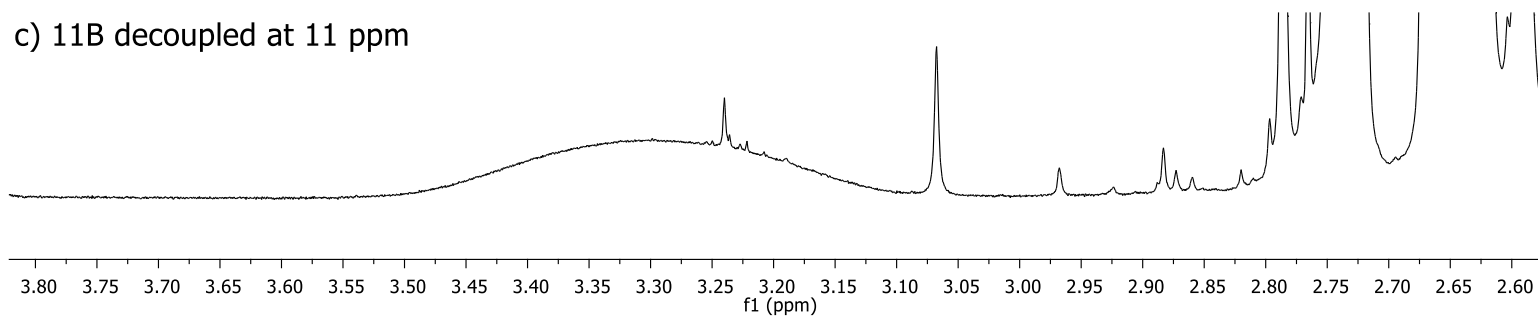
a) not  $^{11}\text{B}$  decoupled



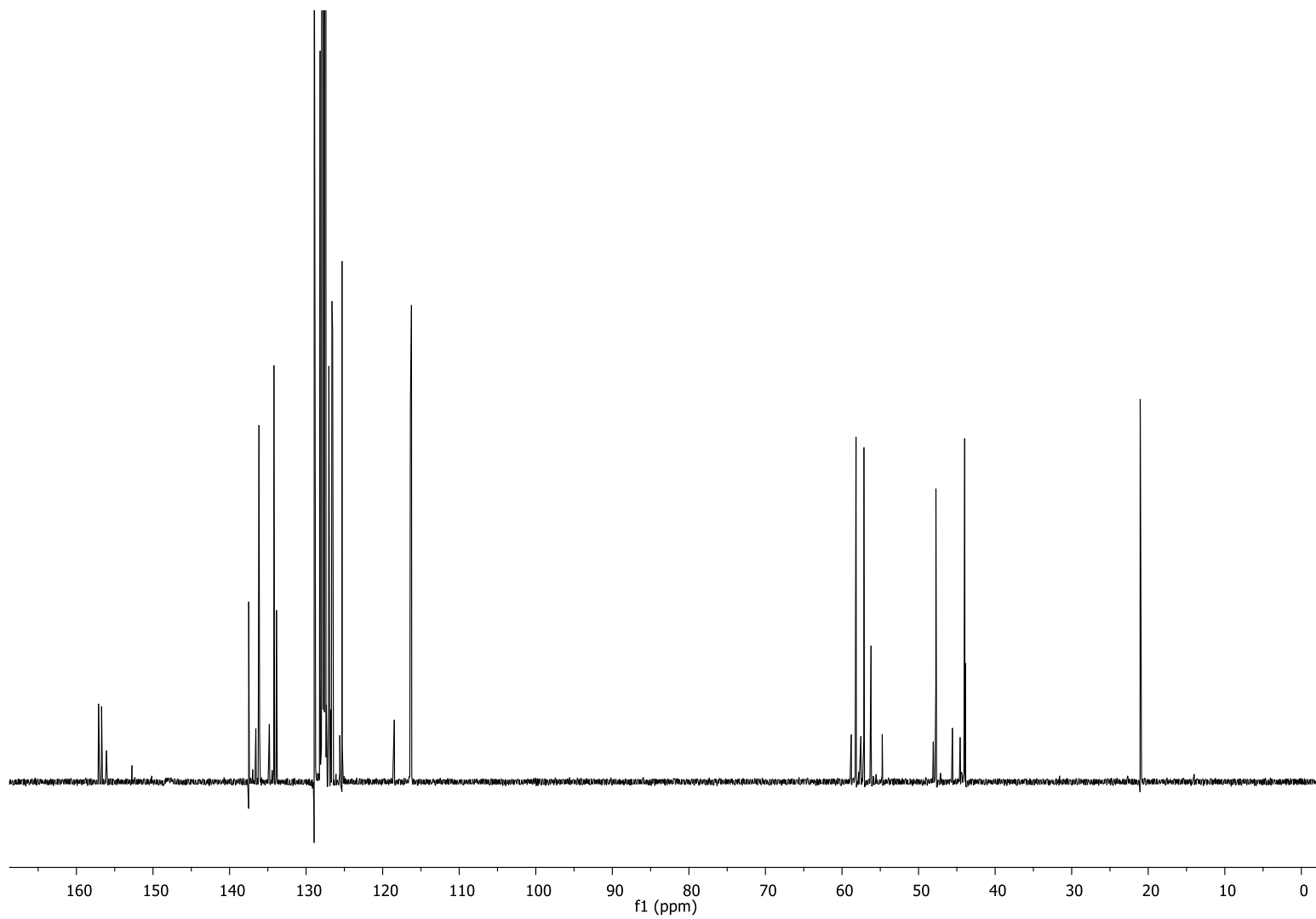
b)  $^{11}\text{B}$  decoupled at 0 ppm



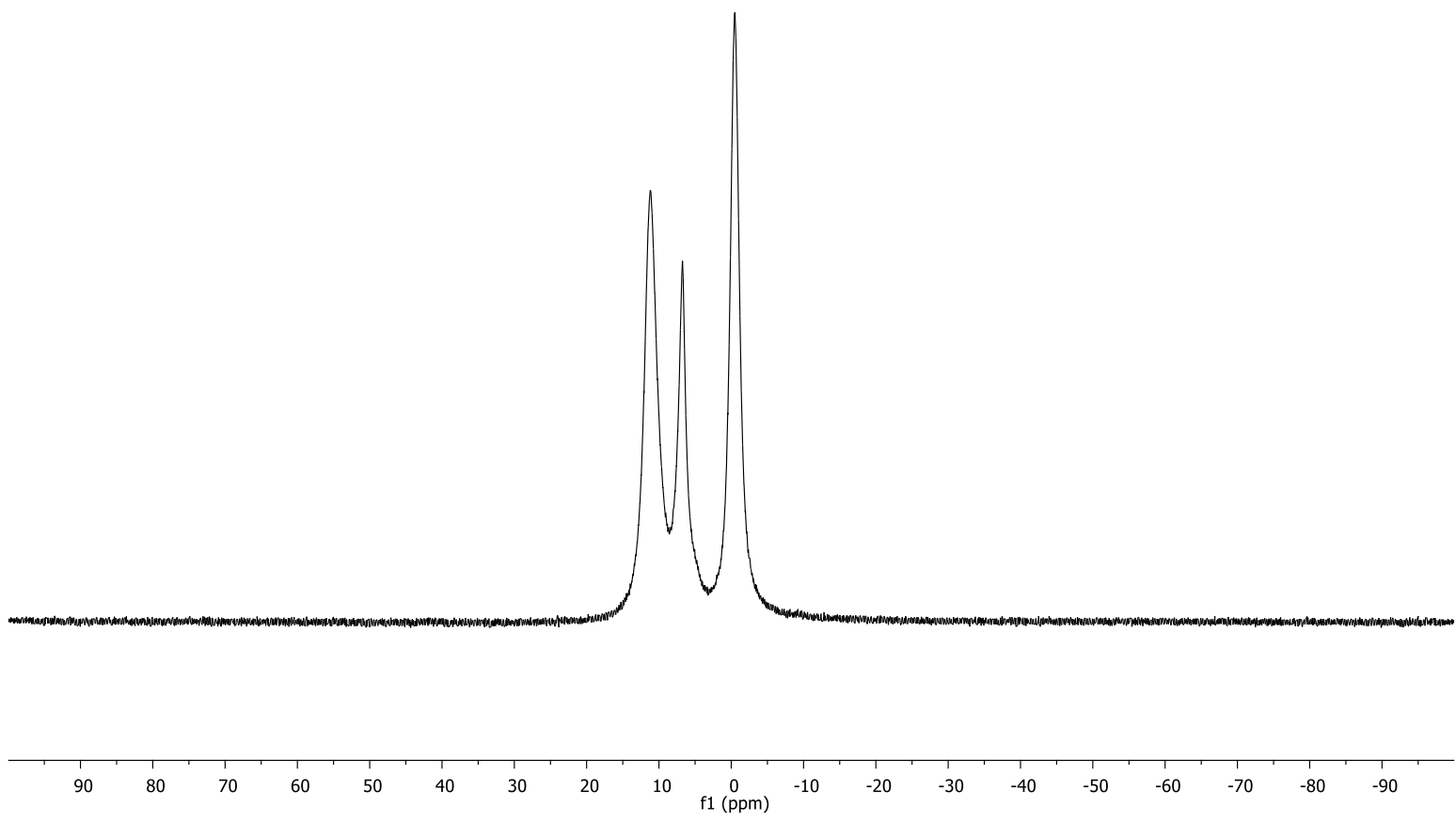
c)  $^{11}\text{B}$  decoupled at 11 ppm



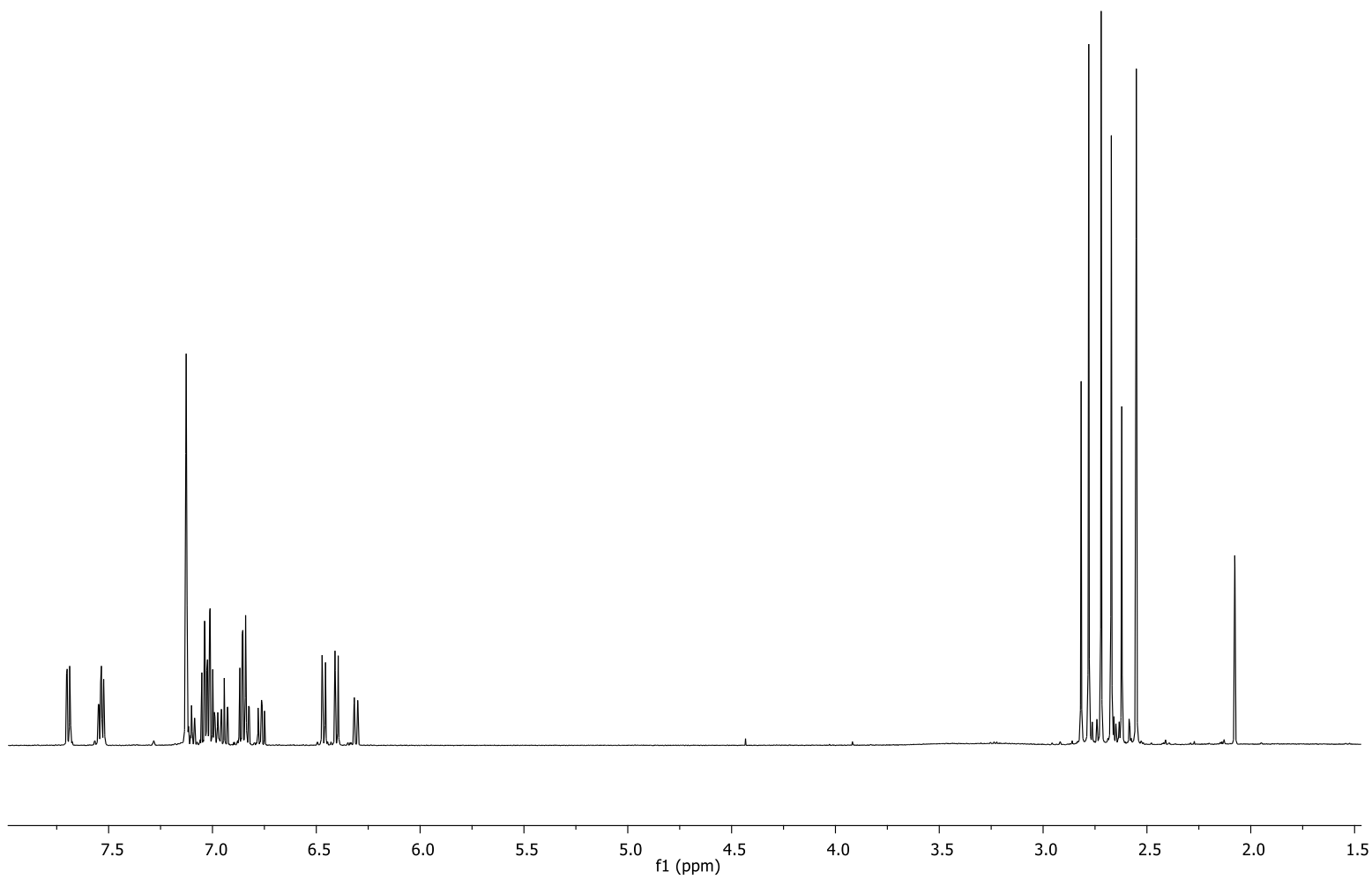
**Figure A2:** Zoom on the borohydride signal of the  $^1\text{H}$  NMR (500 MHz,  $\text{C}_6\text{D}_6$ ) of compound **4.2** with different  $^{11}\text{B}$  decoupling options.



**Figure A3:**  $^{13}\text{C}\{^1\text{H}\}$  NMR (126 MHz,  $\text{C}_6\text{D}_6$ ) of compound **4.2**.

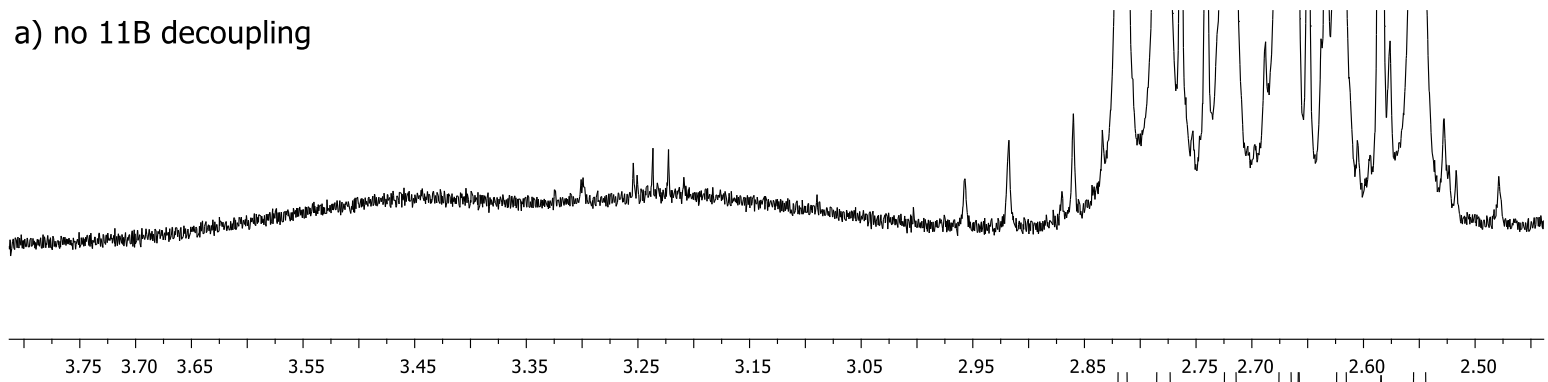


**Figure A4:**  $^{11}\text{B}\{^1\text{H}\}$  NMR (160 MHz,  $\text{C}_6\text{D}_6$ ) of compound **4.2**.

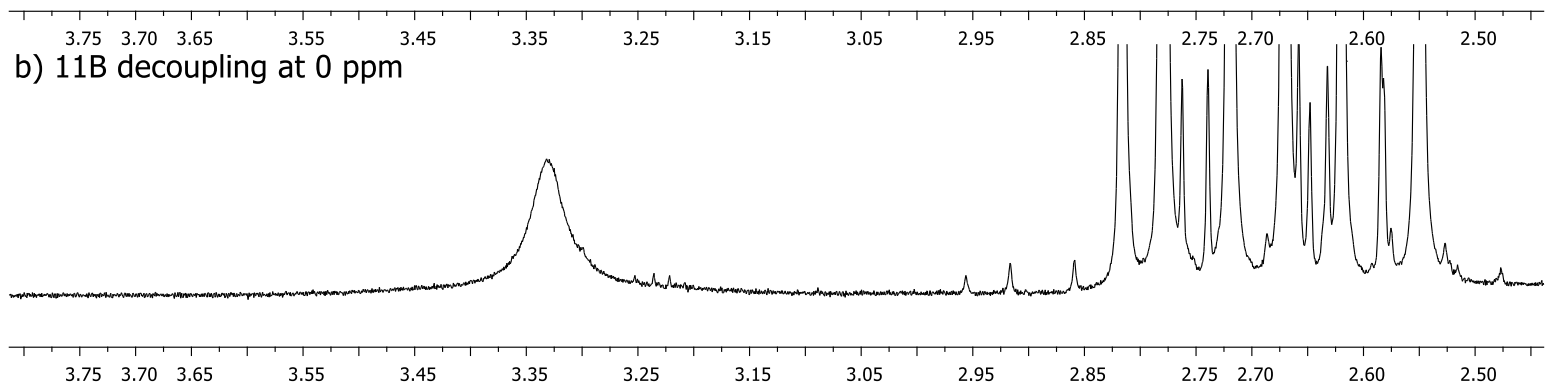


**Figure A5:** <sup>1</sup>H NMR (500 MHz, C<sub>6</sub>D<sub>6</sub>) of compound **4.3**.

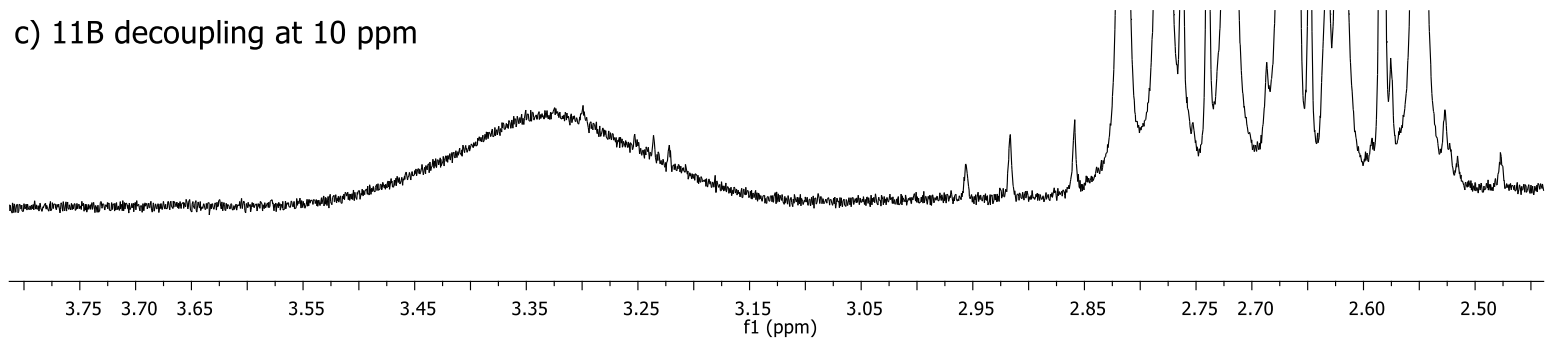
a) no  $^{11}\text{B}$  decoupling



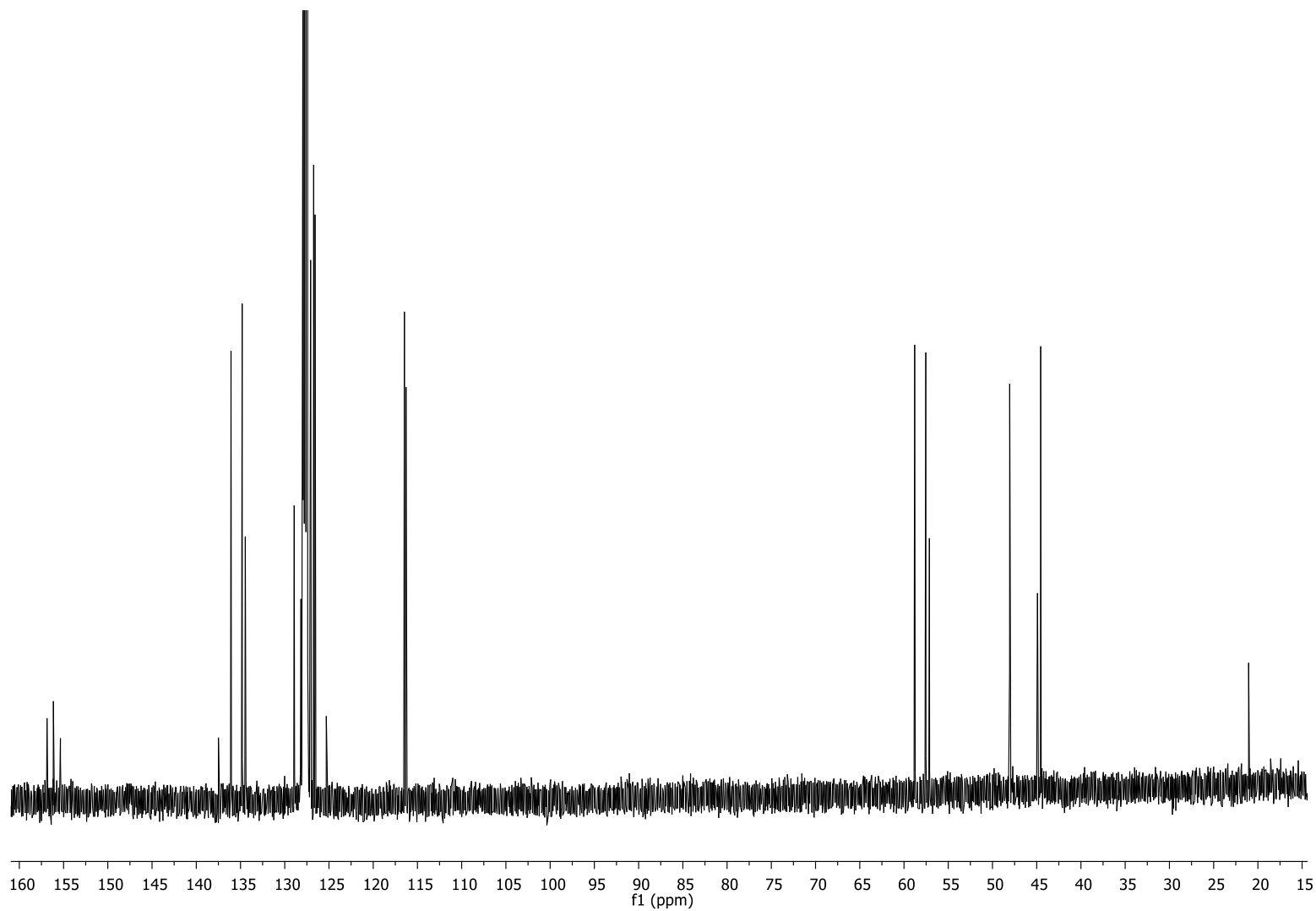
b)  $^{11}\text{B}$  decoupling at 0 ppm



c)  $^{11}\text{B}$  decoupling at 10 ppm

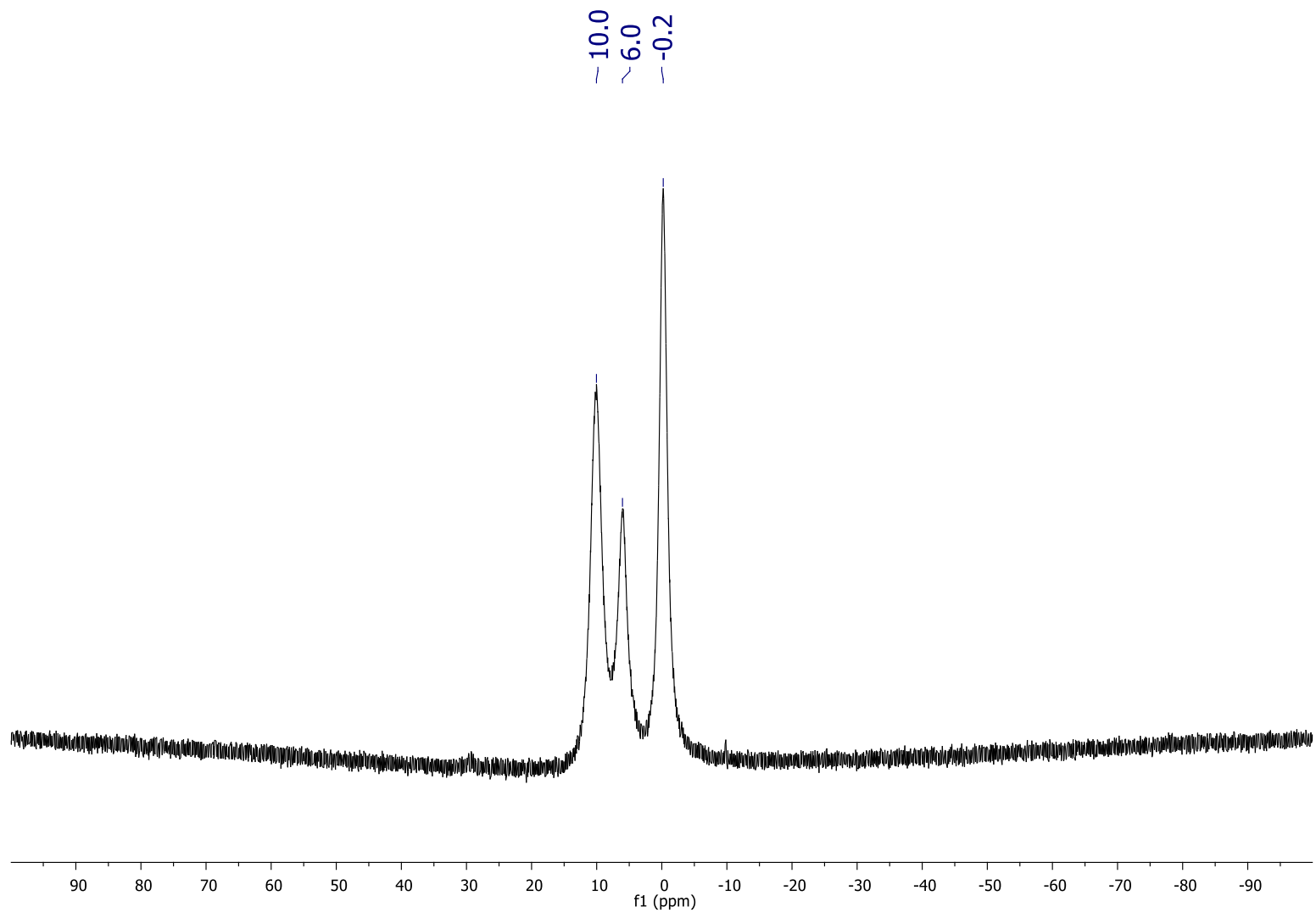


**Figure A6:** Zoom on the borohydride signal of the  $^1\text{H}$  NMR (500 MHz,  $\text{C}_6\text{D}_6$ ) of compound **4.3** with different  $^{11}\text{B}$  decoupling options.

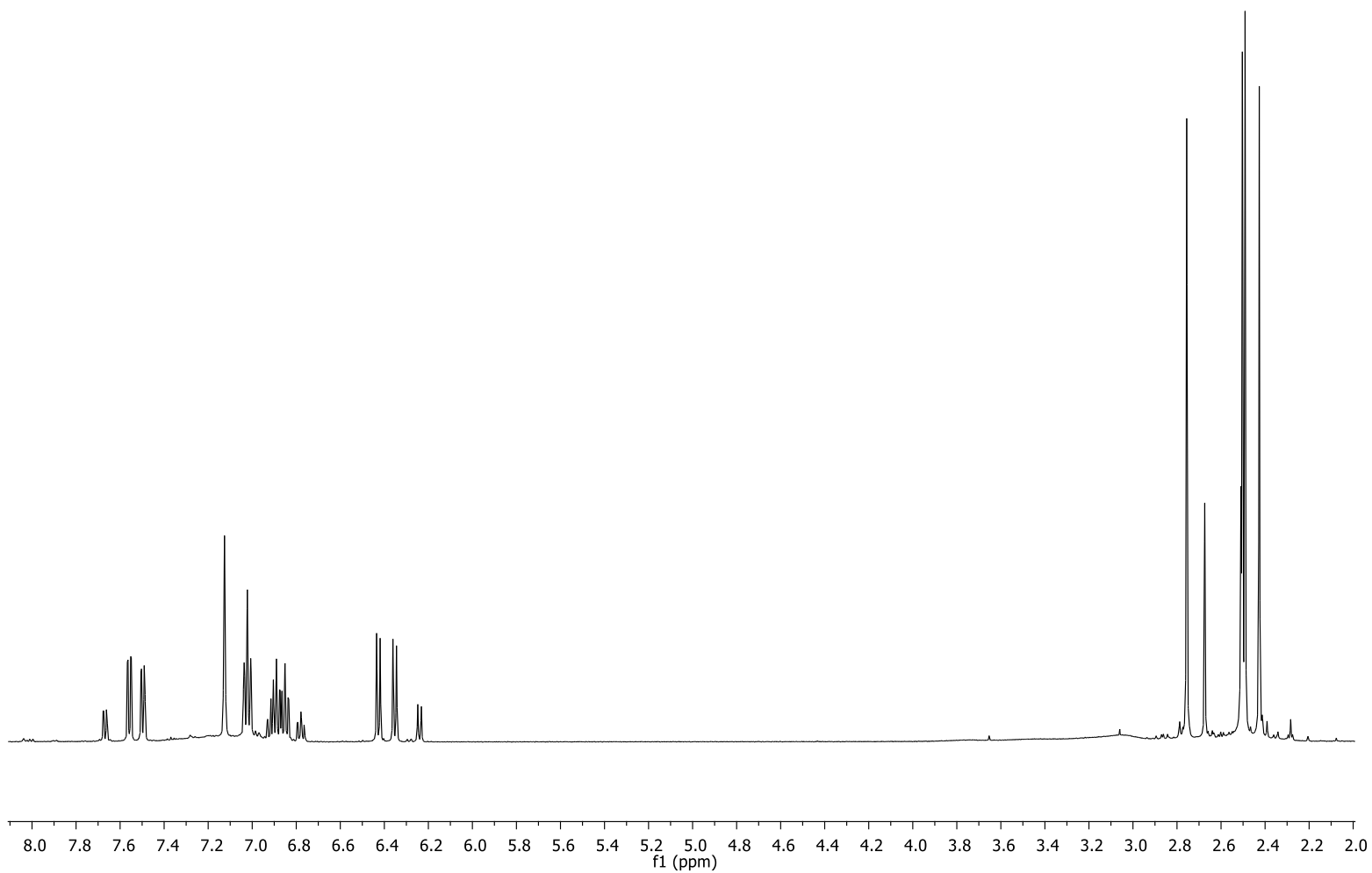


**Figure A7:**  $^{13}\text{C}\{^1\text{H}\}$  NMR (126 MHz,  $\text{C}_6\text{D}_6$ ) of compound **4.3**.

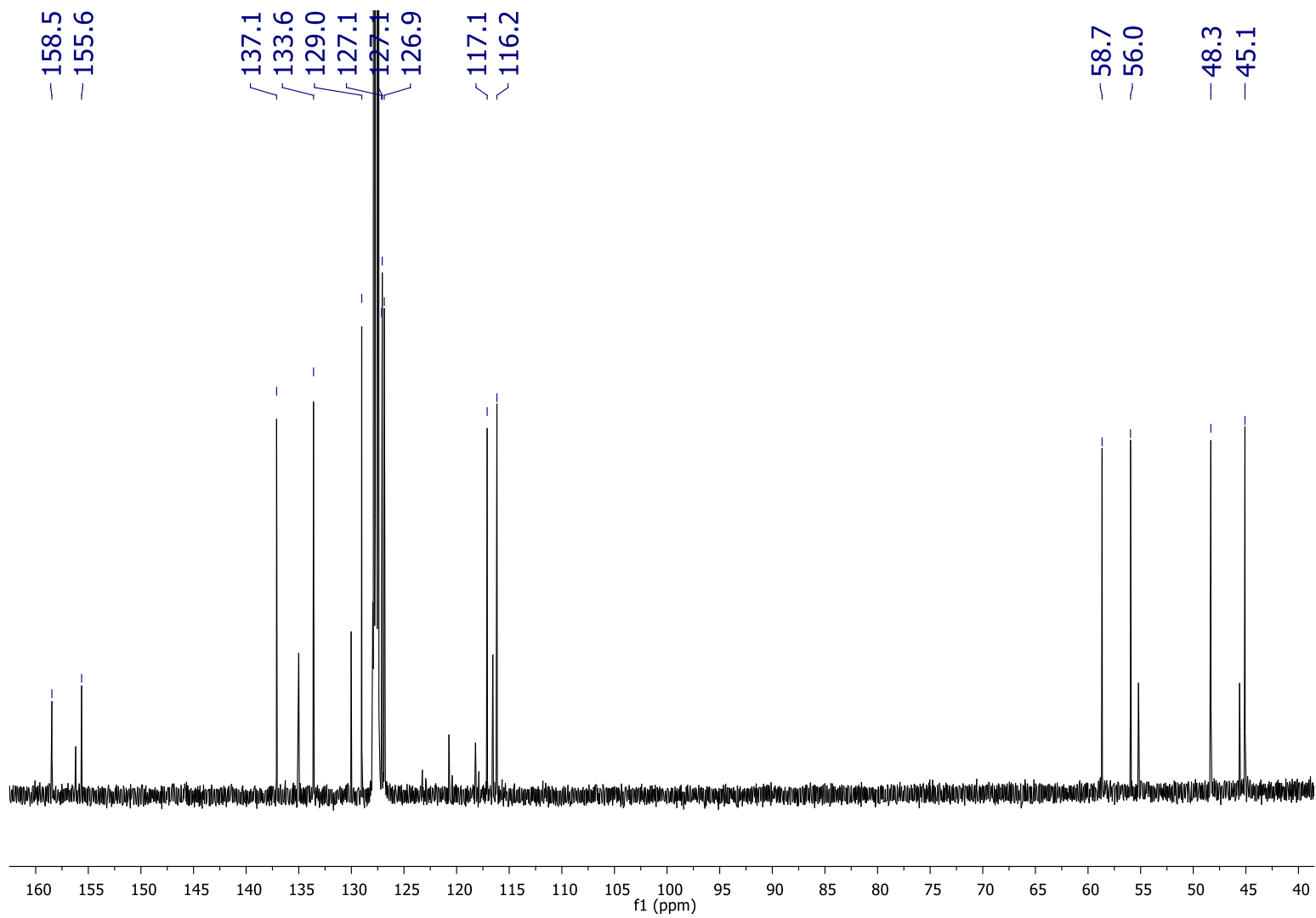




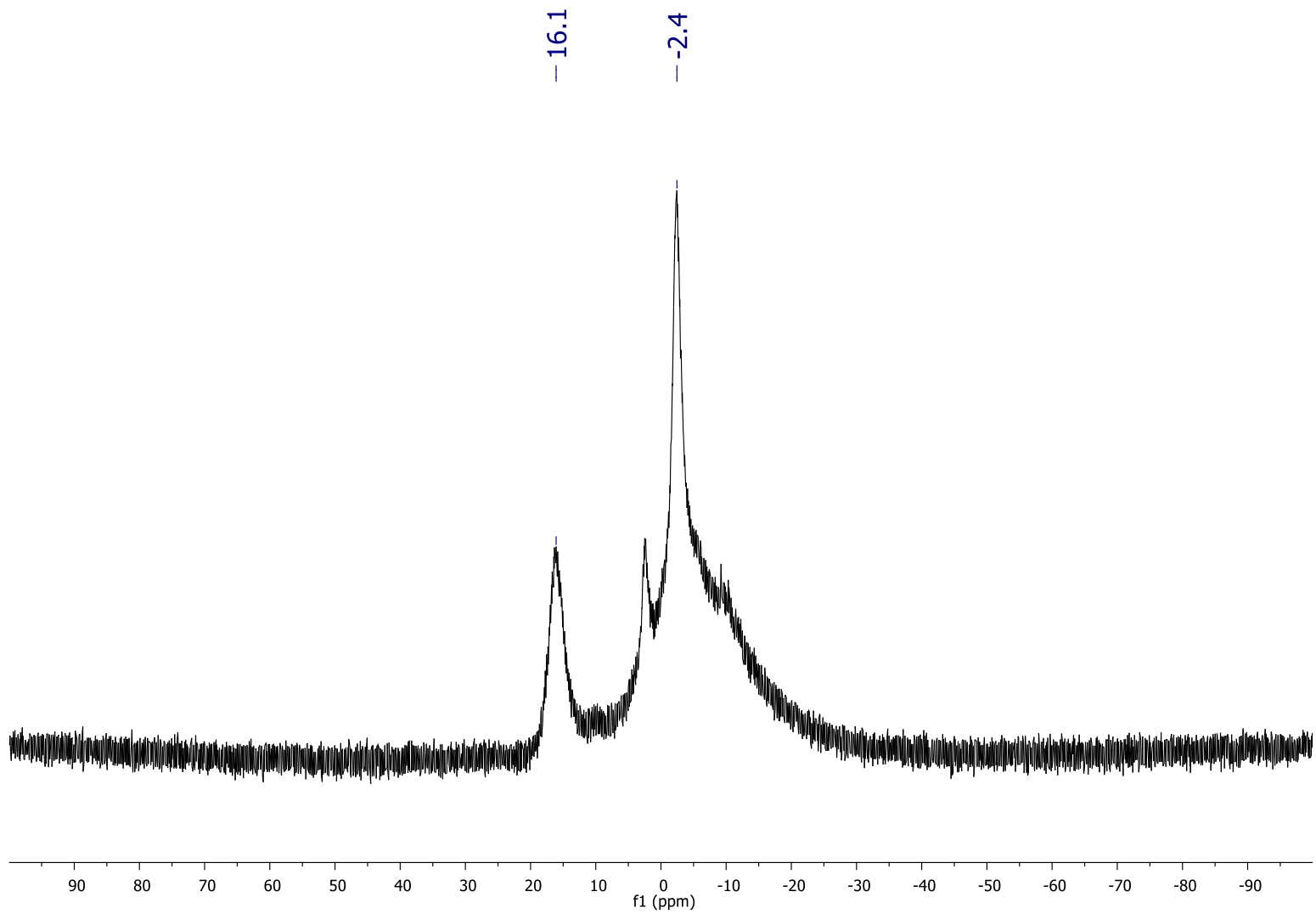
**Figure A8:**  $^{11}\text{B}\{^1\text{H}\}$  NMR (160 MHz,  $\text{C}_6\text{D}_6$ ) of compound **4.3**.



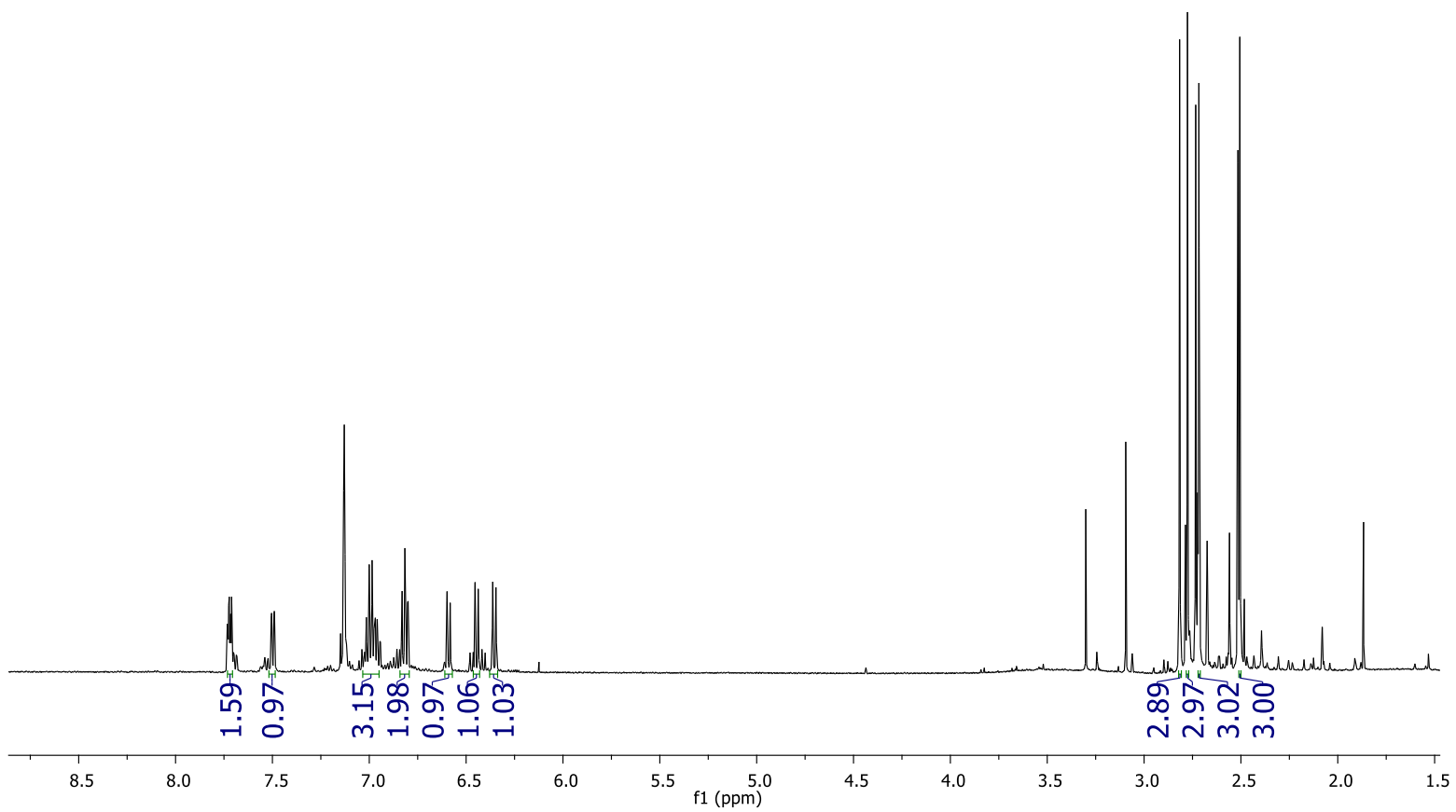
**Figure A9:** <sup>1</sup>H NMR (500 MHz, C<sub>6</sub>D<sub>6</sub>) of compound **4.4**.



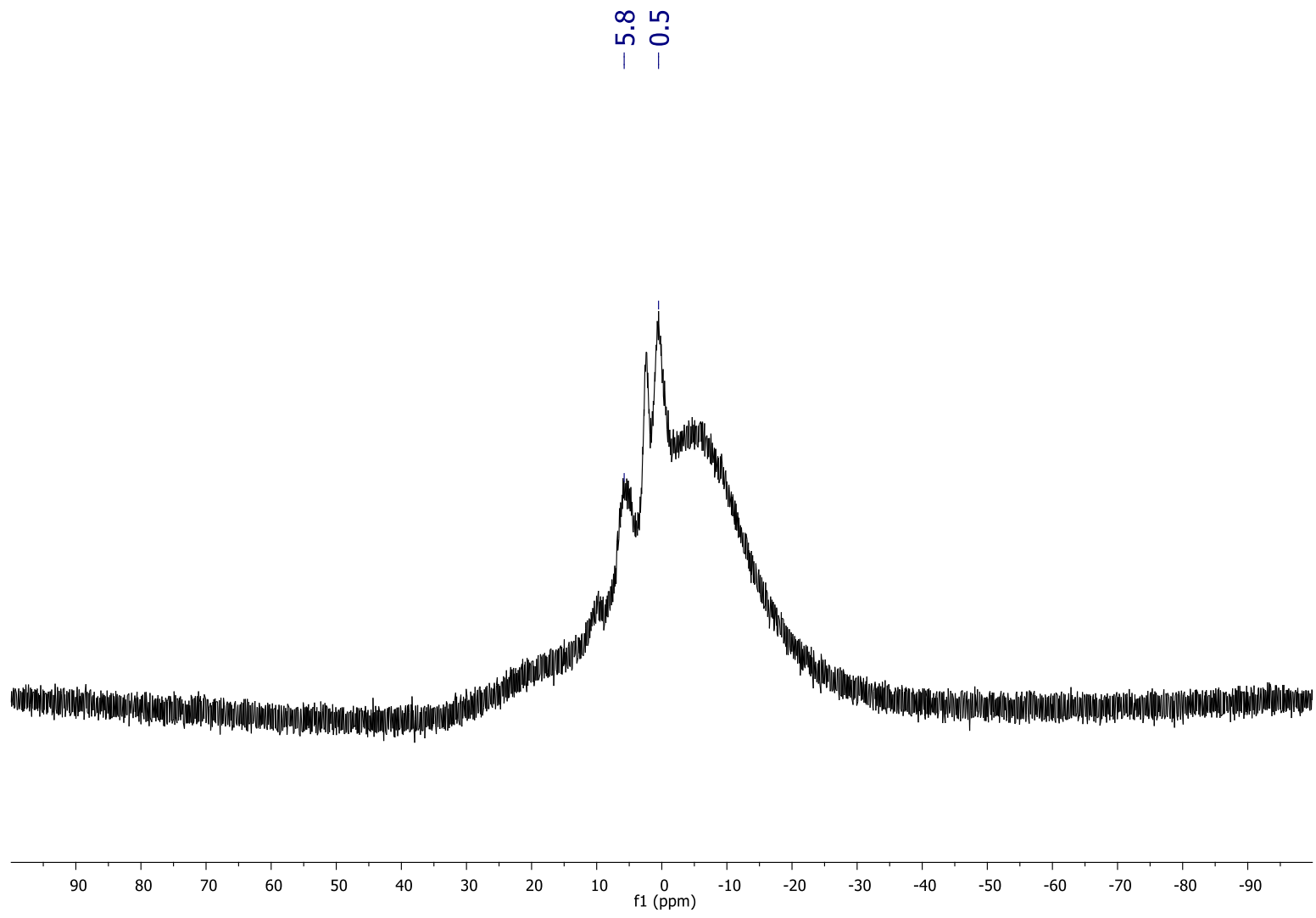
**Figure A10:**  $^{13}\text{C}\{^1\text{H}\}$  NMR (126 MHz,  $\text{C}_6\text{D}_6$ ) of compound **4.4**.



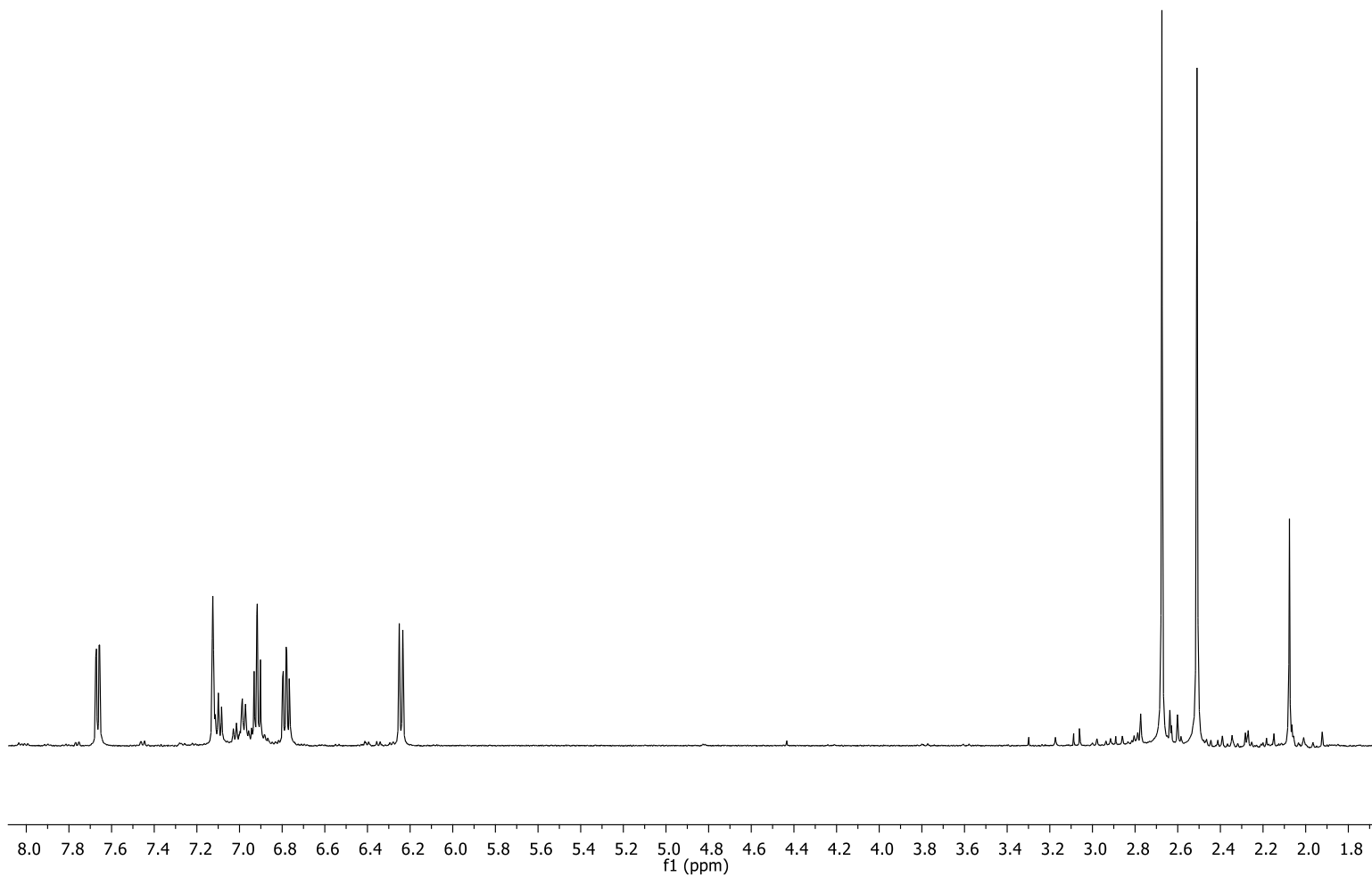
**Figure A11:**  $^{11}\text{B}\{^1\text{H}\}$  NMR (160 MHz,  $\text{C}_6\text{D}_6$ ) of compound **4.4**.



**Figure A12:**  $^1\text{H}$  NMR (500 MHz,  $\text{C}_6\text{D}_6$ ) of compound **4.5**.



**Figure A13:**  $^{11}\text{B}\{^1\text{H}\}$  NMR (160 MHz,  $\text{C}_6\text{D}_6$ ) of compound **4.5**.



**Figure A14:** <sup>1</sup>H NMR (500 MHz, C<sub>6</sub>D<sub>6</sub>) of compound **4.9**.

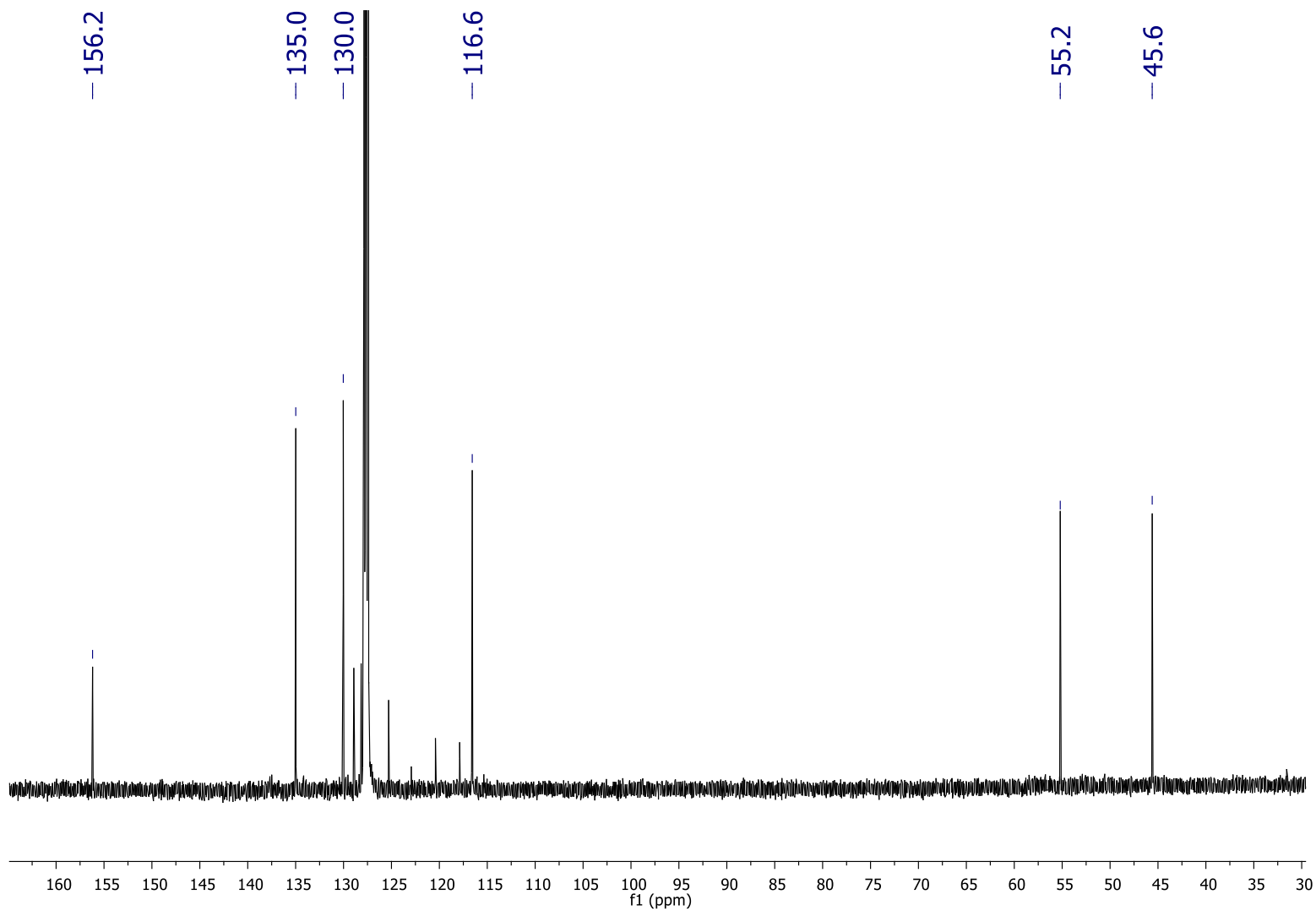
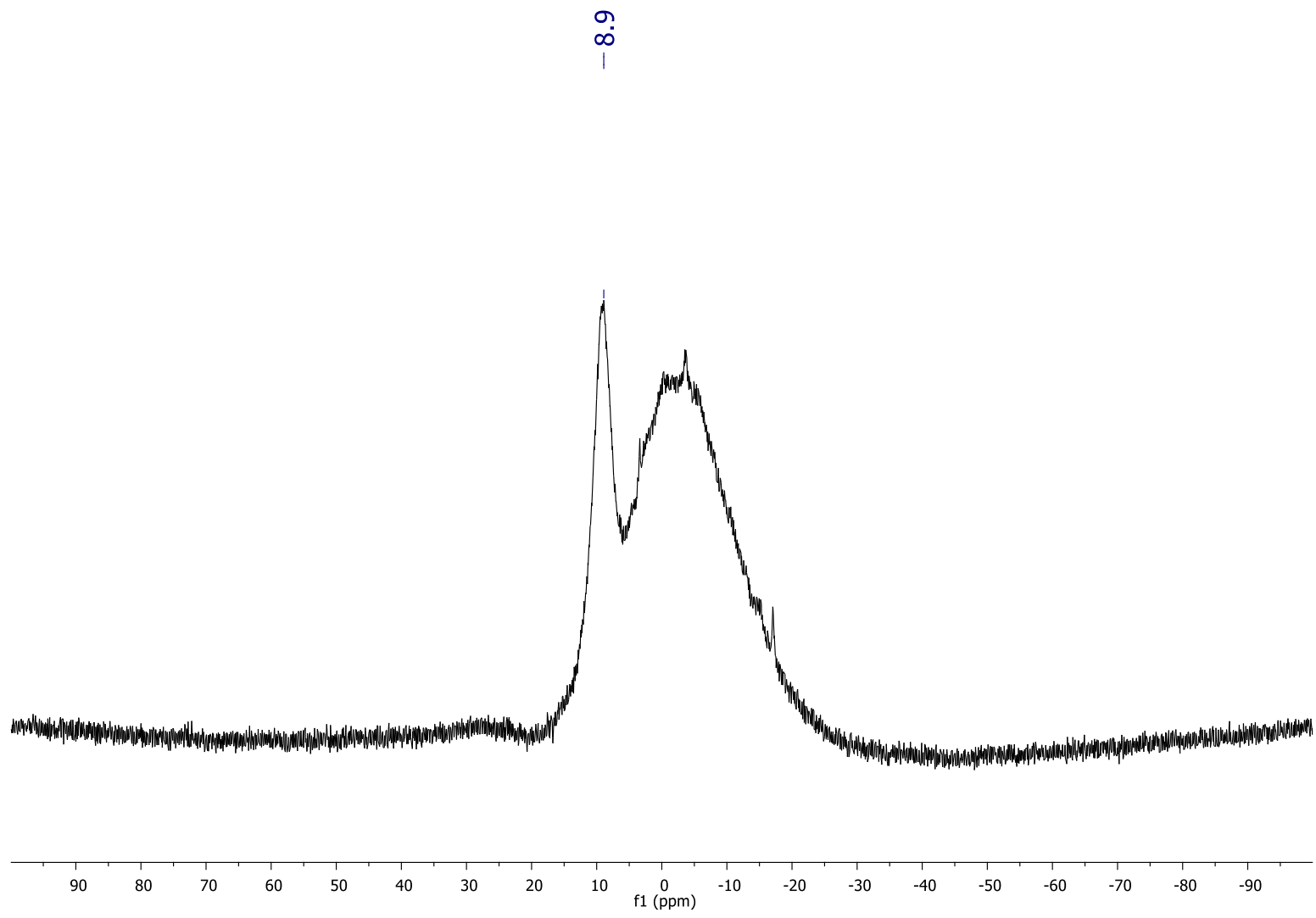


Figure A15:  $^{13}\text{C}\{^1\text{H}\}$  NMR (126 MHz,  $\text{C}_6\text{D}_6$ ) of compound **4.9**.

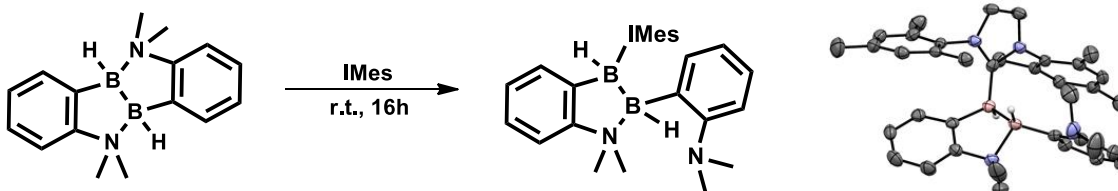




**Figure A16:**  $^{11}\text{B}\{^1\text{H}\}$  NMR (160 MHz,  $\text{C}_6\text{D}_6$ ) of compound **4.9**.

Substitution of the B-N bond of **4.1** by another L or X type “ligand”

Compound **4.1**•IMes

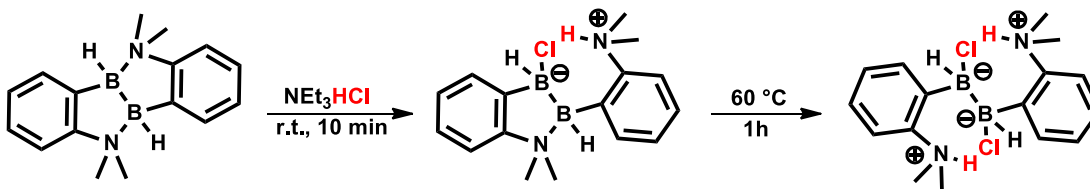


Compound **4.1** (100 mg) was dissolved in toluene, IMes (115 mg, 1 equiv.) was added, the reaction stirred overnight at room temperature and then evaporated to dryness.

$^1\text{H}$  NMR (500 MHz,  $\text{C}_6\text{D}_6$ )  $\delta$  7.92 (d,  $J = 7.4$  Hz, 1H), 7.72 (d,  $J = 7.2$  Hz, 1H), 7.47 (d,  $J = 6.9$  Hz, 1H), 7.34 – 7.27 (m, 1H), 7.18 – 7.11 (m, 2H), 6.87 (t,  $J = 6.9$  Hz, 1H), 6.78 (s, 1H), 6.69 (s, 1H), 6.61 (s, 2H), 6.53 (d,  $J = 8.0$  Hz, 1H), 5.96 (s, 2H), 2.86 (s, 6H), 2.31 (s, 6H), 2.13 (s, 6H), 2.08 (s, 6H), 1.88 (s, 6H).

$^{11}\text{B}\{^1\text{H}\}$  NMR (160 MHz,  $\text{C}_6\text{D}_6$ )  $\delta$  2.4 (s), -22.8 (s).

Compounds **4.1**•HCl and **4.1**•2HCl



Compound **4.1** (10 mg) was dissolved in  $\text{CDCl}_3$ , and  $\text{NEt}_3\cdot\text{HCl}$  (15.6 mg, 3 equiv.) was then dispersed in the solution. The mixture was immediately characterized by NMR and a new species with signals corresponding to **4.1**•HCl were observed. Then the mixture was heated at 60 °C for 1h and characterized again by NMR and this time signals corresponding to **4.1**•2HCl were observed.

Compound **4.1**•HCl

$^1\text{H}$  NMR (500 MHz,  $\text{CDCl}_3$ )  $\delta$  7.71 (d,  $J = 8.3$  Hz, 1H), 7.65 (dd,  $J = 7.0, 1.7$  Hz, 1H), 7.61 (dd,  $J = 7.5, 1.4$  Hz, 1H), 7.47 – 7.42 (m, 1H), 7.35 (td,  $J = 7.4, 0.8$  Hz, 1H), 7.14 – 7.02 (m, 3H), 3.66 (s, 3H), 3.26 (s, 3H), 3.22 (s, 3H), 2.83 (s, 3H).

$^{11}\text{B}\{^1\text{H}\}$  NMR (160 MHz,  $\text{CDCl}_3$ )  $\delta$  3.3 (s), 1.8 (s).

Compound **4.1**•2HCl

$^1\text{H}$  NMR (500 MHz,  $\text{CDCl}_3$ )  $\delta$  7.62 (d,  $J = 8.3$  Hz, 1H), 7.54 (dd,  $J = 7.5, 1.4$  Hz, 1H), 7.40 – 7.36 (m, 1H), 7.31 – 7.27 (m, 1H), 3.58 (s, 3H), 3.14 (s, 3H).

$^{11}\text{B}\{^1\text{H}\}$  NMR (160 MHz,  $\text{CDCl}_3$ )  $\delta$  3.1 (s).

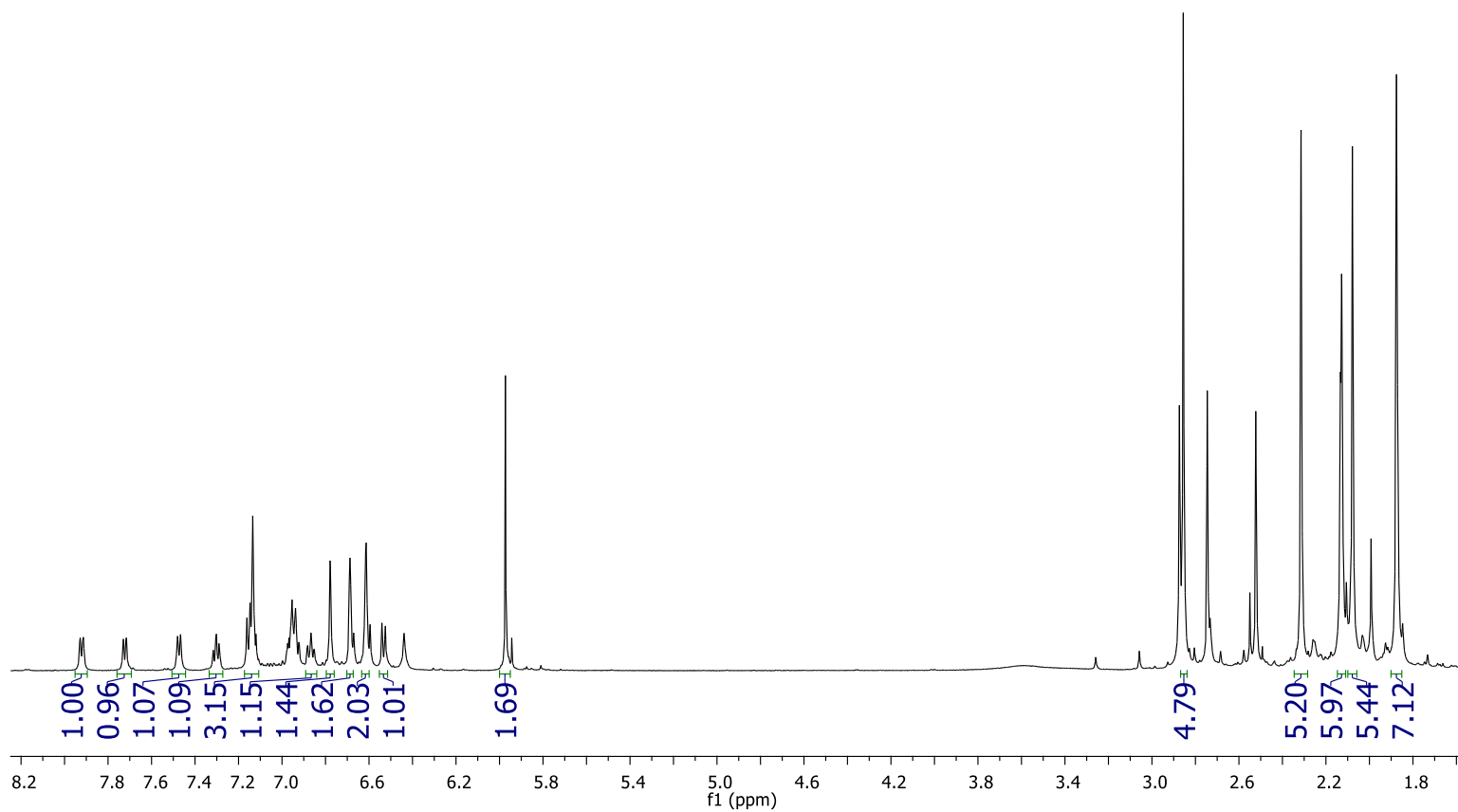
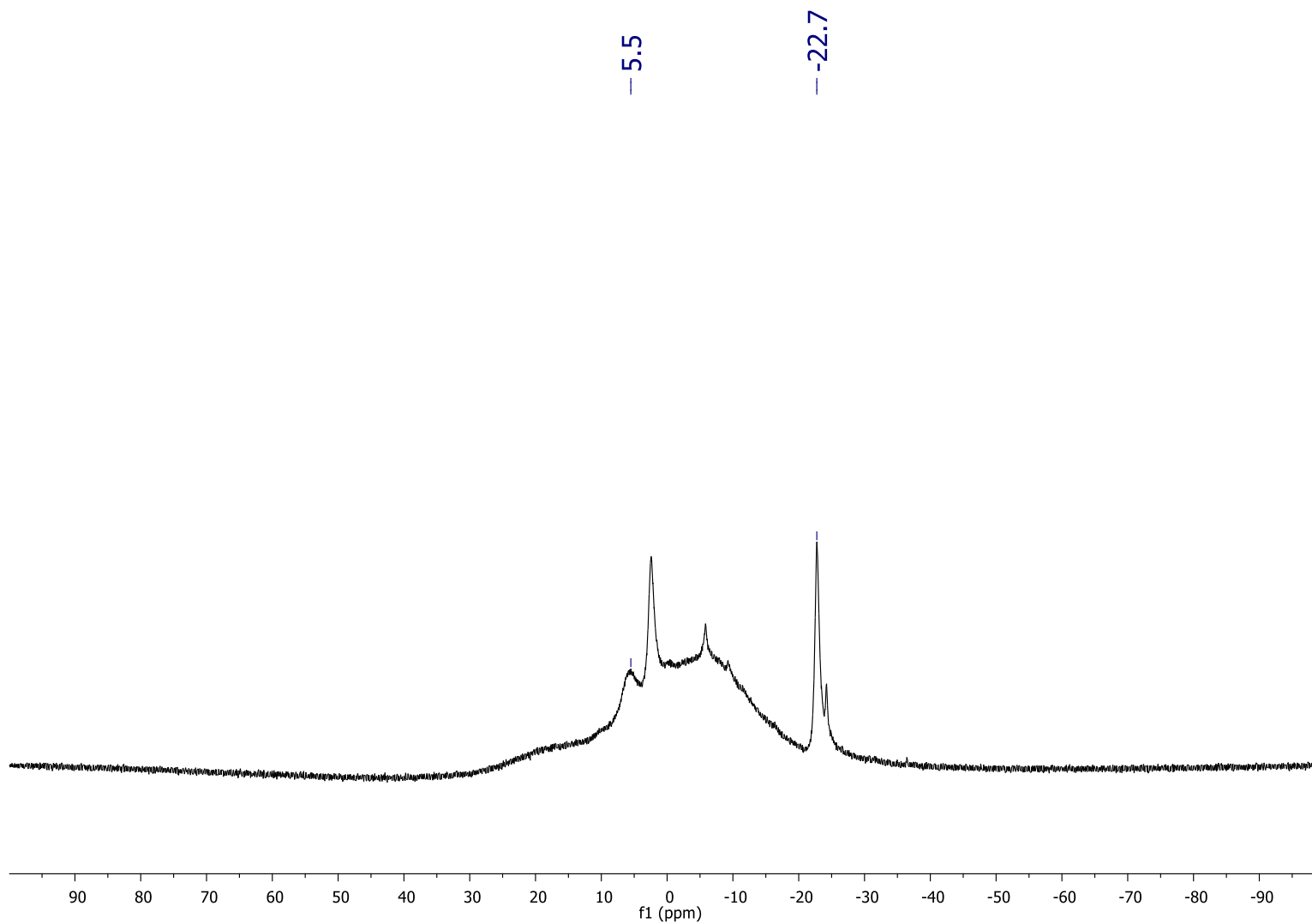


Figure A17: <sup>1</sup>H NMR (500 MHz, C<sub>6</sub>D<sub>6</sub>) of compound **4.1**•IMes.



**Figure A18:**  $^{11}\text{B}\{^1\text{H}\}$  NMR (160 MHz,  $\text{C}_6\text{D}_6$ ) of compound **4.1**•IMes.

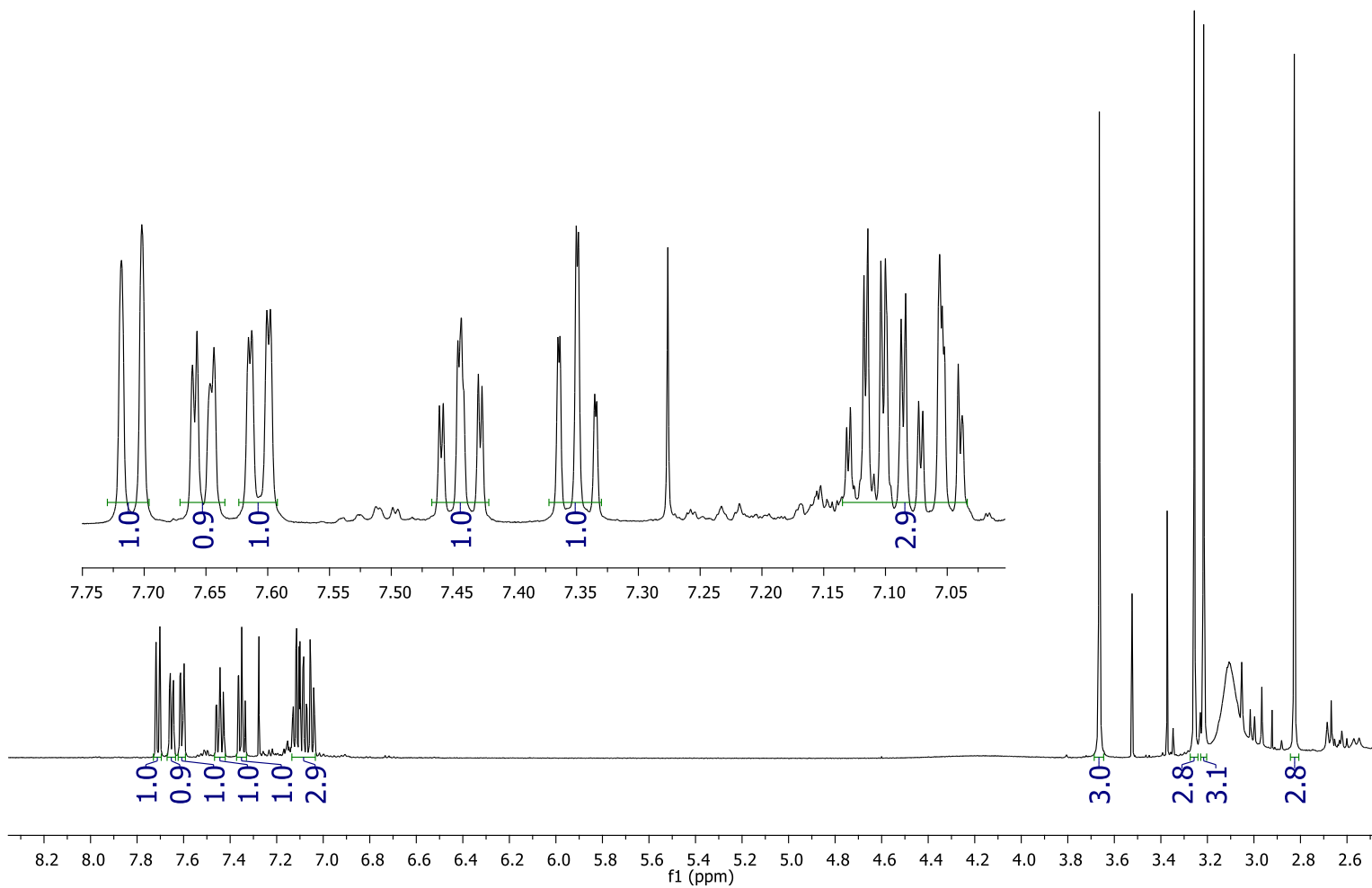
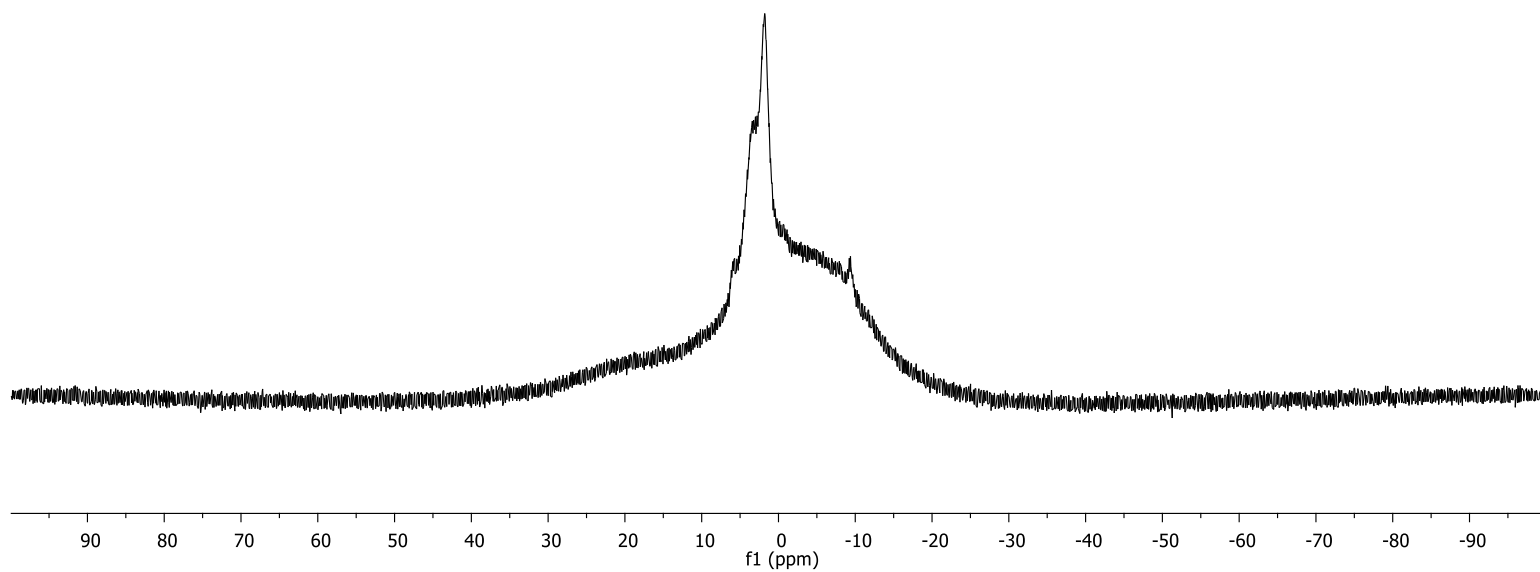
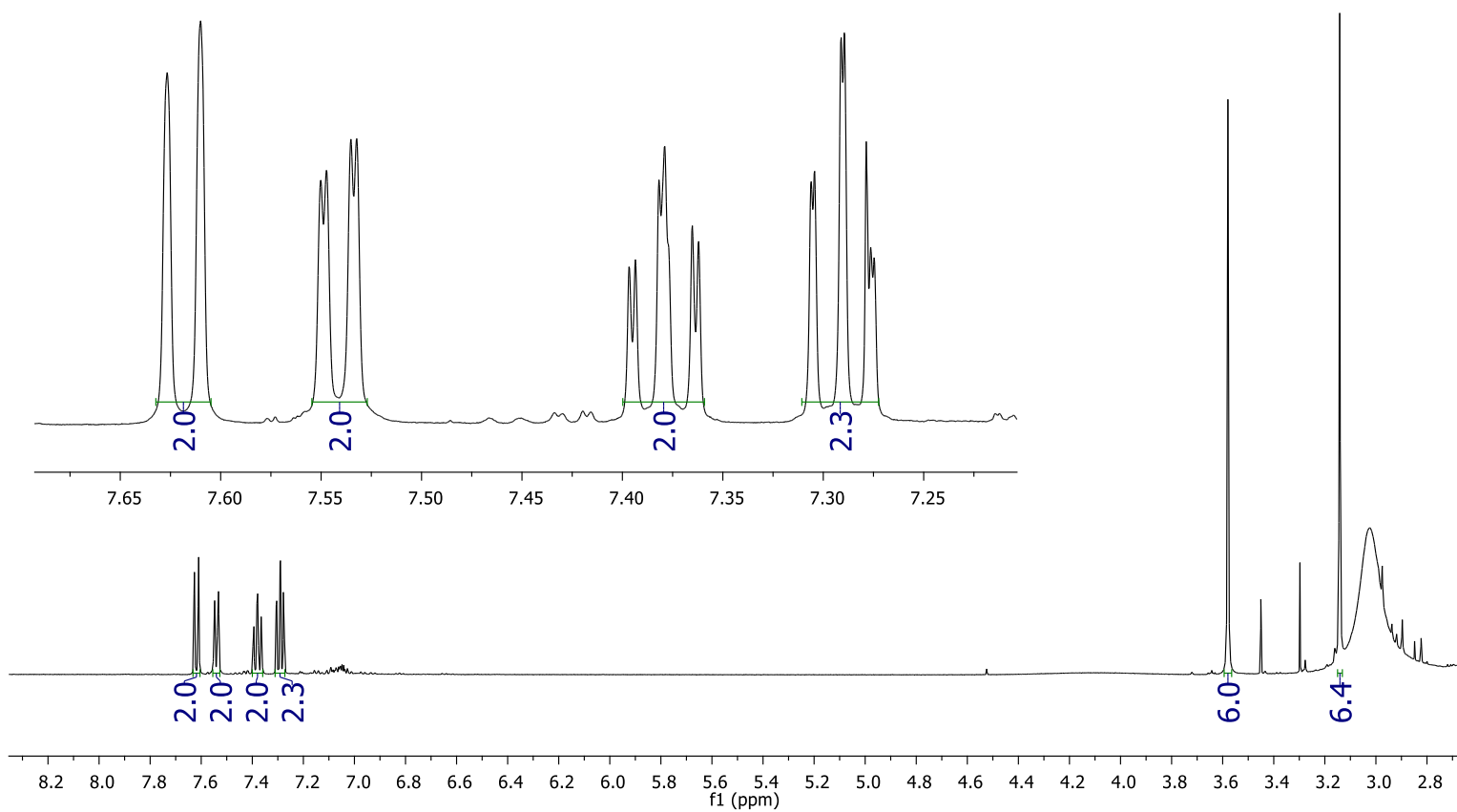


Figure A19: <sup>1</sup>H NMR (500 MHz, CDCl<sub>3</sub>) of compound 4.1.HCl.



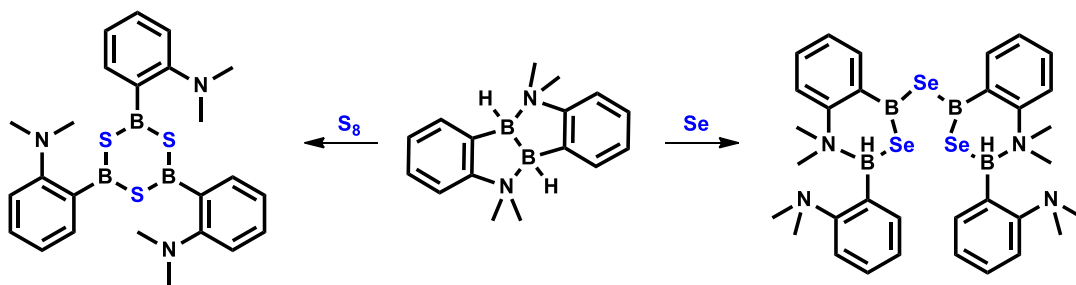
**Figure A20:**  $^{11}\text{B}\{^1\text{H}\}$  NMR (160 MHz,  $\text{CDCl}_3$ ) of compound **4.1**•HCl.



**Figure A21:** <sup>1</sup>H NMR (500 MHz, CDCl<sub>3</sub>) of compound 4.1•2HCl.

Reactivity of **4.1** with  $S_8$  and  $Se_{(s)}$

Compounds **4.10** and **4.11**



Compound **4.1** was dissolved in toluene, 2 equiv. of  $S_8$  or  $Se_{(s)}$  was added and the mixture heated (2 h at 80 °C in the case of  $S_8$  and 2 h at 100 °C in the case of  $Se_{(s)}$ ). The mixture was then filtered to remove excess reagent and evaporated to dryness.

Compounds **4.10**

$^1H$  NMR (500 MHz,  $C_6D_6$ )  $\delta$  8.22 (dd,  $J = 7.5, 1.5$  Hz, 1H), 7.17 – 7.10 (m, 1H), 6.93 (td,  $J = 7.4, 1.0$  Hz, 1H), 6.83 (d,  $J = 7.9$  Hz, 1H), 2.44 (s, 6H).

$^{13}C\{^1H\}$  NMR (126 MHz,  $C_6D_6$ )  $\delta$  158.5 (s), 137.1 (s), 132.7 (s), 123.8 (s), 119.8 (s), 45.4 (s).

$^{11}B\{^1H\}$  NMR (160 MHz,  $C_6D_6$ )  $\delta$  64.6 (s).

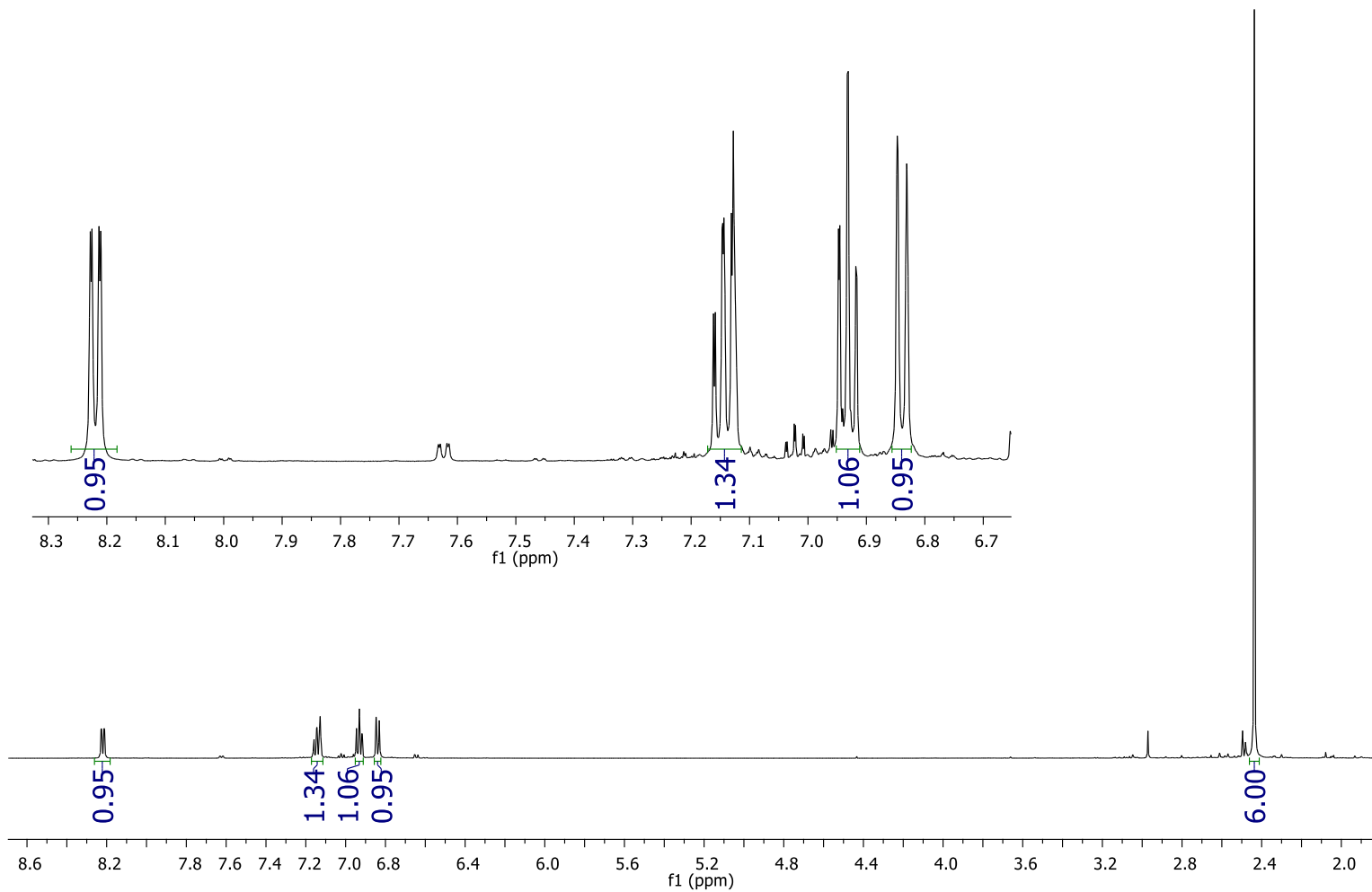
Compounds **4.11**

$^1H$  NMR (400 MHz,  $C_6D_6$ )  $\delta$  8.28 (dd,  $J = 7.5, 1.4$  Hz, 1H), 7.61 (d,  $J = 7.4$  Hz, 1H), 7.13 (td,  $J = 7.7, 1.6$  Hz, 1H), 7.00 – 6.84 (m, 3H), 6.78 (d,  $J = 8.2$  Hz, 1H), 6.60 (d,  $J = 8.1$  Hz, 1H), 2.99 (s, 3H), 2.49 (s, 3H), 2.39 (s, 6H).

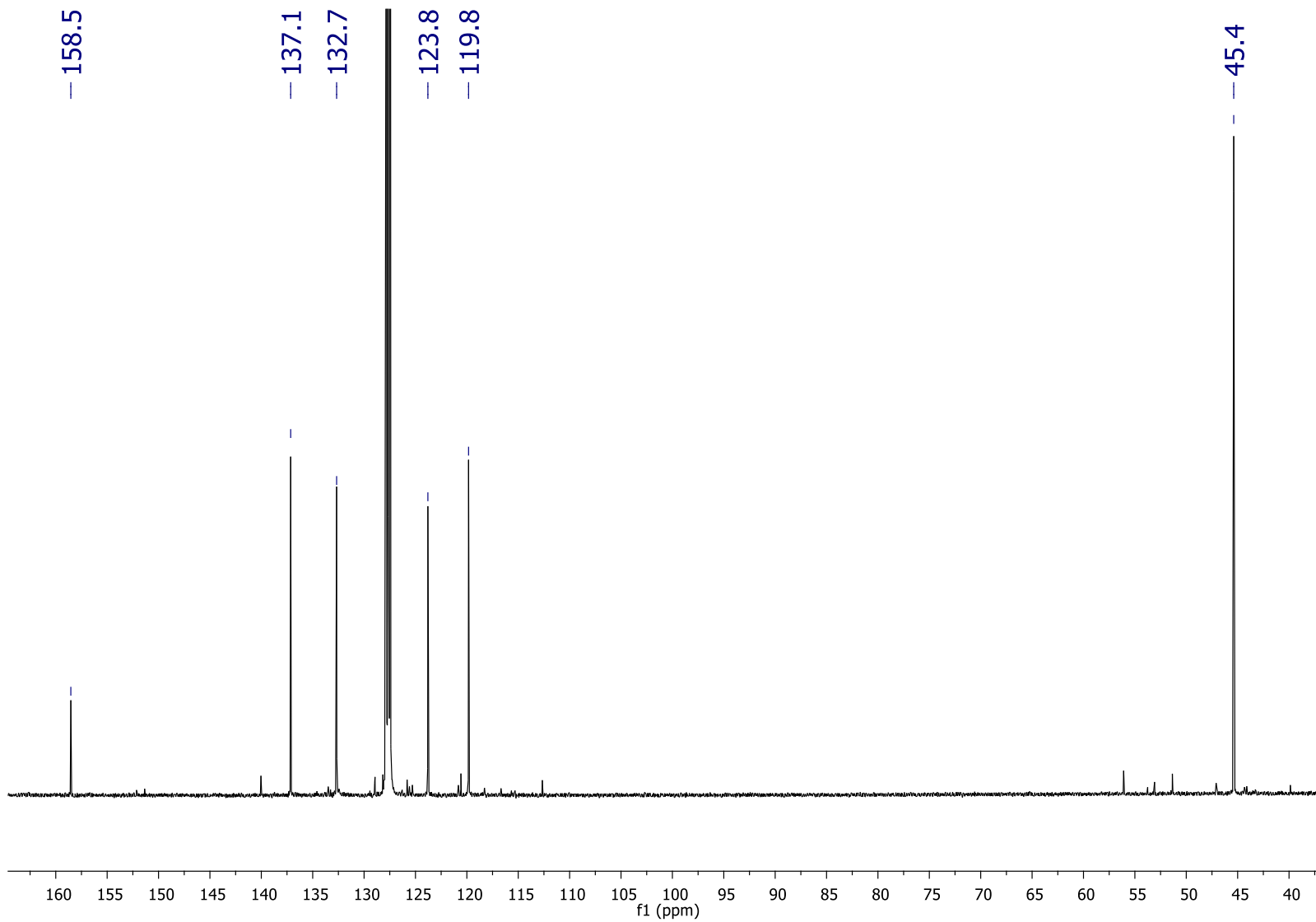
$^{11}B\{^1H\}$  NMR (160 MHz,  $C_6D_6$ )  $\delta$  71.04 (s), -0.50 (s)

$^{11}B$  NMR (160 MHz,  $C_6D_6$ )  $\delta$  71.04 (s), -0.50 (d,  $J = 119.2$  Hz).

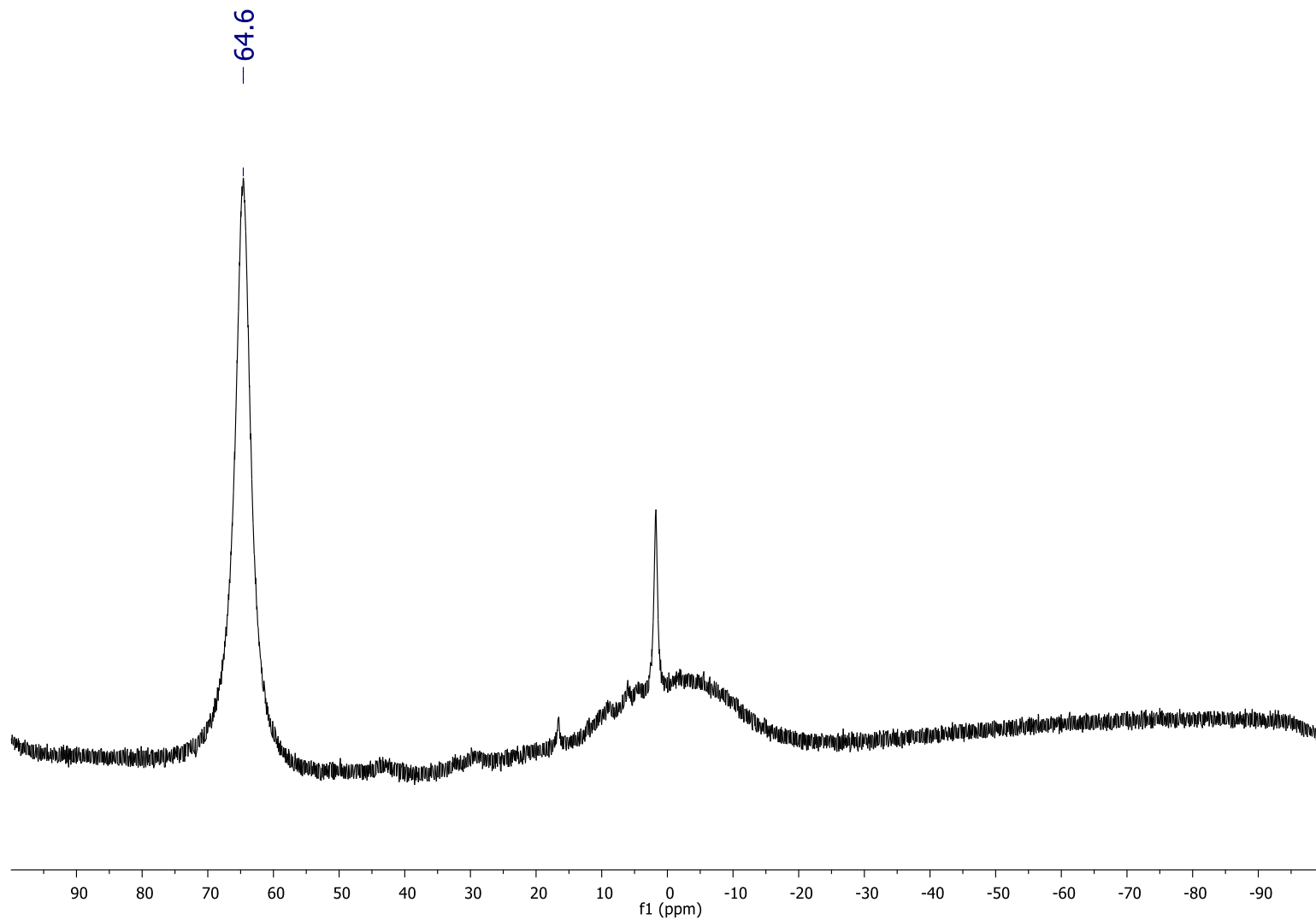




**Figure A22:** <sup>1</sup>H NMR (500 MHz, C<sub>6</sub>D<sub>6</sub>) of compound **4.10**.



**Figure A23**  $^{13}\text{C}\{^1\text{H}\}$  NMR (126 MHz,  $\text{C}_6\text{D}_6$ ) of compound **4.10**.



**Figure A24:**  $^{11}\text{B}\{^1\text{H}\}$  NMR (160 MHz,  $\text{C}_6\text{D}_6$ ) of compound **4.10**.

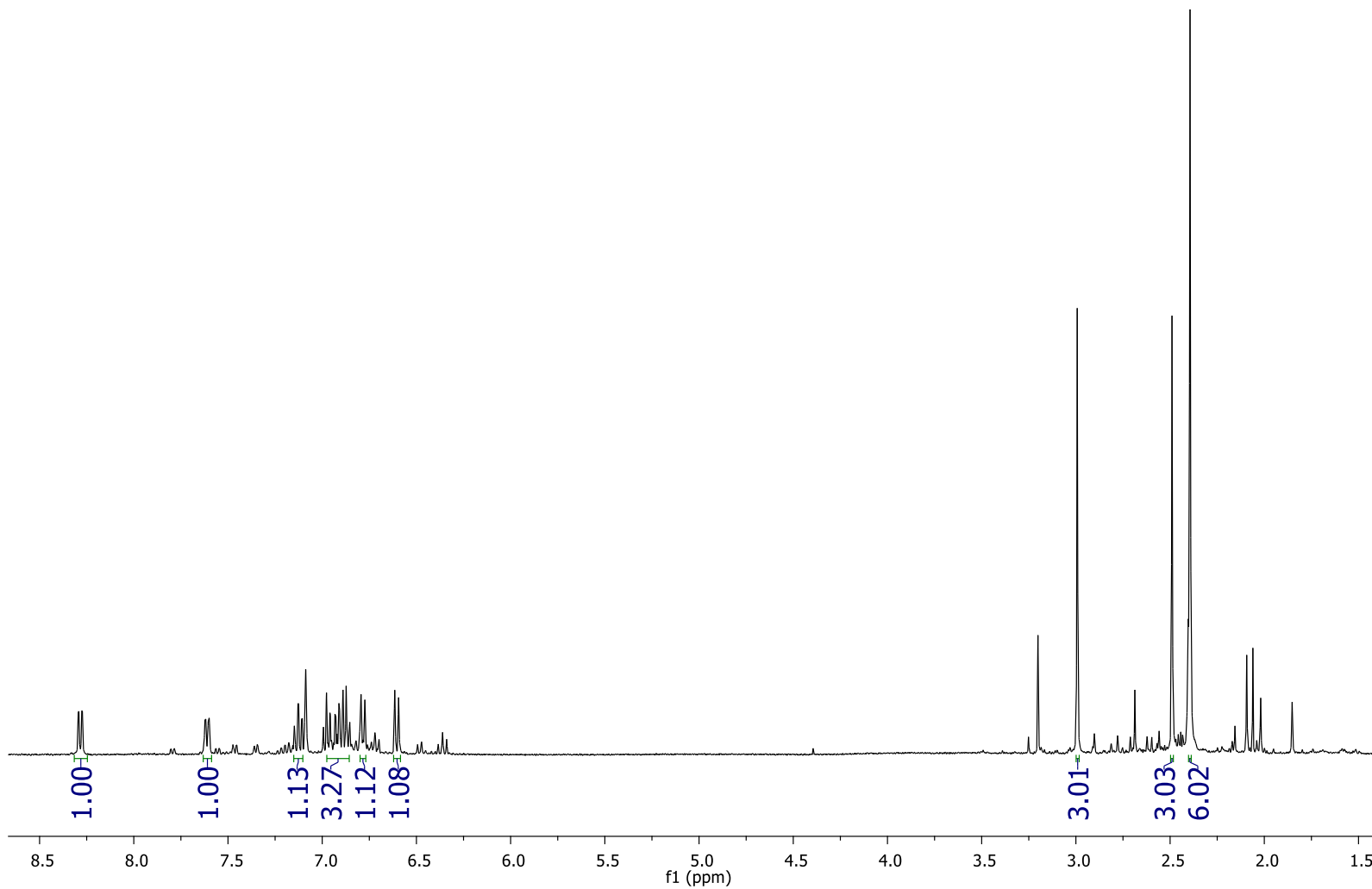
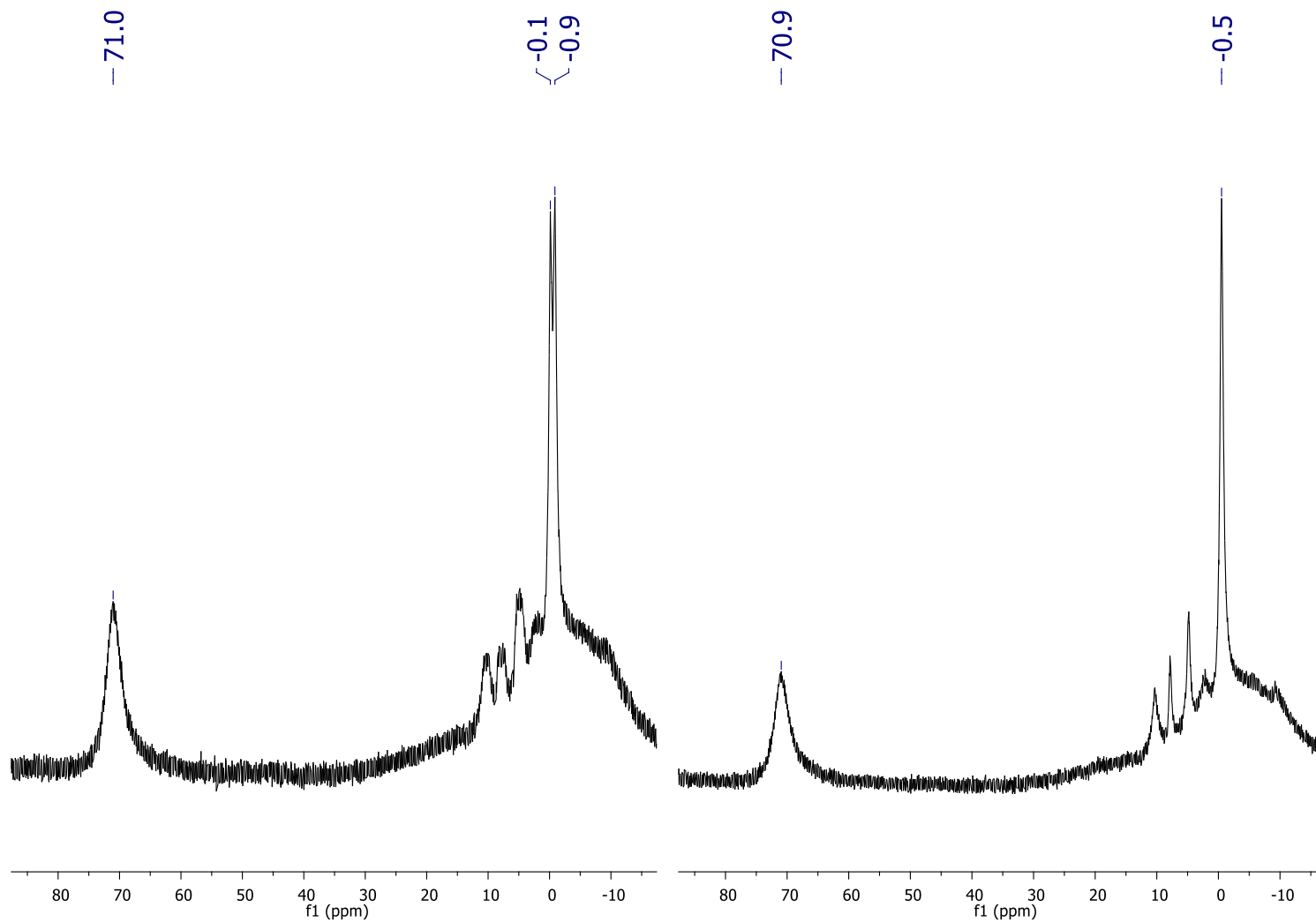


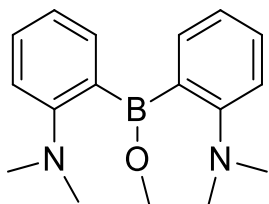
Figure A25:  $^1\text{H}$  NMR (400 MHz,  $\text{C}_6\text{D}_6$ ) of compound **4.11**.



**Figure A26:** Right,  $^{11}\text{B}\{^1\text{H}\}$  NMR (160 MHz,  $\text{C}_6\text{D}_6$ ) of compound **4.11**. Left,  $^{11}\text{B}$  NMR (160 MHz,  $\text{C}_6\text{D}_6$ ) of compound **4.11**.

## Chapter 5

### Compound 5.1



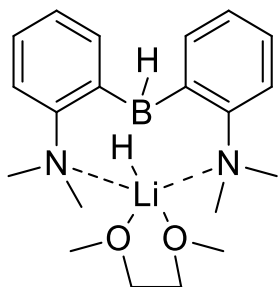
Most of the time, **5.1** was isolated as a side product of the synthesis of  $\text{NMe}_2\text{-C}_6\text{H}_4\text{-B(OMe)}_2$  which is routinely performed in our group. After distillation of  $\text{NMe}_2\text{-C}_6\text{H}_4\text{-B(OMe)}_2$ ,  $(\text{NMe}_2\text{-C}_6\text{H}_4)_2\text{-BOMe}$  was found to be the major product in the residue and could be isolated from crystallization in hexane. An alternative synthesis was also developed.  $\text{NMe}_2\text{-C}_6\text{H}_4\text{-B(OMe)}_2$  (1.53 g, 7.9 mmol, 1 equiv) was dissolved in hexane and added to a  $-78\text{ }^\circ\text{C}$  hexane suspension of 1- $\text{NMe}_2\text{-2-Li-C}_6\text{H}_4$  (1.00 g, 7.9 mmol, 1.00 equiv). The reaction was then left to warm up to room temperature naturally and left at room temperature for 1 h after which  $\text{TMSCl}$  (1.0 mL, 7.9 mmol, 1.00 equiv) was added and the reaction left stirring for an additional 30 min. The mixture was then filtered, the volatiles were removed under vacuum and the green oil obtained distilled under vacuum ( $\approx 1$  torr,  $\approx 150\text{ }^\circ\text{C}$ ) to give 750 mg (34 % yield) of the title compound as a green oil. Single crystals suitable for X-ray diffraction were obtained by recrystallization in hexane at  $-35\text{ }^\circ\text{C}$

$^1\text{H}$  NMR (500 MHz,  $\text{C}_6\text{D}_6$ )  $\delta$  7.54 (d,  $J = 7.2$  Hz, 2H), 7.23 (t,  $J = 7.7$  Hz, 2H), 6.85 (td,  $J = 7.3, 1.5$  Hz, 2H), 6.80 (dd,  $J = 8.2, 1.0$  Hz, 2H), 3.61 (s, 3H), 2.60 (s, 12H).

$^{13}\text{C}\{^1\text{H}\}$  NMR (126 MHz,  $\text{C}_6\text{D}_6$ )  $\delta$  157.1 (s), 136.3 (s), 130.2 (s), 119.3 (s), 115.4 (s), 54.7 (s), 43.8 (s). The carbon linked directly to boron was not observed.

$^{11}\text{B}\{^1\text{H}\}$  NMR (160 MHz,  $\text{C}_6\text{D}_6$ )  $\delta$  46.5 (s)

### Compound 5.2



1.38 g of **5.1** (5.5 mmol, 1.00 eq) was dissolved in toluene and 205 mg of  $\text{LiAlH}_4$  (5.8 mmol, 1.05 eq) was added at room temperature, followed by 1.1 mL (11.0 mmol, 2.00 eq) of DME. After less than five minutes of stirring at room temperature, the green coloration of the mixture disappeared and after 2 h the reaction mixture was filtered and the clear solution was stored at  $-35\text{ }^\circ\text{C}$ . After 48 h an important amount of colorless crystals was present. The solvent was thus removed by filtration through a cannula and the crystals dried under vacuum to give 708 mg (41% yield) of the title compound. By omitting the crystallization step, yields up to 70% were obtained, however the compound was under the form of a white sticky gum and small impurities were present.

Single crystals suitable for X-ray diffraction were obtained by recrystallization in toluene at -35 °C.

$^1\text{H}$  NMR (500 MHz,  $\text{C}_6\text{D}_6$ )  $\delta$  7.76 (s, broad, 2H), 7.21 – 7.09 (m, 4H), 7.6.97 (d,  $J = 7.8$  Hz, 2H), 3.07 (s, 4H), 2.94 (s, 6H), 2.63 (q,  $J = 74$  Hz, 2H), 2.36 (s, 12H).

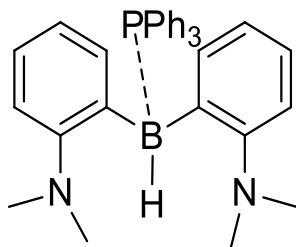
$^1\text{H}\{^{11}\text{B}\}$  NMR (500 MHz,  $\text{C}_6\text{D}_6$ )  $\delta$  7.8 (d,  $J = 6.4$  Hz, 2H), 7.2 – 7.1 (m, 4H), 7.0 (d,  $J = 7.8$ , 2H), 3.1 (s, 4H), 2.9 (s, 6H), 2.6 (s, 2H), 2.4 (s, 12H).

$^{13}\text{C}\{^1\text{H}\}$  NMR (126 MHz,  $\text{C}_6\text{D}_6$ )  $\delta$  155.5 (s), 149.0 (m, broad), 138.4 (s), 125.4 (s), 124.3 (s), 116.9 (s), 71.1 (s), 58.5 (s), 45.9 (s).

$^{11}\text{B}\{^1\text{H}\}$  NMR (160 MHz,  $\text{C}_6\text{D}_6$ )  $\delta$  -20.0 (s).

$^{11}\text{B}$  NMR (160 MHz,  $\text{C}_6\text{D}_6$ )  $\delta$  -20.0 (t,  $J = 74$  Hz)

Compound **5.3**• $\text{PPh}_3$



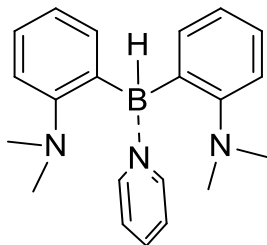
**5.3**• $\text{PPh}_3$  was prepared on a NMR scale by mixing  $(\text{NMe}_2\text{-C}_6\text{H}_4)_2\text{-BH}_2\text{-LiDME}$  (10 mg, 0.03 mmol, 1.00 eq) and  $\text{PPh}_3\text{•HBr}$  (10.2 mg, 0.03 mmol, 1.00 equiv) in  $\text{C}_6\text{D}_6$ . Instantly, a green coloration appeared as well as gas evolution ( $\text{H}_2$ ) and salt precipitation ( $\text{LiBr}$ ).

$^1\text{H}$  NMR (500 MHz,  $\text{C}_6\text{D}_6$ )  $\delta$  7.68 (d,  $J = 6.9$  Hz, 2H), 7.39 – 7.33 (m, 6H), 7.16 (t,  $J = 7.6$  Hz, 2H), 7.03 (t,  $J = 7.1$  Hz, 2H), 6.98 – 6.94 (m, 9H), 6.88 (d,  $J = 7.8$  Hz, 2H), 5.15 (s, very broad,  $\Delta\nu_{1/2}=220$  Hz, 1H), 2.49 (s, 12H).

$^{31}\text{P}\{^1\text{H}\}$  NMR (202 MHz,  $\text{C}_6\text{D}_6$ )  $\delta$  -0.3 (s, broad,  $\Delta\nu_{1/2}=250$  Hz).

$^{11}\text{B}\{^1\text{H}\}$  NMR (160 MHz,  $\text{C}_6\text{D}_6$ )  $\delta$  0.1 (s, broad,  $\Delta\nu_{1/2}=775$  Hz).

Compound **5.3**•Pyridine



**5.2** (750 mg, 2.2 mmol, 1.00 equiv) was dissolved in toluene and pyridine (0.90 mL, 11.2 mmol, 5.00 equiv) was added followed by TMSBr (0.35 mL, 2.6 mmol, 1.20 equiv). The mixture was left to react at room temperature for 2 h, filtered and the volatile were then removed under vacuum to give an orange oil. The product was then washed with ether to give 150 mg (20% yield) of the title compound as a white powder.

Single crystals suitable for X-ray diffraction were obtained by recrystallization in toluene at -35 °C.

$^1\text{H}$  NMR (500 MHz,  $\text{C}_6\text{D}_6$ )  $\delta$  8.15 (d,  $J = 5.3$  Hz, 2H), 7.37 (d,  $J = 7.0$  Hz, 2H), 7.29 (td,  $J = 7.6, 1.6$  Hz, 2H), 7.12 (d,  $J = 7.0$  Hz, 2H, overlapping with  $\text{C}_6\text{D}_6$  residual signal), 7.08 (td,  $J = 7.3, 0.7$  Hz, 2H), 6.55 (t,  $J = 7.6$  Hz, 1H), 6.16 – 6.11 (t,  $J = 7.0$  Hz, 2H), 5.11 (s, very broad,  $\Delta\nu_{1/2}=210$  Hz, 1H), 2.62 (s, 12H).

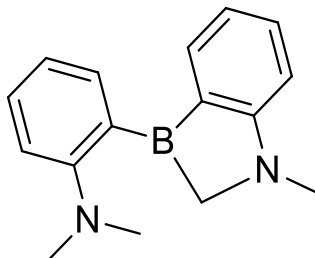
$^1\text{H}\{^{11}\text{B}\}$  NMR (500 MHz,  $\text{C}_6\text{D}_6$ )  $\delta$  8.15 (d,  $J = 5.3$  Hz, 2H), 7.37 (d,  $J = 7.0$  Hz, 2H), 7.29 (td,  $J = 7.6, 1.6$  Hz, 2H), 7.12 (d,  $J = 7.0$  Hz, 2H, overlapping with  $\text{C}_6\text{D}_6$  residual signal), 7.08 (td,  $J = 7.3, 0.7$  Hz, 2H), 6.55 (t,  $J = 7.6$  Hz, 1H), 6.16 – 6.11 (t,  $J = 7.0$  Hz, 2H), 5.11 (s, broad,  $\Delta\nu_{1/2}=25$  Hz, 1H), 2.6 (s, 12H).

$^{13}\text{C}\{^1\text{H}\}$  NMR (126 MHz,  $\text{C}_6\text{D}_6$ )  $\delta$  158.1 (s), 147.4 (s), 137.9 (s), 136.8 (s), 126.6 (s), 122.8 (s), 122.5 (s), 118.0 (s), 44.8 (s). The carbon linked directly to boron was not observed.

$^{11}\text{B}\{^1\text{H}\}$  NMR (160 MHz,  $\text{C}_6\text{D}_6$ )  $\delta$  -0.7 (s).

$^{11}\text{B}$  NMR (160 MHz,  $\text{C}_6\text{D}_6$ )  $\delta$  -0.7 (s), a small broadening of the signal is observed when compared to the  $^{11}\text{B}\{^1\text{H}\}$  NMR spectra.  $\Delta\nu_{1/2}=300$  and 230 Hz respectively

#### Compound **5.4**



**5.2** (10.0 mg, 0.03 mmol, 1.00 eq) was dissolved in  $\text{C}_6\text{D}_6$  and  $\text{PPh}_3\cdot\text{HBr}$  (10.2 mg, 0.03 mmol, 1.00 equiv) was added. The mixture was then placed in a J-young NMR tube and heated at 80 °C for 1 h.

Attempts to isolate the compound in pure form by reacting **5.2** with TMSBr or  $\text{NEt}_3\cdot\text{HCl}$  always led to mixture in which compound **5.4** was the main compound, but we were not able to further purify it. Few small single crystals suitable for X-ray diffraction were obtained by recrystallization from hexanes at -35 °C from one of those attempts, but not enough for NMR characterization.

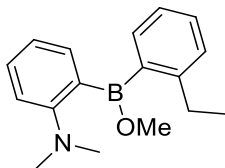
$^1\text{H}$  NMR (500 MHz,  $\text{C}_6\text{D}_6$ )  $\delta$  8.07 (d,  $J = 7.5$  Hz, 1H), 7.69 (dd,  $J = 7.2, 1.7$  Hz, 1H), 7.31 (m, 1H, overlapping with a  $\text{PPh}_3$  signal, observed only the  $^{13}\text{C}\text{-}^1\text{H}$  HSQC), 7.25 (ddd,  $J = 8.2, 7.4, 1.7$  Hz, 1H), 6.96 (td,  $J = 7.2, 0.9$  Hz, 1H), 6.80 (d,  $J = 8.2$  Hz, 1H), 6.71 (t,  $J = 7.2$  Hz, 1H), 6.58 (d,  $J = 8.4$  Hz, 1H), 3.31 (s, 2H), 2.68 (s, 3H), 2.45 (s, 6H).

$^{13}\text{C}\{^1\text{H}\}$  NMR (126 MHz,  $\text{C}_6\text{D}_6$ )  $\delta$  167.9 (s), 158.0 (s), 136.0 (s), 135.8 (s), 134.6 (s), 130.6 (s), 120.2 (s), 115.42 (s), 115.35 (s), 108.7 (s), 54.4 (very weak signal, but well observed on the  $^{13}\text{C}\text{-}^1\text{H}$  HSQC), 45.4 (s), 34.4 (s). Both aromatic carbons linked directly to boron were not observed.



$^{11}\text{B}\{^1\text{H}\}$  NMR (160 MHz,  $\text{C}_6\text{D}_6$ )  $\delta$  65.3 (s).

#### Compound 5.7

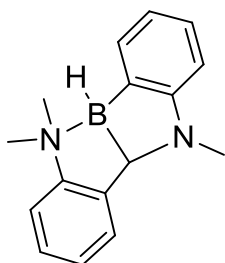


Compound **5.7** was synthesized according to the alternative procedure for the synthesis of **5.1**, but using *ortho*-ethyl- $\text{C}_6\text{H}_4\text{-B(OMe)}_2$  and **2.8**.

$^1\text{H}$  NMR (500 MHz,  $\text{CDCl}_3$ )  $\delta$  7.55 (dd,  $J = 7.5, 1.4$  Hz, 1H), 7.40 – 7.34 (m, 2H), 7.30 – 7.26 (m, 1H), 7.24 (dd,  $J = 7.2, 1.7$  Hz, 1H), 7.16 (td,  $J = 7.4, 1.3$  Hz, 1H), 6.94 (d,  $J = 8.2$  Hz, 1H), 6.89 (td,  $J = 7.2, 1.0$  Hz, 1H), 3.80 (d,  $J = 1.6$  Hz, 3H), 2.97 (q,  $J = 7.5$  Hz, 2H), 2.90 (s, 6H), 1.27 (t,  $J = 7.5$  Hz, 3H).

$^{11}\text{B}\{^1\text{H}\}$  NMR (160 MHz,  $\text{CDCl}_3$ )  $\delta$  47.1 (s).

#### Compound 5.8



**5.2** (500 mg, 1.5 mmol, 1.00 equiv) was dissolved in toluene and  $\text{NEt}_3\text{HCl}$  (205 mg, 1.5 mmol, 1.00 equiv) was added. The mixture was then refluxed for 16 h. The reaction was then filtered, the volatiles evaporated and the resulting thick oil was washed with hexanes to give 118 mg (32 % yield) of the title compound as a pale green solid.

Single crystals suitable for X-ray diffraction were obtained by recrystallization from a diethylether solution stored at  $-35$  °C.

$^1\text{H}$  NMR (500 MHz,  $\text{C}_6\text{D}_6$ )  $\delta$  7.63 (dd,  $J = 6.8, 1.1$  Hz, 1H), 7.37 (td,  $J = 7.6, 1.4$  Hz, 1H), 7.25 (dd,  $J = 7.5, 1.0$  Hz, 1H), 7.01 – 6.95 (m, 2H), 6.89 (td,  $J = 7.8, 1.4$  Hz, 1H), 6.52 (d,  $J = 7.9$  Hz, 1H), 6.45 (d,  $J = 8.0$  Hz, 1H), 3.85 (d,  $J = 5.3$  Hz, 1H), 3.77 (d, very broad,  $J \approx 90$  Hz, 1H), 2.77 (s, 3H), 2.25 (s, 3H), 1.99 (s, 3H).

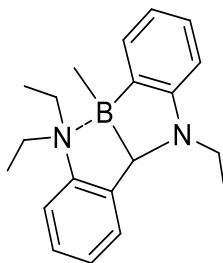
$^1\text{H}$  NMR $\{^{11}\text{B}\}$  (500 MHz,  $\text{C}_6\text{D}_6$ )  $\delta$  7.63 (dd,  $J = 6.8, 1.1$  Hz, 1H), 7.37 (td,  $J = 7.6, 1.4$  Hz, 1H), 7.25 (dd,  $J = 7.5, 1.0$  Hz, 1H), 7.01 – 6.95 (m, 2H), 6.89 (td,  $J = 7.8, 1.4$  Hz, 1H), 6.52 (d,  $J = 7.9$  Hz, 1H), 6.45 (d,  $J = 8.0$  Hz, 1H), 3.85 (d,  $J = 5.3$  Hz, 1H), 3.77 (s, broad, 1H), 2.77 (s, 3H), 2.25 (s, 3H), 1.99 (s, 3H).

$^{13}\text{C}\{^1\text{H}\}$  NMR (126 MHz,  $\text{C}_6\text{D}_6$ )  $\delta$  161.1 (s), 152.5 (s), 142.6 (s), 132.6 (s), 129.4 (s), 128.9 (s), 127.1 (s), 117.8 (s), 116.5 (s), 106.3 (s), 63.0 (s, broad), 52.9 (s), 51.8 (s), 34.7 (s). Both aromatic carbons linked directly to boron were not observed.

$^{11}\text{B}\{^1\text{H}\}$  NMR (160 MHz,  $\text{C}_6\text{D}_6$ )  $\delta$  6.8 (s).

$^{11}\text{B}$  NMR (160 MHz,  $\text{C}_6\text{D}_6$ )  $\delta$  6.8 (d,  $J = 88$  Hz).

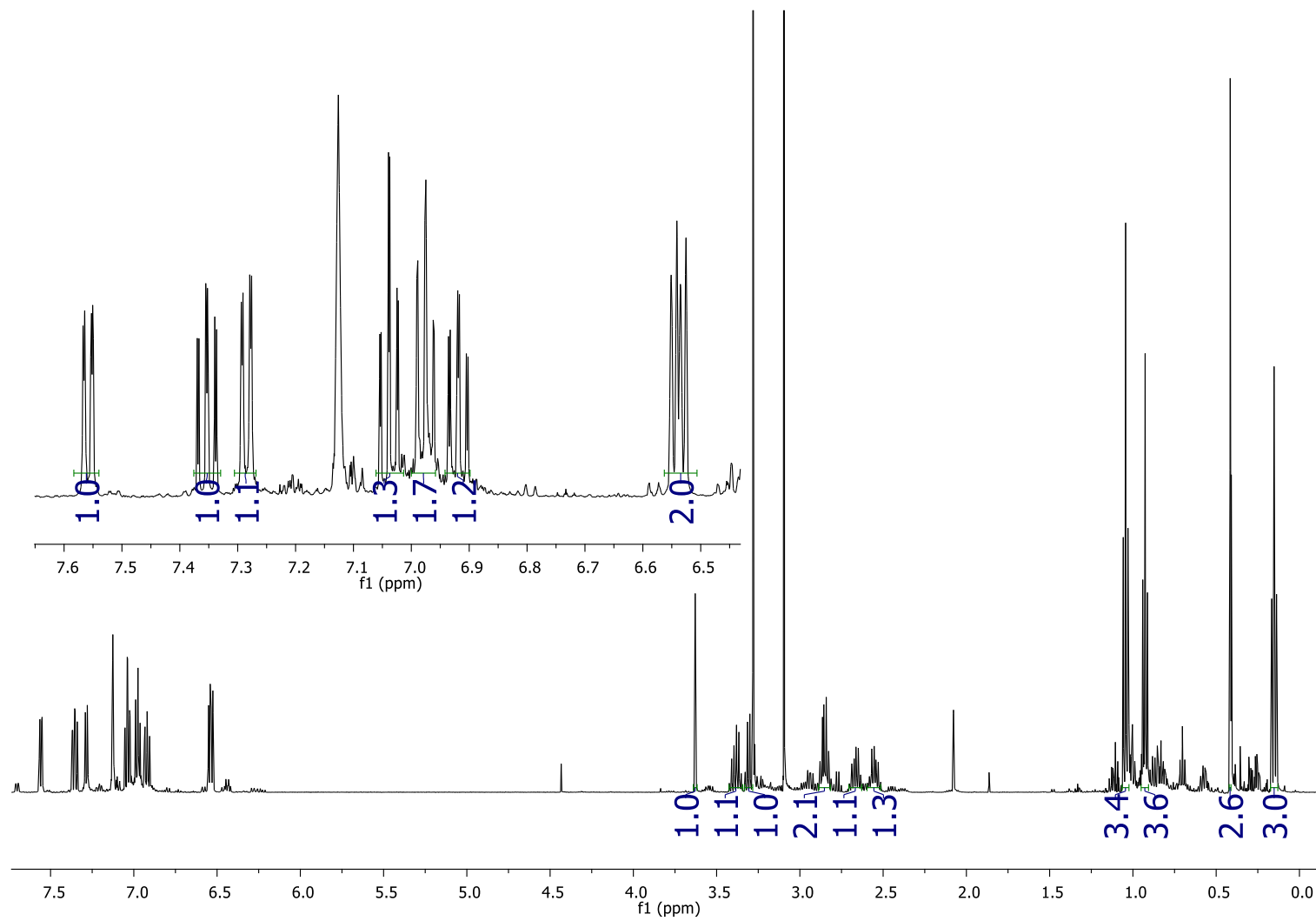
### Compound 5.9



$^1\text{H}$  NMR (500 MHz,  $\text{C}_6\text{D}_6$ )  $\delta$  7.56 (dd,  $J = 6.9, 1.4$  Hz, 1H), 7.35 (ddd,  $J = 7.9, 7.4, 1.5$  Hz, 1H), 7.28 (dd,  $J = 7.4, 1.5$  Hz, 1H), 7.04 (td,  $J = 7.4, 1.1$  Hz, 1H), 6.98 (td,  $J = 7.3, 0.9$  Hz, 1H), 6.94 – 6.90 (m, 1H), 6.54 (dd,  $J = 7.9, 4.9$  Hz, 2H), 3.63 (s, 1H), 3.43 – 3.25 (m, 2H), 2.90 – 2.81 (m, 2H), 2.71 – 2.50 (m, 2H), 1.04 (t,  $J = 7.0$  Hz, 3H), 0.93 (t,  $J = 7.1$  Hz, 3H), 0.42 (s,  $J = 3.1$  Hz, 3H), 0.15 (t,  $J = 7.3$  Hz, 3H).

$^{13}\text{C}\{^1\text{H}\}$  NMR (126 MHz,  $\text{C}_6\text{D}_6$ )  $\delta$  160.1 (s), 149.8 (s), 143.3 (s), 131.1 (s), 130.9 (s), 128.7 (s), 125.8 (s), 120.8 (s), 116.4 (s), 106.8 (s), 71.8 (s), 61.91 (s), 58.4 (s), 49.6 (s), 44.7 (s), 40.5 (s), 10.0 (s), 9.5 (s), 6.6 (s), 3.4 (s).

$^{11}\text{B}\{^1\text{H}\}$  NMR (160 MHz,  $\text{C}_6\text{D}_6$ )  $\delta$  12.4 (s).



**Figure A27**  $^1\text{H}$  NMR (500 MHz,  $\text{C}_6\text{D}_6$ ) of **5.9**.

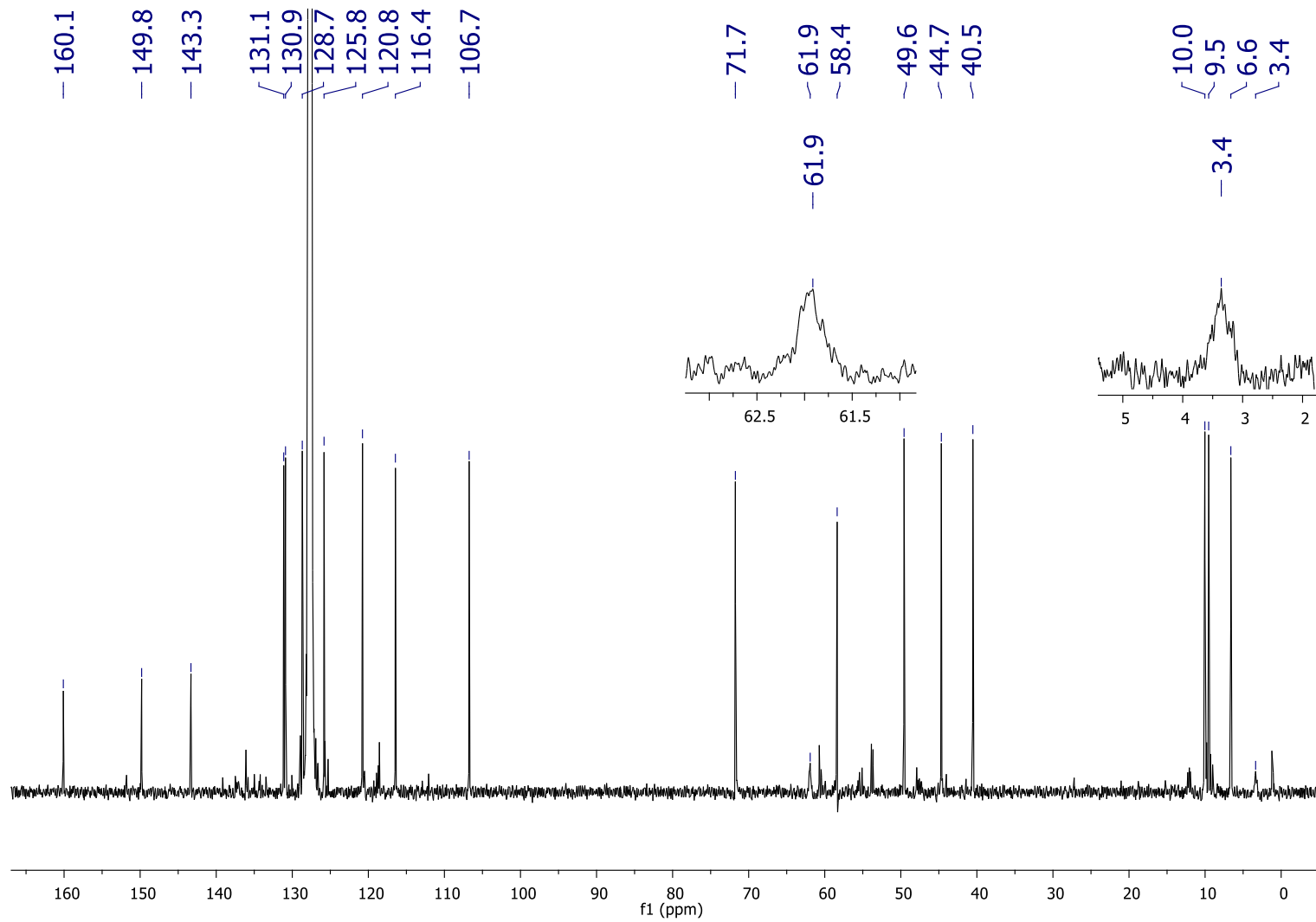
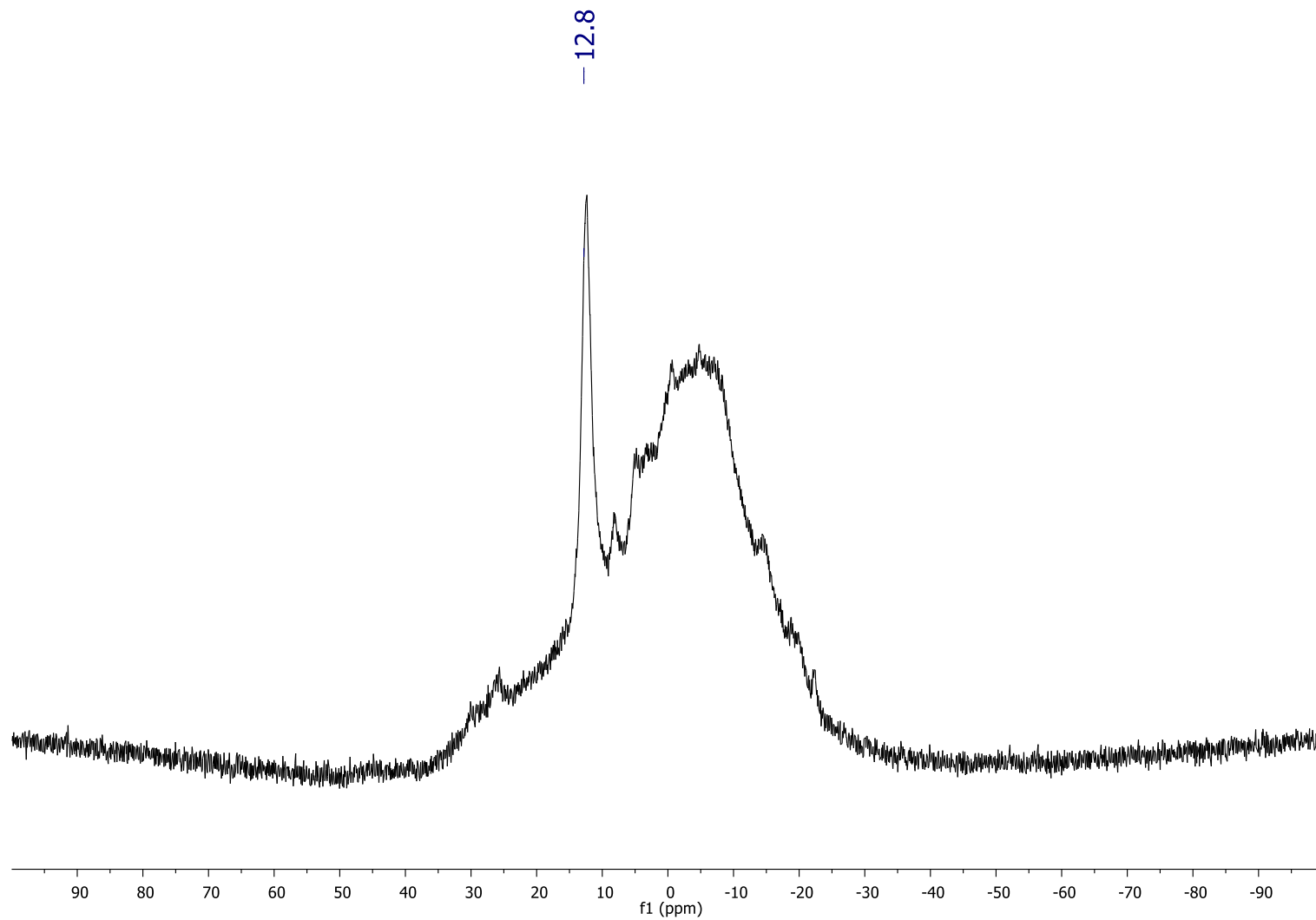
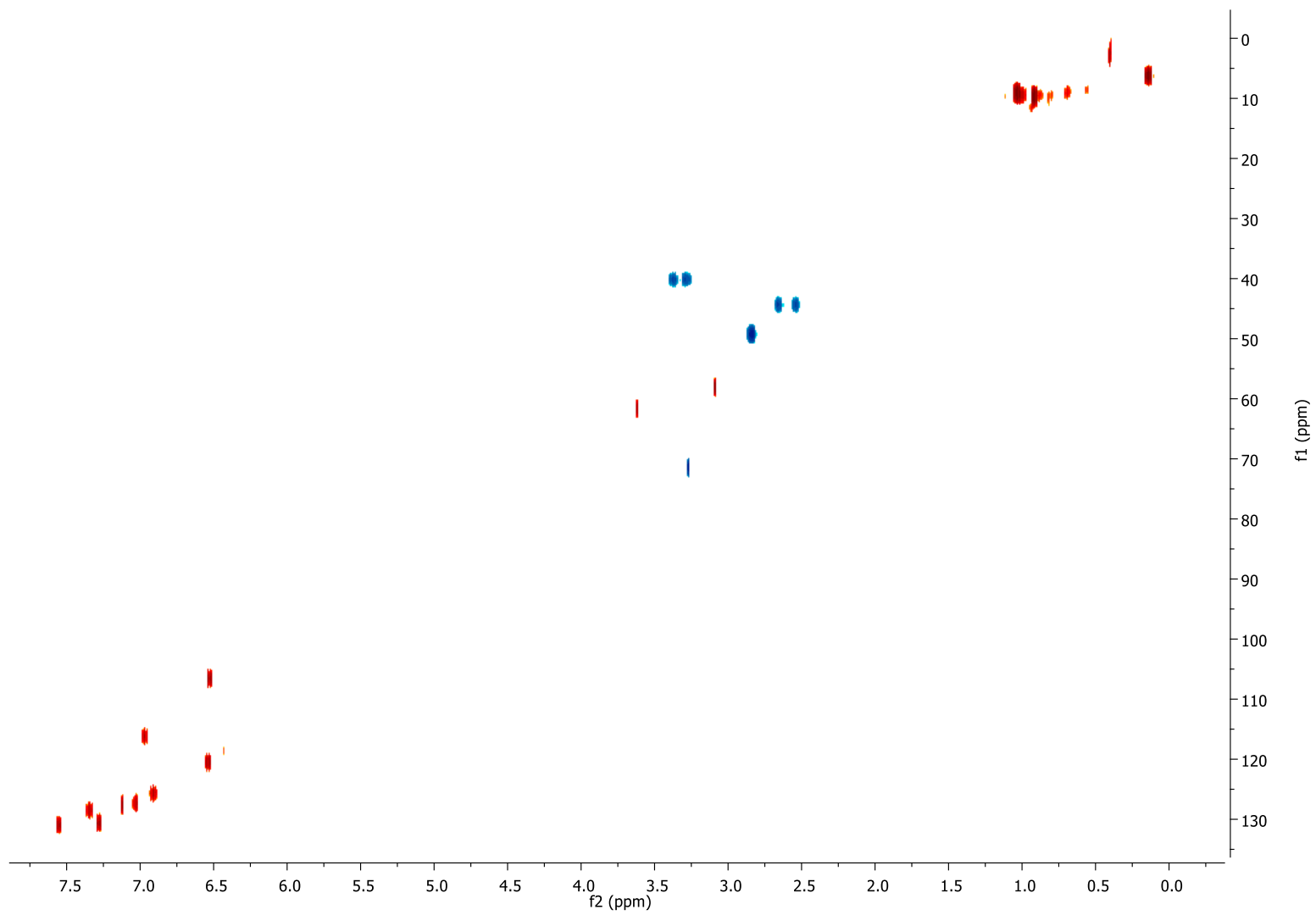


Figure A28  $^{13}\text{C}\{^1\text{H}\}$  NMR (126 MHz,  $\text{C}_6\text{D}_6$ ) of **5.9**.



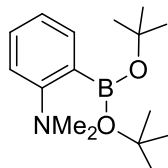
**Figure A29**  $^{11}\text{B}\{^1\text{H}\}$  NMR (160 MHz,  $\text{C}_6\text{D}_6$ , boro-silicate tube) of **5.9**.



**Figure A30** <sup>13</sup>C-<sup>1</sup>H HSQC (126 MHz-500 MHz, C<sub>6</sub>D<sub>6</sub>) of **5.9**.

## Chapter 6

### Compound 6.1



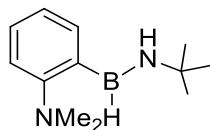
10.0 mg (1.0 equiv) of **3.3** was dissolved in  $\text{CDCl}_3$  and placed in a J-Young NMR tube after which 5.0 equiv (36.0  $\mu\text{L}$ ) of  $t\text{BuOH}$  was added. The reaction was left at room temperature for 30 min and the volatiles were removed under vacuum.  $\text{CDCl}_3$  was then added and the product  $\text{NMe}_2\text{-C}_6\text{H}_4\text{-B(O}t\text{Bu)}_2$  was characterized using multi-nuclear NMR spectroscopy.

$^1\text{H}$  NMR (500 MHz,  $\text{CDCl}_3$ )  $\delta$  7.22 – 7.17 (m, 2H), 6.86 – 6.80 (m, 2H), 2.86 (s, 6H), 1.31 (s, 18H).

$^{13}\text{C}\{^1\text{H}\}$  NMR (126 MHz,  $\text{CDCl}_3$ )  $\delta$  154.5 (s), 132.6 (s), 128.4 (s), 119.5 (s), 115.5 (s), 73.8 (s), 43.7 (s), 30.5 (s). The carbon linked directly to boron was not observed.

$^{11}\text{B}\{^1\text{H}\}$  NMR (160 MHz,  $\text{CDCl}_3$ )  $\delta$  27.3 (s).

### Compound 6.2



10.0 mg (1.0 equiv) of **3.3** was dissolved in  $\text{CDCl}_3$  and placed in a J-Young NMR tube after which 5.0 equiv (39.5  $\mu\text{L}$ ) of  $t\text{BuNH}_2$  was added. The reaction was heated at 80  $^\circ\text{C}$  for 16 h and the volatiles were removed under vacuum.  $\text{CDCl}_3$  was then added and the product  $\text{NMe}_2\text{-C}_6\text{H}_4\text{-B(H)(NH}t\text{Bu)}$  was characterized using multi-nuclear NMR spectroscopy.

$^1\text{H}$  NMR (500 MHz,  $\text{CDCl}_3$ )  $\delta$  7.48 (dd,  $J = 7.5, 1.5$  Hz, 1H), 7.32 – 7.27 (m, 1H), 7.03 – 6.98 (m, 2H), 4.97 (very broad, 1H), 2.78 (s, 6H), 1.32 (s, 9H).

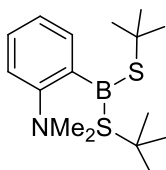
$^1\text{H}\{^{11}\text{B}\}$  NMR (500 MHz,  $\text{CDCl}_3$ )  $\delta$  7.48 (dd,  $J = 7.5, 1.5$  Hz, 1H), 7.32 – 7.27 (m, 1H), 7.03 – 6.98 (m, 2H), 4.97 (s, 1H), 2.78 (s, 6H), 1.32 (s, 9H). The N-H signal was not observed.

$^{13}\text{C}\{^1\text{H}\}$  NMR (126 MHz,  $\text{CDCl}_3$ )  $\delta$  158.3 (s), 137.8 (s), 129.9 (s), 121.7 (s), 116.4 (s), 45.5 (s), 32.3 (s), 28.4 (s). The carbon linked directly to boron was not observed.

$^{11}\text{B}\{^1\text{H}\}$  NMR (160 MHz,  $\text{CDCl}_3$ )  $\delta$  36.5 (s).

$^{11}\text{B}$  NMR (160 MHz,  $\text{CDCl}_3$ )  $\delta$  36.5 (d,  $J = 96$  Hz).

### Compound 6.3



10.0 mg (1.0 equiv) of **3.3** was dissolved in  $\text{CDCl}_3$  and placed in a J-Young NMR tube after which 5.0 equiv (42.0  $\mu\text{L}$ ) of *t*BuSH was added. The reaction was heated at 80 °C for 1 h and the volatiles were removed under vacuum.  $\text{CDCl}_3$  was added and the product  $\text{NMe}_2\text{-C}_6\text{H}_4\text{-B(SiMe}_2)_2$  was characterized using multi-nuclear NMR spectroscopy.

$^1\text{H}$  NMR (500 MHz,  $\text{CDCl}_3$ )  $\delta$  7.21 (ddd,  $J = 8.2, 7.3, 1.8$  Hz, 1H), 7.15 (dd,  $J = 7.3, 1.7$  Hz, 1H), 6.81 – 6.76 (m, 2H), 2.94 (s, 6H), 1.40 (s, 18H).

$^{13}\text{C}\{^1\text{H}\}$  NMR (126 MHz,  $\text{CDCl}_3$ )  $\delta$  153.5 (s), 133.0 (s), 129.3 (s), 118.1 (s), 115.1 (s), 48.0 (s), 43.7 (s), 32.8 (s). The carbon linked directly to boron was not observed.

$^{11}\text{B}\{^1\text{H}\}$  NMR (160 MHz,  $\text{CDCl}_3$ )  $\delta$  62.5 (s).

#### Borylated thiols, product of **Figure 67**

All catalytic experiments were carried out in  $\text{CDCl}_3$  in standard NMR tubes for experiments at 60 °C, and in J-Young tubes for experiments at 80 °C. Some compounds were also prepared starting with 500 mg of the respective thiols and isolated either by distillation or recrystallization, in those cases the complete procedure is described. As previously reported,<sup>214</sup> thioboranes exhibit significant air and moisture sensitivity and no satisfactory EA and HRMS could be obtained.

**Method A:** In a glovebox, 400  $\mu\text{L}$  of a solution containing 2.5 mg/mL (1.0 mg / 400  $\mu\text{L}$ ) of the catalyst **3.3** in  $\text{CDCl}_3$  (0.0038 mmol, 2.5 mol%) and 24  $\mu\text{L}$  of HBPin (0.165 mmol, 1.1 equiv) were added to an NMR tube. The substrate (0.150 mmol, 1.0 equiv) was subsequently added. Liquid substrates were added with a micropipette outside the glovebox and solid substrates were weighted and added inside the glovebox. The reaction was left in an oil bath at 60 °C and  $^1\text{H}$  NMR spectra were taken periodically until complete conversion was observed.

**Method B:** The procedure is the same as in method A with the exception that a solution containing 10 mg/mL of the catalyst (increasing the catalyst loading at 10 mol%) and a temperature of 80 °C were used.

**Method C:** The procedure is the same as in method B with the exception that the quantity of HBPin was doubled (48  $\mu\text{L}$  0.330 mmol, 2.2 equiv).

**Phenylsulfur pinacolborane.** 30.0 mg (2.5 mol%) of **3.3** was placed in a Schlenk tube and dissolved in about 4 mL of toluene. 500 mg of thiophenol (1 equiv) was then added followed by the addition of 725  $\mu\text{L}$  (1.1 eq) of HBPin. The reaction was then heated at 60 °C for about 2 h after which the solution was evaporated to dryness. The reaction was followed by the release of  $\text{H}_2$  causing effervescence. The residual oil was distilled under reduced pressure (boiling point of 75 °C at 1 mbar). 832 mg (78% yield) of the title compound was obtained.  $^1\text{H}$  NMR (400 MHz,  $\text{CDCl}_3$ )  $\delta$  7.53 – 7.47 (m, 2H), 7.31 – 7.19 (m, 3H), 1.31 (s, 12H).  $^{13}\text{C}\{^1\text{H}\}$  NMR (101 MHz,  $\text{CDCl}_3$ )  $\delta$  135.5 (s), 131.6 (s), 129.9 (s), 129.9 (s), 85.2 (s), 24.5 (s).  $^{11}\text{B}\{^1\text{H}\}$  NMR (160 MHz,  $\text{CDCl}_3$ )  $\delta$  32.9.

**ortho-Fluorophenylsulfur pinacolborane.** Synthesized using method A.  $^1\text{H}$  NMR (400 MHz,  $\text{CDCl}_3$ )  $\delta$  7.53 (m, 1H), 7.24 (m, 1H), 7.06 (m, 2H), 1.29 (s, 12H).  $^{13}\text{C}\{^1\text{H}\}$  NMR (126 MHz,  $\text{CDCl}_3$ )  $\delta$  161.9 (d,  $J = 246.4$  Hz), 135.8 (s), 129.2 (d,  $J = 7.66$  Hz), 124.2 (d,  $J = 3.83$  Hz), 116.8 (d,  $J = 18.6$



Hz), 115.7 (d,  $J = 23.3$  Hz), 85.5 (s), 24.4 (s).  $^{11}\text{B}\{^1\text{H}\}$  NMR (160 MHz,  $\text{CDCl}_3$ )  $\delta$  32.4.  $^{19}\text{F}$  NMR (376 MHz,  $\text{CDCl}_3$ )  $\delta$  -106.5 (td,  $J = 7.7, 5.3$  Hz, 1F).

**meta-Fluorophenylsulfur pinacolborane.** Synthesized using method A.  $^1\text{H}$  NMR (400 MHz,  $\text{CDCl}_3$ )  $\delta$  7.32 – 7.13 (m, 3H), 6.97 – 6.86 (m, 1H), 1.31 (s, 12H).  $^{13}\text{C}\{^1\text{H}\}$  NMR (126 MHz,  $\text{CDCl}_3$ )  $\delta$  162.3 (d,  $J = 247.2$  Hz), 131.9 (d,  $J = 8.4$  Hz), 129.7 (d,  $J = 8.5$  Hz), 128.5 (d,  $J = 3.0$  Hz), 119.8 (d,  $J = 23.2$  Hz), 113.8 (d,  $J = 21.1$  Hz), 85.5 (s), 24.5 (s).  $^{11}\text{B}\{^1\text{H}\}$  NMR (160 MHz,  $\text{CDCl}_3$ )  $\delta$  32.6.  $^{19}\text{F}$  NMR (376 MHz,  $\text{CDCl}_3$ )  $\delta$  -112.7 – 112.8 (m, 1F).

**para-Fluorophenylsulfur pinacolborane.** Synthesized using method A.  $^1\text{H}$  NMR (400 MHz,  $\text{CDCl}_3$ )  $\delta$  7.46 – 7.38 (m, 2H), 7.00 – 6.92 (m, 2H), 1.29 (s, 12H).  $^{13}\text{C}\{^1\text{H}\}$  NMR (126 MHz,  $\text{CDCl}_3$ ) :  $\delta$  162.0 (d,  $J = 246.1$  Hz), 134.8 (d,  $J = 8.08$  Hz), 124.6 (d,  $J = 3.51$  Hz), 115.7 (d,  $J = 21.9$  Hz), 85.4 (s), 24.5 (s).  $^{11}\text{B}\{^1\text{H}\}$  NMR (160 MHz,  $\text{CDCl}_3$ )  $\delta$  32.8.  $^{19}\text{F}$  NMR (376 MHz,  $\text{CDCl}_3$ )  $\delta$  -115.6 (ddd,  $J = 13.8, 8.58, 5.08$  Hz, 1F).

**ortho-Chlorophenylsulfur pinacolborane.** Synthesized using method A.  $^1\text{H}$  NMR (500 MHz,  $\text{CDCl}_3$ )  $\delta$  7.69 – 7.65 (m, 1H), 7.43 – 7.39 (m, 1H), 7.23 – 7.16 (m, 2H), 1.31 (s, 12H).  $^{13}\text{C}\{^1\text{H}\}$  NMR (126 MHz,  $\text{CDCl}_3$ )  $\delta$  137.3 (s), 135.8 (s), 129.8 (s), 129.2 (s), 128.5 (s), 126.8 (s), 85.5 (s), 24.5 (s).  $^{11}\text{B}\{^1\text{H}\}$  NMR (160 MHz,  $\text{CDCl}_3$ )  $\delta$  32.4.

**meta-Chlorophenylsulfur pinacolborane.** Synthesized using method A.  $^1\text{H}$  NMR (500 MHz,  $\text{CDCl}_3$ )  $\delta$  7.54 – 7.49 (m, 1H), 7.39 (dt,  $J = 6.7, 1.9$  Hz, 2H), 7.23 – 7.17 (m, 2H), 1.32 (s, 12H).  $^{13}\text{C}\{^1\text{H}\}$  NMR (126 MHz,  $\text{CDCl}_3$ )  $\delta$  134.1 (s, 1C), 132.7 (s), 131.7 (s), 131.1 (s), 129.6 (s), 127.0 (s), 85.5 (s), 24.5 (s).  $^{11}\text{B}\{^1\text{H}\}$  NMR (160 MHz,  $\text{CDCl}_3$ )  $\delta$  32.7.

**para-Chlorophenylsulfur pinacolborane.** Synthesized using method A.  $^1\text{H}$  NMR (400 MHz,  $\text{CDCl}_3$ )  $\delta$  7.45 – 7.38 (m, 2H), 7.27 – 7.19 (m, 2H), 1.30 (s, 12H).  $^{13}\text{C}\{^1\text{H}\}$  NMR (101 MHz,  $\text{CDCl}_3$ )  $\delta$  134.3 (s), 132.9 (s), 128.8 (s), 128.2 (s), 85.4 (s), 24.5 (s).  $^{11}\text{B}\{^1\text{H}\}$  NMR (160 MHz,  $\text{CDCl}_3$ )  $\delta$  32.7.

**ortho-Bromophenylsulfur pinacolborane.** Synthesized using method A.  $^1\text{H}$  NMR (400 MHz,  $\text{CDCl}_3$ )  $\delta$  7.69 (dd,  $J = 7.8, 1.7$  Hz, 1H), 7.59 (dd,  $J = 8.0, 1.5$  Hz, 1H), 7.27 – 7.22 (m, 1H), 7.11 (m, 1H), 1.30 (s, 12H).  $^{13}\text{C}\{^1\text{H}\}$  NMR (126 MHz,  $\text{CDCl}_3$ )  $\delta$  135.6, 133.1, 131.4, 128.6, 127.5, 85.5, 24.5.  $^{11}\text{B}\{^1\text{H}\}$  NMR (160 MHz,  $\text{CDCl}_3$ )  $\delta$  32.6.

**meta-Bromophenylsulfur pinacolborane.** Synthesized using method A.  $^1\text{H}$  NMR (500 MHz,  $\text{CDCl}_3$ )  $\delta$  7.67 (t,  $J = 1.8$  Hz, 1H), 7.43 (ddd,  $J = 7.9, 1.8, 1.0$  Hz, 1H), 7.36 (ddd,  $J = 8.0, 2.0, 1.0$  Hz, 1H), 7.13 (t,  $J = 7.9$  Hz, 1H), 1.32 (s, 12H).  $^{13}\text{C}\{^1\text{H}\}$  NMR (126 MHz,  $\text{CDCl}_3$ )  $\delta$  135.5 (s), 131.6 (s), 129.9 (s), 129.9 (s), 122.2 (s), 85.2 (s), 24.5 (s). The quaternary carbon bonded to the sulfur atom could not be assigned.  $^{11}\text{B}\{^1\text{H}\}$  NMR (160 MHz,  $\text{CDCl}_3$ )  $\delta$  32.6.

**para-Bromophenylsulfur pinacolborane.** Synthesized using method A.  $^1\text{H}$  NMR (500 MHz,  $\text{CDCl}_3$ )  $\delta$  7.41 – 7.35 (m, 4H), 1.31 (s, 12H).  $^{13}\text{C}\{^1\text{H}\}$  NMR (126 MHz,  $\text{CDCl}_3$ )  $\delta$  136.3 (s), 134.6 (s), 132.4 (s), 131.7 (s), 85.5 (s), 24.5 (s).  $^{11}\text{B}\{^1\text{H}\}$  NMR (160 MHz,  $\text{CDCl}_3$ )  $\delta$  32.6.

**ortho-Methoxyphenylsulfur pinacolborane.** Synthesized using method A.  $^1\text{H}$  NMR (400 MHz,  $\text{CDCl}_3$ )  $\delta$  7.53 (dd,  $J = 8.25, 1.67$  Hz, 2H), 7.25 (ddd,  $J = 8.25, 7.47, 1.95$  Hz, 2H), 3.85 (s, 3H), 1.28 (s, 12H).  $^{13}\text{C}\{^1\text{H}\}$  NMR (126 MHz,  $\text{CDCl}_3$ ) 158.5 (s), 135.3 (s), 128.7 (s), 120.8 (s), 117.7 (s), 110.9 (s), 85.0 (s), 55.7 (s), 24.5 (s).  $^{11}\text{B}\{^1\text{H}\}$  NMR (160 MHz,  $\text{CDCl}_3$ ) :  $\delta$  32.7.

**meta-Methoxyphenylsulfur pinacolborane.** 23.7 mg (2.5 mol%) of **3.3** was placed in a Schlenk tubed and dissolved in about 4 mL of toluene. 500 mg of *meta*-methoxythiophenol (1 equiv) was then added and followed by the addition of 570  $\mu\text{L}$  (1.1 equiv) of HBPIn. The reaction was then heated at 60  $^\circ\text{C}$  for about 4 h after which the solution was evaporated to dryness. The reaction can be followed by the release of  $\text{H}_2$  causing effervescence. The residual oil was distilled under reduced pressure (boiling point of 85  $^\circ\text{C}$  at 1 mbar). 761 mg (80% yield) of the title compound was obtained.  $^1\text{H}$  NMR (400 MHz,  $\text{CDCl}_3$ )  $\delta$  7.20 – 7.15 (m, 1H), 7.09 – 7.06 (m, 2H), 6.78 (ddd,  $J = 8.2, 2.3, 1.3$  Hz, 1H), 3.79 (s, 3H), 1.31 (s, 12H).  $^{13}\text{C}\{^1\text{H}\}$  (126 MHz,  $\text{CDCl}_3$ )  $\delta$  159.4 (s), 130.7 (s), 129.4 (s), 125.3 (s), 118.2 (s), 112.9 (s), 85.3 (s), 55.2 (s), 24.5 (s).  $^{11}\text{B}\{^1\text{H}\}$  (160 MHz,  $\text{CDCl}_3$ )  $\delta$  32.8.

**para-Methoxyphenylsulfur pinacolborane.** Synthesized using method A.  $^1\text{H}$  NMR (400 MHz,  $\text{CDCl}_3$ )  $\delta$  7.38 (d,  $J = 8.9$  Hz, 2H), 6.82 (d,  $J = 8.8$  Hz, 2H), 3.78 (s, 3H), 1.29 (s, 12H).  $^{13}\text{C}\{^1\text{H}\}$  NMR

(126 MHz, CDCl<sub>3</sub>) δ 158.8 (s), 134.5 (s), 119.9 (s), 114.4 (s), 85.16 (s), 55.2 (s), 24.5 (s). <sup>11</sup>B {<sup>1</sup>H} NMR (160 MHz, CDCl<sub>3</sub>) δ 33.0.

**ortho-Methylphenylsulfur pinacolborane.** Synthesized using method A. <sup>1</sup>H NMR (400 MHz, CDCl<sub>3</sub>) δ 7.59 – 7.50 (m, 1H), 7.23 – 7.08 (m, 3H), 2.43 (s, 3H), 1.29 (s, 12H). <sup>13</sup>C {<sup>1</sup>H} NMR (126 MHz, CDCl<sub>3</sub>) δ 140.5 (s, 1C), 134.9 (s), 130.2 (s), 128.9 (s), 127.4 (s), 126.1 (s), 85.2 (s), 24.5 (s), 21.6 (s). <sup>11</sup>B {<sup>1</sup>H} NMR (160 MHz, CDCl<sub>3</sub>) δ 32.7.

**meta-Methylphenylsulfur pinacolborane.** Synthesized using method A. <sup>1</sup>H NMR (400 MHz, CDCl<sub>3</sub>) δ 7.37 – 7.28 (m, 2H), 7.16 (dd, *J* = 8.5, 7.4 Hz, 1H), 7.08 – 7.02 (m, 1H), 2.33 (s, 3H), 1.31 (s, 12H). <sup>13</sup>C {<sup>1</sup>H} NMR (126 MHz, CDCl<sub>3</sub>) δ 138.3 (s, 1C), 133.7 (s), 130.1 (s), 128.5 (s), 127.6 (s), 85.2 (s), 24.5 (s), 21.3 (s). The carbon bonded to the sulfur atom could not be assigned. <sup>11</sup>B {<sup>1</sup>H} NMR (160 MHz, CDCl<sub>3</sub>) δ 32.9.

**para-Methylphenylsulfur pinacolborane.** 26.8 mg (2.5 mol%) of **3.3** was placed in a Schlenk tube and dissolved in about 4 mL of toluene. 500 mg of 4-methylthiophenol (1 equiv) was then added, followed by 645 μL of HBPIn (1.1 equiv). The reaction was then heated at 60 °C for 2 h after which the solution was evaporated to dryness. The reaction was followed by the release of H<sub>2</sub> causing effervescence. The residual white solid was dissolved in hot hexane, the mixture was filtered and placed at -35 °C overnight. The next morning, an appreciable amount of white crystals had formed. The supernatant was removed and the crystals dried under vacuum. 525 mg (52% yield) of the title compound was obtained. <sup>1</sup>H NMR (400 MHz, CDCl<sub>3</sub>) δ 7.40 – 7.34 (m, 2H), 7.13 – 7.05 (m, 2H), 2.33 (s, 3H), 1.31 (s, 12H). <sup>13</sup>C {<sup>1</sup>H} NMR (101 MHz, CDCl<sub>3</sub>) δ 136.6 (s, 1C), 133.0 (s), 129.5 (s), 125.9 (s), 85.2 (s), 24.5 (s), 21.1 (s). <sup>11</sup>B {<sup>1</sup>H} NMR (160 MHz, CDCl<sub>3</sub>) δ 32.9.

**Pentafluorophenylsulfur pinacolborane.** Synthesized using method B. <sup>1</sup>H NMR (400 MHz, CDCl<sub>3</sub>) δ 1.28 (s, 12H). <sup>13</sup>C {<sup>1</sup>H} NMR (101 MHz, CDCl<sub>3</sub>) δ 148.6 – 145.0 (m), 142.2 – 139.6 (m), 139.1 – 136.4 (m), 86.4 (s), 24.3 (s). The quaternary carbon bonded to the sulfur atom could not be assigned. <sup>11</sup>B {<sup>1</sup>H} NMR (160 MHz, CDCl<sub>3</sub>) δ 31.6. <sup>19</sup>F NMR (376 MHz, CDCl<sub>3</sub>) δ -131.54 – -131.67 (m, 2F), -154.20 (tt, *J* = 21.1, 1.9 Hz, 1F), -161.70 – -161.97 (m, 2F).

**2,6-dimethylphenylsulfur pinacolborane.** Synthesized using method C. <sup>1</sup>H NMR (500 MHz, CDCl<sub>3</sub>) δ 7.11 (s, 3H), 2.47 (s, 6H), 1.27 (s, 12H). <sup>13</sup>C {<sup>1</sup>H} NMR (101 MHz, CDCl<sub>3</sub>) δ 142.1 (s), 128.5 (s, 1 or 2C), 127.8 (s), 127.4 (s, 1 or 2C), 85.0 (s), 24.5 (s), 22.8 (s). <sup>11</sup>B {<sup>1</sup>H} NMR (160 MHz, CDCl<sub>3</sub>) δ 32.4.

**Decanesulfur pinacolborane.** Synthesized using method B. <sup>1</sup>H NMR (400 MHz, CDCl<sub>3</sub>) δ 2.64 (t, *J* = 7.3 Hz, 2H), 1.63 – 1.53 (m, 2H), 1.43 – 1.14 (m, 26H), 0.87 (t, *J* = 6.9 Hz, 3H). <sup>13</sup>C {<sup>1</sup>H} NMR (126 MHz, CDCl<sub>3</sub>) δ 84.6 (s), 32.4 (s), 31.9 (s), 29.6 (s), 29.5 (s), 29.3 (s), 29.1 (s), 28.5 (s), 26.6 (s), 24.5 (s), 22.7 (s), 14.1 (s). <sup>11</sup>B {<sup>1</sup>H} NMR (160 MHz, CDCl<sub>3</sub>) δ 33.5.

**Cyclohexylsulfur pinacolborane.** Synthesized using method B. <sup>1</sup>H NMR (400 MHz, CDCl<sub>3</sub>) : δ 3.16 – 3.04 (m, 1H), 2.00 – 1.93 (m, 2H), 1.76 – 1.68 (m, 3H), 1.46 – 1.28 (m, 5H), 1.27 (s, 12H). <sup>13</sup>C {<sup>1</sup>H} NMR (126 MHz, CDCl<sub>3</sub>) δ 84.4 (s), 44.1 (s), 40.4 (s), 36.4 (s), 26.2 (s), 25.5 (s), 24.9 (s), 24.5 (s). <sup>11</sup>B {<sup>1</sup>H} NMR (160 MHz, CDCl<sub>3</sub>, borosilicate tube) : δ 33.4.

**tert-Butylsulfur pinacolborane.** 36.8 mg (2.5 mol%) of **3.3** was placed in a Schlenk tube and dissolved in about 4 mL of toluene. 500 mg of *tert*-butylthiol (1 equiv) was then added, followed by the addition of 885 μL (1.1 eq) of HBPIn. The reaction was then heated at 60 °C for about 20 h after which the solution was evaporated to dryness under reduced pressure. The reaction was followed by the release of H<sub>2</sub> causing effervescence. The residual colorless oil was distilled under reduced pressure (boiling point of 35 °C at a pressure of 1 mbar). 1.164 g (76% yield) of the title compound was obtained. <sup>1</sup>H NMR (400 MHz, CDCl<sub>3</sub>) δ 1.46 (s, 9H), 1.28 (s, 12H). <sup>13</sup>C {<sup>1</sup>H} NMR (126 MHz, CDCl<sub>3</sub>) δ 84.1 (s), 43.8 (s), 33.5 (s), 24.5 (s). <sup>11</sup>B {<sup>1</sup>H} NMR (160 MHz, CDCl<sub>3</sub>) δ 33.1.

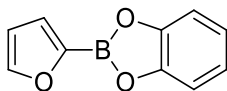
**Benzylsulfur pinacolborane.** Synthesized using method A. <sup>1</sup>H NMR (400 MHz, CDCl<sub>3</sub>) δ 7.38 – 7.35 (m, 2H), 7.33 – 7.28 (m, 2H), 7.26 – 7.22 (m, 1H), 3.92 (s, 2H), 1.32 (s, 12H). <sup>13</sup>C {<sup>1</sup>H} NMR (126 MHz, CDCl<sub>3</sub>) δ 140.5 (s), 128.6 (s), 128.4 (s), 126.8 (s), 85.1 (s), 30.7 (s), 24.6 (s). <sup>11</sup>B {<sup>1</sup>H} NMR (160 MHz, CDCl<sub>3</sub>) δ 33.5.

**Furfurylsulfur Pinacolborane.** 29.0 mg (2.5 mol%) of **3.3** was placed in a Schlenk tube and dissolved in about 4 mL of toluene. 500 mg of 2-furanmethanethiol (1 equiv) was then added and followed by the addition of 700  $\mu\text{L}$  (1.1 eq) of HBPIn. The reaction was then heated at 60 °C for about 2 h after which the solution was evaporated to dryness. The reaction was followed by the release of  $\text{H}_2$  causing effervescence. The residual colorless oil was distilled under reduced pressure (boiling point 60 °C at about 1 mbar). 978 mg (93% yield) of the title compound was obtained.  $^1\text{H}$  NMR (500 MHz,  $\text{CDCl}_3$ )  $\delta$  7.31 (s, 1H), 6.28 (s, 1H), 6.18 (s, 1H), 3.90 (s, 2H), 1.30 (s, 12H).  $^{13}\text{C}\{^1\text{H}\}$  NMR (126 MHz,  $\text{CDCl}_3$ )  $\delta$  153.4 (s), 141.6 (s), 110.3 (s), 106.7 (s), 85.1 (s), 24.5 (s), 22.9 (s).  $^{11}\text{B}\{^1\text{H}\}$  NMR (160 MHz,  $\text{CDCl}_3$ )  $\delta$  33.4.

**Phenylselenenyl pinacolborane.** Synthesized using method C.  $^1\text{H}$  NMR (500 MHz,  $\text{CDCl}_3$ )  $\delta$  7.62 – 7.56 (m, 2H), 7.26 – 7.19 (m, 3H), 1.32 (s, 12H).  $^{13}\text{C}\{^1\text{H}\}$  NMR (101 MHz,  $\text{CDCl}_3$ )  $\delta$  134.4 (s), 129.2 (s), 128.9 (s), 126.7 (s), 85.6 (s), 24.6 (s).  $^{11}\text{B}\{^1\text{H}\}$  NMR (160 MHz,  $\text{CDCl}_3$ )  $\delta$  33.8.

## Chapter 7

### Compound 7.2



In a typical synthesis, 3 g of 2-Furanylboronic acid was dissolved in *ca.* 150 mL of toluene along with 1 equiv. of pyrocatechol. The reaction flask was then directly placed on the rotary evaporator with the heating bath at 50 °C and the solution evaporated at *ca.* 65 mbar. The grayish solid was then further dried on the rotary evaporator at *ca.* 25 mbar. The resulting solid was then dissolved in *ca.* 150 mL of hexane, filtered and stored at -30 °C overnight, during which the title compound crystallized. The supernatant was removed and the solid dried under vacuum. 3.86 g (77 % yield) of the title compound was obtained as a white fluffy powder. Slow degradation of the product was observed at room temperature, so the next product batches were kept at -30 °C as precaution.

$^1\text{H}$  NMR (500 MHz,  $\text{CDCl}_3$ )  $\delta$  7.81 (dd,  $J = 1.6, 0.6$  Hz, 1H), 7.41 (dd,  $J = 3.4, 0.5$  Hz, 1H), 7.32 (dd,  $J = 5.9, 3.3$  Hz, 2H), 7.14 (dd,  $J = 5.9, 3.3$  Hz, 2H), 6.58 (dd,  $J = 3.4, 1.6$  Hz, 1H).

$^{13}\text{C}\{^1\text{H}\}$  NMR (126 MHz,  $\text{CDCl}_3$ )  $\delta$  148.66 (s), 147.99 (s), 125.37 (s), 123.01 (s), 112.68 (s), 110.98 (s), the carbon linked to boron was not observed.

$^{11}\text{B}\{^1\text{H}\}$  NMR (160 MHz,  $\text{CDCl}_3$ )  $\delta$  28.3 (s)

Standart procedure for the transfer borylation reported in **Figure 75**

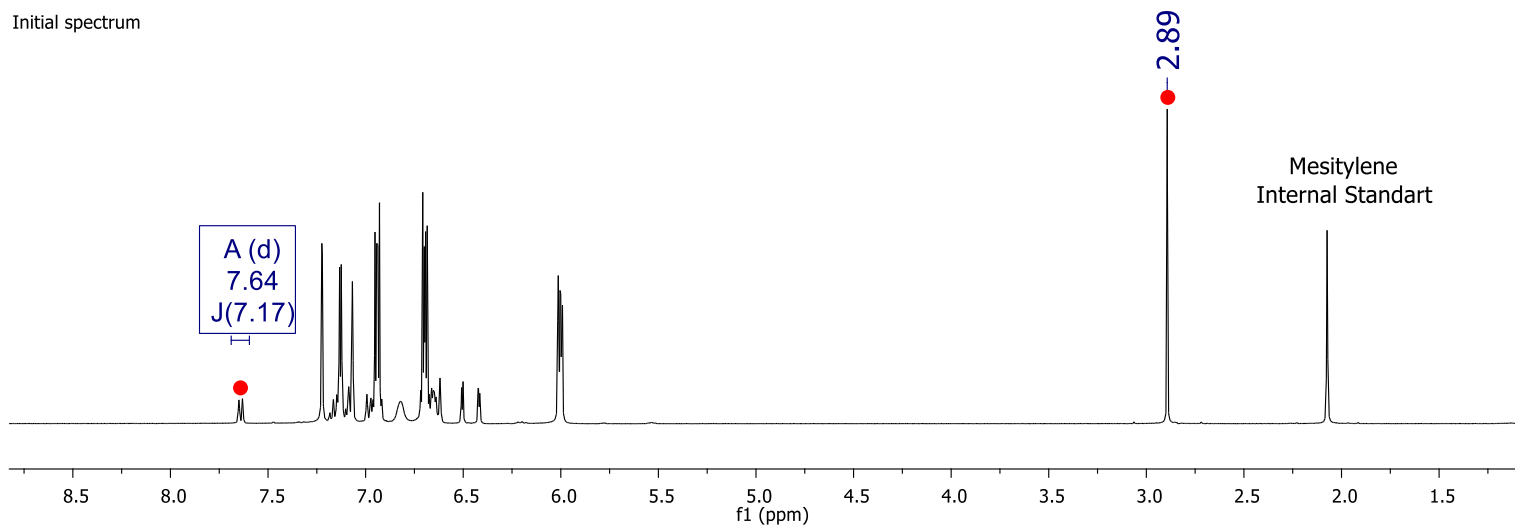
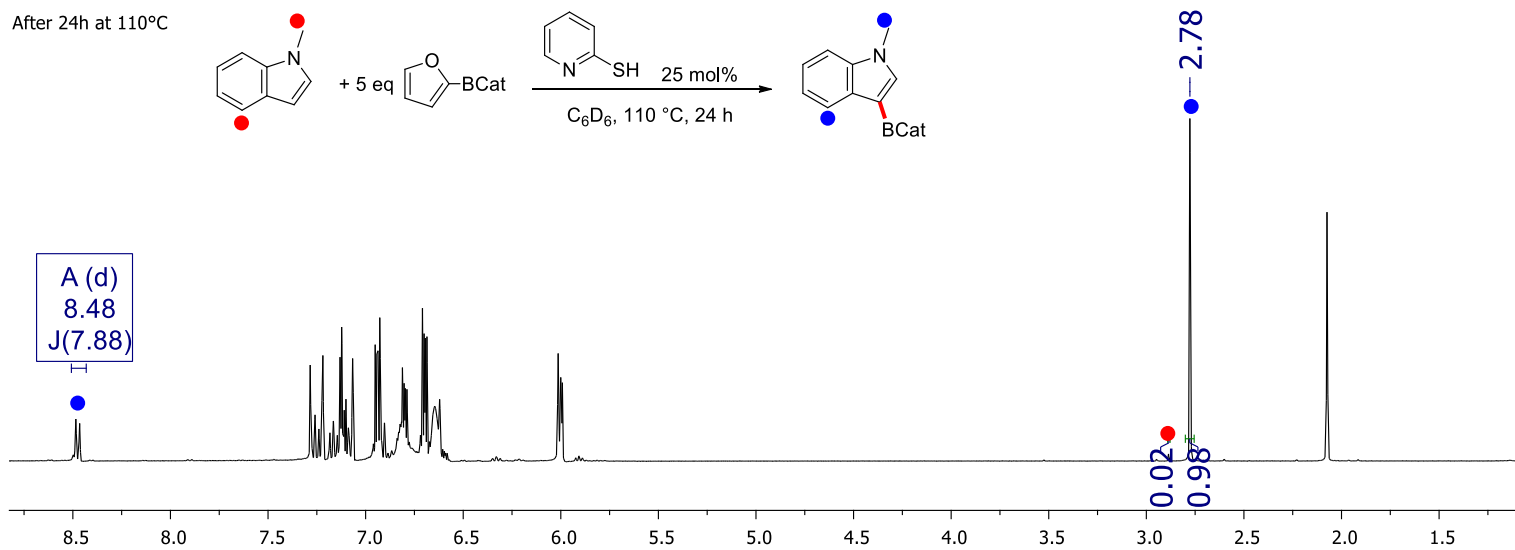
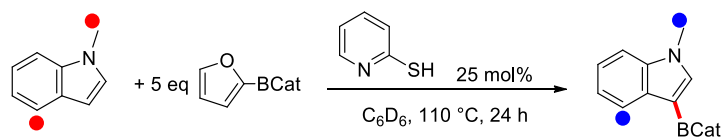
In a standard test run, a solution of 2.5 mg (25 mol%) of 2-mercaptopyridine, 84 mg (5 equiv.) of 2-FurylBCat and 3.2 mg (*ca.* 30 mol%) of mesitylene (internal standart) per 0.5 mL of  $\text{C}_6\text{D}_6$  was prepared. Then, 0.5 mL of the solution was added to 1 equiv. of the substrate, and a small aliquot was taken and analyzed by GC-MS as a reference point. The solution was transferred to a J-Young tube and analyzed by  $^1\text{H}$  NMR as a reference point. The mixture was then heated at 110 °C for 24 h and analyzed by  $^1\text{H}$  NMR. In the following section the initial and final spectra are presented. In all cases the conversion was calculated using the most characteristic signals of the substrates and products. Details for each substrate are given directly on each spectrum. After, 10 equiv. of pinacol and 3.3 equiv. of  $\text{NEt}_3$  in 1 mL of toluene was added to the reaction, the tube was shaken and left to react for 1 h before it was analyzed by GC-MS. GC-MS data are also presented in the following section. It is to note that during the transesterification to pinacol some protodeborylation may occur. Thus the starting materials signals are observed in all GC-traces. Signals of pinacol converted residual

borlyating agent and mesitylene (internal standart) are also present at 5.90 and 4.44 min respectively. All manipulations were performed outside the glovebox in a not air-conditioned laboratory during summer time with temperatures between 25-35 °C and with 80-100 % humidity.

Representative results for compound **7.7a**

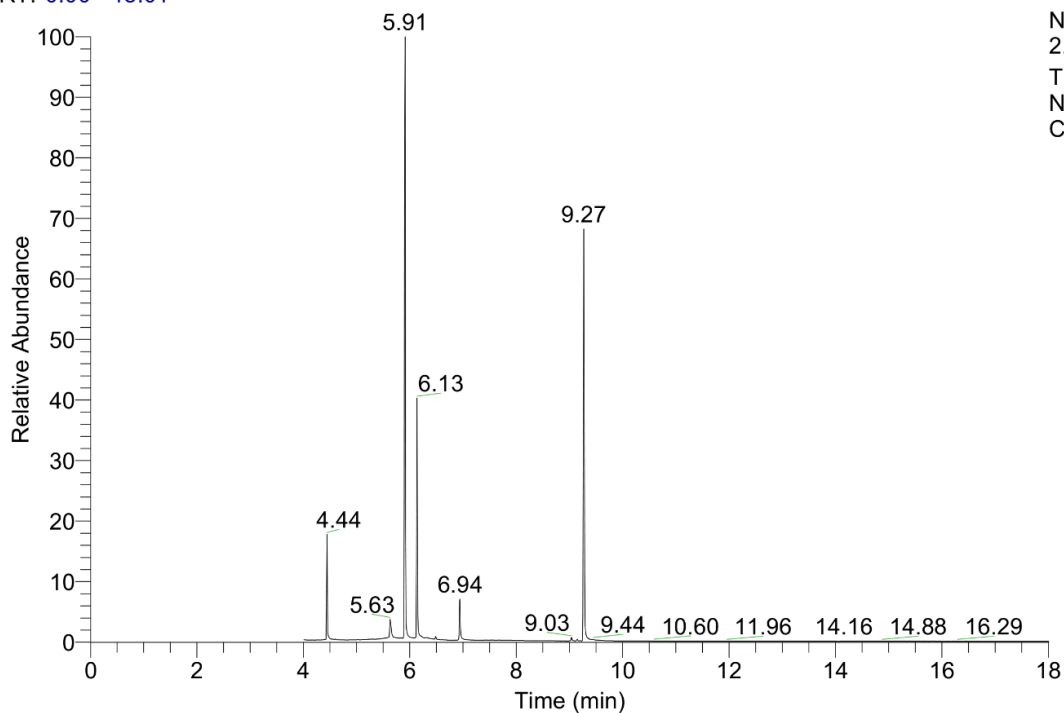
Compounds **7.7b-v** were characterized the same way, but for space and relevance reasons, only **7.7a** data are presented.

After 24h at 110°C

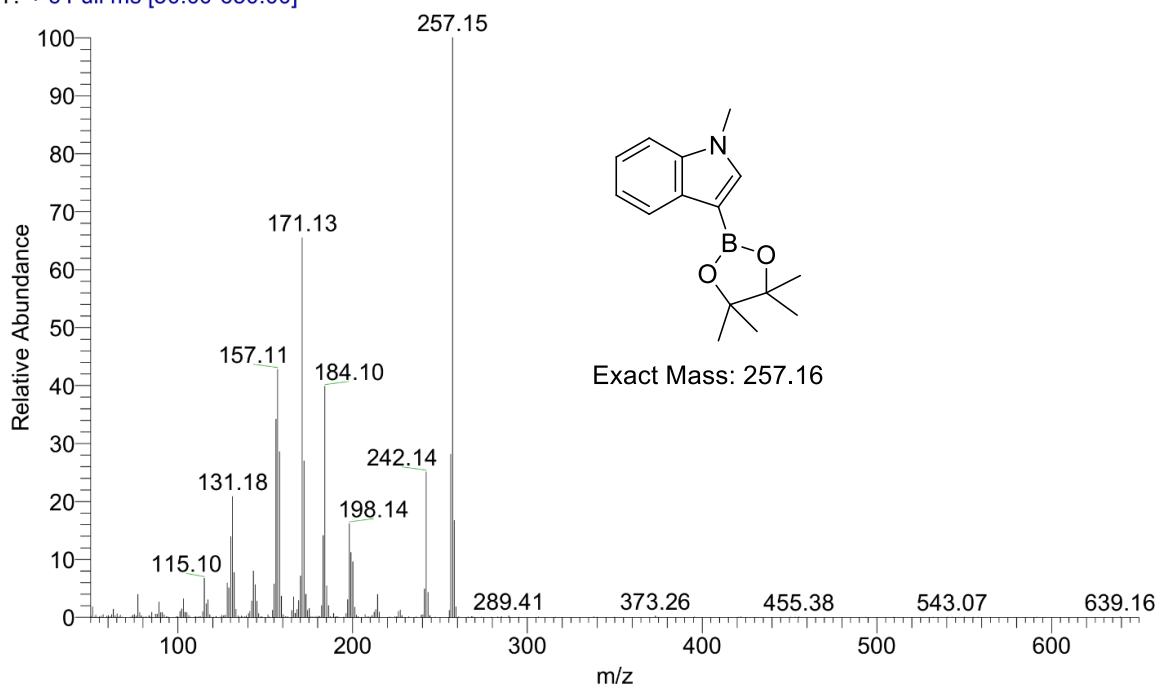


The conversion was determined using the N-Methyl signal that shifts from 2.89 in the starting material to 2.78 ppm in the product. A significant shift of the signal associated to the C4 proton from 7.64 to 8.48 ppm was also observed. The product signals are coherent with the literature

RT: 0.00 - 18.01

NL:  
2.86E7  
TIC MS  
NMeIndole\_  
ConvBPin\_

Created by free version of DocuFreezer

NMeIndole\_ConvBPin #600 RT: 9.27 AV: 1 NL: 2.96E6  
T: + c Full ms [50.00-650.00]

## Bibliography

- (1) Anastas, P. T.; Warner, J. C. *Green Chemistry: Theory and Practice*; 1998.
- (2) Seele, P.; Gatti, L. Greenwashing Revisited: In Search of a Typology and Accusation-Based Definition Incorporating Legitimacy Strategies. *Bus. Strateg. Environ.* **2017**, *26* (2), 239–252.
- (3) Canada, G. of. Canadian Environmental Assessment Act, 2012 <https://laws-lois.justice.gc.ca/eng/acts/C-15.21/> (accessed Jan 10, 2019).
- (4) Center in Green Chemistry and Catalysis <http://ccvc.research.mcgill.ca/research/research.html> (accessed Nov 16, 2018).
- (5) Trost, B. M. Atom Economy—A Challenge for Organic Synthesis: Homogeneous Catalysis Leads the Way. *Angew. Chemie Int. Ed. English* **1995**, *34* (3), 259–281.
- (6) Sheldon, R. A. The: E Factor 25 Years on: The Rise of Green Chemistry and Sustainability. *Green Chem.* **2017**, *19* (1), 18–43.
- (7) Van Aken, K.; Streckowski, L.; Patiny, L. EcoScale, a Semi-Quantitative Tool to Select an Organic Preparation Based on Economical and Ecological Parameters. *Beilstein J. Org. Chem.* **2006**, *2*, 1–7.
- (8) Gałuszka, A.; Migaszewski, Z. M.; Konieczka, P.; Namieśnik, J. Analytical Eco-Scale for Assessing the Greenness of Analytical Procedures. *TrAC - Trends Anal. Chem.* **2012**, *37*, 61–72.
- (9) Klucznik, T.; Mikulak-Klucznik, B.; McCormack, M. P.; Lima, H.; Szymkuć, S.; Bhowmick, M.; Molga, K.; Zhou, Y.; Rickershauser, L.; Gajewska, E. P.; Touthkine, A.; Dittwald, P.; Startek, M. P.; Kirkovits, G. J.; Roszak, R.; Adamski, A.; Sieredzińska, B.; Mrksich, M.; Trice, S. L. J.; Grzybowski, B. A. Efficient Syntheses of Diverse, Medicinally Relevant Targets Planned by Computer and Executed in the Laboratory. *Chem* **2018**, *4* (3), 522–532.
- (10) Nuss, P.; Eckelman, M. J. Life Cycle Assessment of Metals: A Scientific Synthesis. *PLoS One* **2014**, *9* (7), e101298.
- (11) Heck, K. F.; Nolley, J. P. Palladium-Catalyzed Vinylic Hydrogen Substitution Reactions with Aryl, Benzyl, and Styryl Halides. *J. Org. Chem.* **1972**, *37* (14), 2320–2322.
- (12) Cabri, W.; Candiani, I. Recent Developments and New Perspectives in the Heck Reaction. *Acc. Chem. Res.* **1995**, *28* (1), 2–7.
- (13) Beletskaya, I. P.; Cheprakov, A. V. Heck Reaction as a Sharpening Stone of Palladium Catalysis. *Chem. Rev.* **2000**, *100* (8), 3009–3066.
- (14) Miyaura, N.; Yamada, K.; Suzuki, A. A New Stereospecific Cross-Coupling by the Palladium-Catalyzed Reaction of 1-Alkenylboranes with 1-Alkenyl or 1-Alkynyl Halides. *Tetrahedron Lett.* **1979**, No. 36, 3437–3440.
- (15) Miyaura, N.; Suzuki, A. Palladium-Catalyzed Cross-Coupling Reactions of Organoboron Compounds. *Chem. Rev.* **1995**, No. 1, 2457–2483.
- (16) Sonogashira, K. Development of Pd – Cu Catalyzed Cross-Coupling of Terminal Acetylenes with Sp<sup>2</sup>-Carbon Halides. *J. Organomet. Chem.* **2002**, *653*, 46–49.

- (17) Chinchilla, R.; Nájera, C. The Sonogashira Reaction: A Booming Methodology in Synthetic Organic Chemistry. *Chem. Rev.* **2007**, *107* (3), 874–922.
- (18) Chinchilla, R.; Nájera, C. Recent Advances in Sonogashira Reactions. *Chem. Soc. Rev.* **2011**, *40* (10), 5084–5121.
- (19) Paul, F.; Patt, J.; Hartwig, J. F. Palladium-Catalyzed Formation of Carbon-Nitrogen Bonds. Reaction Intermediates and Catalyst Improvements in the Hetero Cross-Coupling of Aryl Halides and Tin Amides. *J. Am. Chem. Soc.* **1994**, *116* (13), 5969–5970.
- (20) Guram, A. S.; Buchwald, S. L. Palladium-Catalyzed Aromatic Animations with in Situ Generated Aminostannanes. *J. Am. Chem. Soc.* **1994**, *116* (17), 7901–7902.
- (21) Knowles, W. S. Application of Organometallic Catalysis to the Commercial Production of L-DOPA. *J. Chem. Educ.* **1986**, *63* (3), 222.
- (22) Gridnev, I. D.; Imamoto, T. On the Mechanism of Stereoselection in Rh-Catalyzed Asymmetric Hydrogenation: A General Approach for Predicting the Sense of Enantioselectivity. *Acc. Chem. Res.* **2004**, *37* (9), 633–644.
- (23) Noyori, R.; Ohkuma, T.; Kitamura, M.; Takaya, H.; Sayo, N.; Kumobayashi, H.; Akutagawa, S. Asymmetric Hydrogenation of  $\beta$ -Keto Carboxylic Esters. A Practical, Purely Chemical Access to  $\beta$ -Hydroxy Esters in High Enantiomeric Purity. *J. Am. Chem. Soc.* **1987**, *109* (19), 5856–5858.
- (24) Lightfoot, A.; Schnider, P.; Pfaltz, A. Enantioselective Hydrogenation of Olefins with Phosphinooxazoline-Iridium Catalysts. *Angew. Chem. Int. Ed.* **1998**, *37*, 2897–2899.
- (25) Church, T. L.; Andersson, P. G. Iridium Catalysts for the Asymmetric Hydrogenation of Olefins with Nontraditional Functional Substituents. *Coord. Chem. Rev.* **2008**, *252* (5–7), 513–531.
- (26) *USP Chapter <232> Elemental Impurities- Limits, Pharmacopeial Forum*, *42*(2), March-April 2016.
- (27) *ICH Guideline Q3D on Elemental Impurities, EMA/CHMP/ICH/353369/2013*, July 2016.
- (28) Hayler, J. D.; Leahy, D. K.; Simmons, E. M. A Pharmaceutical Industry Perspective on Sustainable Metal Catalysis. *Organometallics* **2018**, *acs.organomet.8b00566*.
- (29) Zweig, J. E.; Kim, D. E.; Newhouse, T. R. Methods Utilizing First-Row Transition Metals in Natural Product Total Synthesis. *Chem. Rev.* **2017**, *117* (18), 11680–11752.
- (30) Akiyama, T.; Itoh, J.; Fuchibe, K. Recent Progress in Chiral Brønsted Acid Catalysis. *Advanced Synthesis and Catalysis*. 2006, pp 999–1010.
- (31) Denmark, S. E.; Beutner, G. L. Lewis Base Catalysis in Organic Synthesis. *Angewandte Chemie - International Edition*. 2008, pp 1560–1638.
- (32) Hashimoto, T.; Maruoka, K. Recent Development and Application of Chiral Phase-Transfer Catalysts. *Chemical Reviews*. 2007, pp 5656–5682.
- (33) Jacobsen, E. N.; Doyle, A. G. Small-Molecule H-Bond Donors in Asymmetric Catalysis. *Chem. Rev.* **2007**, *107*, 5713–5743.
- (34) Thadani, A. N.; Stankovic, A. R.; Rawal, V. H. Enantioselective Diels-Alder Reactions Catalyzed by Hydrogen Bonding. *Proc. Natl. Acad. Sci.* **2004**, *101*, 5846–5850.



- (35) Krause, N.; Hoffmann-Röder, A. Recent Advances in Catalytic Enantioselective Michael Additions. *Synthesis (Stuttg)*. **2001**, 2001 (02), 0171–0196.
- (36) Uraguchi, D.; Terada, M. Chiral Brønsted Acid-Catalyzed Direct Mannich Reactions via Electrophilic Activation. *J. Am. Chem. Soc.* **2004**, 126 (17), 5356–5357.
- (37) List, B. *Asymmetric Organocatalysis*; Springer-Verlag: Berlin, Heidelberg, 2010.
- (38) Gaunt, M. J.; Johansson, C. C. C.; McNally, A.; Vo, N. T. Enantioselective Organocatalysis. *Drug Discov. Today* **2007**, 12, 8–27.
- (39) Welch, G. C.; Juan, R. R. S.; Masuda, J. D.; Stephan, D. W. Reversible, Metal-Free Hydrogen Activation. *Science* **2006**, 314, 1124–1126.
- (40) Fontaine, F. G.; Stephan, D. W. On the Concept of Frustrated Lewis Pairs. *Philos. Trans. R. Soc. A* **2017**, 375 (2101), 20170004.
- (41) Lewis, G. N. *Valence and the Structure of Atoms and Molecules*; Chemical Catalog Company: New York, New York, U.S.A., 1923.
- (42) Wikipedia [https://en.wikipedia.org/wiki/Frustrated\\_Lewis\\_pair](https://en.wikipedia.org/wiki/Frustrated_Lewis_pair) (accessed Nov 16, 2018).
- (43) Stephan, D. W. “Frustrated Lewis Pairs”: A Concept for New Reactivity and Catalysis. *Org. Biomol. Chem.* **2008**, 6 (9), 1535–1539.
- (44) Stephan, D. W.; Erker, G. Frustrated Lewis Pairs: Metal-Free Hydrogen Activation and More. *Angew. Chem. Int. Ed.* **2010**, 49 (1), 46–76.
- (45) Stephan, D. W. Frustrated Lewis Pairs. *J. Am. Chem. Soc.* **2015**, 137 (32), 10018–10032.
- (46) Stephan, D. W. The Broadening Reach of Frustrated Lewis Pair Chemistry. *Science* **2016**, 354 (6317).
- (47) Stephan, D. W. “Frustrated Lewis Pair” Hydrogenations. *Org. Biomol. Chem.* **2012**, 10 (30), 5740–5746.
- (48) Erker, G.; Stephan, D. W. *Frustrated Lewis Pairs II: Expanding the Scope*; Erker, G., Stephan, D. W., Eds.; Springer: Berlin, Heidelberg, 2013; Vol. 334.
- (49) Erker, G.; Stephan, D. W. *Frustrated Lewis Pairs I*; Erker, G., Stephan, D. W., Eds.; Topics in Current Chemistry; Springer: Berlin, Heidelberg, 2013; Vol. 332.
- (50) Hounjet, L. J.; Stephan, D. W. Hydrogenation by Frustrated Lewis Pairs: Main Group Alternatives to Transition Metal Catalysts? *Org. Process Res. Dev.* **2014**, 18 (3), 385–391.
- (51) Stephan, D. W.; Erker, G. Frustrated Lewis Pair Chemistry of Carbon, Nitrogen and Sulfur Oxides. *Chem. Sci.* **2014**, 5 (7), 2625–2641.
- (52) Stephan, D. W.; Erker, G. Frustrated Lewis Pair Chemistry: Development and Perspectives. *Angew. Chem. Int. Ed.* **2015**, 54 (22), 6400–6441.
- (53) Stephan, D. W. Frustrated Lewis Pairs: From Concept to Catalysis. *Acc. Chem. Res.* **2015**, 48 (2), 306–316.
- (54) Weicker, S. A.; Stephan, D. W. Main Group Lewis Acids in Frustrated Lewis Pair Chemistry: Beyond Electrophilic Boranes. *Bull. Chem. Soc. Jpn.* **2015**, 88 (8), 1003–1016.
- (55) Dorkó, É.; Szabó, M.; Kótai, B.; Pápai, I.; Domján, A.; Soós, T. Expanding the Boundaries

- of Water-Tolerant Frustrated Lewis Pair Hydrogenation: Enhanced Back Strain in the Lewis Acid Enables the Reductive Amination of Carbonyls. *Angew. Chem. Int. Ed.* **2017**, *56* (32), 9512–9516.
- (56) Fasano, V.; Ingleson, M. J. Expanding Water/Base Tolerant Frustrated Lewis Pair Chemistry to Alkylamines Enables Broad Scope Reductive Aminations. *Chem. Eur. J.* **2017**, *23* (9), 2217–2224.
- (57) Lawson, J. R.; Melen, R. L. Tris(Pentafluorophenyl)Borane and Beyond: Modern Advances in Borylation Chemistry. *Inorg. Chem.* **2017**, *56* (15), 8627–8643.
- (58) Theuergarten, E.; Schlüns, D.; Grunenberg, J.; Daniliuc, C. G.; Jones, P. G.; Tamm, M. Intramolecular Heterolytic Dihydrogen Cleavage by a Bifunctional Frustrated Pyrazolylborane Lewis Pair. *Chem. Commun.* **2010**, *46* (45), 8561–8563.
- (59) Yalpani, M.; Boese, R.; Koster, R.; Yalpani, M. Monomeric and Dimeric 9-Pyrazolyl-9-Borabicyclo[3.3.1]Nonanes. *Chem. Ber.* **1990**, *123*, 1275–1283.
- (60) García, F.; Hopkins, A. D.; Kowenicki, R. A.; McPartlin, M.; Silvia, J. S.; Rawson, J. M.; Rogers, M. C.; Wright, D. S. Pyridyl “ring-Flipping” in the Dimers [Me<sub>2</sub>E(2-Py)]<sub>2</sub> (E = B, Al, Ga; 2-Py = 2-Pyridyl). *Chem. Commun.* **2007**, *2* (6), 586–588.
- (61) Sumerin, V.; Schulz, F.; Atsumi, M.; Wang, C.; Nieger, M.; Leskela, M. Molecular Tweezers for Hydrogen : Synthesis , Characterization , and Reactivity. *J. Am. Chem. Soc.* **2008**, *130*, 14117–14119.
- (62) Winkelhaus, D.; Neumann, B.; Mitzel, N. W. An Intramolecular Boron Nitrogen Lewis Acid Base Pair on a Rigid Naphthyl Backbone. *Zeitschrift fur Naturforsch. - Sect. B J. Chem. Sci.* **2012**, *67* (6), 589–593.
- (63) Kirby, A. J.; Percy, J. M. Synthesis of 8-Substituted 1-Naphthylamine Derivatives. Exceptional Reactivity of the Substituents. *Tetrahedron* **1988**, *44*, 6903–6910.
- (64) Prokofjevs, A.; Jermaks, J.; Borovika, A.; Kampf, J. W.; Vedejs, E. Electrophilic C-H Borylation and Related Reactions of B-H Boron Cations. *Organometallics* **2013**, *32* (22), 6701–6711.
- (65) Brown, H. C.; Schlesinger, H. I.; Cardon, S. Z. Studies in Stereochemistry. I. Steric Strains as a Factor in the Relative Stability of Some Coördination Compounds of Boron. *J. Am. Chem. Soc.* **1942**, *64* (2), 325–329.
- (66) Wittig, G.; Benz, E. Uber Das Verhalten von Dehydrobenzol Gegenuber Nucleophilen Und Elektrophilen Reagenzien. *Chem. Ber.* **1959**, *92*, 1999–2013.
- (67) Roesler, R.; Piers, W. E.; Parvez, M. Synthesis, Structural Characterization and Reactivity of the Amino Borane 1-(NPh<sub>2</sub>)-2-[B(C<sub>6</sub>F<sub>5</sub>)<sub>2</sub>]C<sub>6</sub>H<sub>4</sub>. *J. Organomet. Chem.* **2003**, *680* (1–2), 218–222.
- (68) Mömning, C. M.; Frömel, S.; Kehr, G.; Fröhlich, R.; Grimme, S.; Erker, G. Reactions of an Intramolecular Frustrated Lewis Pair with Unsaturated Substrates: Evidence for a Concerted Olefin Addition Reaction. *J. Am. Chem. Soc.* **2009**, *131* (34), 12280–12289.
- (69) Dureen, M. A.; Stephan, D. W. Terminal Alkyne Activation by Frustrated and Classical Lewis Acid / Phosphine Pairs. *J. Am. Chem. Soc.* **2009**, *131*, 8396–8397.
- (70) Chase, P. A.; Welch, G. C.; Jurca, T.; Stephan, D. W. Metal-Free Catalytic Hydrogenation.

*Angew. Chem. Int. Ed.* **2007**, *46* (42), 8050–8053.

- (71) Spies, P.; Schwendemann, S.; Lange, S.; Kehr, G.; Fröhlich, R.; Erker, G. Metal-Free Catalytic Hydrogenation of Enamines, Imines, and Conjugated Phosphinoalkenylboranes. *Angew. Chem. Int. Ed.* **2008**, *47* (39), 7543–7546.
- (72) Wikipedia [https://en.wikipedia.org/wiki/Carbon\\_dioxide](https://en.wikipedia.org/wiki/Carbon_dioxide) (accessed Jan 30, 2019).
- (73) Olah, G. A.; Goepfert, A.; Surya Prakash, G. K. *Beyond Oil and Gas: The Methanol Economy*; Wiley-VCH, 2009.
- (74) Artz, J.; Müller, T. E.; Thenert, K.; Kleinekorte, J.; Meys, R.; Sternberg, A.; Bardow, A.; Leitner, W. Sustainable Conversion of Carbon Dioxide: An Integrated Review of Catalysis and Life Cycle Assessment. *Chem. Rev.* **2018**, *118* (2), 434–504.
- (75) Fontaine, F. G.; Stephan, D. W. Metal-Free Reduction of CO<sub>2</sub>. *Curr. Opin. Green Sustain. Chem.* **2017**, *3*, 28–32.
- (76) Chakraborty, S.; Zhang, J.; Krause, J. A.; Guan, H. An Efficient Nickel Catalyst for the Reduction of Carbon Dioxide with a Borane Sumit Chakraborty, Jie Zhang, Jeanette A. Krause, and Hairong Guan \*. *J. Am. Chem. Soc.* **2010**, *132* (2), 8872–8873.
- (77) Schmeier, T. J.; Dobereiner, G. E.; Crabtree, R. H.; Hazari, N. Secondary Coordination Sphere Interactions Facilitate the Insertion Step in an Iridium(III) CO<sub>2</sub> Reduction Catalyst. *J. Am. Chem. Soc.* **2011**, *133*, 9274–9277.
- (78) Huff, C. A.; Sanford, M. S. Cascade Catalysis for the Homogeneous Hydrogenation of CO<sub>2</sub> to Methanol. *J. Am. Chem. Soc.* **2011**, *133* (45), 18122–18125.
- (79) Schneidewind, J.; Adam, R.; Baumann, W.; Jackstell, R.; Beller, M. Low-Temperature Hydrogenation of Carbon Dioxide to Methanol with a Homogeneous Cobalt Catalyst. *Angew. Chem. Int. Ed.* **2017**, *56* (7), 1890–1893.
- (80) Mömning, C. M.; Otten, E.; Kehr, G.; Fröhlich, R.; Grimme, S.; Stephan, D. W.; Erker, G. Reversible Metal-Free Carbon Dioxide Binding by Frustrated Lewis Pairs. *Angew. Chem. Int. Ed.* **2009**, *48* (36), 6643–6646.
- (81) Ashley, A. E.; Thompson, A. L.; O’Hare, D. Non-Metal-Mediated Homogeneous Hydrogenation of CO<sub>2</sub> to CH<sub>3</sub>OH. *Angew. Chem. Int. Ed.* **2009**, *48* (52), 9839–9843.
- (82) Ménard, G.; Stephan, D. W. Room Temperature Reduction of CO<sub>2</sub> to Methanol by Al-Based Frustrated Lewis Pairs and Ammonia Borane. *J. Am. Chem. Soc.* **2010**, *132* (6), 1796–1797.
- (83) Berkefeld, A.; Piers, W. E.; Parvez, M. Tandem Frustrated Lewis Pair / Tris (Pentafluorophenyl) Borane-Catalyzed Deoxygenative Hydrosilylation of Carbon Dioxide. *J. Am. Chem. Soc.* **2010**, *132*, 10660–10661.
- (84) Riduan, S. N.; Zhang, Y.; Ying, J. Y. Conversion of Carbon Dioxide into Methanol with Silanes over N-Heterocyclic Carbene Catalysts. *Angew. Chem. Int. Ed.* **2009**, *48* (18), 3322–3325.
- (85) Courtemanche, M. A.; Légaré, M. A.; Maron, L.; Fontaine, F. G. A Highly Active Phosphine-Borane Organocatalyst for the Reduction of CO<sub>2</sub> to Methanol Using Hydroboranes. *J. Am. Chem. Soc.* **2013**, *135* (25), 9326–9329.
- (86) Declercq, R.; Bouhadir, G.; Bourissou, D.; Légaré, M. A.; Courtemanche, M. A.; Nahi, K.

- S.; Bouchard, N.; Fontaine, F. G.; Maron, L. Hydroboration of Carbon Dioxide Using Ambiphilic Phosphine-Borane Catalysts: On the Role of the Formaldehyde Adduct. *ACS Catal.* **2015**, *5* (4), 2513–2520.
- (87) Wencel-Delord, J.; Glorius, F. C-H Bond Activation Enables the Rapid Construction and Late-Stage Diversification of Functional Molecules. *Nat. Chem.* **2013**, *5* (5), 369–375.
- (88) Cho, J. Y.; Tse, M. K.; Holmes, D.; Maleczka, R. E.; Smith, M. R. Remarkably Selective Iridium Catalysts for the Elaboration of Aromatic C-H Bonds. *Science* **2002**, 305–308.
- (89) Ishiyama, T.; Takagi, J.; Ishida, K.; Miyauchi, N.; Anastasi, N. R.; Hartwig, J. F. Mild Iridium-Catalyzed Borylation of Arenes. High Turnover Numbers, Room Temperature Reactions, and Isolation of a Potential Intermediate. *J. Am. Chem. Soc.* **2002**, *124* (3), 390–391.
- (90) Campeau, L. C.; Chen, Q.; Gauvreau, D.; Girardin, M.; Belyk, K.; Maligres, P.; Zhou, G.; Gu, C.; Zhang, W.; Tan, L.; O'Shea, P. D. A Robust Kilo-Scale Synthesis of Doravirine. *Org. Process Res. Dev.* **2016**, *20* (8), 1476–1481.
- (91) Stahl, T.; Müther, K.; Ohki, Y.; Tatsumi, K.; Oestreich, M. Catalytic Generation of Borene Ions by Cooperative B-H Bond Activation: The Elusive Direct Electrophilic Borylation of Nitrogen Heterocycles with Pinacolborane. *J. Am. Chem. Soc.* **2013**, *135* (30), 10978–10981.
- (92) Esteruelas, M. A.; Oliván, M.; Vélez, A. POP-Rhodium-Promoted C-H and B-H Bond Activation and C-B Bond Formation. *Organometallics* **2015**, *34* (10), 1911–1924.
- (93) Takaya, J.; Ito, S.; Nomoto, H.; Saito, N.; Kirai, N.; Iwasawa, N. Fluorine-Controlled C-H Borylation of Arenes Catalyzed by a PSiN-Pincer Platinum Complex. *Chem. Commun.* **2015**, *51* (100), 17662–17665.
- (94) Furukawa, T.; Tobisu, M.; Chatani, N. C-H Functionalization at Sterically Congested Positions by the Platinum-Catalyzed Borylation of Arenes. *J. Am. Chem. Soc.* **2015**, *137* (38), 12211–12214.
- (95) Hatanaka, T.; Ohki, Y.; Tatsumi, K. C-H Bond Activation/Borylation of Furans and Thiophenes Catalyzed by a Half-Sandwich Iron N-Heterocyclic Carbene Complex. *Chem. Asian J.* **2010**, *5*, 1657–1666.
- (96) Mazzacano, T. J.; Mankad, N. P. Base Metal Catalysts for Photochemical C-H Borylation That Utilize Metal-Metal Cooperativity. *J. Am. Chem. Soc.* **2013**, *135* (46), 17258–17261.
- (97) Dombay, T.; Werncke, C. G.; Jiang, S.; Grellier, M.; Vendier, L.; Bontemps, S.; Sortais, J. B.; Sabo-Etienne, S.; Darcel, C. Iron-Catalyzed C-H Borylation of Arenes. *J. Am. Chem. Soc.* **2015**, *137* (12), 4062–4065.
- (98) Borylation, C. C. H.; Obligacion, J. V.; Semproni, S. P.; Chirik, P. J. Cobalt-Catalyzed C – H Borylation. *J. Am. Chem. Soc.* **2014**, *136*, 4133–4136.
- (99) Obligacion, J. V.; Bezdek, M. J.; Chirik, P. J. C(Sp<sup>2</sup>)-H Borylation of Fluorinated Arenes Using an Air-Stable Cobalt Precatalyst: Electronically Enhanced Site Selectivity Enables Synthetic Opportunities. *J. Am. Chem. Soc.* **2017**, *139* (7), 2825–2832.
- (100) Prokofjevs, A.; Kampf, J. W.; Vedejs, E. A Boronium Ion with Exceptional Electrophilicity. *Angew. Chem. Int. Ed.* **2011**, *50*, 2098–2101.

- (101) Del Grosso, A.; Singleton, P. J.; Muryn, C. A.; Ingleson, M. J. Pinacol Boronates by Direct Arene Borylation with Borenium Cations. *Angew. Chem. Int. Ed.* **2011**, *50* (9), 2102–2106.
- (102) Crossley, D. L.; Cade, I. a.; Clark, E. R.; Escande, a.; Humphries, M. J.; King, S. M.; Vitorica-Yrezabal, I.; Ingleson, M. J.; Turner, M. L. Enhancing Electron Affinity and Tuning Band Gap in Donor–acceptor Organic Semiconductors by Benzothiadiazole Directed C–H Borylation. *Chem. Sci.* **2015**, *6* (9), 5144–5151.
- (103) Del Grosso, A.; Pritchard, R. G.; Muryn, C. A.; Ingleson, M. J. Chelate Restrained Boron Cations for Intermolecular Electrophilic Arene Borylation. *Organometallics* **2010**, *29* (1), 241–249.
- (104) Yin, Q.; Klare, H. F. T.; Oestreich, M. Catalytic Friedel–Crafts C–H Borylation of Electron-Rich Arenes: Dramatic Rate Acceleration by Added Alkenes. *Angew. Chem. Int. Ed.* **2017**, *56* (13), 3712–3717.
- (105) Chernichenko, K.; Lindqvist, M.; Kótai, B.; Nieger, M.; Sorochkina, K.; Pápai, I.; Repo, T. Metal-Free Sp<sup>2</sup>-C–H Borylation as a Common Reactivity Pattern of Frustrated 2-Aminophenylboranes. *J. Am. Chem. Soc.* **2016**, *138* (14), 4860–4868.
- (106) Rochette, É.; Fontaine, F. Isodesmic C–H Borylation : Perspectives and Proof of Concept of Transfer Borylation Catalysis. *ChemRxiv* **2018**.
- (107) Neeve, E. C.; Geier, S. J.; Mkhaliid, I. A I.; Westcott, S. A.; Marder, T. B. Diboron(4) Compounds: From Structural Curiosity to Synthetic Workhorse. *Chem. Rev.* **2016**, *116* (16), 9091–9161.
- (108) Braunschweig, H.; Dewhurst, R. D.; Mozo, S. Building Electron-Precise Boron–Boron Single Bonds: Imposing Monogamy on a Promiscuous Element. *ChemCatChem* **2015**, *7* (11), 1630–1638.
- (109) Arrowsmith, M.; Böhnke, J.; Braunschweig, H.; Deißberger, A.; Dewhurst, R. D.; Ewing, W. C.; Hörl, C.; Mies, J.; Muessig, J. H. Simple Solution-Phase Syntheses of Tetrahalodiboranes(4) and Their Labile Dimethylsulfide Adducts. *Chem. Commun.* **2017**, *53* (59), 8265–8267.
- (110) Rochette, É.; Bouchard, N.; Légaré Lavergne, J.; Matta, C. F.; Fontaine, F.-G. Spontaneous Reduction of a Hydroborane To Generate a B–B Single Bond by the Use of a Lewis Pair. *Angew. Chem. Int. Ed.* **2016**, *55*, 12722–12726.
- (111) Ciobanu, O.; Roquette, P.; Leingang, S.; Wadepohl, H.; Mautz, J.; Himmel, H. J. Synthesis and Characterization of a New Guanidine–Borane Complex and a Dinuclear Boron(II) Hydride with Bridging Guanidinate Ligands. *Eur. J. Inorg. Chem.* **2007**, 4530–4534.
- (112) Kaese, T.; Budy, H.; Bolte, M.; Lerner, H. W.; Wagner, M. Deprotonation of a Seemingly Hydridic Diborane(6) To Build a B–B Bond. *Angew. Chem. Int. Ed.* **2017**, *56* (26), 7546–7550.
- (113) Tsukahara, N.; Asakawa, H.; Lee, K. H.; Lin, Z.; Yamashita, M. Cleaving Dihydrogen with Tetra(o-Tolyl)Diborane(4). *J. Am. Chem. Soc.* **2017**, *139* (7), 2593–2596.
- (114) Odom, J. D.; Moore, T. F.; Goetze, R.; Nöth, H.; Wrackmeyer, B. Nuclear Magnetic Resonance Studies of Boron Compounds. *J. Organomet. Chem.* **1979**, *173* (1), 15–32.
- (115) Cole Research Group, SDSU Department of Chemistry & Biochemistry <http://www.chemistry.sdsu.edu/research/BNMR/> (accessed Dec 8, 2018).

- (116) Hohenberg, P.; Kohn, W. Inhomogeneous Electron Gas. *Phys. Rev.* **1964**, *136*, B864–B871.
- (117) Reich, H. J. University of Wisconsin  
<https://www.chem.wisc.edu/areas/reich/chem605/index.htm> (accessed Jan 9, 2019).
- (118) Boudreau, J.; Courtemanche, M.-A.; Fontaine, F.-G. Reactivity of Lewis Pairs ( $R_2PCH_2AlMe_2$ )<sub>2</sub> with Carbon Dioxide. *Chem. Commun.* **2011**, *47* (39), 11131.
- (119) Courtemanche, M. A.; Larouche, J.; Légaré, M. A.; Bi, W.; Maron, L.; Fontaine, F. G. A Tris(Triphenylphosphine)Aluminum Ambiphilic Precatalyst for the Reduction of Carbon Dioxide with Catecholborane. *Organometallics* **2013**, *32* (22), 6804–6811.
- (120) Courtemanche, M.-A.; Légaré, M.-A.; Fontaine, F.-G.; Maron, L. Reducing CO<sub>2</sub> to Methanol Using Frustrated Lewis Pairs: On the Mechanism of Phosphine – Borane-Mediated Hydroboration of CO<sub>2</sub>. *J. Am. Chem. Soc.* **2014**, *136*, 10708–10717.
- (121) Zhou, Q.; Li, Y. The Real Role of N-Heterocyclic Carbene in Reductive Functionalization of CO<sub>2</sub>: An Alternative Understanding from Density Functional Theory Study. *J. Am. Chem. Soc.* **2015**, *137* (32), 10182–10189.
- (122) Riduan, S. N.; Ying, J. Y.; Zhang, Y. Mechanistic Insights into the Reduction of Carbon Dioxide with Silanes over N-Heterocyclic Carbene Catalysts. *ChemCatChem* **2013**, *5* (6), 1490–1496.
- (123) Huang, F.; Lu, G.; Zhao, L.; Li, H.; Wang, Z. X. The Catalytic Role of N-Heterocyclic Carbene in a Metal-Free Conversion of Carbon Dioxide into Methanol: A Computational Mechanism Study. *J. Am. Chem. Soc.* **2010**, *132* (35), 12388–12396.
- (124) Zimmerman, P. M.; Zhang, Z.; Musgrave, C. B. Simultaneous Two-Hydrogen Transfer as a Mechanism for Efficient CO<sub>2</sub> Reduction. *Inorg. Chem.* **2010**, *49* (19), 8724–8728.
- (125) Li, H.; Aquino, A. J. A.; Cordes, D. B.; Hung-Low, F.; Hase, W. L.; Krempner, C. A Zwitterionic Carbanion Frustrated by Boranes - Dihydrogen Cleavage with Weak Lewis Acids via an “Inverse” Frustrated Lewis Pair Approach. *J. Am. Chem. Soc.* **2013**, *135* (43), 16066–16069.
- (126) Mummadi, S.; Unruh, D. K.; Zhao, J.; Li, S.; Krempner, C. “inverse” Frustrated Lewis Pairs - Activation of Dihydrogen with Organosuperbases and Moderate to Weak Lewis Acids. *J. Am. Chem. Soc.* **2016**, *138* (10), 3286–3289.
- (127) Thomas, J. C.; Peters, J. C. Bis(Phosphino)Borates: A New Family of Monoanionic Chelating Phosphine Ligands. *Inorg. Chem.* **2003**, *42* (17), 5055–5073.
- (128) Parks, D. J.; Piers, W. E.; Yap, G. P. A. Synthesis, Properties, and Hydroboration Activity of the Highly Electrophilic Borane Bis(Pentafluorophenyl)Borane, HB(C<sub>6</sub>F<sub>5</sub>)<sub>2</sub>. *Organometallics* **1998**, *17* (25), 5492–5503.
- (129) Albrecht, K.; Kaiser, V.; Boese, R.; Adams, J.; Kaufmann, D. E. Synthesis and Properties of Fluorescent Organoboranes: Triarylmethane-Type Dyes. *J. Chem. Soc. Perkin Trans. 2* **2000**, 2153–2157.
- (130) Slocum, D. W.; Reinscheld, T. K.; White, C. B.; Timmons, M. D.; Shelton, P. a.; Slocum, M. G.; Sandlin, R. D.; Holland, E. G.; Kusmic, D.; Jennings, J. a.; Tekin, K. C.; Nguyen, Q.; Bush, S. J.; Keller, J. M.; Whitley, P. E. Ortho-Lithiations Reassessed: The Advantages of Deficiency Catalysis in Hydrocarbon Media. *Organometallics* **2013**, *32* (6), 1674–1686.

- (131) Tripathy, S.; LeBlanc, R.; Durst, T. Formation of 2-Substituted Iodobenzenes from Iodobenzene via Benzyne and Ate Complex Intermediates. *Org. Lett.* **1999**, *1* (12), 1973–1975.
- (132) Courtemanche, M.-A.; Pulis, A. P.; Rochette, É.; Légaré, M.-A.; Stephan, D. W.; Fontaine, F.-G. Intramolecular B/N Frustrated Lewis Pairs and the Hydrogenation of Carbon Dioxide. *Chem. Commun.* **2015**, *51*, 9797–9800.
- (133) Chernichenko, K.; Madarász, A.; Pápai, I.; Nieger, M.; Leskelä, M.; Repo, T. A Frustrated-Lewis-Pair Approach to Catalytic Reduction of Alkynes to Cis-Alkenes. *Nat. Chem.* **2013**, *5*, 718–723.
- (134) Kang, P.; Cheng, C.; Chen, Z.; Schauer, C. K.; Meyer, T. J.; Brookhart, M. Selective Electrocatalytic Reduction of CO<sub>2</sub> to Formate by Water-Stable Iridium Dihydride Pincer Complexes. *J. Am. Chem. Soc.* **2012**, *134* (12), 5500–5503.
- (135) Rochette, É.; Courtemanche, M.-A.; Pulis, A.; Bi, W.; Fontaine, F.-G. Ambiphilic Frustrated Lewis Pair Exhibiting High Robustness and Reversible Water Activation: Towards the Metal-Free Hydrogenation of Carbon Dioxide. *Molecules* **2015**, *20* (7), 11902–11914.
- (136) Scott, D. J.; Fuchter, M. J.; Ashley, A. E. Nonmetal Catalyzed Hydrogenation of Carbonyl Compounds. *J. Am. Chem. Soc.* **2014**, *136* (45), 15813–15816.
- (137) Mahdi, T.; Stephan, D. W. Enabling Catalytic Ketone Hydrogenation by Frustrated Lewis Pairs. *J. Am. Chem. Soc.* **2014**, *136* (45), 30–33.
- (138) Gyömöre, Á.; Bakos, M.; Földes, T.; Pápai, I.; Domján, A.; Soós, T. Moisture-Tolerant Frustrated Lewis Pair Catalyst for Hydrogenation of Aldehydes and Ketones. *ACS Catal.* **2015**, *5* (9), 5366–5372.
- (139) Scott, D. J.; Simmons, T. R.; Lawrence, E. J.; Wildgoose, G. G.; Fuchter, M. J.; Ashley, A. E. Facile Protocol for Water-Tolerant “Frustrated Lewis Pair”-Catalyzed Hydrogenation. *ACS Catal.* **2015**, *5* (9), 5540–5544.
- (140) Mahdi, T.; Stephan, D. W. Facile Protocol for Catalytic Frustrated Lewis Pair Hydrogenation and Reductive Deoxygenation of Ketones and Aldehydes. *Angew. Chem. Int. Ed.* **2015**, *54* (29), 8511–8514.
- (141) Krempner, C.; Mummadi, S.; Brar, A.; Wang, G.; Kenefake, D.; Diaz, R.; Unruh, D.; Li, S. “Inverse” Frustrated Lewis Pairs - An Inverse FLP Approach to the Catalytic Metal Free Hydrogenation of Ketones. *Chem. Eur. J.* **2018**, 16526–16531.
- (142) Chernichenko, K.; Kótai, B.; Pápai, I.; Zhivonitko, V.; Nieger, M.; Leskelä, M.; Repo, T. Intramolecular Frustrated Lewis Pair with the Smallest Boryl Site: Reversible H<sub>2</sub> Addition and Kinetic Analysis. *Angew. Chem. Int. Ed.* **2015**, *54*, 1749–1753.
- (143) Zalesskiy, S. S.; Ananikov, V. P. Pd<sub>2</sub>(Dba)<sub>3</sub> as a Precursor of Soluble Metal Complexes and Nanoparticles: Determination of Palladium Active Species for Catalysis and Synthesis. *Organometallics* **2012**, *31* (6), 2302–2309.
- (144) Goldman, A. S.; Landis, C. R.; Sen, A. Jack Halpern (1925-2018). *Angew. Chem. Int. Ed.* **2018**, *57*, 4460.
- (145) Simmons, E. M.; Hartwig, J. F. On the Interpretation of Deuterium Kinetic Isotope Effects in C-H Bond Functionalizations by Transition-Metal Complexes. *Angew. Chem. Int. Ed.* **2012**, *51* (13), 3066–3072.

- (146) Jones, W. D. Isotope Effects in C-H Bond Activation Reactions by Transition Metals. *Acc. Chem. Res.* **2003**, *36* (2), 140–146.
- (147) Obligacion, J. V.; Semproni, S. P.; Pappas, I.; Chirik, P. J. Cobalt-Catalyzed C(Sp<sup>2</sup>)-H Borylation: Mechanistic Insights Inspire Catalyst Design. *J. Am. Chem. Soc.* **2016**, *138* (33), 10645–10653.
- (148) Boller, T. M.; Murphy, J. M.; Hapke, M.; Ishiyama, T.; Miyaura, N.; Hartwig, J. F. Mechanism of the Mild Functionalization of Arenes by Diboron Reagents Catalyzed by Iridium Complexes. Intermediacy and Chemistry of Bipyridine-Ligated Iridium Trisboryl Complexes. *J. Am. Chem. Soc.* **2005**, *127* (41), 14263–14278.
- (149) Gorelsky, S. I.; Lapointe, D.; Fagnou, K. Analysis of the Concerted Metalation-Deprotonation Mechanism in Palladium-Catalyzed Direct Arylation across a Broad Range of Aromatic Substrates. *J. Am. Chem. Soc.* **2008**, *130* (33), 10848–10849.
- (150) Toutov, A. A.; Liu, W. B.; Betz, K. N.; Fedorov, A.; Stoltz, B. M.; Grubbs, R. H. Silylation of C-H Bonds in Aromatic Heterocycles by an Earth-Abundant Metal Catalyst. *Nature* **2015**, *518* (7537), 80–84.
- (151) Vitaku, E.; Smith, D. T.; Njardarson, J. T. Analysis of the Structural Diversity, Substitution Patterns, and Frequency of Nitrogen Heterocycles among U.S. FDA Approved Pharmaceuticals. *J. Med. Chem.* **2014**, *57* (24), 10257–10274.
- (152) Tyler McQuade, D.; Pullen, A. E.; Swager, T. M. Conjugated Polymer-Based Chemical Sensors. *Chem. Rev.* **2000**, *100* (7), 2537–2574.
- (153) Cho, J.-Y.; Tse, M. K.; Holmes, D.; Maleczka, R. E. J.; Smith, M. R. I. Remarkably Selective Iridium Catalysts for the Elaboration of Aromatic C-H Bonds. *Science* **2002**, *295* (5553), 305–308.
- (154) Mkhaliid, I.; Barnard, J.; Marder, T. C-H Activation for the Construction of C-B Bonds. *Chem. Rev.* **2009**, *110* (2), 890–931.
- (155) Xu, L.; Wang, G.; Zhang, S.; Wang, H.; Wang, L.; Liu, L.; Jiao, J.; Li, P. Recent Advances in Catalytic C-H Borylation Reactions. *Tetrahedron* **2017**, *73* (51), 7123–7157.
- (156) Hartwig, J. F. Regioselectivity of the Borylation of Alkanes and Arenes. *Chem. Soc. Rev.* **2011**, *40* (4), 1992–2002.
- (157) Liskey, C. W.; Hartwig, J. F. Iridium-Catalyzed C-H Borylation of Cyclopropanes. *J. Am. Chem. Soc.* **2013**, *135* (9), 3375–3378.
- (158) Sadler, S. A.; Tajuddin, H.; Mkhaliid, I. A. I.; Batsanov, A. S.; Albesa-Jove, D.; Cheung, M. S.; Maxwell, A. C.; Shukla, L.; Roberts, B.; Blakemore, D. C.; Lin, Z.; Marder, T. B.; Steel, P. G. Iridium-Catalyzed C-H Borylation of Pyridines. *Org. Biomol. Chem.* **2014**, *12* (37), 7318–7327.
- (159) Ishiyama, T.; Takagi, J.; Yonekawa, Y.; Hartwig, J. F.; Miyaura, N. Iridium-Catalyzed Direct Borylation of Five-Membered Heteroarenes by Bis(Pinacolato)Diboron: Regioselective, Stoichiometric, and Room Temperature Reactions. *Adv. Synth. Catal.* **2003**, *345* (910), 1103–1106.
- (160) Tajuddin, H.; Harrisson, P.; Bitterlich, B.; Collings, J. C.; Sim, N.; Batsanov, A. S.; Cheung, M. S.; Kawamorita, S.; Maxwell, A. C.; Shukla, L.; Morris, J.; Lin, Z.; Marder, T. B.; Steel, P. G. Iridium-Catalyzed C-H Borylation of Quinolines and Unsymmetrical 1,2-Disubstituted



- Benzenes: Insights into Steric and Electronic Effects on Selectivity. *Chem. Sci.* **2012**, *3* (12), 3505–3515.
- (161) Larsen, M. A.; Hartwig, J. F. Iridium-Catalyzed C-H Borylation of Heteroarenes: Scope, Regioselectivity, Application to Late-Stage Functionalization, and Mechanism. *J. Am. Chem. Soc.* **2014**, *136* (11), 4287–4299.
- (162) Press, L. P.; Kosanovich, A. J.; McCulloch, B. J.; Ozerov, O. V. High-Turnover Aromatic C-H Borylation Catalyzed by POCOP-Type Pincer Complexes of Iridium. *J. Am. Chem. Soc.* **2016**, *138* (30), 9487–9497.
- (163) Hartwig, J. F. Evolution of C-H Bond Functionalization from Methane to Methodology. *J. Am. Chem. Soc.* **2016**, *138* (1), 2–24.
- (164) Preshlock, S. M.; Plattner, D. L.; Maligres, P. E.; Krska, S. W.; Maleczka, R. E.; Smith, M. R. A Traceless Directing Group for C-H Borylation. *Angew. Chem. Int. Ed.* **2013**, *52* (49), 12915–12919.
- (165) Robbins, D. W.; Boebel, T. A.; Hartwig, J. F. Iridium-Catalyzed, Silyl-Directed Borylation of Nitrogen-Containing. *J. Am. Chem. Soc.* **2010**, *132*, 4068–4069.
- (166) Chattopadhyay, B.; Dannatt, J. E.; Andujar-De Sanctis, I. L.; Gore, K. A.; Maleczka, R. E.; Singleton, D. A.; Smith, M. R. Ir-Catalyzed Ortho-Borylation of Phenols Directed by Substrate-Ligand Electrostatic Interactions: A Combined Experimental/in Silico Strategy for Optimizing Weak Interactions. *J. Am. Chem. Soc.* **2017**, *139* (23), 7864–7871.
- (167) Smith, M. R.; Bisht, R.; Haldar, C.; Pandey, G.; Dannatt, J. E.; Ghaffari, B.; Maleczka, R. E.; Chattopadhyay, B. Achieving High Ortho Selectivity in Aniline C-H Borylations by Modifying Boron Substituents. *ACS Catal.* **2018**, *8* (7), 6216–6223.
- (168) Su, B.; Hartwig, J. F. Iridium-Catalyzed, Silyl-Directed, Peri-Borylation of C-H Bonds in Fused Polycyclic Arenes and Heteroarenes. *Angew. Chem. Int. Ed.* **2018**, *57* (32), 10163–10167.
- (169) Boebel, T. A.; Hartwig, J. F. Silyl-Directed, Iridium-Catalyzed Ortho-Borylation of Arenes. A One-Pot Ortho-Borylation of Phenols, Arylamines, and Alkylarenes. *J. Am. Chem. Soc.* **2008**, *130* (24), 7534–7535.
- (170) Su, B.; Zhou, T. G.; Xu, P. L.; Shi, Z. J.; Hartwig, J. F. Enantioselective Borylation of Aromatic C-H Bonds with Chiral Dinitrogen Ligands. *Angew. Chem. Int. Ed.* **2017**, *56* (25), 7205–7208.
- (171) Schaefer, B. A.; Margulieux, G. W.; Small, B. L.; Chirik, P. J. Evaluation of Cobalt Complexes Bearing Tridentate Pincer Ligands for Catalytic C-H Borylation. *Organometallics* **2015**, *34* (7), 1307–1320.
- (172) Léonard, N. G.; Bezdek, M. J.; Chirik, P. J. Cobalt-Catalyzed C(Sp<sup>2</sup>)-H Borylation with an Air-Stable, Readily Prepared Terpyridine Cobalt(II) Bis(Acetate) Precatalyst. *Organometallics* **2017**, *36* (1), 142–150.
- (173) Obligation, J. V.; Chirik, P. J. Mechanistic Studies of Cobalt-Catalyzed C(Sp<sup>2</sup>)-H Borylation of Five-Membered Heteroarenes with Pinacolborane. *ACS Catal.* **2017**, *7* (7), 4366–4371.
- (174) Ren, H.; Zhou, Y. P.; Bai, Y.; Cui, C.; Driess, M. Cobalt-Catalyzed Regioselective Borylation of Arenes: N-Heterocyclic Silylene as an Electron Donor in the Metal-Mediated

Activation of C–H Bonds. *Chem. Eur. J.* **2017**, *23* (24), 5663–5667.

- (175) Babudri, F.; Farinola, G. M.; Naso, F.; Ragni, R. Fluorinated Organic Materials for Electronic and Optoelectronic Applications: The Role of the Fluorine Atom. *Chem. Commun.* **2007**, No. 10, 1003–1022.
- (176) Fei, Z.; Shahid, M.; Yaacobi-Gross, N.; Rossbauer, S.; Zhong, H.; Watkins, S. E.; Anthopoulos, T. D.; Heeney, M. Thiophene Fluorination to Enhance Photovoltaic Performance in Low Band Gap Donor-Acceptor Polymers. *Chem. Commun.* **2012**, *48* (90), 11130–11132.
- (177) Zhang, Q.; Yan, L.; Jiao, X.; Peng, Z.; Liu, S.; Rech, J. J.; Klump, E.; Ade, H.; So, F.; You, W. Fluorinated Thiophene Units Improve Photovoltaic Device Performance of Donor-Acceptor Copolymers. *Chem. Mater.* **2017**, *29* (14), 5990–6002.
- (178) Shi, H.; Babinski, D. J.; Ritter, T. Modular C-H Functionalization Cascade of Aryl Iodides. *J. Am. Chem. Soc.* **2015**, *137* (11), 3775–3778.
- (179) Franz, D.; Bolte, M.; Lerner, H.-W.; Wagner, M. Ditopic Hydridoborates and Hydridoboranes: Bridging Ligands in Coordination Polymers and Versatile Hydroboration Reagents. *Dalton Trans.* **2011**, *40* (11), 2433–2440.
- (180) Caubère, P. Applications of Sodamide-Containing “Complex Bases” in Organic Synthesis. *Acc. Chem. Res.* **1974**, *7*, 301–308.
- (181) Caubère, P. Complex Bases and Complex Reducing Agents New Tools in Organic Synthesis. In *Organic Chemistry*; Springer: Berlin, Heidelberg, 1978; pp 49–103.
- (182) Jayaraman, A.; Misal Castro, L. C.; Fontaine, F.-G. Practical and Scalable Synthesis of Borylated Heterocycles Using Bench-Stable Precursors of Metal-Free Lewis Pair Catalysts. *Org. Process Res. Dev.* **2018**, acs.oprd.8b00248.
- (183) Vasko, P.; Zulkifly, I. A.; Fuentes, M. Á.; Mo, Z.; Hicks, J.; Kamer, P. C. J.; Aldridge, S. Reversible C–H Activation, Facile C–B/B–H Metathesis and Apparent Hydroboration Catalysis by a Dimethylxanthene-Based Frustrated Lewis Pair. *Chem. Eur. J.* **2018**, *24* (41), 10531–10540.
- (184) Schulz, F.; Sumerin, V.; Heikkinen, S.; Pedersen, B.; Wang, C.; Atsumi, M.; Leskelä, M.; Repo, T.; Pyykkö, P.; Petry, W.; Rieger, B. Molecular Hydrogen Tweezers: Structure and Mechanisms by Neutron Diffraction, NMR, and Deuterium Labeling Studies in Solid and Solution. *J. Am. Chem. Soc.* **2011**, *133* (50), 20245–20257.
- (185) Ruiz, D. a.; Ung, G.; Melaimi, M.; Bertrand, G. Deprotonation of a Borohydride: Synthesis of a Carbene-Stabilized Boryl Anion. *Angew. Chem. Int. Ed.* **2013**, *52* (29), 7590–7592.
- (186) Himmel, H. J. Repeated Dihydrogen Elimination from Amidine Adducts of Group 13 Element Hydrides: An Evaluation of the Reaction Pathways. *Inorg. Chem.* **2007**, *46* (16), 6585–6593.
- (187) Schulenberg, N.; Litters, S.; Kaifer, E.; Himmel, H. J. Zinc Halide and Alkylzinc Complexes of a Neutral Doubly Base-Stabilized Diborane(4). *Eur. J. Inorg. Chem.* **2011**, No. 17, 2657–2661.
- (188) Wagner, A.; Kaifer, E.; Himmel, H. J. Diborane(4)-Metal Bonding: Between Hydrogen Bridges and Frustrated Oxidative Addition. *Chem. Commun.* **2012**, *48* (43), 5277–5279.

- (189) Litters, S.; Kaifer, E.; Enders, M.; Himmel, H. J. A Boron–boron Coupling Reaction between Two Ethyl Cation Analogues. *Nat. Chem.* **2013**, *5*, 1029–1034.
- (190) Wagner, A.; Kaifer, E.; Himmel, H. J. Bonding in Diborane-Metal Complexes: A Quantum-Chemical and Experimental Study of Complexes Featuring Early and Late Transition Metals. *Chem. Eur. J.* **2013**, *19* (23), 7395–7409.
- (191) Wagner, A.; Litters, S.; Elias, J.; Kaifer, E.; Himmel, H. J. Chemistry of Guanidinate-Stabilised Diboranes: Transition-Metal-Catalysed Dehydrocoupling and Hydride Abstraction. *Chem. Eur. J.* **2014**, *20* (39), 12514–12527.
- (192) Litters, S.; Ganschow, M.; Kaifer, E.; Himmel, H. J. Diboranyl Phosphonium Cations: Synthesis and Chemical Properties. *Eur. J. Inorg. Chem.* **2015**, *2015* (31), 5188–5195.
- (193) Litters, S.; Kaifer, E.; Himmel, H. J. A Radical Tricationic Rhomboid Tetraborane(4) with Four-Center, Five-Electron Bonding. *Angew. Chem. Int. Ed.* **2016**, *55* (13), 4345–4347.
- (194) Litters, S.; Kaifer, E.; Himmel, H. J. Formation of a Radical Tricationic Tetraborane(4) by Hydride Abstraction from Sp<sup>3</sup>–sp<sup>3</sup>-Hybridized Diboranes. *Eur. J. Inorg. Chem.* **2016**, *2016* (25), 4090–4098.
- (195) Frick, M.; Kaifer, E.; Himmel, H. J. Metal-Free Nitrile Diboration through Activation by an Electron-Rich Diborane. *Angew. Chem. Int. Ed.* **2017**, *56* (38), 11645–11648.
- (196) Himmel, H. J. Nucleophilic Neutral Diborane(4) Compounds with Sp<sup>3</sup>–sp<sup>3</sup>-Hybridized Boron Atoms. *Eur. J. Inorg. Chem.* **2018**, *2018* (20), 2139–2154.
- (197) Ciobanu, O.; Himmel, H. J. Repeated Dihydrogen Elimination from Boranes and Gallanes Stabilized by Guanidine-Type Bases: A Quantum Chemical Study Motivated by Recent Experimental Results. *Eur. J. Inorg. Chem.* **2007**, 3565–3572.
- (198) Widera, A.; Kaifer, E.; Wadepohl, H.; Himmel, H. J. On the Dual Reactivity of a Nucleophilic Dihydrido-Diborane: Reaction at the B–B Bond and/or the B–H Bond. *Chem. Eur. J.* **2018**, *24* (5), 1209–1216.
- (199) Horn, J.; Widera, A.; Litters, S.; Kaifer, E.; Himmel, H. J. Tuning the Nucleophilicity of Electron-Rich Diborane(4) Compounds with Bridging Guanidinate Substituents by Substitution. *Dalton Trans.* **2018**, *47* (6), 2009–2017.
- (200) Dinda, R.; Ciobanu, O.; Wadepohl, H.; Hübner, O.; Acharyya, R.; Himmel, H. J. Synthesis and Structural Characterization of a Stable Dimeric Boron(II) Dication. *Angew. Chem. Int. Ed.* **2007**, *46* (47), 9110–9113.
- (201) Ciobanu, O.; Emeljanenko, D.; Kaifer, E.; Mautz, J.; Himmel, H. J. First Dinuclear B(II) Monocations with Bridging Guanidinate Ligands: Synthesis and Properties. *Inorg. Chem.* **2008**, *47* (11), 4774–4778.
- (202) Ciobanu, O.; Allouti, F.; Roquette, P.; Leingang, S.; Enders, M.; Wadepohl, H.; Himmel, H. J. Thermal and Catalytic Dehydrogenation of the Guanidine-Borane Adducts H<sub>3</sub>B·hppH (HppH = 1,3,4,6,7,8-Hexahydro-2H-Pyrimido[1,2-a] Pyrimidine) and H<sub>3</sub>B·N(H)C(NMe<sub>2</sub>)<sub>2</sub>: A Combined Experimental and Quantum Chemical Study. *Eur. J. Inorg. Chem.* **2008**, 5482–5493.
- (203) Ciobanu, O.; Kaifer, E.; Enders, M.; Himmel, H. J. Synthesis of a Stable B<sub>2</sub>H<sub>5</sub><sup>+</sup> Analogue by Protonation of a Double Base-Stabilized Diborane(4). *Angew. Chem. Int. Ed.* **2009**, *48* (30), 5538–5541.

- (204) Schulenberg, N.; Jäkel, M.; Kaifer, E.; Himmel, H. J. The Borane Complexes HtbO-BH<sub>3</sub> and Htbn-BH<sub>3</sub> (Htbo = 1,4,6-Triazabicyclo[3.3.0]Oct-4-Ene, Htbn = 1,5,7-Triazabicyclo[4.3.0]Non-6-Ene) : Synthesis and Dehydrogenation to Dinuclear Boron Hydrides. *Eur. J. Inorg. Chem.* **2009**, 3 (32), 4809–4819.
- (205) Schulenberg, N.; Ciobanu, O.; Kaifer, E.; Wadepohl, H.; Himmel, H. J. The Doubly Base-Stabilized Diborane(4) [HB(μ-Hpp)]<sub>2</sub> (Hpp = 1,3,4,6,7,8-Hexahydro-2H-Pyrimido[1,2-a]Pyrimidine): Synthesis by Catalytic Dehydrogenation and Reactions with S8 and Disulfides. *Eur. J. Inorg. Chem.* **2010**, 2 (33), 5201–5210.
- (206) Schulenberg, N.; Wadepohl, H.; Himmel, H. J. Synthesis and Characterization of a Doubly Base-Stabilized B<sub>3</sub>H<sub>6</sub><sup>+</sup> Analogue. *Angew. Chem. Int. Ed.* **2011**, 50 (44), 10444–10447.
- (207) Lauer, M.; Wulff, G. Arylboronic Acids with Intramolecular B-N Interaction : Convenient Synthesis through Ortho-Lithiation of Substituted Benzylamines. *J. Organomet. Chem.* **1983**, 256, 1–9.
- (208) Polonka-Bálint, Á.; Saraceno, C.; Ludányi, K.; Bényei, A.; Mátyus, P. Novel Extensions of the Tert-Amino Effect: Formation of Phenanthridines and Diarene-Fused Azocines from Ortho-Ortho'-Functionalized Biaryls. *Synlett* **2008**, 4 (18), 2846–2850.
- (209) Colobert, F.; Valdivia, V.; Choppin, S.; Leroux, F. R.; Fernández, I.; Álvarez, E.; Khiar, N. Axial Chirality Control during Suzuki-Miyaura Cross-Coupling Reactions: The Tert-Butylsulfinyl Group as an Efficient Chiral Auxiliary. *Org. Lett.* **2009**, 11 (22), 5130–5133.
- (210) Hanson, J. R. Wagner-Meerwein Rearrangements. *Compr. Org. Synth.* **1991**, 3, 705–719.
- (211) Petasis, N. A.; Akritopoulou, I. The Boronic Acid Mannich Reaction: A New Method for the Synthesis of Geometrically Pure Allylamines. *Tetrahedron Lett.* **1992**, 34 (4), 583–586.
- (212) Candeias, N. R.; Montalbano, F.; Cal, P. M. S. D.; Gois, P. M. P. Boronic Acids and Esters in the Petasis-Borono Mannich Multicomponent Reaction. *Chem. Rev.* **2010**, 110 (10), 6169–6193.
- (213) Romero, E.; Peltier, J. L.; Jazzar, R.; Bertrand, G. Catalyst-Free Dehydrocoupling of Amines, Alcohols, and Thiols with Pinacol Borane and 9-Borabicyclononane (9-BBN). *Chem. Commun.* **2016**, 52, 10563–10565.
- (214) Fernández-Salas, J. A.; Manzini, S.; Nolan, S. P. Efficient Ruthenium-Catalysed S–S, S–Si and S–B Bond Forming Reactions. *Chem. Commun.* **2013**, 49 (52), 5829.
- (215) Civit, M. G.; Sanz, X.; Vogels, C. M.; Webb, J. D.; Geier, S. J.; Decken, A.; Bo, C.; Westcott, S. A.; Fernández, E. Thioboration of α,β-Unsaturated Ketones and Aldehydes toward the Synthesis of β-Sulfido Carbonyl Compounds. *J. Org. Chem.* **2015**, 80 (4), 2148–2154.
- (216) Cuenca, A. B.; Shishido, R.; Ito, H.; Fernández, E. Transition-Metal-Free B–B and B–interelement Reactions with Organic Molecules. *Chem. Soc. Rev.* **2017**.
- (217) Cuenca, A. B.; Shishido, R.; Ito, H.; Fernández, E. Transition-Metal-Free B–B and B–Interelement Reactions with Organic Molecules. *Chem. Soc. Rev.* **2017**, 46 (2), 415–430.
- (218) Bhawal, B. N.; Morandi, B. Isodesmic Reactions in Catalysis – Only the Beginning? *Isr. J. Chem.* **2018**, 58 (1), 94–103.
- (219) Wang, D.; Astruc, D. The Golden Age of Transfer Hydrogenation. *Chem. Rev.* **2015**, 115

- (13), 6621–6686.
- (220) Trnka, T. M.; Grubbs, R. H. The Development of  $L_2X_2Ru=CHR$  Olefin Metathesis Catalysts: An Organometallic Success Story. *Acc. Chem. Res.* **2001**, *34* (1), 18–29.
- (221) Ogba, O. M.; Warner, N. C.; O’Leary, D. J.; Grubbs, R. H. Recent Advances in Ruthenium-Based Olefin Metathesis. *Chem. Soc. Rev.* **2018**, *47* (12), 4510–4544.
- (222) Xianjie, F.; Yu, P.; Morandi, B. Catalytic Reversible Alkene-Nitrile Interconversion through Controllable Transfer Hydrocyanation. *Science* **2016**, *351* (6275), 832–836.
- (223) Preparation Method of Aryl Boric Acid. CN 104119367 A, July 9, 2014.
- (224) Synthetic Method for Diboron Reagents and Related Compounds. US 2016/0090390 A1, 2014.
- (225) Method for Synthesizing Bis(Pinacolato)Diboron. CN 102617623 A, March 5, 2012.
- (226) Preparation Method of Pinacolborane. CN 106008575 A, May 30, 2016.
- (227) Molander, G. A.; Trice, S. L. J.; Kennedy, S. M.; Dreher, S. D.; Tudge, M. T. Scope of the Palladium-Catalyzed Aryl Borylation Utilizing Bis-Boronic Acid. *J. Am. Chem. Soc.* **2012**, *134* (28), 11667–11673.
- (228) 2-Mercaptopyridine, Oakwood Chemicals  
<http://www.oakwoodchemical.com/ProductsList.aspx?CategoryID=-2&txtSearch=17151&ExtHyperLink=1> (accessed Dec 14, 2018).
- (229) García-López, D.; Civit, M. G.; Vogels, C. M.; Ricart, J. M.; Westcott, S. A.; Fernández, E.; Carbó, J. J. Understanding the Mechanism of Transition Metal-Free: Anti Addition to Alkynes: The Selenoboration Case. *Catal. Sci. Technol.* **2018**, *8* (14), 3617–3628.
- (230) Singaram, B. Facile and Convenient Synthesis of B-Amino-9-Borabicyclo[3.3.1] Nonanes. Amino Boration of Isocyanates. *Heteroat. Chem.* **1992**, *3*, 245–249.
- (231) Chernichenko, K.; Nieger, M.; Leskelä, M.; Repo, T. Hydrogen Activation by 2-Boryl-N,N-Dialkylanilines: A Revision of Piers’ Ansa-Aminoborane. *Dalton Trans.* **2012**, *41*, 9029–9032.
- (232) Zulauf, A.; Mellah, M.; Guillot, R.; Schulz, E. Chromium-Thiophene-Salen-Based Polymers for Heterogeneous Asymmetric Hetero-Diels–Alder Reactions. *Eur. J. Org. Chem.* **2008**, 2118–2129.